

UNIVERSITÉ DE SHERBROOKE

Faculté de génie

Département de génie chimique et de génie biotechnologique

Biomatériaux dérivés d'une matrice extracellulaire
(MEC) pour l'ingénierie tissulaire
et les dispositifs médicaux

ExtraCellular Matrix (ECM)-Derived Biomaterials
for Tissue Engineering and Medical Devices

Thèse de doctorat

Spécialité: génie chimique

Vignesh DHANDAPANI

Jury : Professeur Patrick VERMETTE (Directeur)

Professeur Marc-Antoine LAUZON (Rapporteur)

Professeur Denis GROLEAU (Évaluateur)

Professeur Martin BORDUAS (Évaluateur)

Professeure Corinne HOESLI (Évaluatrice externe)

Sherbrooke (Québec), Canada

April 2023

RÉSUMÉ

Le génie tissulaire consiste à construire un organe entier ou une partie de celui-ci *in vitro* ou *in vivo*. Les organes décellularisés utilisés comme échafaudages pour la reconstruction d'organes sont de plus en plus populaires en raison, entre autres, du potentiel de la matrice extracellulaire (MEC). La MEC consiste en un ensemble complexe composé principalement de protéines et de glycosaminoglycanes (GAG). Les protéines les plus courantes comprennent les collagènes, les laminines, les fibronectines et l'élastine. Plusieurs produits commerciaux sont composés de MEC, notamment des papiers tissulaires, des encres pour l'impression 3D et des pansements pour le traitement de plaies. Les bio-adhésifs sont actuellement utilisés seuls ou en complément des sutures pour sceller les fuites d'air ou de sang à la suite d'interventions chirurgicales. On pourrait supposer, par exemple, qu'un bio-adhésif incorporant la MEC permettrait non seulement de sceller une fuite, mais qu'il contribuerait également à la régénération tissulaire.

Cette thèse a pour objectif général d'évaluer la composition et les propriétés de la MEC dérivée de différents organes porcins (vessie, rein, foie, poumon et pancréas) décellularisés à l'aide de méthodes utilisant un détergent et sans détergent. Également, le projet vise à développer une nouvelle famille de biomatériaux à base de MEC pour des applications en médecine.

Le premier travail expérimental comprend la conception d'un système de culture cellulaire pour étudier l'effet des vessies décellularisées, avec ou sans détergent, sur la prolifération et la fonctionnalité des cellules pancréatiques (INS-1 cellules) de rat sécrétant de l'insuline en réponse à des gradients de glucose. Les MECs ont été initialement caractérisées pour la conservation de l'ultrastructure et l'élimination de l'ADN double brin. L'analyse utilisant un test de prolifération CyQUANT a indiqué une prolifération cellulaire après 7 jours de culture sur les vessies décellularisées sans détergent. La sécrétion d'insuline stimulée par le glucose (GSIS) et l'immunomarquage ont confirmé que les cellules étaient également fonctionnelles.

Le deuxième travail expérimental visait la décellularisation des cinq organes porcins à l'aide d'une méthode utilisant un détergent et de méthodes sans détergent. Deux étapes supplémentaires ont été ajoutées à la technique sans détergent (ajustement du pH et traitement par éthylènediaminetétraacétate (EDTA)) afin de réduire la présence d'hémoglobine résiduelle dans les organes décellularisés. Les MECs ont été caractérisées en histologie par différentes colorations pour investiguer l'élimination du contenu cellulaire et la conservation de l'ultrastructure. De plus, la spectrométrie de masse a révélé la conservation d'un plus grand nombre de protéines clés telles que le collagène IV, les laminines, la fibronectine et l'élastine dans les MECs produites avec des méthodes sans détergent par rapport à celles résultantes de la méthode utilisant un détergent. Les mesures de l'orientation du collagène ont indiqué une conservation de l'orientation dans les MECs par rapport à la structure native.

Le troisième travail expérimental a initialement investigué la réponse des cellules INS-1 exposées aux différentes MEC d'organes. Les cellules INS-1 demeuraient fonctionnelles sur certains organes

décellularisés sans détergent après 7 jours de culture. Enfin, des îlots pancréatiques primaires de souris ont été ensemencés sur des vessies décellularisées sans détergent, révélant ainsi que les îlots étaient fonctionnels après 48 heures de culture.

Mots clés : Matrice extracellulaire (MEC), cellules INS-1, organes porcins décellularisés, culture cellulaire en 3D sur des fragments de MEC, caractérisation de protéines par protéomique, cellules et îlots pancréatiques, bio-adhésifs, orientation du collagène, contenu en GAG.

ABSTRACT

Tissue engineering involves the production of whole organ or a part of it *in vitro* or *in vivo*. Decellularized organs as scaffolds for reconstructing organs have been emerging due to the potential of the ExtraCellular Matrix (ECM). ECM is a complex structure primarily composed of proteins and glycosaminoglycans (GAGs). Most common proteins include collagens, laminins, fibronectins and elastins. Several commercial products have been derived from ECM including tissue papers, 3D-printed scaffolds, and wound dressings. Bioadhesives are currently employed alone or as adjuncts to sutures to seal leaks of air or blood from organs following surgical interventions. ECM-incorporated bioadhesives could be hypothesized to not only seal leaks, but also to regenerate tissues.

This thesis aims to investigate the composition and properties of ECMs derived from different porcine organs (bladders, kidneys, livers, lungs, and pancreas) using detergent-based and detergent-free methods.

The first experimental work includes the design of a cell culture system to study the effect of detergent-based and detergent-free decellularized bladders on insulin-secreting rat pancreatic cell (INS-1) proliferation and functionality. ECMs were characterized initially for conservation of ultrastructure and removal of dsDNA. CyQUANT proliferation assay indicated cell proliferation following 7 days of culture on detergent-free decellularized bladders. Glucose-stimulated insulin secretion (GSIS) and immunostaining confirmed that cells were functional.

The second experimental work involved decellularization of the five porcine organs using the detergent-based and detergent-free methods. Two additional steps were added to the detergent-free approach (pH adjustment and ethylenediaminetetraacetic acid (EDTA) treatment) to aid in the removal of residual hemoglobin from the organs. ECMs were characterized by staining for the removal of cellular content and conservation of ultrastructure. Further, mass spectrometry revealed better conservation of a greater number of key proteins such as collagen IV, laminins, fibronectin, and elastin in the ECM resulting from the detergent-free methods, as compared to that produced using the detergent-based one. Collagen fibers orientation measurement indicated preservation of the fibers orientation in the ECMs as compared to that measured in the native organs.

The third experimental work initially screened the INS-1 cell response on different organ ECMs. INS-1 cells were functional on certain detergent-free decellularized organs following 7 days of cell culture. Finally, mouse primary pancreatic islets were seeded on the detergent-free decellularized bladders, revealing functional islets following 48 hours of culture.

Keywords: Extracellular matrix (ECM), INS-1 cells, Decellularized porcine organs, 3D cell culture on ECM pieces, Protein characterization by proteomics, Pancreatic cells and islets, Bioadhesives, Collagen orientation, GAG content.

DEDICATION

I dedicate this thesis to my parents, Dhandapani Kokila Ramalingam and Premila Balasubramanian, for their unconditional love and constant support in every aspect of my life. I am thankful to them for backing me and for their resilience during all the tough times.

For my Parents.....

என் பெற்றோருக்கு அர்ப்பணிக்கிறேன்.....

ACKNOWLEDGEMENTS

I would like to thank my research supervisor Dr. Patrick Vermette for giving me the opportunity to work on the project in the lab, as well as for his support and discussions over the years. It helped me advance my research and grow as a research scientist. I am grateful for the opportunity to explore different avenues in addition to research in the lab.

My sincere wishes to the members of the jury, Dr. Denis Groleau, Dr. Marc-Antoine Lauzon, Dr. Martin Borduas and Dr. Corinne Hoesli for their time in reading and evaluating the thesis. Their inputs have been invaluable and thanks for that. I would like to thank Dr. Martin Borduas for his time and expertise in histology and willingness to help. The help of Dominique Lévesque and technicians Isabelle Arsenaault, Marilène Paquette, Marjolaine Goyette, Martin Thibault, Valérie Larouche, and Serge Gagnon for their assistance in conducting experiments; I am thankful for their services.

I am grateful to all our past and current group members especially Jérémie Chaussé, Vincent-Daniel Girard, Boabekoa Pakindame, Dr. Vickie Ringuette, Dr. Sangamithirai Subramanian, Tamara Challut and Hadrien Le-Nghiem for their help in laboratory and insightful discussions. Times spent had helped me learn and grow with the group.

My sincere gratitude to Dr. Rajinikanth Rajagopal for the brotherhood, love, and support throughout my time in Sherbrooke. I would like to extend my love and gratitude for friendship with Madanraj A S, Raghavendra K G, Prateek J, Rajesh G D, Jamie S, Rajesh M, Charith A, Pavithran I, Akhil S, Edith L, Vasanth K, Audrey L, Avinash V, Irfan V S, Laurine G, Alexandre P, Awais U I, Iulian B Z, Girish N P and Andrea C. I am grateful to the Sherbrooke Cricket Club, parachuting and indoor flying association of Canada for adding a positive outlook to my time in Sherbrooke.

I am thankful to my childhood friends Dr. Brijesh Remin Nelson, Roshan Prabakar, Udaiyali Sivananthan and Suriya T N A for the constant love and encouragement. Finally, words cannot express how thankful I am to my mother Premila Balasubramanian and my father Dhandapani Kokila Ramalingam. They have supported me immensely throughout my journey having been far away from home.

TABLE OF CONTENTS

RÉSUMÉ	iii
ABSTRACT	v
DEDICATION	vi
ACKNOWLEDGEMENTS	vii
LIST OF FIGURES	xii
LIST OF TABLES	xv
LIST OF ABBREVIATIONS	xvi
Chapter 1 Introduction	1
Chapter 2 Composition, Host Responses and Clinical Applications of Bioadhesives ...	5
Foreward.....	6
Résumé.....	7
Abstract.....	8
2.1 Introduction.....	9
2.2 Bioadhesive Classification and Reaction Mechanisms.....	10
2.2.1 Synthetic-derived bioadhesives.....	11
2.2.2 Naturally-derived bioadhesives.....	12
2.3 Bioadhesive Host Responses.....	18
2.3.1 Overview of the steps in wound healing at the site of bioadhesive application...	18
2.3.2 Host responses to bioadhesives.....	19
2.4 Applications.....	23
2.4.1 Clinical applications.....	24
2.4.2 Examples of application-driven requirements for bioadhesives.....	30
2.4.2.1 Lung surgeries.....	30
2.4.2.2 Cardiovascular surgeries.....	30
2.4.2.3 Spinal surgeries.....	31
2.4.2.4 Other applications.....	31
2.5 Conclusions.....	34
Acknowledgements.....	36
Chapter 3 Overview of Approval Procedures for Bioadhesives in the United States of America and Canada	37
Foreward.....	38
Résumé.....	39
Abstract.....	40
3.1 Bioadhesives as Medical Devices.....	41
3.2 FDA Regulations.....	43
3.2.1 Classification.....	43
3.2.2 Tests.....	46
3.2.3 Pre-Submission.....	52

3.2.4 Submission.....	52
3.2.5 Quality System Regulations (QSRs).....	56
3.2.6 Approval and PMS.....	57
3.3 Health Canada Regulations.....	61
3.3.1 Classification.....	61
3.3.2 Forms.....	63
3.3.3 Quality Management System (QMS) Certificate.....	63
3.3.4 Labelling.....	64
3.3.5 Pre-Market Review Document.....	65
3.3.6 Post-market Surveillance (PMS).....	68
3.4 European Regulations.....	69
3.5 Distinguishing features.....	71
3.6 Conclusions.....	73
Acknowledgements.....	74
Chapter 4 Decellularized Bladder as Scaffold to Support Proliferation and Functionality of Insulin-Secreting Pancreatic Cells.....	75
Foreward.....	76
Résumé.....	77
Abstract.....	78
4.1 Introduction.....	79
4.2 Materials and Methods.....	82
4.2.1 Porcine Bladder Decellularization.....	82
4.2.1.1 Detergent-based Decellularization (Det).....	82
4.2.1.2 Detergent-free Decellularization (Det-free).....	83
4.2.2 Histological Characterization.....	85
4.2.3 Scanning Electron Microscopy (SEM) for Ultrastructure Analysis.....	85
4.2.4 DNA Extraction and PicoGreen Assay to Quantify residual dsDNA content.....	85
4.2.5 Three-dimensional Cell Culture System to Validate Decellularized Bladder Parts.....	86
4.2.6 INS-1 Cell Culture Conditions.....	87
4.2.7 MTT Assay for Visual Observation of Viable Cells on ECM Pieces.....	87
4.2.8 CyQUANT™ NF Cell Proliferation Assay Kit to Quantify Cell Proliferation....	88
4.2.9 Immunofluorescence to Investigate Insulin Expression and ECM Interactions...	88
4.2.10 Glucose-Stimulated Insulin Secretion (GSIS) for Functionality Investigation...	89
4.2.11 Statistical Analysis.....	89
4.3 Results and Discussion.....	90
4.3.1 Characterization of Decellularized Bladder Pieces.....	90
4.3.2 Proliferation of INS-1 Cells on Decellularized Bladders.....	94
4.3.3 Functionality of INS-1 Cells.....	99
4.4 Conclusions.....	101

Acknowledgements.....	101
Chapter 5 Characterization of Extracellular Matrix Derived from Decellularized Porcine Organ.....	102
Foreward.....	103
Résumé.....	104
Abstract.....	105
5.1 Introduction.....	106
5.2 Materials and Methods.....	109
5.2.1 Organ Decellularization.....	109
5.2.2 Histological Characterization.....	110
5.2.3 DNA Extraction and PicoGreen Assay for dsDNA Quantification.....	110
5.2.4 Bicinchoninic Acid (BCA) Assay for Protein Quantification.....	111
5.2.5 Digestion of ECM for Mass Spectrometry and Proteomics Analysis.....	111
5.2.6 Mass Spectrometry (LC-MS/MS) for Proteins Identification.....	112
5.2.7 MaxQuant Analysis for Protein Identification.....	113
5.2.8 Polarization Microscopy and Image Analysis for Collagen Fibers Orientation...	113
5.2.9 Data Analysis.....	114
5.3 Results and Discussion.....	115
5.3.1 Decellularization Process.....	115
5.3.2 Characterization of Decellularized Organs.....	118
5.3.3 dsDNA and Protein Quantification.....	121
5.3.4 ECM Composition by Proteomics Analysis.....	123
5.3.5 Collagen Fibers Orientation.....	132
5.4 Conclusions.....	135
Acknowledgements.....	136
Chapter 6 ExtraCellular Matrix from Decellularized Porcine organs as Scaffolds for Insulin-Secreting Cells and Pancreatic Islets.....	137
Foreward.....	138
Résumé.....	139
Abstract.....	141
6.1 Introduction.....	142
6.2 Materials and Methods.....	145
6.2.1 Organs Decellularization.....	145
6.2.2 Culture Setup and INS-1 Cell Culture.....	146
6.2.3 Cell Proliferation Quantification.....	147
6.2.4 Visual Observation of Viable Cells on ECM pieces.....	147
6.2.5 Islet Isolation and Culture.....	148
6.2.6 Insulin and Actin Expression by Immunofluorescence.....	149
6.2.7 Histological Characterization.....	149
6.2.8 Functionality Investigation by Glucose-Stimulated Insulin Secretion (GSIS).....	150

6.2.9 Statistical Analysis.....	151
6.3 Results and Discussion.....	152
6.3.1 Proliferation of INS-1 cells on ECMs.....	152
6.3.2 Functionality of INS-1 cells on ECMs.....	157
6.3.3 Functionality of Pancreatic Mouse Islets seeded on Detergent-free produced Bladder ECM.....	162
6.4 Conclusions.....	166
Acknowledgements.....	167
Chapter 7 Conclusions.....	168
BIBLIOGRAPHY.....	178
APPENDIX A.....	222
APPENDIX B.....	224
APPENDIX C.....	230
APPENDIX D.....	232

LIST OF FIGURES

Figure 2.1: Reaction mechanisms of bioadhesives: a) Cyanoacrylate-based. b) Fibrin-based. c) Chitosan-based. d) BioGlue® Surgical Adhesive (Cryolife Inc.). e) Gelatin-based.....	16
Figure 2.2: Host response towards bioadhesive introduction.....	18
Figure 3.1: Flowchart for medical device regulation according to the FDA. * listed in the exemptions list (21 CFR Parts 862-892).ISO- International Organization for Standardization.....	55
Figure 3.2: Overview of Health Canada regulations for medical devices and examples adapted to bioadhesives.....	67
Figure 4.1: Flowchart of the detergent-based and detergent-free decellularization.....	84
Figure 4.2: Three-dimensional culture system to test intact decellularized bladder pieces.....	87
Figure 4.3: i) Hematoxylin-Eosin (H&E) staining, Alcian Blue and Nuclear Fast Red (AB&NFR) staining and Scanning Electron Microscopy (SEM) pictures of a) Whole native porcine bladders with excised fat and muscle layers, b) Detergent-free decellularized bladder pieces, and c) Detergent-decellularized bladder pieces. The scale bars represent 250 μm . +UT indicates urothelium, *LP indicates lamina propria, ^MU indicates muscle layer. ii) dsDNA content of native, detergent-free-processed (Det-free), and detergent-processed (Det) bladders. Data are presented as means \pm standard errors.....	93
Figure 4.4: MTT staining of a) INS-1 cells on detergent-free-processed bladders (Det-free); b) Detergent-free-processed bladders with no cells (Det-free Ctrl); c) INS-1 cells on SDS-treated bladders (Det); d) SDS-treated bladders with no cells (Det Ctrl). Scale bar represents 1000 μm . e) Quantification of cells using the CyQUANT™ NF Cell Proliferation Assay. Data are presented as means \pm standard errors.....	96
Figure 4.5: Hematoxylin and Eosin (H&E) staining of INS-1 cells cultured for 7 days on detergent-free-processed bladders (Scale bars represent 50 μm for a, b, and c; 250 μm for d and e). The interactions between the ECM and the cells are indicated as black arrows.....	97
Figure 4.6: a) β -actin immunostaining of INS-1 cells. Cell cytoskeleton protruding towards the ECM allows us hypothesizing interactions between the cells and the ECM, as highlighted by white stars. b) Representative images of immunostaining of INS-1 cells on detergent-free-processed bladders for insulin (green) and β -actin (red). Three different samples with 3 images per sample were analyzed. DAPI stained nucleus (blue). Scale bars represent 25 μm	98
Figure 4.7: Functionality of INS-1 cells- validated by a glucose-stimulated insulin secretion (GSIS) assay. S.I. indicates the stimulation index defined as the ratio of insulin concentration secreted at low-glucose to that at high-glucose stimulation. S.I. are represented as means \pm standard deviations.....	100

Figure 5.1: Hematoxylin-Eosin (H&E) staining of native and decellularized porcine organs. Scale bars represent 250 μm . * represents glomerulus, # indicates portal vein, + indicates the alveolar sacs, ^ indicates muscular layer, and \rightarrow indicates lamina propria. Purple-colored nuclei are stained by hematoxylin and ECM in pink by eosin.....	116
Figure 5.2: Alcian Blue/Nuclear Fast Red (AB/NFR) staining of native and decellularized porcine organs. Scale bars represent 250 μm . * represents the glomerulus and \rightarrow represents the lamina propria. The GAGs are coloured in blue, nuclei in red and cytoplasm in pink.....	119
Figure 5.3: Trichrome-Masson staining of native and decellularized porcine organs. Collagen is coloured in blue, nuclei in black, and cytoplasm and muscle fibres in red. Scale bars represent 250 μm	120
Figure 5.4: a-b) dsDNA quantification in native and decellularized organs. c) Protein content in the different ECMs. The protein content has been normalized per mass of wet ECM to compare the protein content of the ECM in its most native form as possible. Also, the ambiguity surrounding the report of dsDNA content normalized to dry mass as reported elsewhere[1], has prompted the normalization per mass of wet ECM.....	122
Figure 5.5: Type IV collagens detected in the decellularized organs: COL4A2, COL4A4, and COL4A5.....	126
Figure 5.6: Laminins detected in the decellularized organs: LAM1, LAMA3, LAMB1, LAMB2, LAMB3, LAMC1, and LAMC2.....	129
Figure 5.7: Other ECM proteins detected in the decellularized organs: Fibronectin 1 (FN1), ExtraCellular Matrix Protein 1 (ECM1), and Elastin (ELN).....	130
Figure 5.8: Venn diagrams of the total number of proteins detected in decellularized bladders, kidneys, lungs, livers, and pancreas. Venn diagrams were prepared using InteractiVenn ©.....	131
Figure 5.9: Percentage relative frequency of orientation of collagen fibers in a) bladders, b) kidneys, c) lungs, d) livers and e) pancreas.....	134
Figure 6.1: Number of INS-1 cells derived from the CyQUANT assay for a) ECMs with no cells, b) 4 hours, and c) 7 days post-seeding of INS-1 cells on ECMs. The statistical analysis was done comparing the detergent-based decellularization to the detergent-free ones. 2-way ANOVA followed by a post-hoc Tukey's multicomparison test was used to analyze significance. **** corresponds to $p < 0.0001$, *** represents $p < 0.001$, ** represent $p < 0.01$, * represents $p < 0.05$ and ns corresponds to non-significant. Bars represent average \pm S.E. Initial cell seeding density is 25,000 cells per well.....	154
Figure 6.2: MTT staining allowing visualizing viable INS-1 cells on decellularized a) detergent-free bladders, b) detergent-free (pH) bladders, c) detergent-free (EDTA) bladders, d) detergent-	

free (pH) kidneys, e) detergent-free (EDTA) kidneys, f) detergent-free (pH) livers, and e) detergent-free (EDTA) lungs.....156

Figure 6.3: Functionality assessed by glucose-stimulated insulin secretion (GSIS) of INS-1 cells seeded on decellularized a) bladders, b) kidneys, c) livers, d) lungs, and e) TCPS. f) Stimulation index in each case (Stimulation index S.I. = concentration of insulin at HG/concentration of insulin at LG1). Ordinary one-way ANOVA with Šidáks multiple comparisons tests was used to determine significance. P<0.05 was significant and indicated by *, p<0.01 indicated by **, p<0.001 indicated by *** and p<0.0001 indicated by ****. TCPS indicates Tissue Culture Polystyrene.....160

Figure 6.4: Immunostaining for insulin (green) and actin (red). INS-1 cells on bladder ECM obtained with the a) bare detergent-free method, b) detergent-free method with pH treatment, and c) detergent-free method with EDTA treatment. INS-1 cells on kidney ECM resulting from d) detergent-free (pH) and e) detergent-free (EDTA) treatments. INS-1 cells on liver ECM produced with the f) detergent-free (pH) method. INS-1 cells on lung ECM obtained from the g) detergent-free (EDTA) treatment. White * indicates focal adhesion points of cells to the ECM. Scale bars indicate 25 µm.....161

Figure 6.5: a) Glucose-stimulated insulin secretion (GSIS) from islets cultured for 48 hours on TCPS and bladder ECM obtained from the bare detergent-free decellularization method. b) Stimulation index of islets. Unpaired t-test was used to determine the significance. ns indicates no significance. Stimulation index = Concentration of secreted insulin at HG / Concentration of secreted insulin at LG1. TCPS refers to Tissue Culture Polystyrene. Bars in the graphs indicate a) Average ± SE and b) Average ± SD.....164

Figure 6.6: Islets cultured for 48 hours on detergent-free decellularized bladder stained by Haematoxylin and Eosin (H&E) (a-d), insulin expression (e-g) and endothelial cells (CD31-positive cells) (h-j). The white arrows indicate the endothelial cells. The islets in panel h correspond to the islets in panel d to highlight the presence and position of the ECM. Black scale bars correspond to 250 µm and white scale bars to 100 µm.....165

LIST OF TABLES

Table 2.1: Advantages and disadvantages of commercially available bioadhesives.....	17
Table 2.2: Inflammatory responses to different bioadhesives.....	22
Table 2.3: Examples of clinical trials associated with commercially available bioadhesives.....	26
Table 2.4: Performance characteristics of commercially available bioadhesives.....	33
Table 3.1: Classes of bioadhesives and examples.....	44
Table 3.2: Performance and biocompatibility tests performed on selected bioadhesives.....	48
Table 3.3: Examples of Class III bioadhesives classified under medical devices and the reported clinical studies and recalls.....	51
Table 3.4: Class II bioadhesives and corresponding tests.....	54
Table 3.5: As of March 2021, user fees related to the FDA services.....	56
Table 3.6: Examples of bioadhesives with licences according to Health Canada.....	62
Table 3.7: As of March 2021, the user application fees related to medical devices, Health Canada.....	63
Table 5.1: Detection of alpha and beta subunits of hemoglobin in the decellularized organs.....	117

ABBREVIATIONS

2D	Two-dimensional
3D	Three-dimensional
AB/NFR	Alcian Blue and Nuclear Fast Red
ANOVA	Analysis of Variance
ASTM	American Society for Testing and Materials
BCA	Bicinchoninic acid assay
BD	Beckton, Dickinson and Company
BSA	Bovine serum albumin
CaCl ₂	Calcium chloride
CAD	Canadian Dollars
CBER	Centre for Biologics Evaluation and Research
CDRH	Centre for Devices and Radiological Health
CE	Conformité Européenne
CFR	Code of Federal Regulations
CHAPS	3-([3-cholamidopropyl]dimethylammonio)-1-propanesulfonate hydrate
CO ₂	Carbon dioxide
COL	Collagen
CPT	Current Procedural Terminology
CSF	Cerebro spinal fluid
CT	Computed Tomography
DAPI	4,6- Diamidino-2-phenylindole, dichloride
Det/D	Detergent-based
Det-free/DF	Detergent-free

DFE	Detergent-free (+EDTA)
DFP	Detergent-free (+pH)
DICE	Division of Industry and Consumer Education
dsDNA	Double-stranded Deoxyribonucleic acid
DTT	Dithiothreitol
ECM	ExtraCellular Matrix
ECM1	ExtraCellular Matrix protein 1
EDTA	Ethylenediaminetetraacetic acid
ELISA	Enzyme linked immunosorbent assay
EMA	European Medicines Agency
EU	European Union
FBR	Foreign body reaction
FBS	Fetal bovine serum
FD & C	Food, Drug and Cosmetics act
FDA	Food and Drug Administration
FDR	False discovery rate
FN	Fibronectin
GAG	Glycosaminoglycan
GCP	Good Clinical Practices
Gel-Ma	Gelatin-Methacryloyl
GLP	Good Laboratory Practices
GMP	Good Manufacturing Practices
GODT	Global Observatory on Donation and Transplantation
GSIS	Glucose-Stimulated Insulin Secretion

H & E	Hematoxylin and Eosin
Hb	Hemoglobin
HBSS	Hanks Buffer Salt Solution
HEPES	(4-(2-Hydroxyethyl)-1-piperazineethanesulfonic acid)
HG	High glucose (28 mM)
HRSA	Human Resources and Services Administration
HSD	Honestly significant differences
IBMX	3-Isobutyl-1-methylxanthine
ICU	Intensive Care Unit
IDE	Investigational Device Exemption
IgG, IgM, IgE	Immunoglobulin G, M and E
IMDRF	International Medical Device Regulators Forum
INS-1	Insulin-secreting rat pancreatic β -like cells
iPSC	Induced Pleuripotent Stem Cells
ISO	International Organization for Standardization
KCl	Potassium chloride
KRBH	Krebs Ringer Buffer with HEPES
LAM	Laminin
LFQ	Label-free quantification
LG1	Low glucose 1 (2.8 mM)
LG2	Low glucose 2 (2.8 mM)
LP	Lamina propria
MDD	Medical Devices Directive
MDR	Medical Devices Regulations

MDSAP	Medical Device Single Audit Program
MeTro	Methacryloyl-substituted Tropoelastin
MgCl ₂	Magnesium chloride
MIN-6	Mouse insulinoma 6
mm Hg	millimetres of Mercury
MS	Mass spectrometer
MTT	3-(4,5-dimethylthiazol-2-yl)-2,5-diphenyl-2h-tetrazolium bromide
MU	Muscle layer
NaCl	Sodium chloride
NaHCO ₃	Sodium bicarbonate
NF-κB	Nuclear factor-kappa B
NHS	n-Hydroxysuccinimide
OC	Office of Compliance
PALS	Pleural Air Leak Sealant
PBS	Phosphate buffered saline
PCI	Phenol, Chloroform and Isoamylalcohol
PEG	Polyethylene glycol
PFA	Paraformaldehyde
PHA	Public Health Agency
PMA	Pre-Market Approval
PMOA	Primary mode of action
PMS	Post-Market Surveillance
PSM	Peptide spectrum match
PTFE	Polytetrafluoroethylene

QMS	Quality Management System
QSR	Quality System Regulations
R&D	Research and Development
RBC	Red blood cell
rpm	revolutions per minute
RPMI	Rosewell Park Memorial Institute medium
RWD	Real-World Data
RWE	Real-World Evidence
S.I.	Stimulation Index
SD	Standard deviation
SDC	Sodium deoxycholate
SDS	Sodium dodecyl sulfate
SE	Standard error
SEM	Scanning Electron Microscope
TCPS	Tissue Culture Polystyrene
TDA	2,4-toluene diamine
TFA	Trifluoroacetic acid
ToC	Table of contents
TSP-1	Thrombospondin-1
USA	United States of America
USD	United States Dollars
USP	United States Pharmacopeia
UT	Urothelium
UV	Ultra-violet

β -actin

Beta-actin

β -cells

Beta-cells

Chapter 1

Introduction

The Global Observatory on Donation and Transplantation (GODT) estimated 144,302 organ transplantations in 2021, out of which kidney transplantation was the most important followed by liver and heart transplantation[2]. Although, procedures in organ transplantation have improved over time, there are certain complications. The Human Resources and Services Administration (HRSA) of the USA has estimated that 17 people die of shortage of organ transplants every day[3]. The quality of the organ for transplantation with the aging population and diseases is of great concern. These grafts are susceptible to ischemia perfusion injury and innate immune-driven tissue damage during organ isolation[4]. Chronic rejection of the transplant due to the recipient's immune response is a conundrum[5]. The increased risks of infections and cancer as side effects of immunosuppression has been researched a lot into recently. To overcome the shortcomings of organ transplantation, tissue engineering was thought to be a solution.

Tissue engineering has emerged recently wherein a whole organ or a part of the tissue could be reconstructed *in vitro* or *in vivo*. Decellularized organs as sources of scaffolds for tissue engineering has gained a lot of research attention owing to the potential of the ExtraCellular Matrix (ECM), a complex mixture of proteins, proteoglycans, glycosaminoglycans (GAGs) that aids in providing a mechanical bioscaffold and biochemical cues for the cells to attach, proliferate and differentiate. Immune rejection associated with transplantation is due to the presence of cellular content. Decellularized organs could quash the organ shortage issue and reduce the number of immune rejections, as the cellular content is removed. Different decellularization techniques have been used to decellularize human, mouse, rat, porcine and bovine tissues that have been recellularized confirming the ability of the ECM to aid in cell attachment, proliferation and functionality[6]. Mechanobiological studies show the significance of scaffold's mechanical properties in recellularization. The advantages of using ECM from decellularized organs as scaffolds to engineer tissue include, being the most native form of ECM, high bioactivity, low immunogenicity, and good biodegradability[7]. However certain challenges associated with using decellularized organs include difficulty to 3D print without solubilization and often complex recellularization strategies using bioreactors. Application-oriented products such as tissue-papers, 3D-printed scaffolds and ECM sheets are already commercialized. Other applications such as bioadhesives-derived from ECM have not been explored extensively.

Surgical intervention is considered an indispensable technique. Staples and sutures are used as gold standards to seal the leak of blood or air. Bioadhesives are used alone or as adjuncts to the standard techniques and have offered multiple advantages. They aid in sealing the leak of blood or air (in case of lung surgeries), in incorporating antibacterial agents and antioxidants, in healing and reduction of post-operative complications[8]. The market share for bioadhesives is currently at 38 billion USD[8]. Although, multiple bioadhesives are already commercialized for internal use, a bioadhesive meant for sealing and regeneration has not been identified. We hypothesized that a bioadhesive incorporating ECM derived from decellularized organs could aid in the repopulation of cells, in tissue regeneration and in reduction of scar formation at the site of application.

This thesis mainly focusses on the characterization of ECMs derived from different porcine organs decellularized by one detergent-based method and by detergent-free ones. Porcine organ decellularization has higher relevance in translational medicine as compared to rat or other subspecies due to the high similarity in the protein biochemical profile with humans and regulatory advantages[9]. Further, the ECMs were investigated *in vitro* for compatibility in recellularization i.e., looking at cell proliferation and functionality. By exploring and understanding the characteristics of the ECMs, a bioadhesive could be derived from ECM and could be potentially used in medicine to not only stop the leak of blood or air but also to regenerate tissues or organs with time.

Chapter 2, entitled “Composition, Host Responses and Clinical Applications of Bioadhesives”, is presenting a review of the scientific literature on the different commercially available bioadhesives and their mechanisms of action. The host responses associated with the bioadhesives, and their individual components are highlighted. In addition, examples of clinical applications and the requirements for bioadhesives to be used for specific applications are detailed.

Chapter 3 entitled “Overview of Approval Procedures for Bioadhesives in the United States of America and Canada” is also a review of the scientific literature. Primarily, the classification of the bioadhesives, the tests to validate them, and the forms to be submitted according to the Food and Drug Administration (FDA) and Health Canada are detailed. Schematic representations, for both FDA and Health Canada, of the steps involved in the regulations are illustrated and the

distinguishing features among the two regulatory bodies listed above. In addition, European regulations are being summarized.

In Chapter 4 entitled, “A Cell Culture System to Investigate the Effect of ExtraCellular Matrix on Insulin-Secreting Pancreatic Cells”, a cell culture system was designed to study the effect of decellularized bladder ECM pieces on insulin-secreting β -like cells from rat. The bladder ECM was extracted using detergent-based and detergent-free decellularization approaches. The cells proliferated on the detergent-free-produced ECM and were functional, as assessed using glucose-stimulated insulin secretion (GSIS).

In Chapter 5 entitled, “Characterization of Extracellular Matrix Derived from Decellularized Porcine Organs”, different porcine organs (i.e., bladders, kidneys, livers, lungs, and pancreas) were decellularized by detergent-based and detergent-free methods. The protein content in the resulting matrices was compared using mass spectrometry and the orientation of collagen fibers was studied using polarization microscopy. The detergent-free decellularizations conserved more proteins, as compared to the detergent-based method.

In Chapter 6 entitled, “Extracellular Matrix from Decellularized Porcine Organs as Scaffolds for Insulin-Secreting Cells and Pancreatic Islets”, the proliferation of INS-1 cells on different organ ECMs was quantified and visualized. The functionality of the cells on the different organs ECMs was verified and primary islets were seeded onto detergent-free decellularized bladder ECM. The primary islets were functional, as confirmed by a GSIS assay.

Finally, Chapter 7 entitled “Conclusions”, consolidates all the experiments, and presents the future scope of the work.

Chapter 2

Composition, Host Responses and Clinical Applications of Bioadhesives

Foreword

Authors and Affiliations:

Vignesh Dhandapani: Ph.D. candidate, Université de Sherbrooke, Département de génie chimique et de génie biotechnologique

Vickie Ringuette: MD, Université de Sherbrooke, Département de chirurgie

Monika Desrochers: M.Sc.A., Université de Sherbrooke, Département de génie chimique et de génie biotechnologique

Marco Sirois: Professor, MD, Université de Sherbrooke, Département de chirurgie

Patrick Vermette: Professor, ingénieur, Université de Sherbrooke, Département de génie chimique et de génie biotechnologique

Date of Submission: February 10th, 2022

State of Acceptance: Published

Journal: Journal of Biomedical Materials Research Part B: Applied Biomaterials

Contribution:

The article comprises a literature review of commercially available bioadhesives as a scope of application to the work done in the thesis. The article is published in *Journal of Biomedical Materials Research Part B: Applied Biomaterials*. The article was written by Vignesh Dhandapani and Patrick Vermette. The section on clinical applications was written by Vickie Ringuette. It was reviewed by Patrick Vermette and Marco Sirois. All the work was done under the guidance and supervision of Patrick Vermette.

Titre en français :

Composition, réponses de l'hôte et applications cliniques des bio-adhésifs

Résumé :

Les bio-adhésifs sont des dispositifs médicaux utilisés pour joindre ou sceller des tissus blessés ou lacérés. Ils sont classés en adhésifs tissulaires, agents d'étanchéité et agents hémostatiques. Les bio-adhésifs tels que FloSeal®, CoSeal®, BioGlue®, Evicel®, Tisseel®, Progel™ PALS, et TissuGlu® sont disponibles commercialement et utilisés cliniquement. Ils peuvent être formulés avec des composants naturels ou synthétiques, ou une combinaison des deux, notamment l'albumine, le glutaraldéhyde, le chitosane, le cyanoacrylate, la fibrine et la thrombine, la gélatine, le polyéthylène glycol (PEG), ainsi que les uréthanes. Chacune de ces formulations possède des propriétés intrinsèques et a été développée et validée pour une application spécifique.

Cet article de synthèse décrit brièvement les mécanismes par lesquels les bio-adhésifs adhèrent aux tissus et met en évidence la corrélation entre leur composition et les réponses potentielles de l'hôte. En outre, les applications cliniques des bio-adhésifs et leurs exigences en matière d'application sont décrites.

Mots clés : Bio-adhésifs ; Agents de scellement ; Agents hémostatiques ; Composition et mécanismes de réaction ; Réponses de l'hôte et biocompatibilité ; Applications cliniques.

Abstract:

Bioadhesives are medical devices used to join or seal tissues that have been injured or incised. They have been classified into tissue adhesives, sealants and hemostatic agents. Bioadhesives such as FloSeal®, CoSeal®, BioGlue®, Evicel®, Tisseel®, Progel™ PALS, and TissuGlu® have been commercialized and used in clinical settings. They can be formulated with natural or synthetic components, or a combination of both, including albumin, glutaraldehyde, chitosan, cyanoacrylate, fibrin and thrombin, gelatin, polyethylene glycol (PEG), along with urethanes. Each formulation has intrinsic properties and has been developed and validated for a specific application. This review article explains the mechanisms by which bioadhesives form adhesion to tissues and highlights the correlation between bioadhesive composition and potential host responses. Furthermore, clinical applications of bioadhesives and their application-driven requirements are outlined.

Keywords: Bioadhesives; Sealants; Hemostatic agents; Composition and reaction mechanisms; Host responses and biocompatibility; Clinical applications.

2.1 Introduction

Bioadhesion can be defined as the adhesion between two components where at least one has a biological origin[10]. Bioadhesives used in clinical applications include tissue adhesives, tissue sealants and hemostatic agents[11]. Adhesive in the term “bioadhesive” indicates any material which is able to polymerize or crosslink[12]. Tissue adhesives are defined as materials, in the form of a patch or a glue, that aid in the wound healing process; examples: intestine, skin, muscle. A hemostatic agent helps in forming blood clots and thereby preventing blood leaks. A sealant is used to seal cracks or gaps in tissues, preventing leakage of fluids or air, as in case of lung surgeries[13,14]. The Food and Drug Administration (FDA) briefly defines the terms tissue adhesives, hemostatic agents and surgical sealants, particularly fibrin sealants, in the Code of Federal Regulations, Title 21, Volume 8, as follows.

1. Tissue adhesives for non-topical use: device employed to adhere vessels and tissues in the body[15].
2. Absorbable hemostatic agents: any device accelerating the clotting process by hemostasis[16].
3. Adjuncts to hemostasis for cases where the bleeding cannot efficiently be controlled by traditional methods such as sutures and ligatures[17].

The broad requirements dictating the development and use of a bioadhesive, as listed in the paper of Spotnitz and Burke[18], include safety, efficacy, usability, cost and approval by regulatory authorities, such as the FDA.

The development of methods to seal wounds is an active field of research at both industrial and academic levels. A report suggests that the global bioadhesive market was valued at 1.40 billion USD in 2016 and is expected to reach around 3 billion USD by 2022[19–21].

The properties and adhesion strength of bioadhesives have been clearly detailed[12]. Bioadhesives used in nanomedicine such as for drug delivery have been presented elsewhere[22]. There are several challenges associated with bioadhesives including biocompatibility, biodegradation, immunogenicity, and performance characteristics for the application indicated. Cost is a significant factor as commercially available bioadhesives are expensive. Future work is directed towards

developing cost-effective bioadhesives and for intricate applications following cranial and gastrointestinal surgeries. Multifunctional bioadhesives such as bioadhesives with self-healing, anti-microbial and hemostatic capacity are researched extensively.

The aim of this review is to summarize, from the scientific literature, the established published correlations between the types of bioadhesives and their clinical applications. A first section lists the primary composition and brief reaction mechanisms of the main bioadhesives found both at the R&D and clinical stages. From this, we highlight and present in the following section, the host responses of the individual components used to formulate only those bioadhesives with evidenced clinical usage, with an aim to depict their potential positive and adverse effects on the host. Finally, the last part aims at presenting the clinical applications of commonly used bioadhesives and properties justifying their usage for the targeted application.

2.2 Bioadhesive Classification and Reaction Mechanisms

This section briefly presents the classification and the reaction mechanisms of bioadhesives available on the market, under R&D or in clinical phases.

Bioadhesives are usually made from a mixture of different components. Firstly, they contain a functional group-bearing compound to induce tissue adhesion and a support to carry this reactive molecule. The latter, in most cases, is made of a protein scaffold or a polymer hydrogel. Adhesion between polymers or proteins in the bioadhesive and the host tissue can occur through covalent bonds as well as through van der Waals, hydrogen bonding, hydrophobic, and/or electrostatic interactions[23].

Basic properties of a bioadhesive include[23]:

1. Safe, sterilizable, non-toxic exhibiting no allergic or histo-toxic reactions.
2. Easily formulated in wet environments at body temperature.
3. Adhesion and, when applicable, acceptable degradation.
4. Cohesion strength in accordance with the application.
5. Preparation time suitable for surgeons.
6. Gelation time suitable for the application.

7. Good adhesion strength.
8. Acceptable shelf life and preferably colored for visualization to facilitate their application.
9. Acceptable swelling index and good elasticity in compliance with the host tissue or organ.
10. Optimal burst pressure and elastic modulus suited for the application.
11. Promoting, or at least not interfering with, tissue repair (or in some cases regeneration).
12. Cost effective and easily available.

Hydrogels form a category of bioadhesives. They are defined as hydrophilic polymer networks that can absorb up to thousands of times their dry weight in water[24]. When used as temporary scaffold, hydrogels can aid the wound healing process by acting as a transient support up to tissue repair[25]. Hydrated adhesives have certain biological advantages by absorbing serous fluid secretion of the wound and keeping the site moist for faster healing[26]. Hydrogels have been extensively used in the preparation of matrices in tissue engineering and have been described elsewhere[27,28].

Bioadhesives can be categorized as synthetic or natural, depending on their composition. See the two sections below for definition and classification.

2.2.1 Synthetic-derived bioadhesives

Synthetic-derived bioadhesives are made solely of synthetic molecules or contain synthetic components. They are formulated with synthetic polymers as a backbone functionalized with reactive groups and are crosslinked or coated using a non-natural cross-linker. The most common synthetic bioadhesives include polyurethane-, polyethylene glycol- and cyanoacrylate-based formulations.

- Cyanoacrylate-based adhesives (e.g., Histoacryl®[29], Dermabond®[30], Indermil™, Glubran 2®[31]) have been on the market for almost four decades now. They contain alkyl-2-cyanoacrylate monomers, which polymerize by an exothermic reaction on exposure to nucleophilic species, such as hydroxyl groups (in the exudate), at room temperature (Figure 2.1a). Most used alkyl groups are n-butyl and octyl groups. The alkyl group influences the properties of polymerization. Longer alkyl groups result in more flexible formulations.

- PEG-based hydrogels consist of chemically functionalized branched or linear PEG molecules. The crosslinking is commonly achieved either by chemical crosslinking or photo-polymerization. CoSeal® (Baxter Inc.)[32] is an example of PEG-based bioadhesive consisting of two PEG fragments, one with a thiol terminal group and the other one with a succinimidyl ester. On mixing, the carbonyl group of the succinimidyl ester reacts with the thiol group forming a covalent thio-ester linkage hence polymerizing. N-hydroxysuccinimide (NHS)-esters modified PEGs in commercially available bioadhesives, such as Duraseal® Dural Spine Sealant (Integralife Inc.)[33] and Progel™ Pleural Air Leak Sealant[34], react with the available proteins, human serum albumin and trily sine, respectively, forming covalent bonds.
- Polyurethane-based bioadhesives (TissuGlu®, Cohera Medical Inc.[35]) consists of a hyperbranched polymer with isocyanate end groups. The isocyanate group reacts with the amine group of the tissue by forming urea. Simultaneously, the crosslinking is achieved as a result of contact of the isocyanate group with water molecules from the body[36].

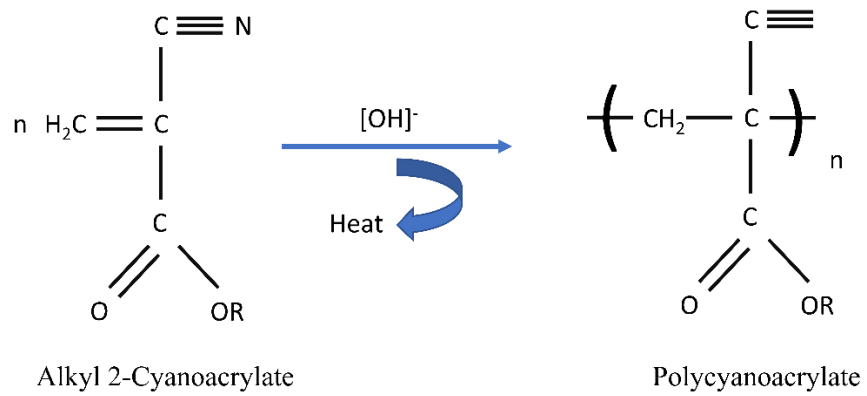
The advantages of synthetic polymers include a better control over the mechanical, material and adhesion properties based on the application. However, biocompatibility has been a concern with some synthetic bioadhesives. At times, there is a need for ultra-purification methods to avoid traces of toxic chemicals in the formulations, such as oxidizing agents. Cyanoacrylates have been known to result in toxic degradation products such as formaldehyde that can cause tissue inflammation, delayed wound healing, cytotoxicity, carcinogenicity and even cell death[37,38].

2.2.2 Naturally-derived bioadhesives

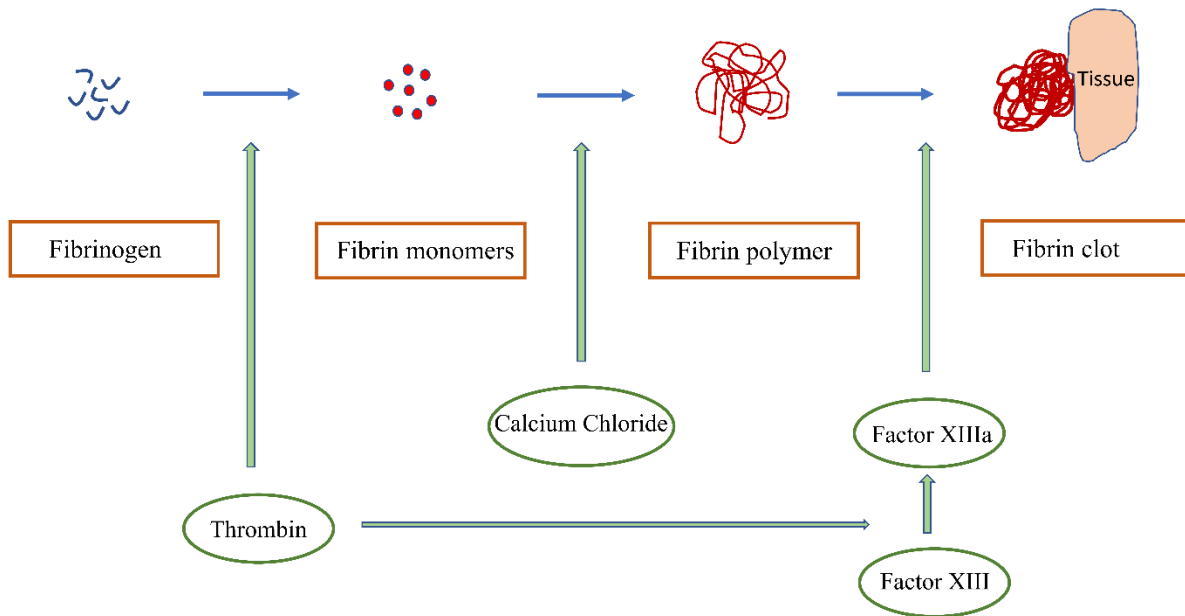
Naturally-derived bioadhesives are extracted purely from biological sources such as human blood, proteins from animal origin (porcine or bovine) or involve an active component (usually crosslinkers like aldehydes), which have been used in combination with animal proteins. A broad classification of naturally-derived bioadhesives include those containing fibrin, chitosan and animal proteins (albumin and gelatin).

- Fibrin sealants (e.g., Tisseel®[39], CryoSeal FS®[40], Evicel®[41], Vitagel™ [42]) function by mimicking the final step of the blood clotting cascade. Thrombin converts fibrinogen into fibrin forming a polymer, as shown in Figure 2.1b. Simultaneously, in the presence of calcium chloride, factor XIII is transformed into factor XIIIa, which stabilizes the clot by creating amide bonds. Often, antifibrinolytic agents such as aprotinin are used to prevent fibrinolysis of the clot. This makes those products expensive.
- Chitosan-based bioadhesives (Chito-Seal™ [43], HemCon Bandage Pro® [44], Syvek Patch® [45,46], BST-Cargel® [47]) contain cationic chitosan. The presence of cationic charges sequesters anionic components such as platelets and clotting factors, activates factor XII and thereby, forming a clot by activating the clotting cascade, as shown in Figure 2.1c.
- BioGlue® Surgical Adhesive (Cryolife Inc.), a surgical sealant approved for use by the Food and Drug Administration (FDA) in 2001, consists of 45% purified bovine serum albumin (BSA) and 10% glutaraldehyde[48]. It has been approved for use in cardiac, thoracic and vascular procedures. By applying it to tissues, the glutaraldehyde acts as a crosslinker forming covalent bonds with the BSA and the tissue proteins, as depicted in Figure 2.1d.
- Gelatin-based bioadhesives (e.g., Gelatin-Resorcinol-Aldehyde glue)[23] consists of gelatin, a biocompatible and biodegradable component. The amine groups in gelatin are crosslinked with the amine groups of the tissue in the presence of aldehyde, as shown in Figure 2.1e. Performance on wet tissues is improved by the addition of a stabilizing agent like resorcinol. MeTro[49], a recently developed bioadhesive, consists of methacryloyl-substituted tropoelastin (MeTro) and gelatin methacryloyl (Gel-MA). A photo-initiator on eosin-Y is responsible for the photo-crosslinking of MeTro and Gel-MA.

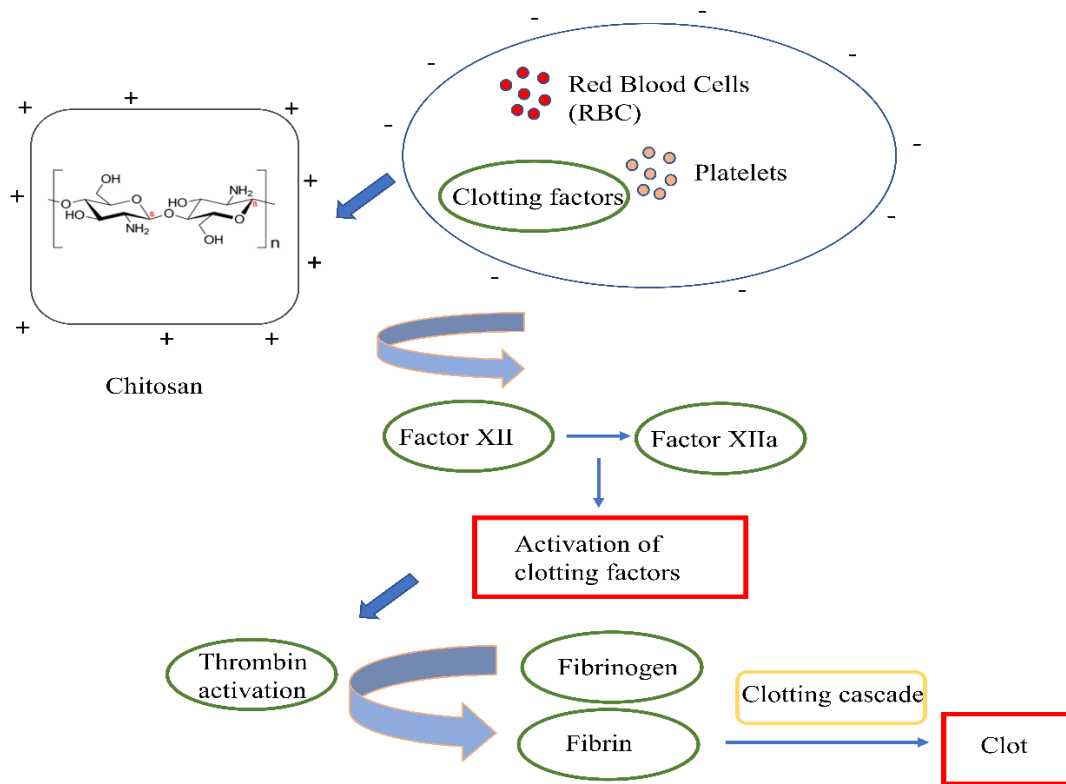
The primary advantages of natural bioadhesives are their good biocompatibility, a degradation resulting into less toxic products and a better elimination from the body. The disadvantages associated with those medical devices are their often poor mechanical properties, possible variations between batches, degradation rate inside the host and poor adherence to wet tissues[38]. The advantages and disadvantages of commonly used, commercially available bioadhesives are summarized in Table 2.1.



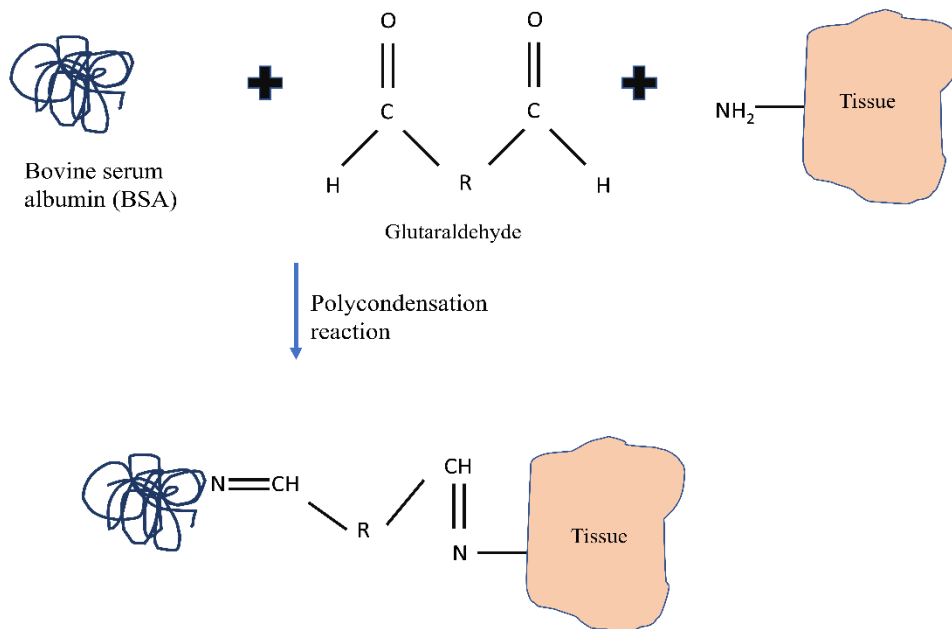
a) Cyanoacrylate-based bioadhesives



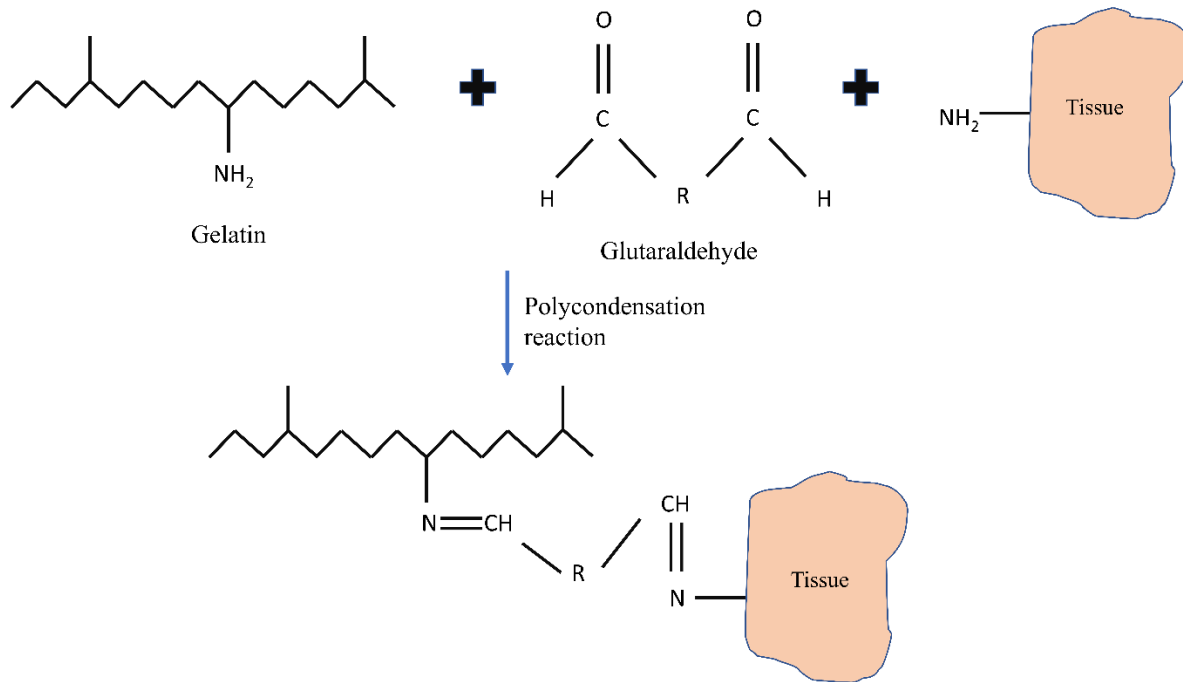
b) Fibrin-based bioadhesives



c) Chitosan-based bioadhesives



d) BioGlue® Surgical Adhesive



e) Gelatin-based bioadhesives

Figure 2.1 Reaction mechanisms of bioadhesives: **a)** Cyanoacrylate-based. **b)** Fibrin-based. **c)** Chitosan-based. **d)** BioGlue® Surgical Adhesive (Cryolife Inc.). **e)** Gelatin-based.

Table 2.1 Advantages and disadvantages of commercially available bioadhesives.

Bioadhesive	Advantages	Disadvantages
Progel™ PALS, BD	Works within 8 seconds, Withstands higher pressures (160±15 mmHg)[50].	Requires refrigeration for storage, Faster degradation following application[51].
Tisseel®, Baxter Inc.	Excellent biocompatibility, low toxicity (detailed in Chapter 3).	Mechanical strength reduction in the presence of a wet environment[52,53], Longer preparation time, slow curing, poor bonding strength, complex preparatory procedures[54], risk of disease transmission[55].
BioGlue® Surgical Adhesive, Cryolife Inc.	Short curing (20 to 30 s), gelation time (within 2 minutes)[56], mechanically strong sealant.	Glutaraldehyde cytotoxic effects, adhesive embolism, tissue compression, need for protection of the surrounding tissue[13].
CoSeal®, Baxter Inc.	Rapid curing and short degradation times[51], weakly toxic.	Stability, weak adhesion to the surrounding tissue and swelling[50].
Omnex™ Ethicon Inc.[57]	Adequate adhesive strength for tissues (Table 2.4), easy to use.	Internal usage can result in necrosis, infections and inflammation[58].
DuraSeal® Sealant System, Integralife Inc.	Longer mean time for leak recurrence[59], shorter time of stay[60] in sealing Cerebro Spinal Fluid (CSF) leaks post posterior fossa surgery.	Swelling on the uptake of water resulting in spinal cord compression[61].
TissuGlu®, Cohera Medical Inc.	Good adhesion strength.	Longer curing time.

2.3 Bioadhesive Host Responses

Biocompatibility of a material is defined as its capacity to elicit a desired host response for a specific application[62]. The introduction of a bioadhesive in the body generates a sequence of reactions as the body recognizes it as a foreign material. The sequence of host reactions to bioadhesives is as shown in Figure 2.2.

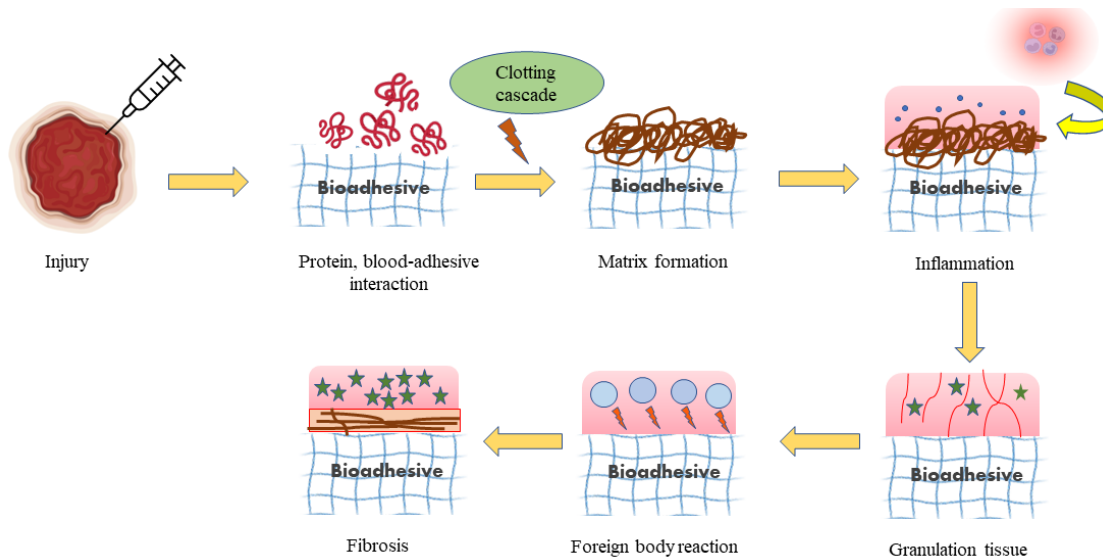


Figure 2.2 Host response towards bioadhesive introduction. 1st step indicates the introduction of bioadhesive at the injury site. 2nd step shows that the proteins (red) and blood interact with the bioadhesive. 3rd step indicates the matrix formation following clotting cascade. The 4th step shows the onset of inflammation. The 5th shows the granulation tissue formation with new blood vessels (red) formed by the fibroblasts (green star). The 6th step depicts the presence of foreign body multinucleated cells (blue) secreting enzymes to engulf or degrade the bioadhesives. The final step illustrates the formation of a fibrotic scar tissue due to the synthesis of extracellular matrix (ECM) by the proliferating fibroblasts (green star).

2.3.1 Overview of the steps in wound healing at the site of bioadhesive application

The introduction of a bioadhesive causes proteins, cells and fluids from the vascular system to rush to the site by a process named “exudation”. The exudate is known to provide the moisture and keeps the injured site always wet, thereby enhancing the healing process[63]. The provisional

matrix is formed by the culmination of a blood clotting cascade that activates the fibrin-fibronectin complex. Platelet activation aids in fibrinogen binding thereby activating a specific matricellular protein called thrombospondin-1 (TSP-1)[64]. Onset of the inflammation reaction occurs due to the complement system, vasoactive agents, kinin system, growth factors, cytokines, etc. The release of cytokines enables the initial recruitment of neutrophils[65]. Following this, monocytes differentiate into macrophages at the site. The neutrophils and macrophages are involved in a process called phagocytosis. Granulation tissue formation is initiated by fibroblasts and vascular endothelial cells[66]. The process called “neo-vascularization or angiogenesis” begins wherein, the existing blood vessels give out new blood vessels by the process of budding. Fibroblasts are involved in the synthesis of collagen and proteoglycans. Type III collagen dominates the formation of granulation tissue and forms the fibrous capsule. Myofibroblasts are involved in wound contraction and can also aid in secretion of an organized extracellular matrix (ECM)[67]. Foreign body reaction (FBR) is elicited by the macrophages, fibroblasts and capillaries. FBR cellular content depends on the topography and the geometry of the biomaterials involved[68–70]. The biomaterials surface-to-volume ratio is found to influence the composition of the FBR. Larger surface-to-volume ratios (e.g., fabrics, microspheres) have larger numbers of macrophages and Langhans giant cells[71]. The process of repair at the implant site depends on the capacity of the existent cells and the persistence of the ECM framework[62]. Myofibroblasts and fibrocytes play an important role in the formation of collagenous fibers, the principal component of the fibrous capsule[72].

2.3.2 Host responses towards bioadhesives

Bioadhesives generally consist of mixtures of different components, as outlined in Section 2. It is therefore important to understand how the host responds to the individual components used to formulate those medical devices. Synthetic bioadhesives generally have stronger adhesion strength but often result in degradation products or are associated with extensive swelling[73].

Bovine serum albumin (BSA) is the protein component of BioGlue® (referred to as only BioGlue® hereafter in the text). It is an allergen and causes immunogenic reactions in various cases. The responses reported include elevated levels of IgG/IgM[74,75] and IgE[76] compared to

normal levels (7-15 g/L for IgG, 600-3000 mg/L for IgM and 3-423 kIU/L) as well as allergic β and T cell response[77]. The crosslinking component of BioGlue® i.e., glutaraldehyde, being an aldehyde on its own, is highly cytotoxic[78–81], results in increased antibody response, inflammation and necrosis[82]. An interesting study evaluating the toxicity of glutaraldehyde has been reported. Acute peroral toxicity of glutaraldehyde in rats showed slight toxicity for concentrations until 5% and moderate toxicity over 5%. The acute percutaneous toxicity was evaluated in rabbits indicating slight toxicity until 25% concentration and moderate for 46%-50% concentrations. The tolerance level and toxicity of glutaraldehyde varied according to the concentration, application, and the model organism under study[83].

Polyurethanes are a family of polymers synthesized by polyaddition reactions of the diisocyanates and diols. Different types of polyurethanes exist of which, aromatic and aliphatic isocyanates with different polyether/polyester diols are used to formulate tissue adhesives[84,85]. Application of polyurethanes as stents in urethral applications have resulted in calcification[86]. A few *in vivo* studies analyzing the biocompatibility of polyurethanes have revealed that polyurethanes results in moderate inflammation, no necrosis and no lesion[87,88]. The breakdown product of certain polyurethanes (especially polyurethanes produced using toluene diisocyanate) , 2,4-toluene diamine (TDA), was long considered to be carcinogenic[89,90].

The toxicity of cyanoacrylates has been suggested to be through two ways. The first one is, low tissue adsorption of cyanoacrylates resulting in macrophages and polymorphonuclear cells infiltration trying to absorb the cyanoacrylate crystals. Cyanoacrylate is scavenged by macrophages, resulting in phagocytosis and lysozyme degranulation, ultimately leading to tissue necrosis[91]. Acrylate monomers and toxic breakdown products of cyanoacrylate i.e., formaldehyde and cyanoacetate[92], react with free radicals and lipids and form lipid hydroperoxide. This results in ischemia, tissue damage and necrosis[91]. Butyl-2-cyanoacrylate has been associated with significant inflammation and foreign body response[93]. The toxicity of cyanoacrylates has been reported elsewhere[94,95]. Increasing the length of the alkyl side chain of the cyanoacrylate has been associated with decreasing level of toxicities[96–98].

PEG is weakly toxic and immunogenic[99]·[100] and results in anti-PEG IgM[101]. The problem associated with PEG-based bioadhesives is that they swell upon administration resulting in adverse responses[50]. Several techniques such as copolymerization, use of clay fillers, thermos-

responsive moieties and hydrophobic motifs could be added to control the swelling properties[73,102].

Natural components such as fibrinogen, thrombin, chitosan, gelatin and factor XIII are generally considered biocompatible because of their origin. The different biocompatibility tests performed to prove the safety and effectiveness of various bioadhesives as required by the regulatory agencies are detailed in Chapter 3. The source of the component could be a significant factor, as it could result in cross-reactive immune responses. Fibrinogen is naturally present in the blood and, in the presence of thrombin, results in fibrin thereby forming a clot. It is considered biocompatible[103]. Antimicrobial activity[104], osteogenic capacity and angiogenesis[105] have been observed with the use of fibrinogen. Factor XIII enhances clot strength, fibrinolysis as well as it results in no adverse responses or anti-Factor XIII antibody production[106]. Thrombin is a serine protease and is formed from the precursor prothrombin. As mentioned above, fibrinogen in the blood is converted to fibrin and this happens in the presence of thrombin, thereby producing a clot. Bovine thrombin was found to be associated to antibodies against coagulation factors and could lead to bleeding on multiple exposures[107,108].

Chitosan aids in ECM regeneration, production of cytokines, cell migration and in granulation tissue formation[109]. Chitosan is also associated with mild-to-moderate inflammatory reactions resulting in accumulation of macrophages and eosinophils (disease-fighting white blood cells)[110–112].

Gelatin is a biocompatible, biodegradable and denatured form of collagen. Increased levels of IgE antibodies[113,114], no inflammatory cell responses and cellular damage were observed with gelatin[115]. Gelatin has been associated with mild inflammatory reactions and anaphylaxis (severe allergic reaction)[116] prior to degradation.

Table 2.2 gives a brief understanding of the inflammatory reactions exhibited by commercially available bioadhesives.

Table 2.2 Inflammatory responses to different bioadhesives.

Bioadhesive	Model	Host responses
No Evident Inflammation		
Tisseel®, Baxter Inc.	Primate brain parenchyma model[117]	Does not induce inflammation
Floseal®	Rat peritoneal injection model[118]	No abnormal or unexpected response
TissuGlu®, Cohera Medical Inc.	Canine abdominoplasty model[36,119]	No cellular response and no accumulation of: macrophages, multinucleated giant cells and seroma formation
CoSeal®, Baxter Inc.	Rabbit subcutaneous and carotid artery model[120]	Compatible with the biological tissue
Mild-to-Moderate Inflammation		
CoSeal®, Baxter Inc.	Canine iliac PTFE-graft model[121]	Moderate-to-marked inflammation at day 7 followed by a mild-to-moderate response at day 30
	Rabbit aorta suture model[122]	Mild B cell infiltration seen in certain samples
BioGlue® Surgical Adhesive, Cryolife Inc.	Sheep aortic repairs[123]	Lack of fibrotic response and multinucleated giant cells
Tisseel®, Baxter Inc.	Spinal cord surgery in rats[124]	Extensive acute inflammation at day 7 turned to be mild at day 28 with mild lymphocyte infiltration
	Colorectal anastomotic procedures in diabetic rat model[125]	Increased collagen and fibroblast formation
ProGel™ PALS, BD	Rat lung air leak model[126,127]	Presence of foreign body giant cells, macrophages and invasion of capillaries
Omnex™ Ethicon Inc.	Rodent intraperitoneal[57]	Mild-to-marked macrophage response
	Ovine venotomy animal study[57]	Minimum-to-moderate pyogranulomatous inflammation
	Rodent subcutaneous implantation[57]	Minimum-to-mild chronic granulomatous inflammation/fibrosis
Moderate-to-Severe Inflammation		
Floseal®	Human trial[128]	IgE-mediated allergic reaction, accumulation of eosinophil-rich inflammatory cells, fibrosis and granulation tissue
BioGlue® Surgical Adhesive, Cryolife Inc.	Rabbit aorta suture model[122]	Increased infiltration of eosinophils and severe infiltration of B cells, lymphocytes and plasma cells
	Spinal surgery[129]	Severe acute inflammation with multiple granulocytes and histiocytes surrounding the BioGlue® site
	Rabbit partial lung resection and liver abrasion model[130]	The released glutaraldehyde (approx. 200 µg/mL) caused high grade inflammation, edema and necrosis
	Rat hernia mesh fixation model[131]	Granuloma formation with severe inflammation resulted in abscess formation
Omnex™ Ethicon Inc.	Ovine graft study[57]	Moderate-to-chronic reaction within 2 to 4 weeks and reduced to mild reaction at 6 and 18 months

From Table 2.2, BioGlue® and Omnex™ cause mostly moderate-to-severe inflammatory reactions. Both are composed of toxic initiators and byproducts. This could be the reason for the severe reactions. Whereas fibrin-based sealant (Tisseel®) and PEG-based (Progel™, CoSeal®) resulted in either no or mild inflammatory reaction. This could be attributed to the natural components of fibrin glue or PEG being weakly toxic. Fibrin adhesives have been shown to be effective, as it is suspected to trigger the body clotting mechanism and eliminating the effect of synthetic components on the immune response. The synthetic adhesive prevents the leaks by forming a mechanical barrier. The primary advantage of synthetic adhesives is that their physical and chemical properties could be fine-tuned based on the application. The host responses exhibited by bioadhesives is a crucial factor in deciding their applications.

2.4 Applications

Sutures and staples are the most used techniques to close and seal wounds during and after surgery. Although sutures have been applied for centuries and are still used largely owing to their efficacy, ease of application and costs, some intricate applications have raised the need for additional sealing techniques. Rare complications related to the use of sutures include: granule formation, chronic wound complications, extended duration to achieve wound closure, extensive pain during application in case the patient is awake and the need to manually remove them after healing, in some cases[132,133]. Moreover, sutures may have limited uses with fragile tissues such as pulmonary parenchyma. Their utility can be limited as in the case of trying to suture the posterior part of a vessel and on very small wounds.

In terms of their clinical applications, bioadhesives can be divided into two distinct categories. These include bioadhesives for topic application, known as extracorporeal adhesives (for example, superficial skin glue) and those applied directly on internal body tissues, known as intracorporeal adhesives. The latter is of higher interest in the surgical field and will be the central theme of this section.

Bioadhesives are associated with reduced pain on application, do not need removal and permit faster wound closure, thus, decreasing the risk of bleeding and infections. Also, tissue adhesives are easy to apply, allowing them to be used in wounds that are difficult to access. Due to their

physical properties, bioadhesives can also be used on brittle tissues and on microscopic wounds[134].

The differences between standard sutures and adhesives have been analyzed. Firstly, cosmetic outcomes are important characteristics compared to surgeries where the appearance of the wound is substantial. This feature was studied in randomized clinical trials like breast surgery for benign breast lump, repair of cutaneous and subcutaneous lacerations on children or repair of maxillofacial incisions[132,135,136]. Bioadhesives and sutures had comparable results in terms of cosmetic outcomes. Consequently, the choice of sutures or adhesives should not depend on this characteristic.

Secondly, bioadhesives have been reported equivalent to sutures for certain postoperative complications. For example, in endodontic surgical procedures like apicoectomy, less postoperative inflammation and better clinical and histological healing were associated with the use of cyanoacrylate-based adhesives in comparison to silk sutures. There was no significant statistical differences between complications of those two methods in circumcision surgeries and in the repair of herniotomy wound[137,138].

2.4.1 Clinical applications

Clinical applications of bioadhesives play an important role in classifying the adhesive for specific purposes and body parts, since organs have different architectures and characteristics. Overall, clinical studies demonstrate that adhesives are safe for the indicated conditions.

FloSeal® is a gelatin-based hemostatic sealant used to control bleeding in surgical procedures where conventional hemostasis methods prove inefficient or non-feasible. According to Baxter, based on a prospective randomized controlled trial comparing the use of FloSeal® to a gelatin sponge with thrombin, anemia, atrial fibrillation, infection and hemorrhage were the most common adverse events noted during or after the use of FloSeal®.

CoSeal® is a polyethylene glycol (PEG)-based adhesive used to control bleeding in the vascular area as an adjunct for mechanical sealing.

BioGlue® is a surgical adhesive composed of bovine serum albumin and glutaraldehyde used to control bleeding in open surgical repair of large vessels as an adjunct to standard methods of achieving hemostasis such as sutures and staples.

Evicel®, a fibrin sealant, is used to achieve hemostasis when standard surgical techniques are inefficient. Tisseel® like Evicel® is also indicated for use as an adjunct to hemostasis. Its main uses are in conventional surgical techniques, during surgery for trauma of solid organs and as an alternative to sutures in hernia mesh fixation.

Progel™ PALS, a human albumin serum and PEG-based adhesive, is used mostly to control postoperative air leaks after a thoracic surgery. Finally, TissuGlu® is a surgical adhesive intended to be used in abdominoplasty and mastectomy for the approximation of tissue layers and to prevent fluid accumulation.

Some of the commercially available bioadhesives and their clinical applications are presented in Table 2.3.

Table 2.3 Examples of clinical trials associated with commercially available bioadhesives.

Commercial Bioadhesives	Clinical Trials	Clinical Outcomes
FloSeal®, Baxter Inc.	Hemostasis in cardio-vascular surgeries [139][140][141]	<ul style="list-style-type: none"> • Hemostasis in more patients with FloSeal® than in the control group with a gel foam with thrombin at 3 minutes. • Cessation of bleeding within 10 minutes of the first lesion was higher with FloSeal® than in the control group for cardiac surgeries and vascular surgeries. • FloSeal® led to less postoperative bleeding, lower rate of transfusion of blood products. • Rates of revision for bleeding and minor complications were not different.
	Hemostasis in spinal surgeries [139][142][143][144]	<ul style="list-style-type: none"> • Hemostasis achieved in more patients with FloSeal® than with a gel foam+thrombin at 3 minutes. • Cessation of bleeding within 10 minutes of the first lesion was higher with FloSeal® than in the control group for the spinal or orthopedic surgeries. • With FloSeal®, decreased risk of blood product transfusion, shorter surgery time and decreased product usage in spine surgeries compared to control group (Surgiflow, a flowable gelatin matrix with thrombin). • Risk of complications and hospital length of stay did not differ. • No difference in time to hemostasis between FloSeal® and Surgiflow for patients under laminectomy or laminarthrectomy with a bleeding not responding to standard hemostatic techniques.
	Hemostasis in neurosurgical surgery [145]	<ul style="list-style-type: none"> • Shorter surgery duration, lower estimated blood loss, shorter hospital stays, fewer intensive care unit days and shorter time-to-recovery with FloSeal® than with the local bleeding control guidelines. • No patient with FloSeal® required blood transfusion compared to the control, where in 5 units of blood were administered.
	Hemostasis in ear-nose-throat (ENT) surgeries [146][147][148]	<ul style="list-style-type: none"> • Hemostasis successful in all the application sites and no reported intraoperative complications during endoscopic sinus surgery. • Use of FloSeal® during thyroidectomy showed reduction of the mean operating time and an earlier wound drain removal, resulting in shorter postoperative hospital stay. • No difference of postoperative morbidity between the two groups. • During tonsillectomy, improved wound healing, a trend for less postoperative pain, a shorter duration of pain-medication use and reduced pain-medication consumption/demand associated with the use of FloSeal®.
	Hemostasis in laparoscopic cholecystectomy [149]	<ul style="list-style-type: none"> • Shorter operating time and lower intraoperative complications rate with FloSeal® (differences not significant). • Conversion rate in laparotomy lower with FloSeal®. • Time to drain removal and length of hospital stay were not different.
	Hemostasis in robot-assisted laparoscopic radical prostatectomy [150]	<ul style="list-style-type: none"> • Blood transfusion rate decreased with FloSeal® compared to control group. • FloSeal® was associated with improvements in the difference between the immediate postoperative hemoglobin (Hb) and post-operative day 1 Hb levels as well as between the mean immediate postoperative Hb and least Hb levels.
CoSeal®, Baxter Inc.	Hemostasis in vascular surgeries [151]	<ul style="list-style-type: none"> • Immediate anastomotic sealing after an implantation of polytetrafluoroethylene grafts was done in more patients with CoSeal® than with an absorbable gelatin sponge soaked in thrombin. • Cessation of bleeding within 10 min. was equivalent between CoSeal® and the control. • The median time to stop bleeding in controls was longer than with CoSeal®.

	Hemostasis in cardiac surgeries [152]:[153]	<ul style="list-style-type: none"> • CoSeal® reduced intraoperative and postoperative transfusion requirements of red blood cells and fresh frozen plasma as well as postoperative bleeding within 48h at the anastomotic closure of the aorta in Bentall procedure. • Shorter length of stay in the intensive care unit and in the hospital with CoSeal®. • No difference in the rethoracotomy between the 2 groups. • Extent of pericardial adhesion and adhesion tenacity during the second sternotomy operation were lower with CoSeal® after a surgical correction of congenital heart malformations through median sternotomy.
	Postsurgical drainage and lymphocele formation after axillary surgery for breast cancer [154]	<ul style="list-style-type: none"> • No difference noted with CoSeal® with a vacuum drain compared to vacuum drain alone, in terms of drainage on postoperative day 4, total drainage, days to drain removal, and hospitalization duration.
	Control of air leaks after thoracic surgeries [155]:[156]:[157]:[158]:[144]	<ul style="list-style-type: none"> • After lung resection, CoSeal® group had a lower incidence of air leaks and prolonged air leaks compared to the use of staples/sutures alone. • The duration of drainage and the mean length of hospital stay were shorter with CoSeal® than with the control.
BioGlue® Surgical Adhesive, Cryolife Inc.	Hemostasis in cardiac surgeries [159]:[160]:[161]:[162]:[163]:[164]	<ul style="list-style-type: none"> • In aortic anastomosis after an acute aortic dissection, BioGlue® had a tendency for a shorter circulatory arrest time. • BioGlue® had less bleeding and a tendency to receive less units of blood cells. • Even when studies showed no differences in the length of stay in the ICU, the total length of hospital stay was shorter with BioGlue®. • No differences in term of risk of reoperation, stroke, hemothorax, mediastinitis, wound infection and early or late mortality between both groups. • For reinforcement of thoracic aortic suture lines, bleeding control and obliteration of the false lumen in aortic dissection, BioGlue® had a lower mortality rate compared to a control (as a perioperative complication or in long-term follow-up). • No perioperative death and no evidence of systemic embolization or neurologic complications when BioGlue® was used for reinforcement of suture line and bleeding control during repair of intracardiac structural defects.
	Control of air leaks after thoracic surgeries [165]:[166]:[167]:[168]	<ul style="list-style-type: none"> • After a thoracotomy, the mean duration of air leaks, the intercostal chest drainage and the length of hospital stay were shorter with BioGlue®. • No difference between BioGlue® and Peri-strips® or Vivostat® groups in terms of median duration of air leaks or intercostal drainage duration after lung resection.
	Hemostasis in open nephron-sparing surgery at the tumor-bed site [169]	<ul style="list-style-type: none"> • Reduced mean estimate blood loss leading to lower transfusion rate with BioGlue®. • A correlation was found between estimated blood loss and transfusion rate and date of surgeries.

	Sealant for dura mater during neurosurgical procedures [170]	<ul style="list-style-type: none"> • Post-surgical cerebrospinal fluid leak rate of 0.93% using BioGlue® was lower than the incidence reported in the literature (2.7% to 6%).
	Hemostasis and sealing in hemorrhoidopexy [171]	<ul style="list-style-type: none"> • Less anastomosis leaks with BioGlue®. • With the overall complications, less were observed with BioGlue®.
Evicel®, Ethicon Inc.	Hemostasis in vascular surgeries [172]	<ul style="list-style-type: none"> • Hemostasis in polytetrafluoroethylene-ethylene arterial anastomoses within 4, 7 and 10 min. from the intervention was higher with Evicel® than with the control using manual compression alone. • Lower incidence of treatment failure with Evicel®. • No differences between Evicel® and the control in terms of complications related to bleeding such as anemia, haematoma or increased sanguineous drainage.
	Overall healing at the osteotomy site after rhinoplasty [173]	<ul style="list-style-type: none"> • Lower bruising and swelling with Evicel® on postoperative days 1 and 7. • On postoperative day 21, bruising was lower, but swelling was not different. • There was no difference between both sides in terms of pain and overall rate of recovery on postoperative days 1, 7 and 21.
	Hemostasis in laparoscopic sleeve gastrectomy [174]	<ul style="list-style-type: none"> • No differences in hemoglobin levels between the Evicel® group and the control. • No differences in drainage volume (first 24h), number of patients who received packed cell and late infected hematoma.
	Hemostasis in total knee arthroplasty [175]	<ul style="list-style-type: none"> • No difference in blood volume loss between the Evicel® group and the control. • Transfusion rate was not significant.
	Control of air leaks after a pulmonary resection [176]	<ul style="list-style-type: none"> • Less air leaks with Evicel® on immediate postoperative, postoperative days 1, 3 and 7.
	Sealing in pterygium surgery with conjunctival autograft [177]	<ul style="list-style-type: none"> • Fashioning and repositioning of the conjunctival autograft were shorter with Evicel® than the control. • Pain level was lower with Evicel®. • No significant differences in recurrence rate, change in logarithm of the minimum angle of resolution and in surgically-induced refractive change.
	Hemostasis after a thyroidectomy or hemithyroidectomy [178]	<ul style="list-style-type: none"> • Less drainage output and drainage time in the total thyroidectomy subgroup with Evicel®. • Hospital lengths of stay in this subgroup were not shorter with Evicel®. • No outcomes were statistically significant in the hemithyroidectomy subgroup.
Tisseel®, Baxter Inc.	Hemostasis in cardiac surgeries [179–181]	<ul style="list-style-type: none"> • Use of Tisseel® during cardiac or redo cardiac surgery was more effective for hemostasis than conventional agents. • Reduction of perioperative blood loss was observed with Tisseel®. • Literature studies were not unanimous about the reduction of blood products used. • Resternotomy due to bleeding was lower with Tisseel®. • No difference in duration of hospital stay and mortality.

	Hemostasis in vascular surgeries [182]	<ul style="list-style-type: none"> Hemostasis rate after an implantation of polytetrafluoroethylene grafts was done in more patients with Tisseel® than in the control group (manual compression).
	Hemostasis in traumatic injury to the spleen and liver [183]	<ul style="list-style-type: none"> Tisseel® was effective to achieve hemostasis in 21 of the 26 patients who had splenic or liver trauma.
	Sealing in pterygium surgery with conjunctival autograft ¹⁷⁶	<ul style="list-style-type: none"> Flap time (fashioning and repositioning of the conjunctival autograft) was shorter with Tisseel® compared with the control. Pain level was lower with Tisseel® than with the control. No differences in recurrence rate, change in logarithm of the minimum angle of resolution and in surgically induced refractive change.
Progel™ PALS, BD	Control of air leaks after thoracic surgeries [184–188]	<ul style="list-style-type: none"> Intraoperative and postoperative air leaks were lower with Progel™ as an adjunct to standard closure methods after a pulmonary resection. There was a tendency for a shorter chest tube duration for patients who underwent a lung resection surgery with Progel™. Progel™ was associated with a shorter hospital length of stay for patients undergoing pulmonary surgery. No differences in mortality and morbidity were reported.
TissuGlu®, Cohera Medical Inc.	Wound drainage after an abdominoplasty [189,190]	<ul style="list-style-type: none"> Use of TissuGlu® in abdominoplasty was associated with a tendency of lower total wound drainage and time to drain removal compared to the control where the same procedure was done but without application of the adhesive. Number of needle aspirations for fluid collection was more important with TissuGlu®, where no drain was installed during surgery.
	Wound fluid formation after a mastectomy [191–193]	<ul style="list-style-type: none"> Even if the total volume of the wound fluid with TissuGlu® was lower than with the control where patient had drain placement during surgery, the number of clinically relevant seroma was more important. Patients who received intraoperative application of TissuGlu® required additional postoperative intervention such as fluid aspiration. Shorter hospitalisation was observed with TissuGlu® after a mastectomy.

ICU: Intensive Care Unit

2.4.2 Examples of application-driven requirements for bioadhesives

2.4.2.1 Lung surgeries

Lung is a soft spongy tissue. Bioadhesives for sealing air leaks in lungs have been studied extensively. The elastic modulus of a guinea pig lung was found to be 5-6 kPa[194]. A bioadhesive meant for sealing air leaks in lungs should typically be highly elastic (40% extensibility) and contain an elastic modulus between 5-30 kPa to support the inflation/deflation cycle of the lung[37,195]. The most common bioadhesives used in clinic to prevent air leaks following lung surgery include ProGel™ Pleural Air Leak Sealant and Tisseel®. Fibrin glues[196–199] have been identified as the most suitable in addition to ProGel™ [126]. *In vitro* studies were conducted to compare the burst pressures of some commercially available bioadhesives[50]. The highest mean burst pressure was achieved by ProGel™ (160.60±15 mmHg), followed by BioGlue® (115.47±21.21 mmHg) and Tisseel (13.98±5.50 mmHg) at day 0. MeTro, a newly developed bioadhesive intended to be used for sealing air-leaks, had a burst pressure of 6.2±0.7 kPa immediately following curing and was significantly higher as compared to ProGel[37]. From Table 2.3, considering ProGel™ as the only sealant clinically approved by FDA for sealing air leaks in lung surgery, a bioadhesive meant for preventing air leaks should have an average *in vitro* burst pressure of 114.3 mm Hg, an *in vivo* burst pressure of up to 77±19.1 mmHg in a rat lung incision model at time 0, a quick gelation time (approx. 13.7 s) and a quick preparation time (few minutes)[50]. Thus, a bioadhesive intended for lung surgery should have short preparation and gelation times.

2.4.2.2 Cardiovascular surgeries

Bioadhesives have been extensively applied in cardiovascular surgeries. Sealants used in cardiovascular surgeries should be able to withstand a high dynamic and pulsatile pressure and must be able to adhere to wet environments. The minimum pressure that the sealant must withstand is at least 140 mmHg[200]. BioGlue® is the most used bioadhesive for aortic repair. CoSeal®, Evicel®, and Omnex™ are used for vascular reconstruction. Clinical studies were done to investigate the effectiveness of BioGlue® in cardiac, aortic and peripheral vascular repairs. A hemostasis success rate of 61% compared to 39% for controls indicated effective treatment with

BioGlue®[56]. BioGlue® exhibited a significantly higher burst pressure of 596±71.5 mmHg in an arterial burst test as compared to CoSeal® (343±91 mmHg)[200]. CoSeal® had a shorter *in vitro* degradation of 6 days as compared to BioGlue®. Bioadhesive applied following aortic procedures must have high burst pressures (approx. 600 mmHg), a considerably shorter gelation time (up to 2 minutes). CoSeal® and BioGlue® were found to be effective in major aortic reconstruction procedures[201]. However, the use of BioGlue® to enforce anastomosis in the cardiovascular operations resulted in leaking of the glue through the needle holes onto the prosthetic grafts and aortic tissue causing concerns of embolization[202].

2.4.2.3 Spinal surgeries

Spinal cord is a cylindrical fragile tube of nervous tissue. The elastic modulus of spinal cord in human and rat was measured to be 89 kPa[203] and 27 kPa[204], respectively. The sealant approved to be used as an adjunct to sutures in dural repair following spinal surgery is DuraSeal® Exact Spine Sealant system (Integralife Inc.). The optimal characteristic values to be considered for a sealant designed for spinal surgeries are a gelation time of ≤ 3.5 s, a pressure integrity (the structural and leak resistant capability of a product to contain applied pressure) of at least 68 psi, an average *in vitro* burst pressure of up to 78 mmHg[205], an *in vitro* degradation within 1.3 to 3.6 days[206] and *in vivo* degradation within 9 to 12 weeks[207]. Use of BioGlue® for pediatric neurosurgical procedures resulted in post-operative wound complications[208].

2.4.2.4 Other applications

TissuGlu® (Cohera Medical Inc.) is currently used in joining the tissue layers following abdominoplasty when the underlying fatty layers of the abdomen are excised. TissuGlu® exhibits a longer gelation time (approx. 11 minutes) as compared to the bioadhesives used for other applications listed above.

Different bioadhesives along with the reported mechanical characteristics have been listed in Table 2.4. Correlations have been established for commercially available bioadhesives for specific applications.

From the scientific literature, it appears that active efforts are made to develop bioadhesives as gastro-intestinal drug delivery systems[73,209–211]. Complications associated with the gastro-intestinal applications include the smooth mucus lining and pH due to the secretion of enzymes, which could further complicate the adhesion and biodegradation of bioadhesives, respectively.

Table 2.4 Performance characteristics of commercially available bioadhesives.

Commercial Adhesive	Properties								Primary Applications
	Shear Strength (N)	Gel Point	Tensile Strength (N)	Peel Strength (N)	Burst Pressure	Degradation	Shelf-life (months)	Sterilization	
CoSeal®, Baxter Inc.[212]	0.8-0.95 [213]	< 3 s	0.6-1.02[213]	0.18[213]	660±150 mmHg[120]	30 days[121]	36[214]	Gamma[214]	Vascular (arterial or venous) reconstruction in adjunctive hemostasis
BioGlue® Surgical Adhesive, Cryolife Inc.[56]	1-2.25[213]	2 min	1-1.6[213]	0.1-0.2[213]	560 mmHg	24 months	36	Irradiation [215]	Cardiac, vascular, thoracic[161,165,216], genitourinary, neurosurgery, gastrointestinal, Ear, Nose and Throat (ENT)
Tisseel®, Baxter Inc.	-	4-5 min[217]	-	-	8.1±6.2 mm H ₂ O[218]	10-14 days[217]	-	-	Adjunct to hemostasis in patients, wherein conventional techniques prove to be ineffective[217]
Progel™ PALS, BD[219]	-	13.7 s	-	-	114.3 mmHg	14 days	12	E-beam	Lung parenchymal resection to prevent air leaks[219]
TissuGlu®, Cohera Medical Inc.[220]	32.6	11.74 min	12.9-21.8	0.36-0.92	-	24 months	12	Gamma	Abdominoplasty, aiding in approximation of tissue layers reducing the dead space and collection of fluids[189]
Omnex™ Ethicon Inc.[57]	2.2-4[213]	<15 s	1.5-3.2[213]	0.4[213]	118 mmHg (day 10) [221]	24-30 months	12	Dry heat and Ethylene oxide	Adjunctive hemostasis in vascular reconstruction[57]
DuraSeal® Exact Spine Sealant System, Integralife Inc.[206]	0.38-0.79[213]	≤ 3.5s	0.21-0.28[213]	0.1[213]	Approx. 80 mmHg [205]	1.3-3.6 days	18	E-beam	Adjunct to sutures in spinal surgery[222,223]. Scar tissue inhibitor in lumbar microdissectomy[224]

Adapted from Dhandapani et al.[225].

2.5 Conclusions

Bioadhesives are classified as medical devices and prove to be a good addition to the field of surgery and medicine. Different bioadhesives made from various sources have been identified including synthetic- and natural-based formulations as well as combination of those. The most frequently used components in the formulation of commercial bioadhesives are albumin, glutaraldehyde, chitosan, cyanoacrylate, fibrin and thrombin, gelatin, polyethylene glycol (PEG), as well as urethanes. From our analysis of the scientific literature and our clinical experience, the most frequently reported used bioadhesives in clinical applications are FloSeal®, CoSeal®, BioGlue® Surgical Adhesive, Evicel®, Tisseel®, Progel™ PALS and TissuGlu®.

The most common binding mechanism to tissues has been targeting the amine groups available in the tissue and organ structures. With no surprise, those molecules used to formulate bioadhesives differ greatly in their crosslinking mechanisms as well as in their properties and, as revealed in this review, also result in very different host responses ranging from mild to more considerable ones. Overall, host responses to fibrin- and PEG-based bioadhesives resulted in no to mild inflammation. Whereas the reactions were moderate-to-severe for BioGlue® Surgical Adhesive and Omnex™. Some bioadhesives trigger adverse reactions in addition to the normal response to wounds. They have been approved for applications considering their added benefits. Biocompatibility of bioadhesives has been closely related to the initiators used and the degradation products released in the body.

In some cases, it appears that a single bioadhesive, developed for a very specific application, is tried in other applications commanding quite different requirements from the initial intended usage. In fact, each bioadhesive has been shown to be effective for a specific use. For example, Progel™ PALS is indicated to seal air leaks and BioGlue® Surgical Adhesive in surgical repair of large vessels such as aorta. It can be tempting to consider the use of bioadhesives for other purposes than the ones for which they have been validated, but in some cases, this would result in an unacceptable mismatch between the mechanical properties of the bioadhesive and those of the tissue or organ on which it is applied. As a specific example, when applied, BioGlue® Surgical Adhesive results in a stiff material, which could exclude its use with some soft tissues and organs because of the resulting mismatch between the mechanical properties of the material and the tissue or organ. The properties of certain organs and applications of bioadhesives have been detailed in

Section 2.4.2. The level of swelling of the bioadhesives after application could be a critical factor dictating beneficial effects.

The clinical use of bioadhesives can be justified only for specific applications for which they have been developed and validated. They need to meet the strict requirements dictated by clinical applications. As for all medical devices, their clinical usage is justified only if their clinical benefits outweigh their associated deleterious effects. Finally, from a clinician's point of view, traditional methods such sutures and staples remain the most appreciated and applied methods in wound closure. Bioadhesives need to add real benefits over those traditional methods to justify their application or, when sutures and staples cannot be applied or result in poor outcomes for the patient, then they become applicable. We should not forget that they are expensive.

We hope that this review paper would aid academics, clinicians, and researchers to better understand the reaction mechanisms of currently available bioadhesives and the correlation between composition, host response and intended clinical applications.

Acknowledgments

This research project was supported by NSERC through a Discovery Grant awarded to Patrick Vermette (Grant # 250296-2012). All authors have approved the final manuscript. Patrick Vermette owns shares in SherMATRIX Inc., a company developing biomaterials for clinical uses.

Chapter 3

Overview of Approval Procedures for Bioadhesives in the United States of America and Canada

Foreword

Authors and Affiliations:

Vignesh Dhandapani: Ph.D. candidate, Université de Sherbrooke, Département de génie chimique et de génie biotechnologique

Prashanth Saseedharan: Ph.D. student, Université de Sherbrooke, Département de génie chimique et de génie biotechnologique

Denis Groleau: Professor, Université de Sherbrooke, Département de génie chimique et de génie biotechnologique

Patrick Vermette: Professor, ingénieur, Université de Sherbrooke, Département de génie chimique et de génie biotechnologique

Date of Submission: May 6th, 2021

State of Acceptance: Published

Journal: Journal of Biomedical Materials Research Part B: Applied Biomaterials

Contribution:

The article presents the regulatory steps to be followed for the commercialization of bioadhesives as medical devices in the United States of America and Canada. The article is published in *Journal of Biomedical Materials Research Part B: Applied Biomaterials*. The skeleton of the article was designed by Vignesh Dhandapani and Patrick Vermette. The initial draft of the article was written by Vignesh Dhandapani. It was rewritten and edited by Vignesh Dhandapani and Patrick Vermette. A part of post-market surveillance section was supported by Prashanth Saseedharan. It was reviewed by Patrick Vermette and Denis Groleau. All the work was done under the guidance and supervision of Patrick Vermette.

Titre en français :

Survol des procédures d'approbation des bio-adhésifs aux États-Unis d'Amérique et au Canada

Résumé :

Les bio-adhésifs sont des dispositifs médicaux utiles qui contribuent à réduire les complications postopératoires et agissent comme adjuvants aux sutures et aux agrafes pour sceller les plaies. Les entreprises biomédicales travaillent activement au développement de nouveaux bio-adhésifs. Comme pour d'autres dispositifs médicaux, la mise sur le marché de technologies prometteuses nécessite plusieurs étapes réglementaires, au cours desquelles leur sécurité et leur efficacité sont évaluées alors que les remboursements par les payeurs sont évalués. Les procédures réglementaires impliquent une classification basée sur les facteurs de risque, des études, la soumission de demandes aux autorités compétentes, l'obtention d'une certification et enfin la commercialisation, tout en conservant un historique des données du service après-vente. L'importance des données du monde réel a été récemment réalisée. L'objectif de cette revue est de se concentrer sur les aspects suivants : les objectifs translationnels ainsi que les attentes et les nécessités des dispositifs médicaux en focalisant sur les bio-adhésifs. Cet article devrait aider les chercheurs désireux de développer et de commercialiser de nouveaux bio-adhésifs à comprendre la nécessité des aspects réglementaires de base qui sous-tendent leur commercialisation à des fins médicales, surtout en médecine interne, et ce, spécifiquement aux États-Unis d'Amérique, au Canada et en Europe (en partie). Les principales différences entre les aspects réglementaires de ces pays sont mises en évidence. Les réglementations changent constamment avec l'introduction de nouveaux produits et de nouvelles lois gouvernementales. Elles sont mises à jour dans ce manuscrit jusqu'en mars 2021.

Abstract:

Bioadhesives are useful medical devices to help reduce post-operative complications and as adjuncts to sutures and staples in sealing wounds. Biomedical companies have been promoting research and development into new bioadhesives. As for other medical devices, translating promising candidates to market involves the need to pass through several regulatory steps, wherein their safety and effectiveness are evaluated and proper reimbursements from payors are assessed. The regulatory procedures involve classification based on the risk factors, support studies, submission of applications to relevant authorities, procurement of certification and finally commercialization, while keeping a track record of the post-market data. The importance of Real-World Data (RWD) has been recently realized.

The aim of this review is to focus on the translational goals, expectations and necessities of medical devices focusing on the bioadhesives to be commercialized. It should aid researchers inspired to discover and market new bioadhesives in understanding the need for basic regulatory procedures behind their commercialization for medical usage, most importantly, for internal medicine in the United States of America, Canada and Europe, in part. The key differences in the regulatory aspects among those are highlighted. Regulations keep changing with the introduction of new products and governmental laws. They are updated in this manuscript till March 2021.

3.1 Bioadhesives as Medical Devices

Developments in the field of wound closure have led to bioadhesives of different compositions and reaction mechanisms. Leaders in medical technologies have been probing more into identifying an ideal and suitable bioadhesive for closing surgical wounds. Current leaders in the manufacture of medical bioadhesives include Cryolife Inc., Ethicon Inc., Baxter, Covidien, Cohera Medical, only to name a few.

Medical devices make a clinical impact only if they are commercially available for use. Approval for marketing and manufacturing of the medical devices only comes with successful regulatory approval and establishment of proper reimbursements from payors, as they create the market for the device. The reimbursements for medical devices refer to the payment by a third-party public or private insurance that pays the healthcare provider for the costs incurred in the use of the medical device. Considering the costs of medical devices, the success of a medical device would depend on whether the cost for the device would be reimbursed. Knowledge about the reimbursements would enable the manufacturer to predict whether investing in the product would provide sufficient returns [226]. Recently, the reimbursement strategy for medical devices has been shifting from a volume-based approach to a value-oriented one where the reimbursement is decided on better care, cost and quality of the treatment [226]. The process of reimbursement for medical devices involves coding, coverage and payment. The code is an alphanumeric indication of the described medical device. The most common system used is the Current Procedural Terminology (CPT) code. Coverage refers to whether the payers would pay for the device and it depends on FDA approval and evidence of safety and efficacy of a new device over available devices. Different payers have different criteria to determine coverage. Payment is a fee-for service model where the payer pays the healthcare provider for the use of the new device and depends on the cost of the product, coding and contracts between the parties involved [227].

The regulatory bodies involved in the approval of medical devices to be commercialized in the United States of America (USA), Canada and Europe are the Food and Drug Administration (FDA), Health Canada and the European Medicines Agency (EMA), respectively. The primary goal of the regulatory authorities is to ensure that the medical device is “safe and effective” for use in humans.

The FDA defines a medical device according to the 201 (h) section of the Food, Drug and Cosmetics (FD &C) act as “any instrument, contrivance, implant, apparatus, machine, implement, *in vitro* reagent, or other similar articles, including the accessory which is [228]:

1. recognized in the official United States Pharmacopeia including the supplement sections;
2. intended for use in the diagnosis, treatment, mitigation and cure of diseases in man or other animals, or;
3. intended to affect the function or structure of the body of animals or man, the primary purpose of which is achieved not through chemical action within the body and does not depend on being metabolized to achieve the function.”

Classification of a combination product involving a device and a drug into one or the other is based on the *Primary Mode of Action* (PMOA). FDA defines PMOA as the “primary mode of action of a combination product that provides the most significant therapeutic effect of the product.” [229]

Health Canada defines medical devices as any instrument used to treat, mitigate, diagnose and prevent a disease or an abnormal physical condition in humans excluding animals [230]. Bioadhesives meant for human applications are classified under the category “medical devices”.

The EMA is responsible for regulating the safety and performance of medical devices in Europe. The introduction of new *Medical Devices Regulations* (MDRs) since 2017, replacing the Medical Devices Directive (MDD), has changed the European legal framework for medical devices and has introduced new responsibilities for the EMA and the national regulatory authorities [231]. EMA defines medical devices as “an instrument, appliance, software, apparatus, implant, reagent or any other article, that is used for:

1. Diagnosis, prevention, monitoring, alleviation or treatment of disease, injury or disability;
2. Replacement, investigation of anatomical, physiological and pathological process;
3. Providing data by *in vitro* examination of samples derived from the human body.”

The following sections in the review article will detail the classifications, key regulatory requirements according to the FDA and Health Canada, examples of bioadhesives and their related regulatory aspects.

3.2 FDA Regulations

The primary mission of the FDA is “to protect the public health by ensuring the safety, efficacy and security of human and veterinary drugs, biological products and medical devices and by ensuring the safety of our nation’s cosmetics, food supply and products that emit radiation” [232]. The FDA consists of different organizations of which, the Center for Devices and Radiological Health (CDRH) and the Center for Biologics Evaluation and Research (CBER) are key for bioadhesives, as they are classified accordingly. The CBER regulates medical devices related to licensed blood and cellular products by applying appropriate medical device laws and regulations. They are intimately associated with blood collection, processing and cellular therapies. CBER has developed specific expertise in blood, blood products and cellular therapies [233].

Products containing both biological and synthetic components are analyzed based on their PMOA and are assigned to either the CDRH or CBER [234]. For example, Progel™ Pleural Air Leak Sealant (BD) is a product combining Human Serum Albumin (HSA) and Polyethylene Glycol (PEG) and was reviewed by CDRH. Evicel®, a fibrin-based sealant containing only biological products, was processed by CBER. An understanding of which branch processes the product application facilitates communication during the preparation of the application or application review. The following is a summary of the sequential regulatory steps in bringing an identified bioadhesive to market.

3.2.1 Classification

Medical devices have been classified into three classes (Class I, Class II and Class III) based on the risks they pose. Class I medical devices include low-to-moderate risk medical devices such as bandages, handheld surgical instruments and non-electric wheelchairs. Class II medical devices are moderate-to-high risk devices and includes Computed Tomography (CT) scanner and infusion pumps. Class III medical devices pose the highest risk and they are involved in sustaining life such as pacemakers and deep-brain stimulators [235]. FDA has provided a list of 1700 distinct types of medical devices organized in the 21 Code of Federal Regulations (CFRs) Parts 862-892. They are divided into different parts based on applications (e.g., anesthesiology, cardiovascular, dental,

etc.). Finding a matching description and classification would ease the classification of the medical device. Traditionally as medical devices, bioadhesives meant for superficial and internal applications can be categorized into three classes based on the risk they pose (see Table 3.1 for specific examples) [236]. The term ‘controls’ refers to requirements from a regulatory perspective. This is not used in the same context in academia, where controls are used in experiments to ensure that an effect is observed due to the independent variable.

Table 3.1 Classes of bioadhesives and examples.

Class	Risk Level	Controls and Requirements	Examples of Bioadhesives
I	Low-to-moderate	General controls (510 (k) or pre-market notification)	ProDerma liquid bandage (Procurement Technology Systems LLC)[237], Kerisure™ Advanced liquid bandage (Kerisure™)[238]
II	Moderate-to-high	General, special controls (510 (k) or pre-market notification)	Glustitch® Tissue Adhesive (Glustitch Inc.)[239], Liquiband Exceed (Advanced Medical Solutions Group Plc.)[240]
III	High	General, special controls (pre-market approval)	TissuGlu® (Cohera Medical Inc.)[220], Ethicon™ Omnex™ (Ethicon Inc.)[57]

The approval process through FDA also considers the classification of medical devices based on the benefit-risk determination. The benefits of the device are assessed based on the type, magnitude, probability, necessity and the duration of the benefits for the patients. Risk assessment is done based on the severity of harmful events (Serious Adverse Events), probability, duration of occurrence, patient tolerance of the risk and distribution of the product. Other factors that influence the benefit-risk assessment include characteristics of the disease, patients’ perspectives and reported outcomes, availability of alternative treatment methods, post-market data, risk mitigation, scope of the device and breakthrough technologies solving an unmet medical need[241,242].

Pre-market (or) 510 (k) notification refers to submission and decision made by the FDA for Class I and II medical devices (unless exempt) that exhibit a substantial equivalence to a previously identified predicate device [243]. The tests usually done are equivalence studies (performance and biocompatibility) and animal studies to determine substantial equivalence of a proposed device to an approved marketed predicate device.

Pre-market approval (PMA) is applicable for high-risk medical devices i.e., Class III [244], unless it is a pre-amendment device marketed before 1976. The device must prove safety and effectiveness through extensive studies including performance, animal studies and clinical trials.

Classification of a medical device is done through the product code classification database [245]. Keywords of similar products are fed in, and the list of products is analyzed. For example, search for sealants in the device field results in 7 products within the Class II and III categories and their regulation numbers. If the classification panel (i.e., the list of matching device descriptions) is known, it may be readily accessed through the Code of Federal Regulations (CFR)[246]. Bioadhesives meant for internal surgical applications posing higher risks and aiding in the sustaining of human life are automatically classified under class III. Most of the bioadhesives meant for topical applications that do not pose risk to human life and have a predicate device (i.e., a previously legally marketed device to which an equivalence is drawn), are classified under either Class I or II. BioGlue® (Cryolife Inc., Kennesaw, Georgia, USA) a bioadhesive used as a patch in cardiovascular surgical procedures, is classified as Class III, as it aids in sustaining a person's life. However, GluStitch® Tissue Adhesive (GluStitch Inc., Delta, British Columbia, Canada) is considered as a Class II tissue adhesive. In fact, it is applied as a topical adhesive for surgical incisions and trauma-induced lacerations and it has used Indermil™ Tissue adhesive (Tyco Healthcare Group LP, Norwalk, Connecticut, USA) as a predicate device [247].

General controls include basic provisions in the Medical Devices Amendment Act (1976), wherein, the most basic studies are sufficient to prove the safety and effectiveness of the device. Examples of general controls for medical devices are no adulteration (501), no misbranding (502), device registration (510), absence in the banned list of devices (516), different notifications (518), control of reports (519) and adherence to Good Manufacturing Practices (GMP) (520) [248].

Special controls are device-specific and are mandatory for Class II medical devices. They are included when general controls alone are insufficient to prove the safety and effectiveness of the device. Examples of special controls include performance standards, patient registries, post-market surveillance, pre-market data requirements and special labelling requirements [249].

3.2.2 Tests

Evidence for safety and effectiveness of a bioadhesive is obtained through preclinical and clinical tests. The preclinical tests broadly include biocompatibility studies, performance testing and animal studies (based on the application). The biocompatibility tests are performed following Good Laboratory Practices (GLP; 21 CFR 58) in accordance with International Organization for Standardization (ISO) 10993 “Biological Evaluation of Medical Devices Part-1: Evaluation and Testing” [250]. Laboratory tests proving the safety and effectiveness prior to animal studies include the following:

- Cytotoxicity – International Organization for Standardization (ISO 10993-5)
- Sensitization and irritation (ISO 10993-10)
- Implantation (ISO 10993-6)
- Pyrogenicity, acute, sub-chronic and chronic toxicity (ISO 10993-11)
- Hemolysis (ISO10993-4)
- Genotoxicity (ISO 10993-3)

Examples of performance testing for bioadhesives included adhesive strength, polymerization time, heat of polymerization, volumetric swelling, burst pressure, gel point, shear strength, sterilization, degradation and shelf life. Animal studies for specific applications of bioadhesives are performed in a variety of animals including sheep, dogs, rats, mice and pigs. The FDA has proposed a framework for determining the biocompatibility studies associated with the medical devices based on the mode of contact and the duration i.e., limited (≤ 24 hours), prolonged (24 hours-30 days) and permanent (more than 30 days) [251].

Class III bioadhesives meant for permanent use (e.g., ProGel™ Pleural Air Leak Sealant) must include cytotoxicity, sensitization, irritation, toxicity (acute system and sub-chronic), pyrogenicity, genotoxicity, chronic toxicity, carcinogenicity and implantation studies. In addition to these tests, if the bioadhesives degrade with time, a degradation study must be included. Class III bioadhesives meant for contact with the blood must include the hemocompatibility study. Reproductive toxicity study must be done for the bioadhesives if it is targeting pregnant women or intended for applications close to the reproductive organs or in cases where a novel material is used. Class II

bioadhesives such as GluStitch® Tissue Adhesive (GluStitch Inc.), were classified as meant for prolonged use with breached surfaces and included cytotoxicity, sensitization, irritation, pyrogenicity, acute system toxicity, implantation and sub-chronic toxicity studies. Class II bioadhesives meant for a limited term topical application must include cytotoxicity, sensitization, irritation, pyrogenicity and acute system toxicity studies [239,252]. Hence, Class III bioadhesives meant for permanent internal use require more exhaustive biocompatibility testing, as compared to Class II adhesives meant for limited or prolonged topical use. Bioadhesives with their reported performance and biocompatibility studies are listed in Table 3.2.

Successful translation of results from animal studies to clinical trials depends on the selected animal model. Studies have revealed that animal models are not always a standard for the targeted application. Bioadhesives or medical devices made of human origin (e.g., Tisseel®) are more demanding as they need to be tested and assessed in immunocompromised animal models and this would defeat the purpose as the immune response is a key to clinical presentation and patient outcomes [253]. To date, only genetically engineered rats have been used to test devices of human origin and they are not always accepted for regulatory submissions [254].

Table 3.2 Performance and biocompatibility tests performed on selected bioadhesives.

Tissue Adhesives, Performance and Biocompatibility Tests	TissuGlu® , Cohera Medical Inc.[220]	ProGel™ PALS , BD[219]	Ethicon™ Omnex™ , Ethicon Inc.[57]	DuraSeal® Spine sealant , Integralife Inc.[206]	CoSeal® , Baxter Inc.[212]	BioGlue® , Cryolife Inc.[56]
A) Performance Tests						
Gel point	11.74 min	13.7 s	< 15 s	≤ 3.5 s	< 3 s	2 min [215]
Shear strength (N) (approx.)	32.6	-	2.2-4 [213]	0.38-0.79 [213]	0.8-0.95 [213]	1-2.25 [213]
Tensile strength (N) (approx.)	12.9-21.8	-	1.5-3.2 [213]	0.21-0.28 [213]	0.6-1.02 [213]	1-1.6 [213]
Peel strength (N) (approx.)	0.36-0.92		0.4 [213]	0.1 [213]	0.18 [213]	0.1-0.2 [213]
Burst pressure (approx.)	-	77.5±19.1 mmHg [127]	118 mmHg (day 10) [221]	68 psi	660±150mm Hg [120]	86 mmHg (day 10) [221]
Heat evolution	< 3° C	-	-	No [255]	-	-
Volumetric swelling	27.6%	-	-	≤ 200%	2-4 times [120]	-
Sterilization (ANSI/AAMI/ISO 11137) Sterility Allowance Limit (SAL) = 1 x 10 ⁻⁶	Gamma	E-beam	Dry heat and ethylene oxide	E-beam	Gamma [214]	Irradiation [215]
Degradation	24 months No systemic effects	14 days	2.1-2.5 years	1.3-3.5 days	30 days[121]	24 months
Shelf life	12 months (if stored at 25°C)	12 months	12 months	18 months	36 months [214]	3 years (if stored at 25°C)

B) Biocompatibility Tests						
Cytotoxicity (ISO 10993-5)	No	No	No	No	No	Mild- moderate
Sensitization (ISO 10993-10)	No	Mild	No	No	Very mild	No
Irritation (ISO 10993-10)	No	Mild Ocular	No	No	-	
Acute toxicity (ISO 10993-11)	No	No	No	No	-	No
Implantation (ISO 10993-6)	Slight irritant	-	-	Slight irritant	-	-
Sub-chronic toxicity (ISO 10993-6)	26 weeks slight irritant 52 weeks - no	No	-	No	No	No
Pyrogenicity (ISO 10993-11)	No	No	No	No	-	No ($< 0.5^{\circ} \text{C}$ in rabbits)
Hemolysis (ISO 10993-4)	No	No	No	No	-	No (4.45% of the total cells tested)
Genotoxicity (ISO 10993-3)	No	No	-	No	No	No
Clastogenicity	No	No	No	No	No	-

Clinical trials are performed for bioadhesives to evaluate their safety and effectiveness. Understanding the difference between efficacy and effectiveness to be applied to the clinical setting is of great importance. Efficacy compares the bioadhesive to no treatment and is used by researchers to grade the product. Effectiveness compares the bioadhesive to a standard procedure in the clinic and is found to yield high external validity and applicability in clinical settings[256]. Randomized multicenter trials are briefly described in Table 3.3.

The term “recall” refers to the removal or correction of a product that is marketed and considered to be a violation of the laws governing the FDA. The FDA could initiate a legal action for the violation. Recalls may be mandatory or voluntary. Voluntary recall refers to when the firm (manufacturer or the distributor) does its duty of protecting public health from the products that cause injury or gross deception. FDA classifies these recalls as Class I, II and III depending on whether the violating product causes, may cause or not cause adverse reactions. When the manufacturer fails to voluntarily recall the violating device, the FDA initiates a mandatory recall to the manufacturer. On identifying reasonable evidence that the adverse event is related to the device, the FDA may notify health professionals and users to cease the use of the device or issue a ceasing order [257]. Voluntary recalls for different bioadhesives are listed in Table 3.3.

Table 3.3 Examples of Class III bioadhesives classified under medical devices and the reported clinical studies and recalls.

Adhesive	PMA	Examples of Clinical Trials Reported to the FDA	Voluntary Recalls
BioGlue® Surgical Adhesive (CryoLife Inc.) [56]	P010003	Cardiac procedures (aortic valve replacement, aortoplasty, aorto valve annuloplasty, Bentall procedure, mitral valve replacement, coronary artery bypass grafting, ross procedure), aortic aneurysm repair (abdominal, ascending, descending, thoracoabdominal, transverse aortic arch aneurysms), peripheral vascular procedures (carotid endarterectomy), bypass (aorto-femoral, aorto-iliac, aorto-innominate, femoral-distal, femoral-femoral, renal, hepatic-renal).	Class 2 (2014) – Serum albumin monomer failed to meet the internal shelf life specification [258]. Class 2 (2017) – Error in the labelling of the lot number [259]. Class 2 (2018) – Syringe spreader tip not included and incorrect labelling of pouches [260].
Progel™ Pleural Air Leak Sealant (BD)[219]	P010047	Adjunct to closure in lobectomy when using standard procedures alone such as staples, sutures resulted in visible air leaks, segmentectomy, lobectomy with wedges, bilobectomy, lung volume reduction.	Class 2 (2012) – Errors in the expiration date of the distributed product [261].
TissuGlu® Surgical Adhesive (Cohera Medical Inc.) [220]	P130023	TissuGlu® in addition to standard wound closure in abdominoplasty, TissuGlu® and standard wound closure with no drain in abdominoplasty.	-
CoSeal® (Baxter) [212]	P030039	Sealing of anastomotic suture lines during vascular graft placement.	Class 2 (2010) - Out of specification parameter during stability study at 18- and 21-month period affecting gel properties [262]. Class 2 (2012) - Out of specification parameter during stability study at 24-month period affecting gel properties [263]. Class 2 (2016) - Potential of incomplete dissolution of PEG resulting in inconsistent hydrogel [264].
Omnex™ Surgical Sealant (Ethicon Inc.) [57]	P060029	Sealing anastomotic suture lines in patients undergoing arteriovenous shunt procedures receiving an expanded polytetrafluoroethylene (ePTFE) graft, anastomotic sealant in vascular reconstruction procedures involving ePTFE graft and different types of graft materials.	-
FloSeal® Hemostatic Sealant (Baxter) [265]	P990009	Adjunct to control intraoperative bleeding in cardiac, vascular and orthopedic/spinal surgical procedures.	Class 2 (2008) - Discoloration of FloSeal matrix during endoscopic application using the applicator [266]. Class 2 (2018) - Use of incorrect plastic formulation in the malleable tips [267].

PMA: Pre-Market Approval

3.2.3 Pre-Submission

To determine whether an identified product is a medical device, a first step is carried out by contacting the Division of Industry and Consumer Education (DICE) at *dice@fda.hhs.gov*. This process, called *device determination*, involves submitting its intended use, physical description, mechanism of action, public claims and contact information. If the information is incomplete, informal device determination could be obtained for no fee and used to determine whether the identified product is a medical device. The informal e-mail enquiry can be written to the Device Determination team at *devicedetermination@fda.hhs.gov* [268]. The e-mail should include a brief description of the product, its intended use and pictures of the claims (if available). The FDA should reply within 7 days. If the enquiry is complex and the FDA cannot reply by mail, the FDA will recommend a 513 (g) submission. The FDA 513 (g) program consists of a formal device determination or classification and involves user fees. The request for classification through this process includes a cover letter, a device description and use as well as the proposed labelling [269]. Responses to the questions should be issued by the FDA within 60 days after receiving the application.

Q-submission is an inquiry made to the FDA requesting for its feedback or for a meeting regarding the application to be submitted for a potential medical device. It could be done for potential *de novo* requests, PMA, 510 (k) and Investigational Device Exemption (IDE) [270]. Communication is established between the FDA and the submitter via teleconferencing or meeting in person. The Q-submission could also be used in cases where the FDA could recommend whether the planned clinical studies are of significant risk or not. It could also result in informational meetings during which the submitter enters into a discussion with the FDA review team making it aware of the product and of the progress but without feedback [271].

3.2.4 Submission

The *de novo* process for bioadhesives is possible when general and special controls provided reasonable assurance for safety, but for which there is no previously identified equivalent devices for comparison. The *de novo* request is filed when the sponsor is unable to identify a benchmark to compare its device to a previously identified bioadhesive or where the 510 (k) application for a bioadhesive is rejected. For example, the Closure Medical Corporation went for an Automatic

Class III request to the FDA for its PRINEO® Skin closure system. The FDA thereafter classified the bioadhesive as a Class II device. The FDA indicated that this was acceptable because the new bioadhesive was able to satisfy the controls listed in the document entitled “Class II Special Controls Document: Tissue Adhesive with Adjunct Wound Closure Device Intended for the Topical Approximation of Skin” [272].

Classes I and II devices to be marketed in the USA require 510 (k) notification or pre-market notification unless they are exempt from it. Most of the Class I devices and very few Class II devices are exempt from 510 (k) notification. For a device to be exempted from 510 (k) notification, it must be listed in 21 CFR Parts 862-892 [273]. The list classifies the devices under different categories such as dental, anesthesiology, hematology devices, etc., which have been exempted from 510 (k) notification. The device should be shown to be safe and effective for use and should have a substantially equivalent or predicate device already on the market (Section 513(i)(1)(A)). A new device is substantially equivalent to a predicate device if the use and their technological characteristics are similar or, if the use is similar (even if the technological characteristics are different) satisfying the FDA that the device is safe and effective [243]. Liquiband® Exceed™, Advanced Medical Solutions Group Plc., (Plymouth, Devon, United Kingdom) is a cyanoacrylate-based Class II tissue adhesive used for approximation of skin edges of wounds resulting from incisions for surgery, trauma and in combination with deep stitches. The product demonstrated substantial equivalence to a predicate bioadhesive called Barle Tissue Adhesive 2 (Advanced Medical Solutions Group Plc). The reasons cited for substantial equivalence included similarities (cyanoacrylate-based, ampoule type and applicator devices), differences (applicator design and volume of adhesive) and containing sufficient volume to seal wounds up to a length of 30 cm. Certain performance tests (lap-shear strength, wound closure strength, force to actuate, degradation, viscosity, purity and wound closure length) and biocompatibility tests (cytotoxicity, irritation, sensitivity, intramuscular implantation and subdermal toxicity) were done to support evidence that the device is comparable to the predicate device [240]. The tests performed and submitted to the FDA requesting for 510 (k) notification approval for two Class II bioadhesives are listed in Table 3.4.

Table 3.4 Class II bioadhesives and corresponding tests.

Bioadhesive	Predicate Device	Tests Performed for 510 (k) (Equivalence)
Glustitch® Tissue Adhesive, GluStitch Inc. [239]	Indermil™ Tissue Adhesive	Biocompatibility tests (ISO 10993-5,6,10), sterilization, shelf life and comparative testing (tensile strength [American Society for Testing and Materials (ASTM) F2458-05, F2258-05, F2255-05], polymerization time, viscosity, heat of polymerization, chemical analysis, hydrolytic degradation, applicator expression force.
LiquiBand Exceed, Advanced Medical Solutions Group Plc [240]	Barle Tissue Adhesive 2	Sterilization, shelf life, performance testing (wound closure strength [ASTM F2458-05], adhesive strength in tension [ASTM F2258-05], lap-shear strength [ASTM F2255-05], peel adhesion strength [ASTM F2256-05]), polymerization time, force to actuate, intraoperative reuse, viscosity, degradation rate, purity, moisture, heat of polymerization, microbial barrier, biocompatibility tests (ISO 10993-1 including cytotoxicity, sensitization, irritation, acute dermal toxicity).

PMA is a mandatory requirement for Class III medical devices unless it is a pre-amendment device (i.e., on the market prior to the approval of the 1976 FDA medical devices amendments or substantially equivalence to such a device). The technical section of the PMA exercise consists of non-clinical lab tests (biocompatibility, animals, toxicology, immunology, microbiology, wear, stress, shelf-life testing) and clinical tests (patient information, study design, protocols, adverse reactions, end points and demography). ProGel™ (PALS, BD) is a Class III bioadhesive for which PMA was obtained. The initial sections include a device description, indications for use, a list of contraindications, warnings, marketing history and potential adverse effects[219]. Following the initial sections, the technical section describes the preclinical studies on biocompatibility carried out under GLP in accordance with ISO 10993. The clinical studies concerning ProGel™ and several other bioadhesives are listed in Table 3.3. Fees related to the various submissions may be found in Table 3.5. A brief flowchart for medical devices regulatory pathways, which also incorporates bioadhesives, is shown in Figure 3.1.

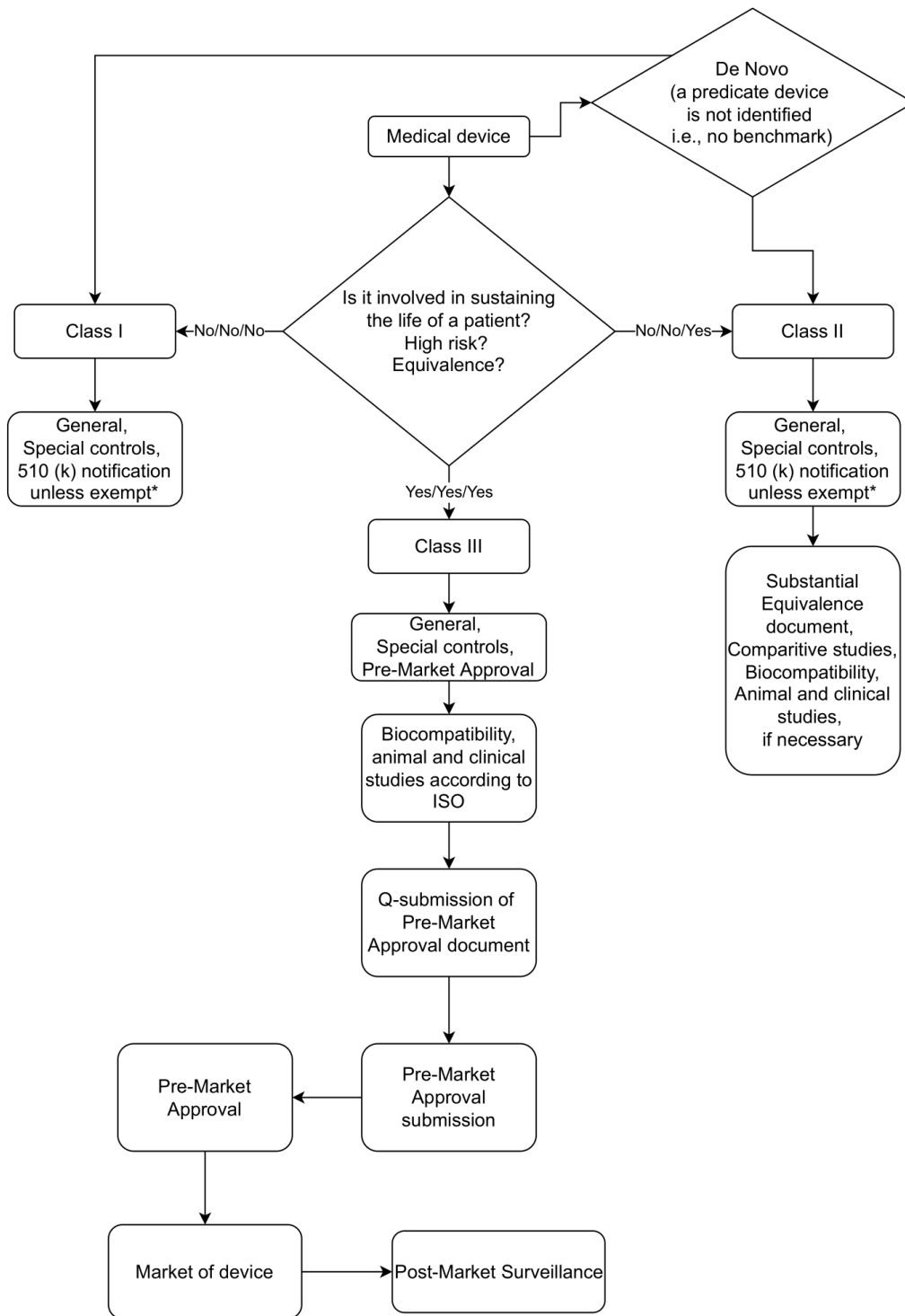


Figure 3.1 Flowchart for medical device regulation according to the FDA.

* listed in the exemptions list (21 CFR Parts 862-892).ISO- International Organization for Standardization

Table 3.5 As of March 2021, user fees related to the FDA services [274].

Application	Purpose	Small Business Fees (USD)	Standard Fees (USD)
513 (g)	Aid from the FDA for classification, preparation of documents.	2,468	4,936
<i>De Novo</i> classification request	Novel medical device that does not have a predicate device to be compared to.	27,424	109,697
510 (k)	Class II and a few Class I medical devices.	3,108	12,432
PMA	Class III medical devices.	91,414	365,657
180-day Supplement	Supplements that include changes to safety and effectiveness of the device including significant change in the materials, design, components or labelling.	13,712	54,849
Panel Track Supplement	Significant change in the design and performance wherein additional clinical data are required.	68,561	274,243
Real Time Supplement	Minor changes to the design, labelling, sterilization.	6,399	25,596

Abbreviations: FDA, Food and Drug Administration; PMA, pre-market approval

3.2.5 Quality System Regulations (QSRs)

Manufacturers of medical devices must follow QS according to the 21 CFR 820 to help ensure that the device consistently meets the applicable requirements and specifications. They are called Current GMPs. ISO 9001:1994 were established and revised to ISO 13485:2003 in order to obtain a harmonized and international standard as part of the QS. The regulations do not instruct the manufacturer to a specific method to produce the device, rather, they offer an umbrella approach, that is, providing a framework that all manufacturers must use to create their systems, specific for the device [275]. QSRs are applicable to finished medical devices. All PMA applications are required to include a complete description of the methods, facilities and controls for the FDA to assess the quality control. The Office of Compliance (OC) of the CDRH reviews the QS portion. The sections of the QS document include [276]

1. Device-related design controls, input, output, review, verification, validation, transfer, changes and history of the device according to the 21 CFR 820.30(a)-(j) and
2. Manufacturing-related QS audits, production flow, use of standards, purchasing controls, production and process controls, inspection, process validation, acceptance activities, non-conforming products, corrective actions, complaint files and servicing [277].

3.2.6 Approval and PMS

The FDA uses the term ‘PMS’ explicitly and it requires the manufacturers to conduct studies for high-risk devices, which were granted 510 (k) clearance or PMA.

Following the filing of the PMA, an acceptance review is done within Day 15 of submission. Following the acceptance review, the FDA either accepts the PMA or not. On acceptance, the PMA proceeds to the filing review which is done within Day 45. The purpose of both reviews is to ensure that the PMA is sufficiently complete to proceed to the substantive review. On acceptance of the review, the substantive review is carried out. A “Major/Minor Deficiency Letter” is issued to the applicant if further information is required to complete the review within Day 90. The decision of approval or conditional approval or rejection is given by the FDA within Day 180. Based on the overall reported findings, the FDA can approve the product. If there is a lack of clarity in the overall reported findings, the FDA decision might be “Not Approved” or “Approval pending GMP or deficiencies” [278].

Post-approval, medical devices are marketed following the regulations of the FDA. Recalls are voluntarily done by the manufacturer according to the 21 CFR 7 [279], if the medical device present risks of injury or defects, keeping in mind health safety of the public. In rare cases, wherein the manufacturer fails to recall a device with defects, the FDA could initiate itself the recall according to 21 CFR 810. Examples of recalls for bioadhesives are found in Table 3.3.

A PMA supplement is needed when there is a change in the device that would alter its safety and its effectiveness, and for which a PMA was issued earlier [280]. Several types of PMA supplements and their associated fees as listed in Table 3.5. The following conditions require the manufacturer to add a supplement to the PMA:

1. Changes in labelling, sterilization, manufacturing, performance or design specifications.
2. Extension of the expiry date of the product.
3. New indications for use.
4. Use of a different facility to process and package the device.

Bioadhesives approved through a PMA have included many PMA supplements. For example, CoSeal® fabricated by Baxter (California, USA) with the PMA number P030039 has included a series of 23 supplements including addition of a manufacturing site, change of label, addition of device components, addition of a new setup in the production site, change of warehouse, and change of material(s) used to manufacture the syringe. These supplements have been submitted under different categories including 180-day track, real time, site change, panel track, special and 30-day notice supplements [281].

The FDA also has the authority to withdraw a product from the market if it supposes that the product poses considerable risk upon use. As an example, FocalSeal-L Surgical Sealant was approved for commercialization by the FDA in 2000, was used as an adjunct to seal air leaks during pulmonary resection, and was withdrawn from the market in 2016 [282].

According to section 522 of the FD & C Act, the FDA could request the manufacturers to conduct post-market surveillance of certain Class II and III medical devices that:

1. are likely to cause serious adverse health consequences, or
2. are significantly used in pediatric populations, or
3. are intended to be implanted for more than a year, or
4. are life-supporting devices used outside the facility.

The pre-522 team at the FDA evaluates the device under consideration and issues a 522 order that contains intricate details such as the type of submission involved, public health questions, suggested PMS design and the rationale for the 522 issuance.

The manufacturer has 30 days since the issuance of the 522 to submit a PMS plan. The plan must contain details that help support and clarify the rationale for the original PMS order. Most inclusions in a PMS order include [283], not exclusively:

1. Background of the device, regulatory history, description, and indications for use.

2. PMS plan purpose, PMS plan objectives and hypotheses as well as PMS design.
3. Descriptions of the follow-up schedule, length, and assessment procedures.
4. Relevant data collection forms as well as description of data collection procedures and statistical analysis.
5. Reporting schedules for interim and final reports.
6. Interim and final data analyses.
7. Milestones/timeline elements.

According to the PMS plan, the interim and final PMS reports must be submitted to the FDA. Data from the PMS are the clinical performance data for the use of the device in a real-world setting, as the data are gathered from an uncontrolled patient population. Real-World Data (RWD) are data related to patient health status or delivery of healthcare and are derived from varying sources including [284]:

1. Electronic health records.
2. Billing and claims.
3. Disease, product and patient registries.
4. Data gathered from other sources such as mobile devices.
5. Health insurance and healthcare databases.
6. Social media.

The Real-World Evidence (RWE) is the evidence derived from the analysis of the RWD. The validity of the RWD to prove the safety and effectiveness of a device has been established by the FDA. The data have been used to bring new devices to market or to evaluate the safety and effectiveness of a device for a new condition or to continuously assess the safety of the products on market [285]. The RWE can be used:

1. To generate hypotheses for testing in a prospective clinical trial;
2. As a historical control;
3. As a concurrent control;
4. As evidence to support approval of the PMA;

5. To support reclassification of a device;
6. To support validity for additional indications for use;
7. For generating medical device reports and public health surveillance methods [286].

Recent advances have enabled health information technology developers to adopt applications programming interface in collecting and storing data using the HL7 FHIR® standard. The Medicare and Medicaid programs in the United States have recently opted for electronic access to medical claims through the HL7 FHIR® standard [284].

3.3 Health Canada Regulations

The Minister of Health is responsible for Canada's health portfolio, which includes Health Canada, the Public Health Agency of Canada and the Canadian Institute of Health Research. The primary mission of the Health Products and Food Branch of Health Canada is "to minimize the health risk factor to Canadians while maximizing the safety provided by the regulatory system for health products and to provide information to Canadians so they can make informed, healthy decisions about their health"[287]. The role of Health Canada is to ensure the safety and effectiveness of a drug, gene therapy, medical devices, etc. Here, a "medical device" is defined as an instrument used to treat, mitigate, diagnose and prevent a disease or an abnormal physical condition in humans. Examples of medical devices include bandages, glucose monitoring tests, hospital beds, toothbrushes, cancer-screening tools and blood-screening tools. Bioadhesives come under the category of medical devices.

Key steps in regulating medical devices according to Health Canada include classification, performing tests according to norms, preparation of documents (application, fee form), quality management system (QMS) certification, labelling and submission.

3.3.1 Classification

According to Health Canada, medical devices are classified into four classes based on the associated risks. The Class I product posing the least risks and Class IV involving the highest.

For device classification, the special rules must be given priority and checked first before comparing with other categories of the classification including invasive, non-invasive and active devices.

Bioadhesives incorporating human or animal cells and their derivatives are categorized under Class IV, according to the special rule 14.1(a). Bioadhesives for use in diagnosis, control, monitoring and correction of defects of cardiovascular and central nervous system are automatically classified as Class IV according to rule 1.1. Bioadhesives for internal use and which are intended to remain for more than 30 days and absorbed in the body are classified under Class III according to rule 1 (3), which states that "surgically invasive devices intended to be absorbed

by the body or stay in the body for more than 30 days are classified under Class III.” The classification of medical devices and the active licenses in Canada may be accessed through the Health Canada website [288]. The database lists the name, manufacturer, license number, device family and device class for each one of various medical devices.

The classification of bioadhesives may be found in Table 3.6.

Table 3.6 Examples of bioadhesives with licences according to Health Canada.

Bioadhesives	License Number	Class
Bioglue® surgical adhesive, Cryolife Inc.	15891	IV
FloSeal® Hemostatic matrix, Baxter	8797	IV
Glubran® 2 surgical glue, Galenmedical	86241	IV
CoSeal® Surgical Sealant, Baxter	37017	IV
DuraSeal® Dural Sealant, Integralife	68781	IV
Liquiband FIX8, Advanced Medical Solutions Plc.	98068	III
Liquiband® Exceed, Advanced Medical Solutions Plc.	82194	II
GluStitch® Tissue Adhesive, GluStitch Inc.	11549	II

3.3.2 Forms

Application forms are a key to register a new medical device or amend an existing medical device license. Different forms are used for different classes of medical devices [289]. There are fees for processing the application. The fee form contains the following details: Name of the device, license number, contact details of the manufacturer, fees for the application and proof of fees remittances. The user fees concerning different applications are listed in Table 3.7.

Table 3.7 As of March 2021, the user application fees related to medical devices, Health Canada [290].

Application Class	Description	Standard Fees \$ (CAD)
II	New license application.	478
III	New license application.	8,895
III	Amendment application for a significant change in manufacturing.	2,375
III	Amendment application for no significant change in manufacturing but that could change classification of the device.	7,543
IV	New license application.	24,699
IV	Amendment application for a significant change in manufacturing.	1,375
IV	Amendment application for no significant change in manufacturing but that could change classification of the device.	9,964

3.3.3 Quality Management System (QMS) Certificate

The QMS certificate role is to verify that the QMS under which a device is manufactured and designed, obeys ISO 13485 - QMSs for Regulatory Purposes. Health Canada only accepts a QMS certificate issued by third party auditing organizations recognized and listed under section 32.1 of Medical Devices Regulations [291]. An example of a Medical Device Single Audit Program (MDSAP) model is shown in Figure 3.2. A copy of the Medical Device Single Audit Program (MDSAP) is required and it is designed in such a way that a single audit performed by an auditing

organization meets the quality threshold. The MDSAP is based on a three-year audit cycle. The initial certification audit is performed in two stages, Stage 1 and Stage 2, in accordance with ISO 17021-9.3.1.2 and 9.3.1.3. Stage 1 includes a document review and preparedness for the Stage 2 audit. Stage 2 audit ensures that all ISO 13845 procedures are followed by the manufacturer and verifies whether the product or the process has complied with the regulations. Following this initial audit, partial surveillance audit is done every 2 years according to ISO 17021-9.6.2.2. The purpose of the surveillance audit is to ensure that manufacturers have incorporated the new QMS requirements, modifications to the product (if any), technology and amendments in the technical documentation. The recertification audit is done during the third year, in accordance with ISO 17021-9.6.4.2. The recertification audit ensures continued relevance, suitability and applicability of the organization's QMS in accordance to ISO 13485 [292].

3.3.4 Labelling

As the title indicates, each medical device should be identified uniquely. For labelling, all devices should include the following details [293]:

- Label: Any word, legend or mark attached to the package of a cosmetic, food, drug, or device.
- Control number: Unique set of letters, numbers which can identify a lot such that the lot history can be traced back to.
- Directions for use: Indicate the procedures that result in optimal performance of the device.
- Identifier: Barcode with unique set of letters that distinguishes it from similar devices.
- Name of the device.

The requirements for labelling include the following[294] :

- **Section 21:** No person shall import or sell a device unless the device has information such as the name of the device, name and address of the manufacturer, device identifier, Class III or IV device control number, the word sterile, if intended to be used sterile, expiry date of the device, medical conditions, whether the device is to be used safely (or) safely and effectively.
- **Section 22:** Conditions set out in Section 21 and intended to be sold to the public, all the information needs to be set out on the package for sale or visible under normal conditions. In cases when the package is too small to indicate all the conditions, a pamphlet indicating the directions for use could be accompanying the device.
- **Section 23:** For devices sold to the public, the information should be in English and French. For all other medical devices, the information could be in English or French. If a particular province has two different languages, the information can be made available in one initially. The information in the other language should be made available as soon as the manufacturer could provide on the request of the purchaser.

3.3.5 Pre-Market Review Document

The purpose of the *pre-market review document* is to prove that the device is safe and effective to be used. It is the manufacturer's responsibility to prove that the device is safe and effective by comparing their devices to the various resources available that include the following:

- Seeking advice through meetings with Health Canada.
- National or international standards.
- Relevant information in peer-reviewed scientific publications.
- Published guidance documents from Health Canada indicating the basic requirements.

Class II medical device manufacturers must attest that they have evidence for demonstrating the safety and effectiveness of the device but need not submit the evidence along with the pre-market review document unless Health Canada requests for it. Class III and IV device manufacturers must attach the evidence describing the safety and effectiveness of their product while submitting the

application form. The International Medical Device Regulators Forum (IMDRF) has established a harmonized Table of Contents (ToC) structure for medical device submission [295]. The purpose of ToC is to help in reducing the cost and time needed for preparing the documents, in maintaining consistency by the use of a specific format, in reducing the probability of information missing together with timely access to the internationally approved medical devices. Health Canada strongly recommends that all Class III and IV applications be in accordance with the IMDRF-ToC. An overview of the medical device regulations according to Health Canada is shown in Figure 3.2.

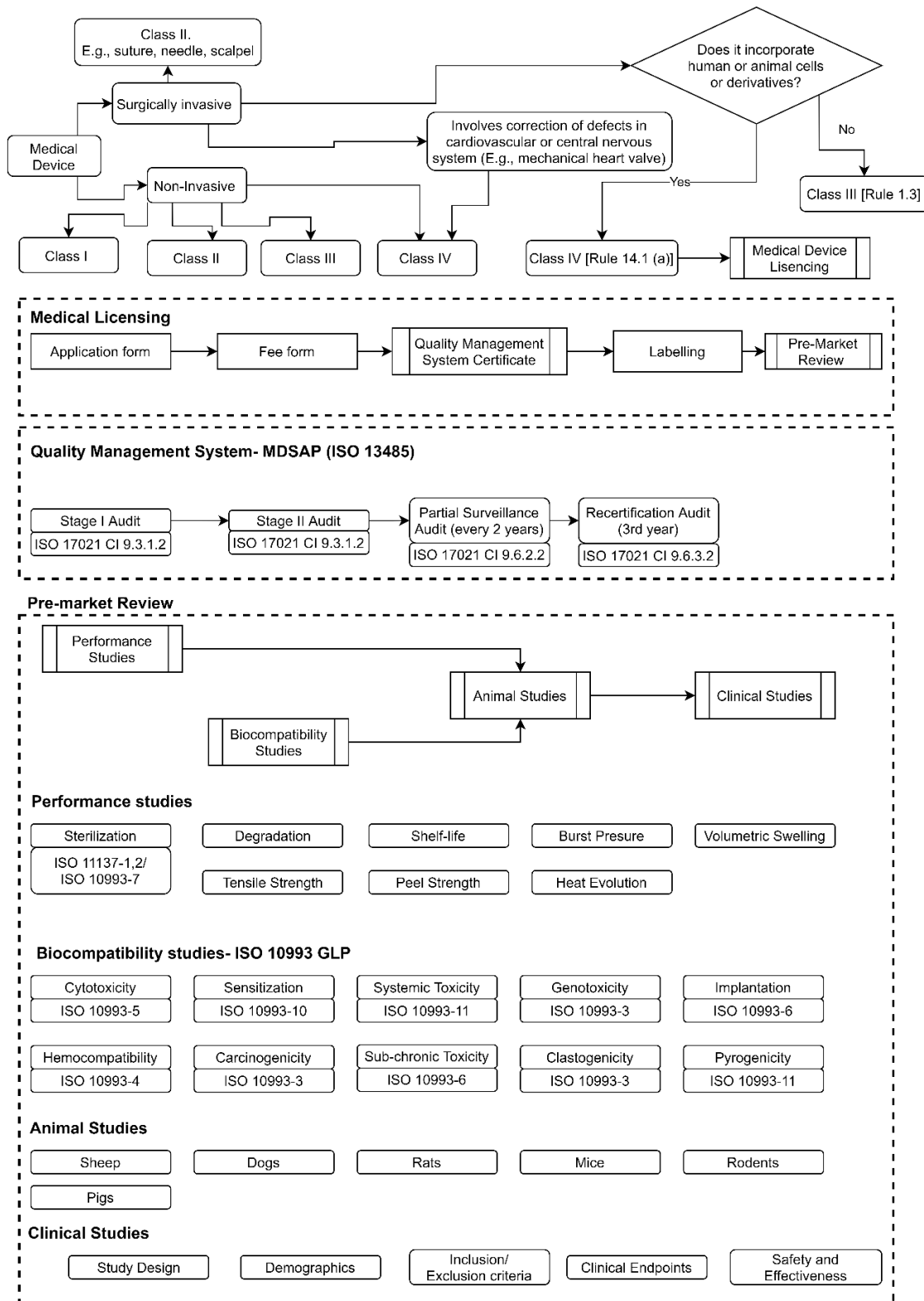


Figure 3.2 Overview of Health Canada regulations for medical devices and examples adapted to bioadhesives. GLP, Good Laboratory Practices; ISO, International Organization for Standardization; MDSAP, Medical Device Single Audit Program

The pdf format is highly preferred for submission of applications, while Microsoft Office formats (.docx, .xlsx) are also accepted. The formats not accepted include image files (.jpeg, .bmp, .tiff), outlook items (.msg), thumbnail cache files (Thumbs.db), pdf files with attachments, and documents containing macros (.docm).

The applications are submitted via e-mail at

hc.devicelicensing-homologationinstruments.sc@canada.ca if the size of the file is under 20 MB or submitted in hard copy.

3.3.6 Post-market Surveillance (PMS)

Following submission of the document to Health Canada, the administration conducts a screening of the application with the pre-market review document. Further information will be requested if something is missing and, on acceptance of the same, the documents are forwarded for “validation screening”. If the information is not available, the documents are rejected while, with proper documentation, the documents are forwarded for “technical screening”.

Technical Screening is carried out and a screening acceptance letter is generated. On identification of “deficiencies” or “gross errors”, another kind of report is generated. If the technical screening detects gross errors, the documents are rejected and not considered for further validation. Deficiencies would be reported with the deficiency letter and the documents should be resubmitted within 15 days for a new round of technical screening. If approved after screening, a screening acceptance letter will be generated [293].

On issuance of the acceptance letter, a review will be conducted over a period of 60-75 days, following which there could be multiple decisions such as

1. More information could be requested within the first 60 days and an additional information letter needs to be submitted.
2. The review could directly lead to the refusal communicated by a letter.

3. Acceptance, either the first time or after submission of an additional information letter, following which an acceptance letter is issued and a medical device license is generated.

3.4 European Regulations

It might be of interest to make an opening towards the situation in Europe. The primary goal of the European Medicines Agency (EMA) is “to foster scientific excellence in the evaluation and supervision of medicines, for the benefit of animal and public health in the European Union (EU)” [296]. According to the EMA, medical devices are classified into 4 classes including Class I, Class IIa, Class IIb and Class III. Class III medical devices pose the highest risk and includes devices such as cardiovascular catheters, aneurysm clips, prosthetic heart valves and others. Class IIa includes low-to-medium risk devices that stay in the body for less than 30 days, such as hearing aids, diagnostic ultrasound machines and others. Class IIb includes medium-to-high risk devices that are in the body for more than 30 days such as contact lenses, defibrillators, etc. [297,298]. Bioadhesives meant for internal use comes under the Class III category. The medical devices in Europe must undergo conformity assessment to indicate that they are safe to use and perform as intended. Medical Device Regulations (MDRs) indicate the devices that need the *Conformité européenne* (CE) label and the devices that pass the conformity assessment can affix this CE label for marketing [231].

The European MDRs have changed. New MDRs have been introduced by the European Commission and have been implemented since May 2017 (EU 2017/745). The new regulations have combined Medical Device Directive 93/42 EEC and Active implantable MDD 98/79 EC into one single entity, the MDR EU 2017/745. The transitional period was initially thought to be for three years but the European Parliament and the Council of European Union have extended it until May 26, 2021, due to the outbreak of the COVID-19 pandemic [299]. Annexure 1 of MDRs lists the new updates regarding the safety and performance requirements and, hence, CE recertification of existing devices is now required. The definition of medical device is also broadened to include nonmedical and cosmetic devices not previously regulated such as disinfectants and liposuction equipment. A unique Device Identifier is now employed to keep track of the device and it should be affixed on all labels. Many medical devices have been classified to a higher class thereby requiring more stringent testing. Manufacturers are required to provide more in-depth clinical

assessments with tighter equivalency standards to prove the safety and performance of the medical device [300]. The reason for new regulations include stricter regulations for high-risk devices, introduction of new categories for certain devices, improved transparency, strengthening PMS and an improved coordination system [301].

3.5 Distinguishing Features

It is common to believe that the regulations followed in most countries are similar to FDA's ones. This is not accurate considering the vast regulations and updates. Consolidating and distinguishing the concepts of regulations for medical devices in the USA, Canada and European Union is crucial and are listed below [302,303]

1. Classification

FDA classifies medical devices into three classes, whereas Health Canada and the EMA classified them into four classes. The procedures to classify the medical device are similar in the EU and Canada following the Medical Device Regulations (MDR's) EU 2017/745 and SOR/98-282, respectively. In the United States, the different medical devices and classes are published in the CFRs Title 21 Part 862-892 and manufacturers can use this information for comparison and device classification purposes.

2. Licenses and Registration

Medical device manufacturers in Canada intending to market a Class I device require an establishment license. For Class II, III and IV, manufacturers require a medical device license from Health Canada for which they have to attach a certificate demonstrating compliance to ISO 13485:2003. Applications for Class III include summary documents whereas submissions for Class IV requires study reports, extensive data, quality plans, risk assessment, etc.

In the United States, most Class I devices are exempt from registration requirements and just need to register their establishment with the FDA and comply with QSR. The remaining Class I and Class II devices require pre-market notification submission, as described earlier. All Class III medical devices must go through the extensive PMA procedure.

EMA states that for low-risk medical devices (Class I and IIa), the manufacturer can declare a self-assessed statement of the declaration of conformity without the involvement of the notified body. For the other classes, a notified body must be involved. Annex I of the MDRs details the essential requirements. Technical documentation submission should include performance data, procedures, standards, labelling and certifications from the Notified Bodies.

3. Fees

As described above in Tables 3.5 and 3.7, fees are different for different applications with Health Canada and the FDA. The submissions are very costly with the FDA, as compared to Health Canada.

4. Clinical Investigations

Health Canada expects that manufacturers to comply with Good Clinical Practices of ISO 14155:2011 as standard for conducting clinical studies with human subjects. In the United States, ISO 14155 is not a law, it is just a standard recognized by the FDA. The FDA requires compliance to 21 CFR Part 11, 50, 54, 56, 812.

5. MDSAP

Health Canada has made it mandatory for all submission to follow the MDSAP in order to obtain a harmonized global model or audits and this enables manufacturers to comply with regulatory requirements of multiple jurisdictions. The FDA is just a member of MDSAP, and therefore, it does not intend to oblige manufacturers to follow MDSAP.

6. Post-Market Requirements

The FDA authorizes to request the manufacturer to run PMS on certain Class II and Class III medical devices. The post-market requirements in the USA include tracking systems, establishment registration and reporting of device malfunction and of serious injuries or deaths. The PMS of Health Canada requires maintenance of distribution records, recalls, mandatory problems reporting and complaint handling. There are other differentiating features considering the market size, varying QS and health-care reimbursement systems.

3.6 Conclusions

A key factor dictating the commercialization of medical devices relates to regulations. In brief, the steps to bring a medical device to market are classification, submission document preparation, consultation, submission, approval and PMS. According to the FDA, Class I and II medical devices require 510 (k) notification, exhibiting substantial equivalence to a predicate device unless exempt. All Class III medical devices require pre-market approval unless they are either listed as or substantially equivalent to a pre-amendment device. The percentage of Class I, II and III approved by the FDA are 38, 53 and 9%, respectively.

Most bioadhesives meant for topical applications (e.g., Liquiband® Exceed™, Glustitch® Tissue Adhesive) have been commonly classified under Class I or II and those intended for internal usage (e.g., Coseal®, BioGlue®, Progel™ Pleural Air Leak Sealant System) under Class III. The risk class of the bioadhesive influences the requirement to prove the safety and effectiveness of a medical device to the FDA, that is, evidence to support the safety and effectiveness of a Class III bioadhesive involves more stringent screening as compared to a Class II or Class I bioadhesive. RWD obtained from trials provide a bigger picture of the effects of the device. Real-World Data (RWD) are crucial in deriving Real-World Evidences (RWE) that has extensive uses in clinical research (i.e., to establish controls to demonstrate the safety and effectiveness of the device).

Health Canada regulations categorize medical devices into four classes, as opposed to three by the FDA. Health Canada regulations and information for bioadhesives have been more vaguely identified and published. As of December 23, 2020, Health Canada has modified slightly the MDRs including additional requirements for post-market requirements for Class II, III and IV medical devices and certain regulations for medical device license holders. The situation in Europe has changed with the introduction of the new MDRs. The new regulations have added stricter regulations regarding the requirement to prove the safety and effectiveness for medical device approval.

It is often a perception that regulations worldwide are following those of the FDA. Although there are certain similarities in the operations, it is not always true and the major differences have been described in this document. Since, December 2022, animal studies are not needed for proving the

safety and effectiveness of drugs according to FDA. The current case for medical devices requires animal studies and could change in the future with more stricter regulations coming up.

In summary, researchers intending to bring a bioadhesive to market must give prime importance to regulations throughout its life cycle i.e., from its design, even at the laboratory/research stage, to preclinical/clinical validation and to the post-market analysis.

Acknowledgements

We thank Jérémie Chaussé and Vincent-Daniel Girard for their help with the final formatting of the article. This research project was supported by NSERC through a Discovery Grant awarded to Patrick Vermette (Grant # 250296-2012). All authors have approved the final manuscript.

Chapter 4

Decellularized Bladder as Scaffold to Support Proliferation and Functionality of Insulin-Secreting Pancreatic Cells

Foreword

Authors and Affiliations:

Vignesh Dhandapani: Ph.D. candidate, Université de Sherbrooke, Département de génie chimique et de génie biotechnologique

Patrick Vermette: Professor, ingénieur, Université de Sherbrooke, Département de génie chimique et de génie biotechnologique

Date of Submission: February 2nd, 2023

State of Acceptance: Published

Journal: Journal of Biomedical Materials Research Part B: Applied Biomaterials

Contribution:

The article details a cell culture system to study the effect of porcine bladder ExtraCellular Matrix on insulin-secreting pancreatic cells. The article was published in *Journal of Biomedical Materials Research Part B: Applied Biomaterials*. The experimental design was done mainly by Vignesh Dhandapani and Patrick Vermette. All the experimental work was performed by Vignesh Dhandapani and assisted by Hadrien Le-Nghiem. The results were analyzed by Vignesh Dhandapani and Patrick Vermette. The article was written by Vignesh Dhandapani and Patrick Vermette. It was reviewed by Patrick Vermette. All the work was done under the guidance and supervision of Patrick Vermette.

Titre en français :

Système de culture cellulaire pour étudier l'effet de la matrice extracellulaire sur des cellules pancréatiques sécrétrices d'insuline

Résumé :

La perte du nombre ou de la fonction de cellules β productrices d'insuline dans les îlots pancréatiques a été associée au diabète de type 1. Bien que la transplantation d'îlots puisse être un traitement alternatif, des complications telles que l'apoptose, l'ischémie et la perte de viabilité ont été signalées. L'utilisation d'organes décellularisés en tant qu'échafaudages en ingénierie tissulaire présente un intérêt certain en raison de l'ultrastructure et de la composition uniques de la matrice extracellulaire (MEC), avec un potentiel de favoriser la régénération des tissus. Dans cette étude, un système de culture cellulaire a été conçu pour investiguer l'effet de morceaux de vessie porcine décellularisée sur les cellules INS-1, une lignée cellulaire sécrétant de l'insuline en réponse à une stimulation au glucose. Des vessies de porc ont été décellularisées à l'aide de deux techniques, soit une méthode avec et une autre sans détergent. Les MECs résultantes ont été caractérisées pour investiguer l'élimination des cellules et de l'ADNdb. Les cellules INS-1 n'étaient pas viables sur la MEC produite à l'aide d'un détergent (i.e., dodécylsulfate de sodium (SDS)). Les cellules INS-1 ont été observées après 7 jours de culture sur des morceaux de vessie décellularisée sans détergent à l'aide d'un test de viabilité et de métabolisme cellulaire (MTT) et la prolifération cellulaire a été quantifiée (CyQUANT™ NF Cell Proliferation Assay). Aussi, la sécrétion d'insuline stimulée par le glucose (GSIS) et l'immunomarquage ont confirmé que les cellules étaient fonctionnelles en réponse à la stimulation par le glucose, en plus d'exprimer l'insuline. Elles interagissaient également avec la MEC produite sans détergent.

Mots clés : Vessie décellularisée, Matrice extracellulaire (MEC), Sécrétion d'insuline, Pancréas, Ingénierie tissulaire.

Abstract:

Loss in the number or function of insulin-producing β -cells in pancreatic islets has been associated with Diabetes mellitus. Although islet transplantation can be an alternative treatment, complications such as apoptosis, ischaemia and loss of viability have been reported. The use of decellularized organs as scaffolds in tissue engineering is of considerable interest owing to the unique ultrastructure and composition of the ExtraCellular Matrix (ECM) believed to promote tissue regeneration. In this study, a cell culture system has been designed to study the effect of decellularized porcine bladder pieces on INS-1 cells, a cell line secreting insulin in response to glucose stimulation. Porcine bladders were decellularized using two techniques *i.e.*, a detergent-containing and a detergent-free method. The resulting ECMs were characterized for the removal of both cells and dsDNA. INS-1 cells were not viable on ECM produced using detergent (*i.e.*, sodium dodecyl sulfate (SDS)). INS-1 cells were visualized following 7 days of culture on detergent-free decellularized bladder pieces using a cell viability and metabolism assay (MTT) and cell proliferation quantified (CyQUANT™ NF Cell Proliferation Assay). Further, glucose-stimulated insulin secretion (GSIS) and immunostaining confirmed that cells were functional in response to glucose stimulation, as well as they expressed insulin and interacted with detergent-free produced ECM, respectively.

Keywords: Decellularized bladder, ExtraCellular Matrix (ECM), Insulin secretion, Pancreas, Tissue engineering.

4.1 Introduction

Type-I diabetes is due to T cell-mediated autoimmune destruction of insulin-producing β -cells in the endocrine region of the pancreas leading to deficiency in insulin production[304,305]. Current treatment strategies include exogenous supply of insulin through multiple daily injections or insulin pumps coupled with strict diet restrictions[306]. Those treatments expose patients to the risk of hypoglycaemia[307–310], insulin resistance[311], and obesity as well as to a lifelong dependency on external insulin supply, and psychiatric conditions[312]. Preliminary testing of islet transplantation dates back to 1977[313] and the first two decades resulted in unsatisfactory results[314]. Islet transplantation optimized through the Edmonton protocol in 2000 improved methods of islet transplantation by using: 1. corticosteroid-free immunosuppression, 2. an increased number of islets isolated from pancreas from multiple donors, 3. avoiding the use of non-human medium for islet purification, and 4. short cold ischemic storage time[315–317]. Comparison of islet transplantation and insulin therapy following severe hypoglycaemia or kidney transplantation has revealed that islet transplantation had improved metabolic outcomes[316,318–320]. Intrahepatic islet transplantation has been shown to improve glucose counter regulation and hypoglycaemia control in the long term[321]. However, complications such as ischaemia, apoptosis[322], loss of islets viability and detrimental effects of immunosuppressive agents still occur with islet transplantation[323–327]. The need for alternative strategy in tissue engineering arose due to the complications associated with transplantation. Tissue engineering techniques include the use of decellularized organs, 3D bioprinting, organ-on-a-chip for multiple medical applications.

Decellularized organs and tissues have been used to design biological scaffolds for pre-clinical and clinical applications[328–330]. The removal of cells from tissues or organs yields a residual complex material composed of structural and functional proteins, which constitute the ExtraCellular Matrix (ECM). The ECM is generally composed of structural, globular proteins (e.g., collagens, laminins, fibronectin, elastin and tenascins) and proteoglycans (e.g., glycosaminoglycans (GAGs)). The ECM components interact with each other giving a structure and shape to organs, aid in cell signaling and ECM network remodeling and contribute to hydration of the ECM and interactions with growth factors, cytokines and cell receptors[331]. The production of ECM through recombinant DNA engineering is nearly impossible, due to the

complex composition and ultrastructure of the ECM, that vary from one tissue or organ to another. Therefore, various organs have been decellularized by different methods involving mechanical, physical, chemical and/or enzymatic means, as reported elsewhere[6,332–335]. The most common detergents used in decellularization protocols include sodium dodecyl sulfate (SDS), Triton X-100, sodium deoxycholate (SDC) and 3-([3-cholamidopropyl]dimethylammonio)-1-propanesulfonate hydrate (CHAPS).

SDS, an anionic detergent, functions by solubilizing membrane proteins and penetrating the outer membrane layer, thereby resulting in disruption[336]. SDS, at different concentrations, has been extensively used to decellularize mouse pancreas[337], rat kidneys[338], ovine small intestine submucosa[339], porcine pulmonary arteries[340], kidneys[341], lungs[342], and bladders[343]. SDS is efficient to decellularize tissues and organs. However, the use of high SDS concentrations over a prolonged period can affect the glycosaminoglycan (GAG) and collagen content, and can result in other detrimental effects[344–347]. To further investigate and address the effect of SDS, considering some contradictions found in the literature, SDS was used in this study as one of the methods to decellularize porcine bladders.

Freeze-thaw cycles for cell lysis in decellularization involves cycles alternating between cold (often -80°C) and higher (37°C) temperatures[334]. The freeze-thaw process has been shown to be effective in cell disruption of zebra fish heart[348] and of fibroblast sheet[349], however, remnant nucleic material has been reported without the use of additional ribonucleases or trypsin. Protocols combining detergents and physical methods have proven to be effective in obtaining scaffolds[350,351]. Combination of freeze-thaw, hypertonic solution treatment, and polar solvent led to efficient decellularization of human adipose tissue[352]. Previous studies have indicated the cytocompatibility of decellularized porcine bladder when seeded with urothelial, stromal and fibroblastic cell lines[343,353]. We therefore hypothesized that decellularized porcine bladder pieces containing preserved ECM would aid in providing a favorable micro-environment for the survival, proliferation and function of INS-1 cells, a rat insulin-secreting β -like cell line. Although various studies have been conducted to study the effect of porcine bladder ECM on multiple cell lines, the use of insulin-secreting pancreatic cells seeded on detergent-free decellularized porcine bladder is performed for the first time in this study.

The objective of this research study was to compare the responses of INS-1 cells cultured on decellularized porcine bladder pieces produced by two techniques: 1) 0.5% SDS treatment and 2)

freeze-thaw combined with hypertonic sodium chloride treatments and ethanol extraction. ECM pieces were neither further treated nor modified to preserve as much as possible the ECM ultrastructure, but this requirement complicates cell culture experiments, justifying the design and validation of the cell culture system described in this study. The decellularization was characterized by immunohistochemical analysis, scanning electron microscopy (SEM) and double stranded (ds)DNA quantification. INS-1 cells were seeded and cultured on the produced ECM pieces and viability, proliferation and functionality of the cells were characterized by MTT, Cyquant, glucose-stimulated insulin secretion (GSIS) and immunostaining.

4.2 Materials and Methods

4.2.1 Porcine Bladder Decellularization

Porcine bladders from three different porcine donors (N=3) were freshly procured from a slaughterhouse (Abattoir Régional de Coaticook, Coaticook, Québec) within 24 hours of animal sacrifice and were placed on ice until use. The porcine bladders were procured from a licensed slaughterhouse and since the animal sacrifice was performed under strict regulated conditions, the tissues needed no approval from the ethics committee of the Université de Sherbrooke. Fat and muscular layers of the bladder were excised and delaminated using scissors and a surgical blade. The resulting tissue was diced into approx. 5mm x 5mm pieces. Decellularization was carried out by two techniques, as depicted in Figure 4.1. The different decellularization steps are shown in Appendix A (Supplementary Figure 1) and the video showing the initial procedure of delamination and mincing is shown as Supplementary Video 1.

4.2.1.1 Detergent-based Decellularization (Det)

Bladder pieces (approx. 40-50g) were washed with distilled water (300 mL) for 4 hours in a shaker (New Brunswick Innova® 44/44R, Eppendorf, Hamburg, Germany) at 180 rpm with a change of water once. The process of decellularization was carried out using 0.5% Sodium Dodecyl Sulfate (SDS) (161-032, Biorad, Hercules, CA, USA) for 30 ± 1 hours at 180 rpm with the solution replaced thrice during the procedure. The decellularized samples were washed again in distilled water for 36 ± 1 hours at 180 rpm with 3 changes of water in between and the final 12-hour water rinse contained 1% penicillin/streptomycin (15140122, Life Technologies, Carlsbad, CA, USA). The samples were filtered, water discarded, and stored at -20°C until further use.

4.2.1.2 Detergent-free Decellularization (Det-free)

Bladder pieces (approx. 40-50g) were washed using Milli-Q water (300 mL) for 4 hours in a shaker (Innova® 44/44R, New Brunswick™) at 37°C and 200 rpm with a change of water once. The process of decellularization was initiated using 2M sodium chloride for an hour followed by an overnight step in Milli-Q water at 37°C and 200 rpm. The tissues underwent an hour of freezing in liquid nitrogen followed by a thawing step for one hour in Milli-Q water at 37°C. The tissues were again submerged in liquid nitrogen for an hour. Samples were thawed partially in Milli-Q water at 37°C and were blended (Osterizer 12-speed Blender, Brampton, ON, Canada) with ice, filtered, and washed for one hour in 2M sodium chloride, thrice in Milli-Q water for one hour, and then underwent a final overnight Milli-Q wash at 37°C and 200 rpm. Samples were washed twice in 70% ethanol, once in 1X PBS (BP665-1, Thermo Fisher Scientific, Waltham, MA, USA) and were subjected to an overnight wash in 1X PBS containing 1% penicillin/streptomycin at room temperature and 200 rpm. They were filtered and stored at -20°C until further use.

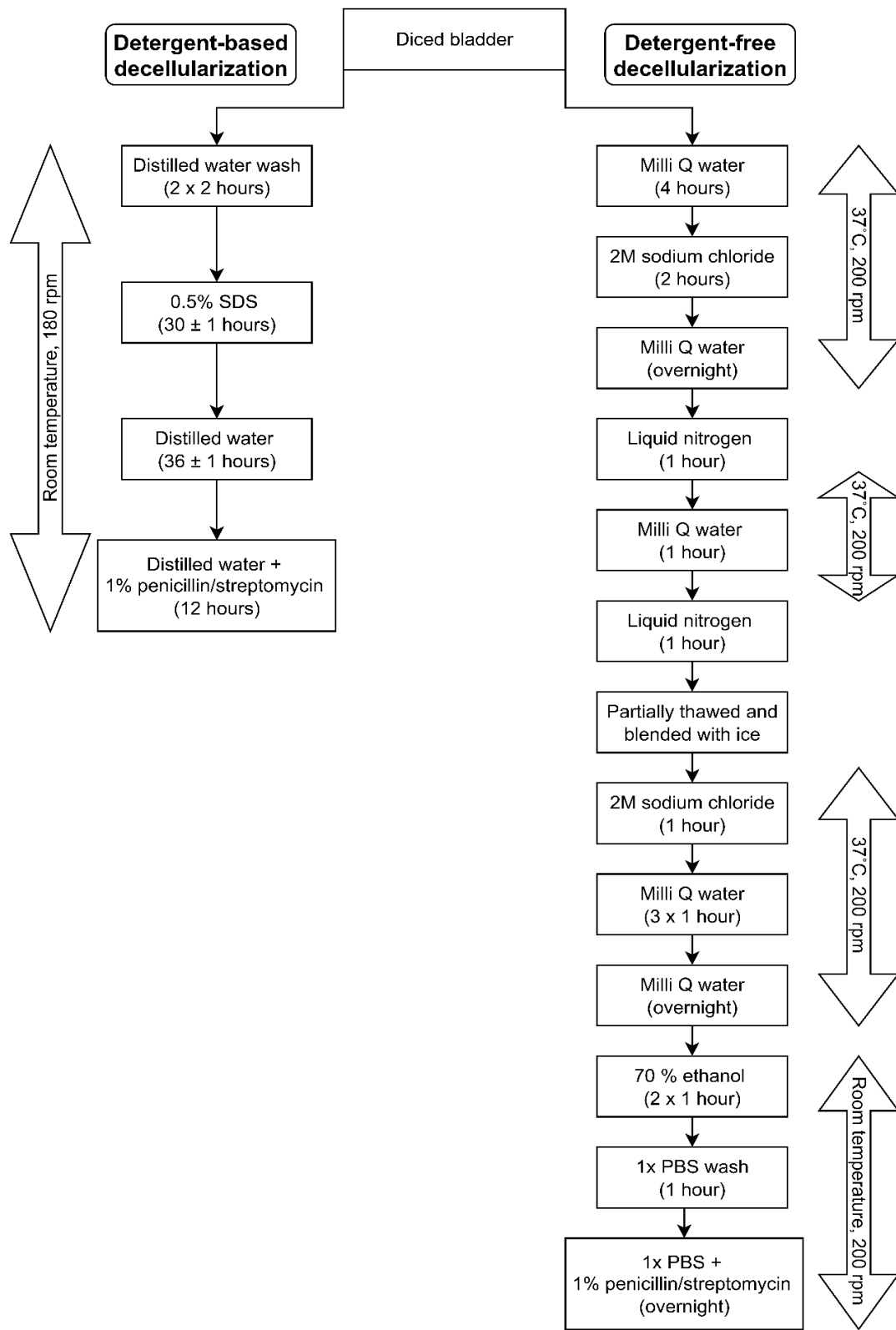


Figure 4.1 Flowchart of the detergent-based and detergent-free decellularization.

4.2.2 Histological Characterization

Bladders (native, detergent-processed, and detergent-free-processed samples) were fixed in 4% paraformaldehyde (PFA) (P16148, Sigma-Aldrich, St-Louis, Missouri, USA) for 48 hours. The samples were processed in a tissue processor, embedded in paraffin, and then sliced into 4- μ m thick sections. The sections on glass slides were dried for 48 hours at 37°C. The sections were characterized using 1) Hematoxylin and Eosin, for confirming the absence of nuclei and presence of collagen; 2) Alcian Blue and Nuclear Fast Red staining, for detecting the presence of glycosaminoglycans and nuclei.

4.2.3 Scanning Electron Microscopy (SEM) for Ultrastructure Analysis

The second method to characterize decellularized bladder pieces was SEM to reveal the absence of cells and presence of the 3D fibrous collagen network. Samples were frozen and fixed in 4% PFA. They were washed in PBS twice, fixed in 1% osmium tetroxide and washed twice in distilled water. Dehydration of the samples was achieved by successive ethanol treatments and a final critical point drying step in liquid carbon dioxide. The samples were imaged using a Hitachi S-3000N scanning electron microscope after mounting on a stub and coating with gold/palladium.

4.2.4 DNA Extraction and PicoGreen Assay to Quantify Residual dsDNA

Content

Samples of native and decellularized bladders were solubilised in a proteinase K digestion solution (BP1700, Thermo Fisher Scientific). This step was necessary to eliminate interference from ECM molecules with the assay and to dissolve the proteins to extract the DNA. DNA extraction was performed by the conventional phenol, chloroform and isoamylalcohol (PCI) method[354] and finally precipitated in a mixture of ethanol and sodium acetate. The pelleted DNA was suspended in 1X Tris EDTA buffer (pH 8). The quantification of double-stranded (ds)DNA was performed using the Quant-iT™ PicoGreen™ dsDNA assay kit (P7589, Thermo Fisher Scientific). The

fluorescence was measured at 480 nm excitation (Synergy HT Microplate Reader, Biotek, Agilent, Santa Clara, CA, USA).

4.2.5 Three-dimensional Cell Culture System to Validate Decellularized Bladder Pieces

As ECM was neither treated nor modified following bladder decellularization, it was necessary to design a 3D culture system to investigate cell responses towards ECM pieces (typical diameter of ca. 1 cm).

The ECM was aseptisized under ultra-violet (UV) light in a sterile hood for 20 minutes. A 2% (w/v) agarose solution (A0169, Sigma-Aldrich) was prepared in the INS-1 cell culture medium made from RPMI-1640 with L-glutamine (31800-022, Life Technologies) supplemented with 1 mM sodium pyruvate (11360-070, Gibco), 50 μ M β - mercaptoethanol (M7522, Sigma-Aldrich), 10 mM HEPES (BP310, Thermo Fisher Scientific), 10% fetal bovine serum (FBS) (12483020, Life Technologies), and a 1% penicillin/streptomycin mixture.

A first layer was deposited at the bottom of the wells of 24-well cell culture plates. The bladder ECM pieces were transferred to these wells covering approx. 90% of the total surface area, as shown in Figure 4.2. One ECM piece per well was added. A second layer of agarose was poured surrounding the ECM part and the whole setup with 1X PBS was UV-asepticized in the hood for 90 minutes. The second layer of agarose was added to create a meniscus wherein the cells would form non-adherent aggregates when in contact with agarose and would ensure the interaction of the cells with the ECM pieces. The wells with ECM pieces were soaked for 48 hours in culture medium at 37°C.

4.2.6 INS-1 Cell Culture Conditions

INS-1 (C0018007, AddexBio) cells were cultured in flasks in the culture medium at 37°C under 5% carbon dioxide. The culture medium was changed once every two days. Upon confluence, cells were trypsinized (25200072, Life Technologies) and 25,000 cells were added in each well containing the ECM pieces. The cells were cultured for 7 days with medium change once every two days.

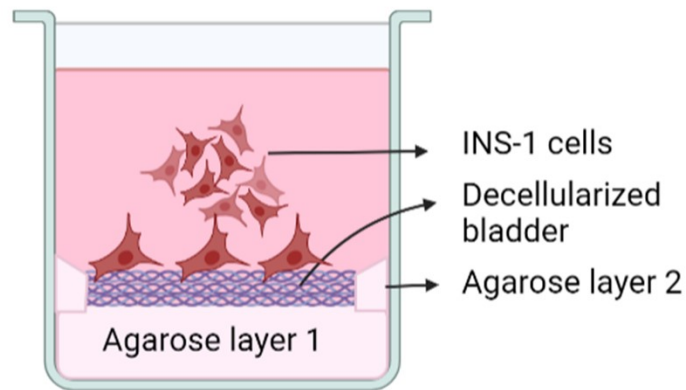


Figure 4.2 Three-dimensional culture system to test intact decellularized bladder pieces. The second layer of agarose was added surrounding the ECM pieces to keep them in place, to create a meniscus and to facilitate the interaction of INS-1 cells with the ECM.

4.2.7 MTT Assay for Visual Observation of Viable Cells on ECM Pieces

Thiazolyl blue tetrazolium bromide (M5655, Sigma-Aldrich) was solubilized in 1X Hanks Buffer Salt Solution (HBSS) at 0.5 mg/mL. The medium from each well was centrifuged, the supernatant fluid discarded and the pellet resuspended in 1 mL of the prepared 3-(4,5-dimethylthiazol-2-yl)-2,5-diphenyltetrazolium bromide (MTT) solution. The solution was transferred to the ECM-containing wells and incubated at 37°C for 1 hour under humidified conditions. Afterwards, the MTT solution was discarded and 1X PBS was added to the wells. A digital microscope, VHX-6000 series (Keyence Canada Inc., Mississauga, ON, Canada), was used to capture the images.

4.2.8 CyQUANT™ NF Cell Proliferation Assay Kit to Quantify Cell Number

The CyQUANT™ NF Cell Proliferation Assay Kit (C35006, Thermo Fisher Scientific) was used to quantify cells. The media were transferred into vials. The cells in each well were collected and transferred to the same vial by trypsinization (6-7 minutes) followed by vigorous repeated pipetting. The sample was centrifuged at 1200 rpm for 5 minutes. The medium was discarded, and the pellet was rinsed in 1X HBSS (provided with the kit) and centrifuged again. The 1X HBSS buffer was discarded, and the cells were suspended in diluted CyQUANT™ NF reagent (according to the supplier's protocol) and transferred to a 96-well microplate. The plate was incubated at 37°C for 1 hour and the fluorescence read at 480 nm excitation (Synergy HT Microplate Reader, Biotek).

4.2.9 Immunofluorescence to Investigate Insulin Expression and ECM

Interactions

Bladder ECM pieces populated with cells were fixed in 4% PFA for 48 hours. The samples were processed (to dehydrate), embedded in wax, and 4- μ m slices were cut. The dried sections were deparaffinized, hydrated and blocked in 2% bovine serum albumin. The primary antibodies to insulin (ab181547, Abcam, Cambridge, UK) and β -actin (ab8226, Abcam) were added at the recommended dilution and left undisturbed overnight at 4°C. The secondary antibodies anti-rabbit Alexa 488 (Invitrogen, Waltham, MA, USA) and anti-mouse Alexa 647 (Invitrogen) were added and left for 1 hour at room temperature and were counterstained with 4,6-diamidino-2-phenylindole, dichloride (DAPI, D1306, Invitrogen). Three fluorescence images from three different samples were observed using an Olympus IX83 inverted confocal microscope (Olympus life sciences, PA, USA) at 63x and the images were acquired using the Olympus FV-31S-SW software.

4.2.10 Glucose-Stimulated Insulin Secretion (GSIS) for Functionality

Investigation

Medium was centrifuged, the supernatant fluid discarded, to obtain the cell pellet. Further, the pellet was washed in 1X PBS, centrifuged, and the supernatant fluid discarded. The washing step was followed by incubation in different concentrations of glucose, as described below. Initially, the cell pellet along with the content of the entire well was washed twice (30-minute and 1-hour incubation) in low glucose (2.8 mM)-containing Krebs-Ringer buffer (KRBH) supplemented with 115 mM NaCl, 25 mM HEPES, 5mM KCl, 24 mM NaHCO₃, 1mM MgCl₂, 5mM CaCl₂ and 0.1% bovine serum albumin to remove the residual insulin present in the culture. Further, the whole well with the cells was incubated for 1 hour at 37°C, sequentially, in each one of the following conditions: 1) low-glucose (2.8 mM); 2) high glucose (28 mM); 3) high glucose (28 mM) + 50µM 3-isobutyl-1-methylxanthine (IBMX, I5879, Sigma-Aldrich); and 4) low-glucose (2.8 mM). All the glucose solutions were prepared in KRBH buffer. Post-incubation at each step, the buffer was collected, centrifuged and the supernatant fluid (insulin-containing solution) was stored at -20°C. The step involving washing the well and cell pellet with 1X PBS following centrifugation was done in-between each step with the wash solution discarded every time to remove residual insulin from the previous step. The different insulin solutions were stored at -20°C until ELISA quantification. Rat High Range Insulin ELISA (80-INSRTH-E01, Alpco Diagnostics, Salem, NH, USA) was used to estimate insulin secretion. The secreted insulin was normalized to 100,000 cells in the appropriate condition and the stimulation index was calculated for each condition by dividing the insulin concentration at high-glucose stimulation to that at low-glucose stimulation.

4.2.11 Statistical Analysis

R-studio (Version 4.2.0) was used to perform Tukey's HSD two-way analysis of variance (ANOVA) statistical analysis. Microsoft Office 365 Excel version 2206 was used to plot the graphs. A p value < 0.05 was considered statistically significant. The bars in the graph represent the mean of three experiments ± standard error.

4.3 Results and Discussion

At first, bladders were cut into smaller pieces after removing fat and muscular layers. Several studies have reported decellularization of porcine bladders by keeping the organ intact following delamination of the fat and muscular layers[343,353,355]. Dicing the organ into smaller pieces and performing decellularization under agitation yields a larger surface area, allowing for a reduction of the duration of the whole process[356]. Porcine skeletal and cardiac muscles have been reported to be successfully decellularized following mincing into smaller pieces (2-5mm) that have been used to create bioinks[357,358]. Perfusion decellularization has been of great interest with different vascular organs, as it minimizes the diffusion distance for the decellularizing agent(s)[333,355,359]. However, perfusion decellularization could be difficult to scale-up. In the present study, decellularization of porcine bladders was done using two techniques. A detergent-free and a detergent-based decellularization have resulted in complete decellularization of bladders, as we were able to observe the change in organ colour from pink to opaque white through the process. The images of native and decellularized bladders are shown in Appendix A (Supplemental figure 1).

4.3.1 Characterization of Decellularized Bladder Pieces

Hematoxylin-Eosin (H&E) and Alcian Blue-Nuclear Fast Red (AB/NFR) staining of the native bladder (Figure 4.3i) revealed the presence of urothelium, as 5-6 layers of transitional epithelial cells. Next to the urothelium, the lamina propria was identified to contain different cell types. The muscularis layer containing the smooth muscle cells have been also identified, densely stained in pink by eosin-containing stretched muscle cells. The detrusor muscular layer was not visible, as the process of delamination might have removed it. Following detergent-free decellularization, Figure 4.3i shows that nuclei are absent and certain regions of the lamina propria and muscularis have been preserved. The detergent-based decellularization also revealed the absence of nuclei but the overall microstructure was not preserved. One % SDS has been used to decellularize porcine bladders elsewhere[343] and the histological characterization revealed a similar analysis. Alcian Blue staining revealed the presence of glycosaminoglycans (GAGs) in decellularized samples

produced with both methods. GAGs aid cell attachment and proliferation as well as wound healing[360,361]. The detergent-free method has been reported for the decellularizing of porcine corneas, and results were comparable to SDS and Triton X-100 treatments[346]. The combination of freeze-thaw, hypertonic treatment and solvent extraction is reported for the first time here with porcine bladders.

SEM of native bladders revealed the presence of circular or oval shaped cells attached to a fibrous matrix (Figure 4.3i-SEM). Representative images are shown in Figure 4.3i-SEM and three images from three different bladder samples were analyzed. Cells were absent in the detergent-based and detergent-free decellularized samples. Collagen fibres, being the most abundant, were seen as fibrous structures preserved in the decellularized samples.

dsDNA quantification in native bladders indicated approximately 20 times the dsDNA concentration than those in decellularized bladder pieces, as revealed in Figure 4.3ii. This value is comparable to that (i.e., 13 times) reported elsewhere for a porcine bladder decellularized by perfusion[355]. The concentration of dsDNA in the detergent-free-treated bladders was comparable to the detergent-treated samples, as no statistical difference was found between the two groups. The histological characterization and dsDNA quantification revealed that the bladders were decellularized. dsDNA content was found to be in a range comparable to the values reported elsewhere, wherein sodium deoxycholate was used to decellularize porcine bladders[355]. Reports revealed reduced concentrations of dsDNA normalized to wet mass of the ECM (per milligram of sample) compared to native organs for decellularized corneas[362] and liver[363]. We have chosen to report the concentration of dsDNA normalized to mg of wet mass of the ECM produced using the detergent-free protocol because, as revealed in Appendix A, the measured dsDNA concentration depends on the ECM state used to extract DNA. We have tested three protocols to extract DNA and to report dsDNA concentration, as follows:

1. Wet ECM samples were weighted, then DNA extracted from those, and dsDNA concentration quantified and normalized per mg of wet mass of ECM. Results are presented in Figure 4.3 below.
2. DNA extracted from wet ECM samples and dsDNA quantified and normalized per mg of dry ECM mass. The dry mass was estimated by weighing a lyophilized sample obtained

from ECM having a wet mass equivalent to that used to extract the DNA. Results are presented in Appendix A (Supplemental figure 2).

3. Lyophilized ECM was weighted, then DNA extracted from this same lyophilized ECM sample and dsDNA quantified and normalized per mg of dry mass of ECM. Results are presented in Appendix A (Supplemental figure 2).

The ambiguity surrounding normalization of dsDNA content per mg dry mass of ECM has been reported elsewhere[364]. Crapo et al. [365] established that a decellularized organ should contain less than 50 ng of DNA per mg dry mass of ECM, as an arbitrary criterion for an acceptable decellularization. However, many commercial products such as TissueMend™ (TEI Biosciences, currently Stryker), Restore Orthobiologic Implant™ (DePuy Synthes, currently a part of Johnson and Johnson), GraftJacket™ Regenerative Tissue Matrix (LifeCell Corporation, currently Wright Medical Group), and AlloDerm Select™ Regenerative Tissue Matrix (Allergan Aesthetics, currently AbbVie) contain higher values of DNA[366,367] than that arbitrary threshold value.

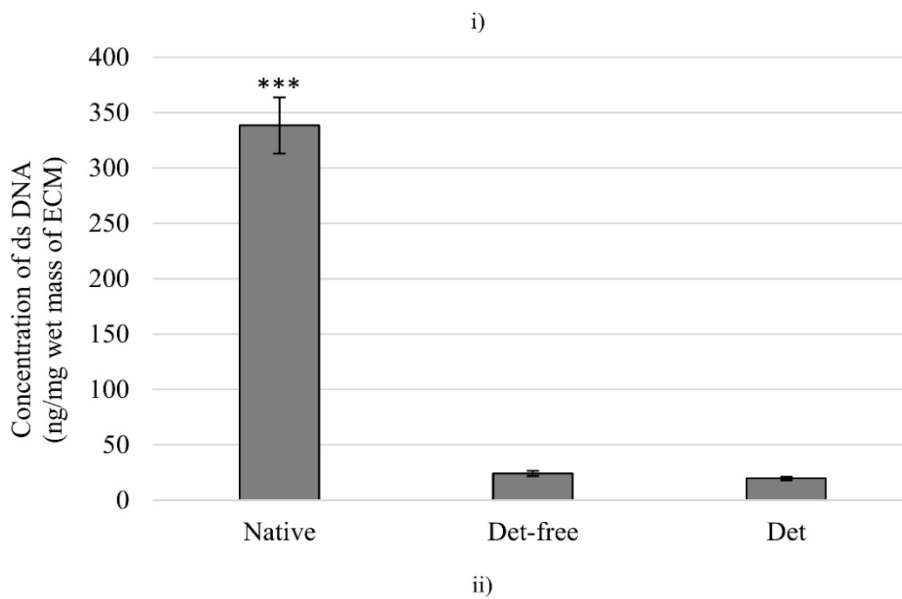
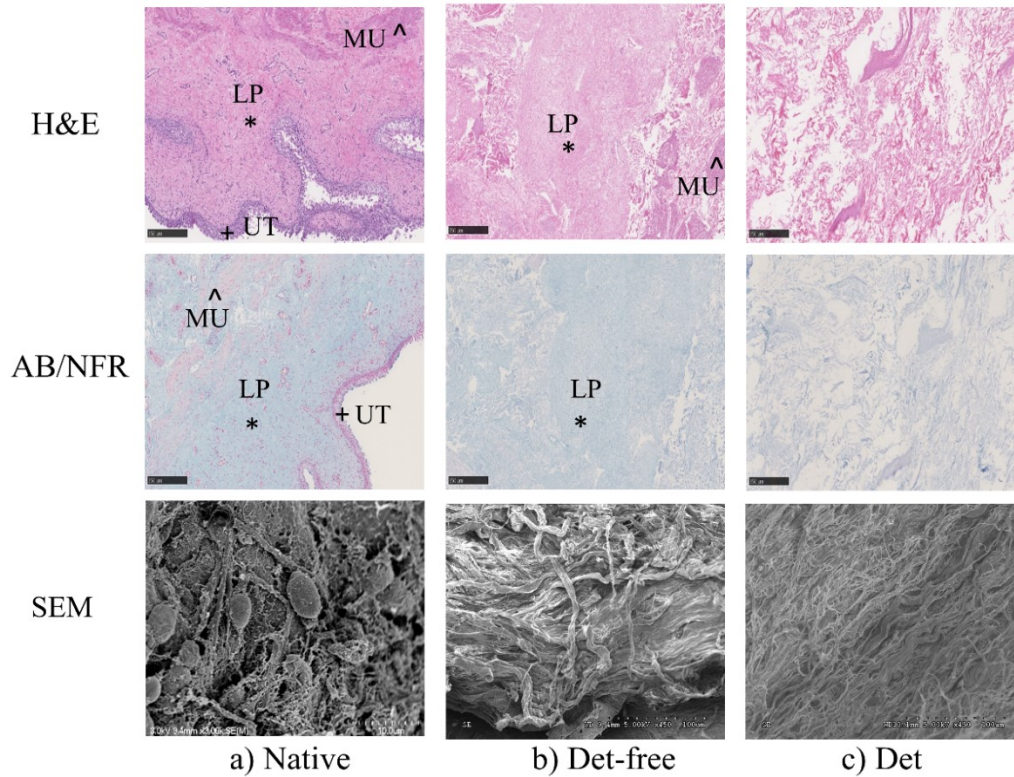


Figure 4.3 i) Hematoxylin-Eosin (H&E) staining, Alcian Blue and Nuclear Fast Red (AB&NFR) staining and Scanning Electron Microscopy (SEM) pictures of **a)** Whole native porcine bladders with excised fat and muscle layers, **b)** Detergent-free decellularized bladder pieces, and **c)** Detergent-decellularized bladder pieces. The scale bars represent 250 μ m. +UT indicates urothelium, *LP indicates lamina propria, ^MU indicates muscle layer. **ii)** dsDNA content of native, detergent-free-processed (Det-free), and detergent-processed (Det) bladders. Data are presented as means \pm standard errors.

4.3.2 Proliferation of INS-1 Cells on Decellularized Bladders

INS-1 cells cultured for 7 days on decellularized bladders were imaged using MTT. Representative images are shown in Figure 4.4a, whereas 3 different samples were inspected. Metabolically active cells were observed on detergent-free-processed bladders, as purple-stained cells were visualized (Figure 4.4a). Comparing to the controls, this confirms that the crystals did not arise from the matrix itself (Figure 4.4b). No purple spots were observed on detergent-processed bladders and control samples, suggesting that cells were not metabolically active and/or could possibly be dead (Figures 4.4c and 4.4d). Studies have reported proliferation of skeletal muscle cells[368], fibroblasts[343], adipose-derived stem cells[369] and myoblasts[370] on biomimetic materials derived from decellularized bladders.

The CyQUANT™ NF Cell Proliferation Assay indicated that INS-1 cells proliferated by approximately 14 times, as compared to the cell number of 25,000 initially seeded on detergent-free-processed bladders. Cell proliferation on tissue culture polystyrene (TCPS) and agarose was comparable to that on detergent-free-processed bladders (Figure 4.4e). The results obtained on TCPS were comparable to those of a study done earlier[371]. Detergent-free-processed bladders not seeded with cells (Det-free) revealed that the signal was not remnant from the ECM. Detergent-processed bladders did not support cell proliferation, as there was no significant difference when comparing to the detergent-processed bladders not seeded with cells (Det Ctrl). The use of multiple surfactants as post-treatment to SDS decellularization has been reported to potentially reduce the cytotoxicity of SDS[372,373]. In the present study, since no metabolically active cells were observed on SDS-processed bladders, we decided it was not worth performing immunostaining and glucose-stimulated insulin secretion (GSIS) with INS-1 cells seeded on those. Previously, studies have been conducted to characterize INS-1 cell proliferation and functionality on fibronectin-coated TCPS, RGD-coated TCPS, and fibrin[371,374,375]. Here, TCPS was selected as positive control, as it is our established reference for INS-1 cell attachment and functionality[376]. Culturing INS-1 cells on commercially available matrices such as MatriStem, Oasis or others could have been an option for instance, but it would be a study on its own, as no study of INS-1 cells on these matrices has been reported. Those materials cannot be used as established controls. For the 3D cell culture, control cultures were performed on INS-1 cell aggregates resulting from agarose exposure. In this case, aggregates were non-adherent, and

proliferation of cells was evaluated. Previously, we found that INS-1 cells form similar aggregates on low-fouling surfaces made from carboxy methyl dextran (CMD)[371]. Finally, the negative controls used here were ECMs with no cells. Hence, comparing cells responses on ECMs to those on TCPS and agarose allowed highlighting and isolating the effect of the ECM. Better visualization of the interaction between cells and detergent-free-processed bladders was observed by hematoxylin-eosin (H&E) staining of the samples (Figure 4.5), revealing that INS-1 cells were interacting with the ECM. Interactions were hypothesized from H&E-stained sections of cells on ECM, as shown in Figure 4.5. We noted that cells were firmly attached to the ECM pieces, as they were resisting media/solution changes and rinsing procedures performed during MTT and CyQUANT™ assays, while this was not the case for agarose *i.e.*, cells formed aggregates in suspension that were not attached to the agarose layer. In addition, immunostaining revealed cells having extensions pointing towards the ECM, as shown in Figure 4.6a. The interactions between the pancreatic β -cells and matrix proteins such as laminin-1, fibronectin and collagen IV are known to be vital to their survival[377–379]. Rat bladder carcinoma 804G-derived ECM was found to help in the attachment, proliferation and functionality of β -cells[380].

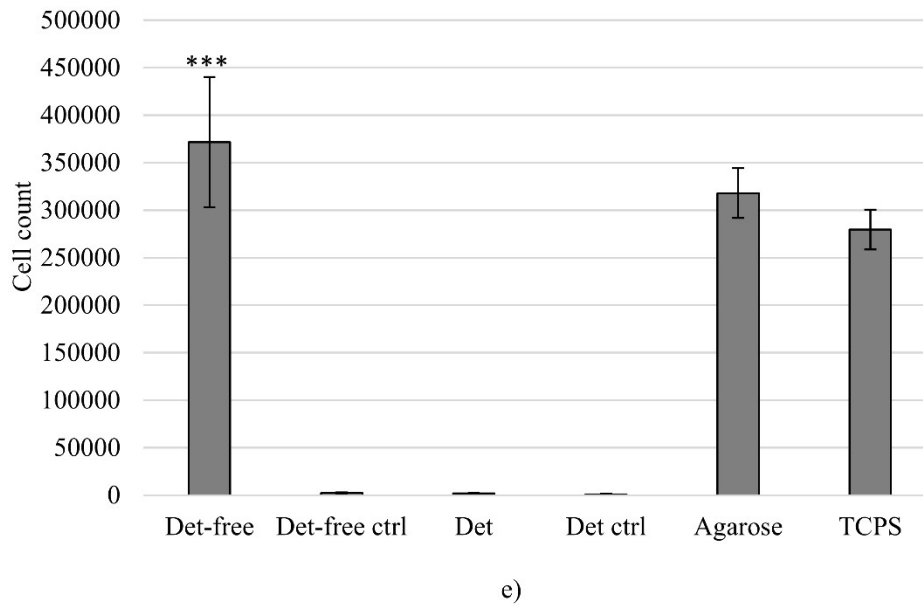
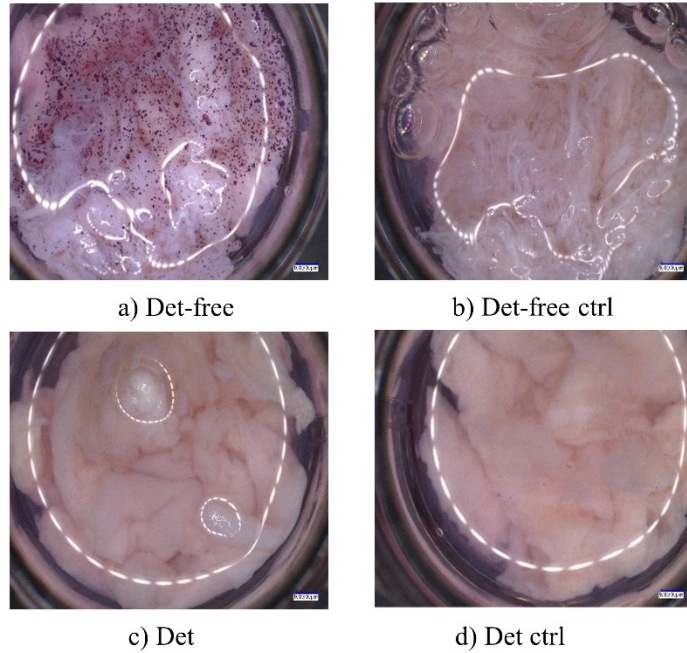


Figure 4.4 MTT staining of **a)** INS-1 cells on detergent-free-processed bladders (Det-free); **b)** Detergent-free-processed bladders with no cells (Det-free Ctrl); **c)** INS-1 cells on SDS-treated bladders (Det); **d)** SDS-treated bladders with no cells (Det Ctrl). Scale bar represents 1000 μm . **e)** Quantification of cells using the CyQUANT™ NF Cell Proliferation Assay. Data are presented as means \pm standard errors.

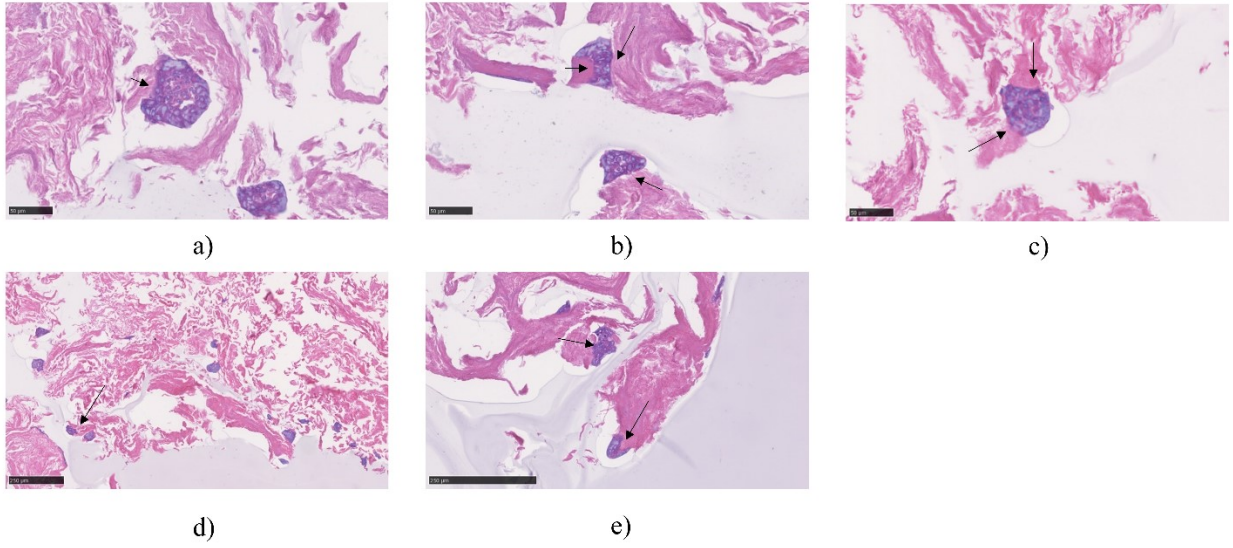
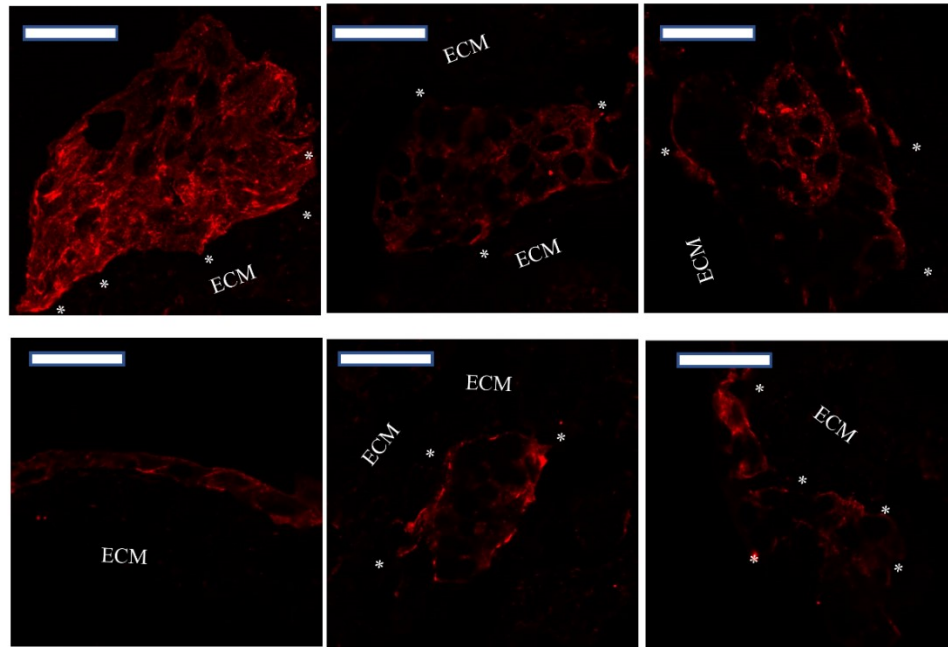
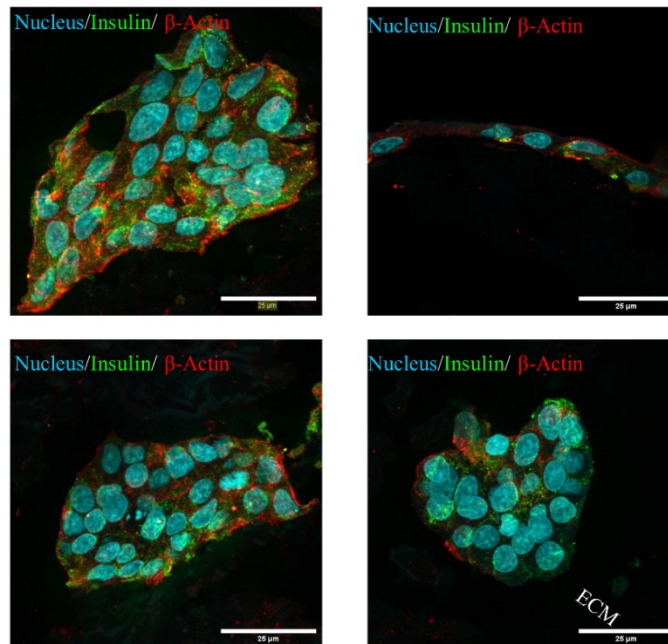


Figure 4.5 Hematoxylin and Eosin (H&E) staining of INS-1 cells cultured for 7 days on detergent-free-processed bladders (Scale bars represent 50 μm for a, b, and c; 250 μm for d and e). The interactions between the ECM and the cells are indicated as black arrows.



a)



b)

Figure 4.6 a) β -actin immunostaining of INS-1 cells. Cell cytoskeleton protruding towards the ECM allows us hypothesizing interactions between the cells and the ECM, as highlighted by white stars. **b)** Representative images of immunostaining of INS-1 cells on detergent-free-processed bladders for insulin (green) and β -actin (red). Three different samples with 3 images per sample were analyzed. DAPI stained nucleus (blue). Scale bars represent 25 μ m.

4.3.3 Functionality of INS-1 Cells

The glucose-stimulated insulin secretion (GSIS) assay revealed that INS-1 cells cultured on detergent-free-processed bladders were functional following 7-day cultivation, as shown in Figure 4.7. The trend in insulin secretion in response to the different glucose concentrations was as reported in a previous study in which mouse islets were seeded in decellularized mouse pancreas[337]. Comparing insulin secretion of INS-1 cells on TCPS, the insulin secretion was higher for the INS-1 cells on detergent-free-processed bladders. The stimulation index *i.e.*, ratio of insulin concentration at high-glucose stimulation to that at low-glucose, was higher for cells on TCPS compared to that on detergent-free-processed bladders. The stimulation index of cells on bladders (1.3 ± 0.2) was comparable to that of INS-1 cells cultured in fibrin for 48 hours[376]. The stimulation index of INS-1 cells on TCPS (2.1 ± 0.5) was comparable to that of a culture on fibronectin-coated plates[381]. The stimulation index according to the insulin secretion in a 3D hydrogel was lower as compared to 2D culture[382]. However, it is difficult to compare the two systems (TCPS and 3D culture), as the 3D culture system may create a diffusional barrier and/or can result in trapped insulin content[337,383]. Cell-matrix interactions were reported to influence survival and insulin secretion of β -cells by activation of NF- κ B signaling[374,384–386]. Laminins were reported to be the basement membrane proteins responsible for insulin gene expression and β -cell proliferation[387]. Laminins could have potentially been conserved in the Det-free samples and could have supported insulin expression and, thereby, functionality (this aspect is the subject of a subsequent study in preparation).

Functionality was also confirmed by immunostaining (Figure 4.6b). The intracellular insulin was revealed in green, confirming that INS-1 cells expressed insulin after the 7-day culture period. The nuclei, stained in blue, showed a regular nuclear structure. The staining for β -actin in red revealed the cell cytoskeleton. The formation and structure of actin along the bladder ECM pieces, shown in Figure 4.6a, revealed that cells were aligned towards the ECM. Certain proteins such as vinculin, talin and integrins are involved in establishing a protein-mediated ECM-actin linkage[388]. Regions of cell attachment to the ECM, also known as the focal adhesion points, could be hypothesized from the observed extensions of the cytoskeleton. Staining for vinculin was not performed as the primary mouse antibody needed for staining vinculin in rat cells could not be shipped to Canada.

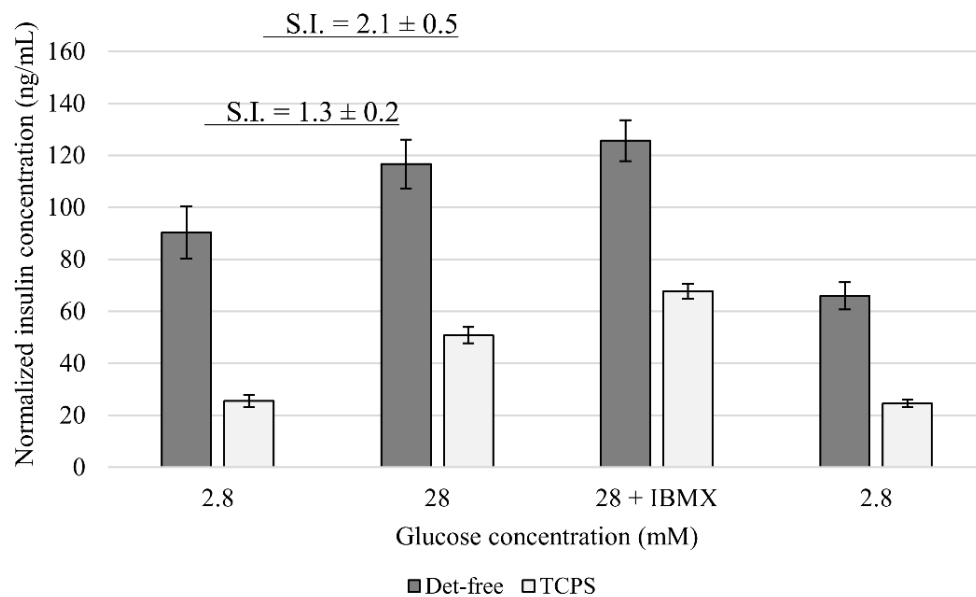


Figure 4.7 Functionality of INS-1 cells- validated by a glucose-stimulated insulin secretion (GSIS) assay. S.I. indicates the stimulation index defined as the ratio of insulin concentration secreted at high-glucose to that at low-glucose stimulation. S.I. are represented as means \pm standard deviations. S.I. for the Det-free condition was 1.3 ± 0.2 and for the TCPS condition was 2.1 ± 0.5 .

4.4 Conclusions

This study presents the design of a 3D cell culture system and its validation in the cultivation of a β -like cell line (INS-1 cells). The system was successfully used to validate the effect of Extracellular Matrix (ECM) pieces on cells in a 3D environment, while preserving as much as possible the ECM (ultra)structure. The study reveals that ECM derived from decellularized porcine bladders can be used as a biocompatible scaffold for the culture of pancreatic β -like cells. Also, it illustrates that the method of decellularization plays a crucial role in the process. One of the goals of this experimental work was to study the effect of two decellularization methods on the ECM activity towards INS-1 cells. Our work is one of the few studies that maintains the ECM as much as possible in its original form in contrast to other studies transforming the ECM into gels or membranes to perform *in vitro* cell culture. The scope of this article extends to other applications of this 3D tissue culture system to investigate the effect of ECMs derived from different organs or tissues on the recellularization using different cell lines (attachment, proliferation, and functionality) and primary tissues. ECM-derived scaffolds, with preserved (ultra)structure, open the door to support the culture of stem cells including iPSCs.

Acknowledgements

We thank Vincent-Daniel Girard for the statistical analysis and graph preparation. We thank Pakindame Boabekoa and Tamara Challut for technical help. We thank Marilène Paquette and the histology research core facility of the Faculté de Médecine et des Sciences de la Santé (Université de Sherbrooke) for the histology service, and Charles-Bertrand for the SEM sample preparation and operation.

This research project was supported by NSERC through a Discovery Grant awarded to Patrick Vermette (Grant # 250296-2012). All authors have approved the final manuscript.

Patrick Vermette owns shares in SherMATRIX Inc., a company developing biomaterials for clinical uses.

Chapter 5

Characterization of Extracellular Matrix Derived from Decellularized Porcine Organs

Foreword

Authors and Affiliations:

Vignesh Dhandapani: Ph.D. candidate, Université de Sherbrooke, Département de génie chimique et de génie biotechnologique

Boabekoa Pakindame: Training student, Université de Sherbrooke, Département de génie chimique et de génie biotechnologique

Martin Borduas: Professor, MD, Département de pathologie de l'Université de Sherbrooke, Faculté de médecine et des sciences de la santé

Patrick Vermette: Professor, ingénieur, Université de Sherbrooke, Département de génie chimique et de génie biotechnologique

Date of Submission: March 17th, 2023

State of Acceptance: Under Review

Journal: Journal of Biomedical Materials Research Part B: Applied Biomaterials

Contribution:

The article presents the characterization of extracellular matrix (ECM) derived from different porcine organs decellularized by detergent-based and detergent-free techniques. The article was submitted to the *Journal of Biomedical Materials Research Part B: Applied Biomaterials*. The experimental design was done mainly by Vignesh Dhandapani and Patrick Vermette. All the experimental work was performed by Vignesh Dhandapani, assisted by Boabekoa Pakindame and Tamara Challut. The results were analyzed by Vignesh Dhandapani, Martin Borduas and Patrick Vermette. The article was mainly written by Vignesh Dhandapani and Patrick Vermette. It was reviewed by Patrick Vermette and Martin Borduas. All the work was done under the guidance and supervision of Patrick Vermette.

Titre en français :

Caractérisation de la matrice extracellulaire dérivée d'organes porcins décellularisés

Résumé :

La médecine régénérative a repoussé les capacités de la médecine à un point tel que la fabrication de tissus et d'organes pourrait être industrialisée. Cela pourrait résoudre les problèmes liés à la transplantation d'organes. Le principal composant des tissus et des organes responsable de leur structure et de leur fonction est la matrice extracellulaire (MEC). La MEC fournit un échafaudage de soutien et des signaux biochimiques permettant aux cellules de se fixer, de proliférer et de se différencier. La MEC est composée de différentes protéines fibreuses et de protéoglycanes. Dans cette étude, quatre protocoles ont été utilisés pour décellulariser des organes porcins. Les MEC ont été caractérisées par des méthodes histologiques illustrant l'absence de noyaux et la présence de glycosaminoglycanes (GAG) et de collagène. L'analyse à l'hématoxyline et à l'éosine du pancréas natif a révélé une nécrose par autodigestion, corroborée par une teneur réduite en ADNdb, et pourrait avoir conduit à la destruction du collagène de type IV, des laminines et d'autres protéines dans les MECs résultantes, comme le confirme la spectrométrie de masse. La quantification de l'ADN de la MEC a révélé des contenus résiduels d'ADNdb inférieurs à ceux des organes natifs. Le dosage par l'acide bicinchoninique (BCA) a montré une différence de contenu protéique entre les organes. La spectrométrie de masse couplée à une analyse protéomique a mis en évidence une différence significative dans la composition protéique. Le nombre de protéines différentes, dans certains cas plus de 2700, dans la MEC ainsi produite dépendait de la technique de décellularisation appliquée. La microscopie à polarisation a indiqué des différences dans l'orientation des fibres de collagène. L'étude pourrait aider à caractériser en détail les MEC (matrices extracellulaires) obtenues à l'aide de différentes techniques de décellularisation. De plus, elle pourrait contribuer à trouver un équilibre entre le maintien de l'ultrastructure et la composition de la MEC et l'élimination des composants cellulaires.

Mots clés : Matrice extracellulaire (MEC), Décellularisation de tissus et d'organes, Glycosaminoglycanes (GAG), Collagènes, Laminine, Spectrométrie de masse et protéomique.

Abstract:

Regenerative medicine has extended the capacity of medicine to a point where tissues and organs could potentially be manufactured. This could resolve issues associated with organ transplantation. The Extracellular Matrix (ECM) provides a supportive scaffold and biochemical cues allowing cells to attach, proliferate and differentiate. The ECM is composed of different fibrous proteins and proteoglycans. In this study, four protocols were applied to decellularize porcine organs. The ECMs were characterized by histological methods illustrating the absence of nuclei and presence of glycosaminoglycans (GAGs) and collagen. Hematoxylin and eosin analysis of native pancreas revealed necrosis by auto-digestion, also supported by a reduced dsDNA content, and could have led to the destruction of type IV collagen, laminins, and other proteins in the resulting ECMs as confirmed by mass spectrometry. DNA quantification of ECM revealed residual dsDNA contents lower than those of the native organs. Bicinchoninic acid (BCA) assay showed a difference in protein content between organs. Mass spectrometry coupled with proteomic analysis highlighted a significant difference in protein composition. The number of different proteins, in some cases with more than 2700, in the produced ECM depended on the applied decellularization technique. Polarization microscopy indicated differences in the orientation of collagen fibers. The study could help characterize ECMs obtained using different decellularization techniques in detail. Further, it could aid in finding a balance between maintaining the ultrastructure and composition of ECM and removing the cellular components.

Keywords: Extracellular Matrix (ECM), Tissue and Organ Decellularization, Glycosaminoglycans (GAGs), Collagens, Laminin, Mass Spectrometry and Proteomics.

5.1 Introduction

Scaffolds made of ExtraCellular Matrix (ECM) are more and more considered in reconstructive surgery and regenerative medicine. Each organ and tissue in the body has a distinctive ECM with unique composition and topology[389]. Synthetic or natural materials have been investigated to create three-dimensional scaffolds with the aim to mimic the ECM of organs. This has raised significant interest about the scope of application of ECM-derived scaffolds in tissue engineering and regenerative medicine. The ECM includes the secretory products of cells providing cues for cell proliferation, migration and differentiation[389–391]. The ECM is generally composed of 1) structural proteins (e.g., collagens, laminins, fibronectin, elastin and tenascins) that are fibrillar and insoluble, interacting with each other giving a structure and shape to organs; 2) globular proteins (e.g., cytokines, growth factors and other matrix metalloproteinases (MMPs)) aiding in cell signalling and ECM network remodelling[392] and; 3) proteoglycans (e.g., glycosaminoglycans (GAGs)) contributing to hydration of the ECM and interactions with growth factors, cytokines and cell receptors[331].

Decellularized organs are one of the sources to obtain ECM. It involves the removal of cellular components from the tissue or organ hence, leaving the ECM[334]. Different techniques have been applied to decellularize organs. Examples include: 1) chemical and enzymatic methods[337,338,340,341,393–397] involving the use of detergents such as sodium dodecyl sulfate (SDS), sodium deoxycholate, Triton X-100, 3-([3-cholamidopropyl]dimethylammonio)-1-propanesulfonate hydrate (CHAPS), trypsin, ethylene diamine tetracetic acid (EDTA) and hypertonic solutions and 2) mechanical and physical methods, which include snap-freezing, agitation, freeze-thawing, sonication and hydrostatic pressure. Combination of these methods have been reported to be effective to remove cellular materials, while preserving the ECM[398–400].

Understanding ECM organization and composition is necessary to appreciate its full potential. Several characterization techniques have been used. Alcian blue staining has been applied to confirm the conservation of GAGs[401,402]. GAGs such as hyaluronic acid, chondroitin sulfate, keratan sulfate, dermatan sulfate and heparan sulfate[403] have been used to engineer constructs for a myriad of diseases and for cartilage regeneration[404–407].

Collagen is the main constituent of connective tissues, such as tendons, bones and skin[408]. In vertebrates, 28 types of collagens (I-XXVIII) have been identified[409–411]. They occur as triple-helix of α -polypeptide chains. In the ECM, collagens are organized as supramolecular entities defined by the type of collagen composed from different amino-acid sequences and by the 3D folding of their tertiary structures[412]. Fibrillar collagens include type I, II, III, V and XI. They merge to form collagen fibers of micrometric sizes and are present in all tissues. Collagen I is the most prominent in the body and is predominantly present in the dermis and bones[413], while it is collagen II for cartilage[414]. Basement membranes are found in every tissue and are organized glycoproteins providing a structural and functional support to cells. Collagen type IV is predominant in basement membranes[415,416].

Laminins, heterotrimeric glycoproteins made of α , β and γ polypeptide chains[417] are associated with collagen IV and are present in basement membranes. They are important for cell attachment, as they help cell integrin receptors to attach to the ECM. Overall, 16 distinct forms of laminins have been identified, made from three different chains: 5 α , 3 β and 3 γ chains[418,419].

Fibronectin is a dimeric glycoprotein formed by association of two non-identical monomers making two disulfide bridges at the C-terminal. Fibronectin is coded by one gene and is found in the ECMs of most organs, a soluble form also circulates in the blood[420]. It interacts with collagens or integrins[421].

Tropoelastin monomers coordinate to form elastin fibers and are associated with fibrillar collagen to impart elasticity to the ECM and compensate for the tensile strength of collagen[422].

Although extensive studies have reported on the organization and composition of ECM in native or diseased organs, very few have reported on the composition of ECM in decellularized organs. The objective of the present study was to investigate the structure and composition of the ECM resulting from four decellularization techniques. Five porcine organs (bladder, kidney, lung, liver, and pancreas) were decellularized. The techniques included 1) SDS-decellularization, 2) Freeze-thawing and osmotic cell lysis followed by an ethanol extraction, 3) EDTA treatment, freeze-thawing and osmotic cell lysis, followed by an ethanol extraction, and 4) Isoelectric extraction with pH adjustment, freeze-thawing and osmotic cell lysis, followed by an ethanol extraction. SDS was chosen as it is one of the most common detergents used in decellularization, resulting in effective removal of cells from different organs[337,423,424]. The freeze-thaw method was

selected as some organs have been decellularized using this detergent-free method[335,351], showing potential to maintain the ECM ultrastructure. Combined with the freeze-thaw method, isoelectric treatment using pH adjustment and EDTA-chelating methods were used with the hypothesis that they would result in the removal (or reduction at least) of hemoglobin content from the resulting ECMs. ECMs were further characterized by Hematoxylin and Eosin (H&E) staining to detect the presence of nuclear materials, Alcian Blue and Nuclear Fast Red (AB/NFR) staining to investigate the presence of GAGs, and Trichrome-Masson staining to visualize collagens. The double stranded (ds)DNA content and protein content in the extracted and purified ECMs were quantified. Exploring the ECM composition and collagen orientation was done using mass spectrometry coupled with proteomics analysis, and polarized light microscopy, respectively.

5.2 Materials and Methods

5.2.1 Organ Decellularization

Porcine bladders, kidneys, lungs, livers, and pancreas from three different porcine donors (N=3) were freshly acquired from a slaughterhouse (Abattoir Régional de Coaticook, Coaticook, Québec, Canada) within 24 hours of animal sacrifice, transferred to the lab and put on ice. The porcine bladders were procured from a licensed slaughterhouse and since the animal sacrifice was performed under strict regulated conditions, the tissues needed no approval from the ethics committee of the Université de Sherbrooke. Fat and muscle layers of bladders were excised followed by delamination[343,353]. The resulting tissues were diced into approx. 5mm x 5mm pieces. Fat from the other organs were excised, the organs cut into pieces, weighed, and fed into a meat grinder (Heavy-duty Electric Meat Grinder, Model #8 ¾ HP Motor, Weston, Southern Pines, NC, USA). Grinding organs was done with ice to prevent damage due to the generated heat during grinding, as shown in Appendix B (Supplemental figure 3). Further, decellularization was carried out by four techniques of which the first two techniques have been described elsewhere[1].

- 1. Detergent (SDS)-based decellularization (Det):** Briefly, bladder pieces (approx. 40-50g) and, for the other organs, slurries were washed in distilled water and decellularization was done for 30 ± 1 hours using 0.5% Sodium Dodecyl Sulfate (SDS, 161-032, Biorad, CA, USA). The decellularized samples were washed again in distilled water containing 1% penicillin/streptomycin to remove the residual SDS, filtered and stored at -20°C until further use.
- 2. Detergent-free decellularization (Det-free):** Bladder pieces (approx. 40-50g) and, for the other organs, slurries were washed in Milli-Q water and decellularization was initiated using 2M sodium chloride under agitation (New Brunswick Innova® 44/44R, Eppendorf, Hamburg, Germany) at 37°C . An overnight washing step in Milli-Q water was performed at 37°C . Tissues were subject to 2 freeze-thaw cycles in liquid nitrogen and Milli-Q water at 37°C . Samples were then blended with ice, filtered, and washed for 1 hour each in 2M sodium chloride, 3 times in Milli-Q water, and finally overnight in Milli-Q water at 37°C , 200 rpm. They were washed twice in 70% ethanol, once in 1X PBS and overnight in 1X PBS containing 1% penicillin/streptomycin. Samples were filtered and stored at -20°C until further use.

3. Detergent-free decellularization with EDTA-chelating treatment (Det-free + EDTA):

This third protocol is based on the second, with the exception that the first Milli-Q water overnight incubation was substituted by an overnight incubation in 0.5% ethylenediamine tetra acetic acid (EDTA) with the aim to limit blood clotting[425], so the hemoglobin still present in the organs could be washed away.

4. Detergent-free decellularization with isoelectric extraction using pH adjustment (Det-free + pH):

This fourth protocol is also based on the second one, with the first Milli-Q water overnight incubation replaced by an overnight incubation in Milli-Q water with pH adjusted to 6.6 using sodium hydroxide and ammonium sulfate to extract/precipitate the residual hemoglobin in the tissue at its isoelectric point[426].

5.2.2 Histological Characterization

Native and decellularized organs were fixed in 4% paraformaldehyde (PFA) (P16148, Sigma-Aldrich) for 48 hours. Samples were treated in a tissue processor, embedded in wax, then sliced into 4- μ m sections. Sections on glass slides were dried for 48 hours at 37°C. They were analyzed using 1) Hematoxylin and Eosin (H&E) staining to detect the presence of nuclei and collagen, 2) Alcian Blue and Nuclear Fast Red (AB/NFR) to investigate the presence of glycosaminoglycans (GAGs), negatively charged polysaccharides involved in cell signalling, ECM hydration and structural scaffolding[427], 3) Masson-Trichrome (MT) for better contrast visualization of collagens, and 4) Picrosirius Red (PR) to evaluate collagen fibers orientation, according to the standard laboratory protocol. The prepared glass slides were visualized, and the images were acquired in visible mode using a NanoZoomer 2.0-RS (Hamamatsu Photonics K.K, Bridgewater, NJ, USA) at a magnification of 20x.

5.2.3 DNA extraction and PicoGreen Assay for dsDNA Quantification

Samples of native and decellularized organs were weighed and solubilised in proteinase K solution to digest proteins in the ECM. The DNA extraction was performed by the conventional phenol,

chloroform and isoamylalcohol (PCI) method[354]. Briefly, the digested solution was centrifuged multiple times with a mixture of phenol:chloroform:isoamyl alcohol (25:24:1 volume ratios) to extract DNA. A centrifugation step with chloroform:isoamyl alcohol (24:1) was done to remove residual phenol. Finally, the DNA was precipitated in ethanol containing 3M sodium acetate overnight at -20°C. DNA was pelleted by centrifugation and suspended in 1X Tris EDTA buffer. The dsDNA quantification was performed using the Quant-iT™ PicoGreen™ dsDNA assay kit (P7589, Thermo Fisher Scientific, Waltham, MA, USA). The fluorescence was measured at an excitation 480 nm using a plate reader (Synergy HT Microplate Reader, Biotek, Agilent, Santa Clara, CA, USA).

5.2.4 Bicinchoninic acid (BCA) Assay for Protein Quantification

Initially, 200 mg of the organs were weighed and solubilized in 10 mL of 1M sodium hydroxide (NaOH) at 37°C under an agitation of 250 rpm for 24 hours. The solution was filtered using a 0.45 µm pore size syringe filter (SLHV033RB, Millipore Sigma, St-Louis, Missouri, USA). Pierce™ BCA Protein Assay Kit (23227 Thermo Fisher scientific, Waltham, MA, USA) working reagent was prepared by mixing Reagent A and Reagent B in the ratio of 50:1. 200 µL of the working reagent were added to 25 µL of the protein solution in a 96-well plate. The plates were incubated at 37°C for 30 minutes and the absorbance was recorded at 562 nm using a plate reader (Synergy HT Microplate Reader, Biotek, Agilent, Santa Clara, CA, USA).

5.2.5 Digestion of ECM for Mass Spectrometry and Proteomics Analysis

ECMs were solubilized in 8M urea containing 10 mM HEPES followed by pulse sonication. Subsequently, 100 µL of the solubilized solution containing a maximum of 75 µg of extracted proteins (quantified by the BCA kit) were transferred to a low protein binding tube. Boiling and incubation in 5 mM dithiothreitol (DTT) was done to remove the disulfide bonds. Incubation in 7.5 mM chloroacetamide was done to reduce the reformation of the disulfide bonds by reacting with the reduced cysteines. Ammonium bicarbonate (50 mM) was added to lower urea

concentration and to optimize the action of trypsin at pH 8. Overnight trypsin (1 μg) treatment at 30° C under agitation was done to digest the proteins into peptides. The samples were vacuum-dried and acidified using 0.2% trifluoroacetic acid (TFA). Zip-Tip technique was performed to extract the peptides by repeated pipetting of samples through the special membrane designed to capture the peptides. Elution of the captured peptides was done using repeated pipetting in the elution buffer containing 1% formic acid and 50% acetonitrile.

5.2.6 Mass Spectrometry (LC-MS/MS) for Protein Identification

The Dionex Ultimate 3000 nanoHPLC system was used to separate the trypsin-digested samples. Samples of 10 μL volume (1.5 μg in total) in 1% formic acid (FA) were loaded with a 4 $\mu\text{L}/\text{min}$ constant flow onto an Acclaim PepMap100 C18 nanocolumn (75 μm x 50 cm, Dionex Corporation)[428,429]. A linear gradient of 5-35% of solvent B (80% acetonitrile with 0.1% FA) was established with a flow of 200 nL/min over 240 minutes. An EasySpray Source was used to couple the HPLC system to the OrbiTrap QExactive mass spectrometer (Thermo Fisher Scientific, Waltham MA, USA). The temperature of the column and spray voltage were set to 40°C and 2.0 kV, respectively. Full scan MS survey spectra (m/z 350-1600) in profile mode were acquired in the OrbiTrap at a resolution of 70,000 following the accumulation of 1,000,000 ions. From the preview scan, the top 10 most intense peptide ions were further fragmented by collision-induced dissociation (resolution of 75,000 and normalized collision energy 25%) after 50,000 ions accumulation. The maximal filling times for full scans and MS/MS scans were 250 ms and 60 ms, respectively. Precursor ion charge state screening was enabled and all unassigned charged states, singly, 7 and 8 charged species were rejected. The dynamic exclusion list was limited to 500 entries with a relative mass window and retention period of 10 ppm and 40 s, respectively. The lock mass option for survey scans was enabled to improve mass accuracy and the data were gathered using the Xcalibur software (version 4.3.73.11).

5.2.7 MaxQuant Analysis for Protein Identification

Following the run, peptides were identified and quantified using MaxQuant software version 2.0.3.0 with Uniprot proteome database (*Sus scrofa*)[429]. The MaxQuant analysis was performed with the following settings: 2 miscleavages allowed, fixed modification of carbamidomethylation on cysteine, trypsin as enzyme (K/R not before P), variable modifications including methionine oxidation, protein carbamylation (K,N-terminal) and protein N-terminal acetylation. Mass tolerances of 4.5 ppm and 20 ppm were used for precursor ions and fragment ions, respectively. The identification values such as the “Protein FDR”, “Site Decoy Fraction” and “PSM FDR” were set to 0.05. The minimum peptide count was set to 1. The Label-Free-Quantification (LFQ) was selected, and a minimal ratio count of 2 was fixed. “Second peptides” was selected and the results were organized and sorted according to different parameters. Proteins positive for either “Reverse”, “Only.identified.by.site” or “Potential.contaminant” were eliminated along with proteins identified from single peptides. The intensity values for each proteins identified were exported in Excel. The number of proteins in each condition was plotted using InteractiVenn©[430].

5.2.8 Polarization Microscopy and Image Analysis for Collagen Fibers Orientation

ECM sections stained for Picrosirius Red were imaged using a Polarization Microscope Zeiss Axioscope 5 (Carl Zeiss Microscopy GmbH, Oberkochen, Germany). Collagen fibers were observed using polarized light at 10X magnification. The Axiocam 305 (Carl Zeiss Microscopy GmbH, Oberkochen, Germany) was used to live capture the image with a gamma of 0.45 and intensity of 43.1%. Image J version 1.53r (Bethesda, Maryland, USA) was used to analyse the captured images. Briefly, the image was converted into 8-bit and the orientation was observed using the Orientation J Analysis with Gaussian gradient and a local window of 1-pixel. For the distribution of orientation, a Gaussian gradient was used, with a local window of 1-pixel, a minimum coherency, and an energy of 10%.

5.2.9 Data Analysis

Microsoft Excel (version 2208) was used to prepare the graphs. The data were gathered from 3 different experiments. The mean values were plotted in graphs with standard errors indicated by the bars.

5.3 Results and Discussion

5.3.1 Decellularization Process

Perfusion decellularization has been used to decellularize whole organs allowing for retaining the whole architecture of the ECM[337,355]. The initial step of grinding the organs (except for the bladder) was done to increase surface area to facilitate their decellularization. This step enables efficient decellularization with minimal time of exposure[356]. Since bladder is a muscular tissue, it was diced into smaller pieces with scissors following delamination instead of grinding. Appendix B (Supplemental figure 4) indicates that the process of grinding did not affect the organs, as H&E images of ground organs were comparable to those of native ones, as shown in Figure 5.1.

The glomerulus in kidneys was clearly visible in grounded samples. For grounded lungs, the bronchioles and alveolar sacs were also visible. Delaminated and diced bladders contained the urothelium and the lamina propria with reduced muscularis. The livers populated with cells along with the septum were identified in grounded native samples.

Hemoglobin is a tetramer containing 2 alpha and 2 beta subunits[431]. Following decellularization by the SDS-based and detergent-free methods, samples were analyzed using a mass spectrometer for the presence of hemoglobin. The SDS-based method was able to remove cytochrome c and the alpha and beta subunits of hemoglobin, as compared to the detergent-free method (Table 5.1). The release of massive amounts of hemoglobin subunits in the blood plasma has been reported to lead to toxicity in the kidneys[432]. Hence, two additional protocols were developed and applied, based on the detergent-free method. 1) Isoelectric extraction/precipitation by adjusting the pH of the suspension to 6.6 using sodium hydroxide and ammonium sulfate during decellularization to precipitate and remove hemoglobin, as the isoelectric point of its β -subunits is 6.1-6.8[433]. 2) Addition of 0.5% EDTA to chelate the iron molecules in hemoglobin. Decellularization using pH adjustment and EDTA treatment resulted in pale brown ECMs for kidneys, livers, and lungs, as compared to dark brown ECMs obtained by the bare detergent-free method not using pH and EDTA treatments, as shown in Appendix B (Supplemental figure 5). Although mass spectrometry has qualitatively indicated the presence of the hemoglobin A and hemoglobin B subunits in the pH-adjusted and EDTA-treated samples, we hypothesize that a significant amount of hemoglobin has been removed from the tissues, as indicated by the colour change.

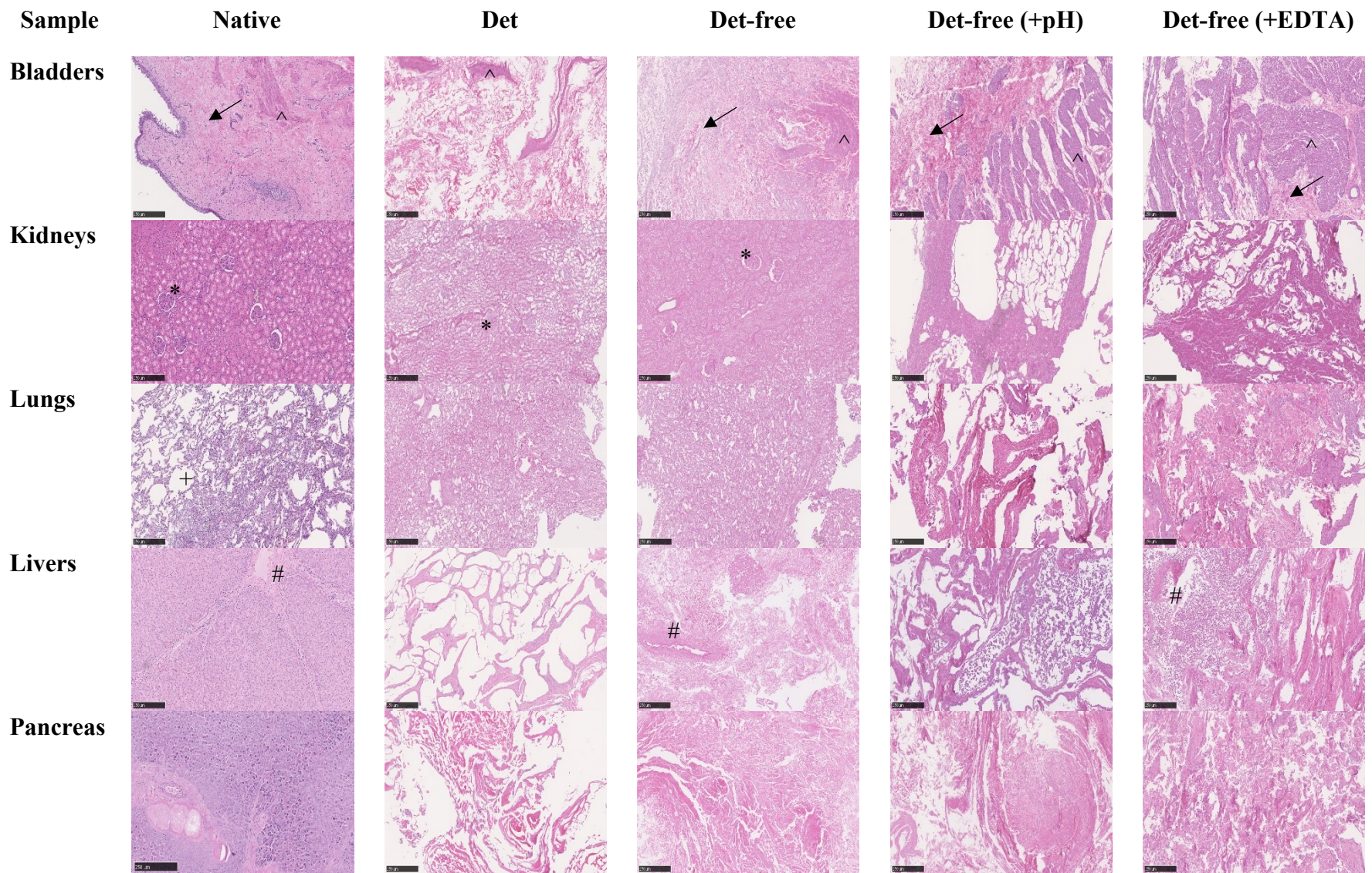


Figure 5.1 Hematoxylin-Eosin (H&E) staining of native and decellularized porcine organs. Scale bars represent 250 μm . * represents glomerulus, # indicates portal vein, + indicates the alveolar sacs, ^ indicates muscular layer, and \rightarrow indicates lamina propria. Purple-colored nuclei are stained by hematoxylin and ECM in pink by eosin.

Table 5.1 Detection of alpha and beta subunits of hemoglobin in the decellularized organs.

Hemoglobins	Bladders				Kidneys				Lungs				Livers				Pancreas			
	D	DF	DFP	DFE	D	DF	DFP	DFE	D	DF	DFP	DFE	D	DF	DFP	DFE	D	DF	DFP	DFE
Hemoglobin alpha subunit	-	+	+	+	+	+	+	+	+	+	+	+	+	+	+	+	-	-	+	+
Hemoglobin beta subunit	-	+	+	+	+	+	+	+	+	+	+	+	+	+	+	+	-	-	+	+

D indicates detergent (SDS)-based, DF indicates detergent-free, DFP indicates detergent-free + pH adjustment and DFE indicates detergent-free with EDTA-treatment decellularization.

5.3.2 Characterization of Decellularized Organs

H&E staining of native organs revealed the presence of nuclei as dark purple spots (Figure 5.1). The cytoplasm appeared as pale pink with the ECM stained as dark pink. All tested methods yielded efficient decellularization, as evidenced by the lack of nuclei in Figure 5.1, compared to the native organs. The detergent-free method was able to preserve certain structures in the organs, such as the lamina propria and the muscularis in bladders, the glomerulus and the distal convoluted tubules in kidneys, bronchioles in lungs and the septum in livers. Our H&E analysis was similar to those obtained with different techniques used to produce decellularized porcine bladders[353,434], livers[435], kidneys[436] and lungs[437,438]. An important observation was made for the native pancreas, from Figure 5.1. The H&E staining of the harvested pancreatic tissue, even when procured from the slaughterhouse, indicated that the native pancreas seemed necrotic with a fat-necrosis appearance, probably the result of an auto-digestion with a beginning of saponification and surrounding apoptosis. Pancreas is a sensitive organ and, with acinar cells secreting digestive enzymes, the pancreas could start auto-digestion process when removed and kept too long[439–441]. We decided to pursue the analysis of the resulting tissue to compare with the others. The detergent (SDS)-based method resulted in matrices in which we could not identify any structures. The preservation of GAGs in the decellularized organs was revealed in Figure 5.2. The significance of GAGs in the ECM obtained after decellularization has been highlighted elsewhere[442]. However, in the detergent-free decellularized kidneys and livers, remnant cytoplasm was visible. As most studies have defined decellularization by the removal of nuclear content, however, some have indicated the presence of cytoplasmic content in the resulting matrices and have defined the decellularization to be inefficient[343] or incomplete[372]. Trichrome-Masson staining revealed the presence of collagen fibers in the ECM of native and decellularized organs (Figure 5.3). Muscle fibers were stained in red.

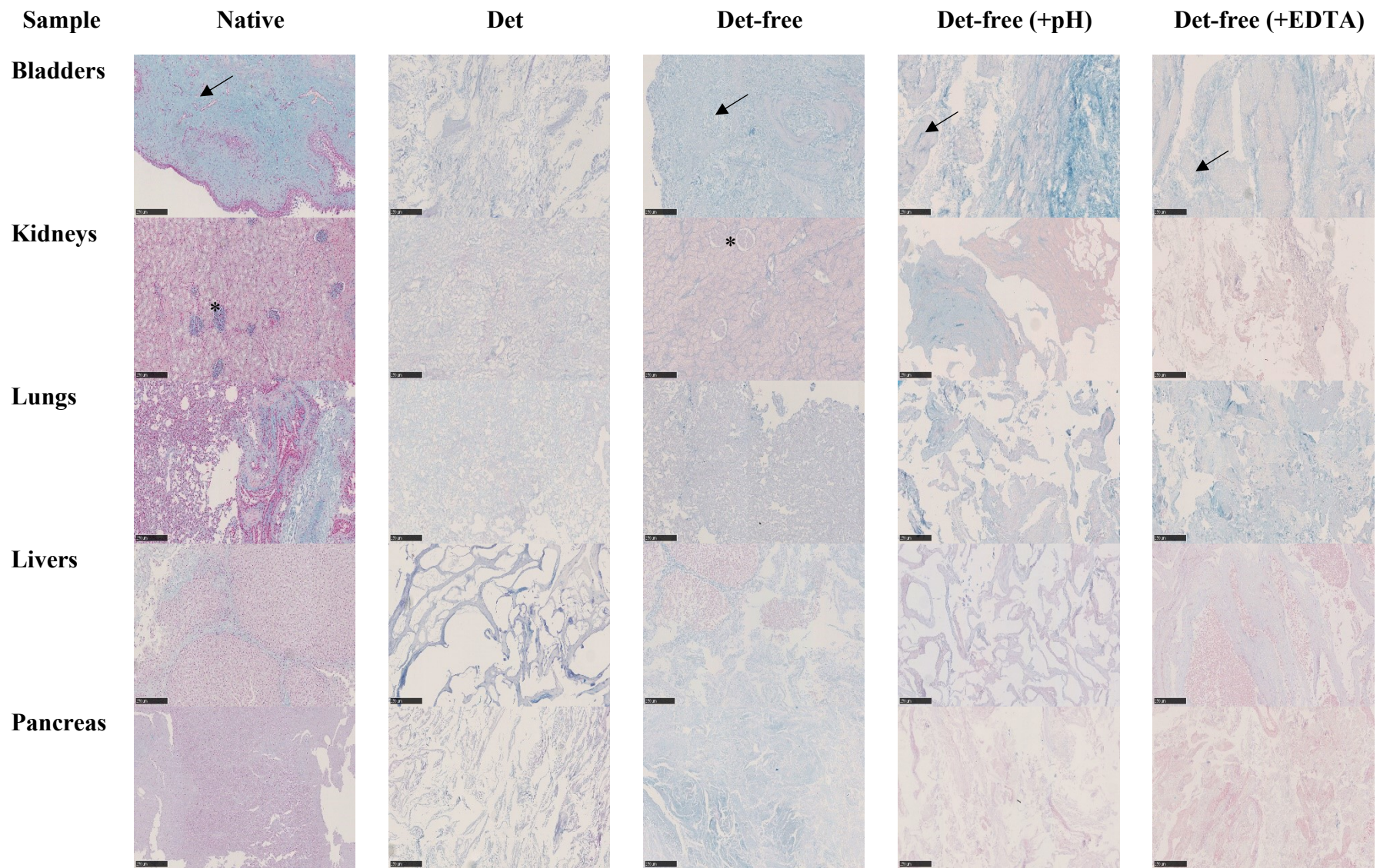


Figure 5.2 Alcian Blue/Nuclear Fast Red (AB/NFR) staining of native and decellularized porcine organs. Scale bars represent 250 μm .

* represent glomerulus and \rightarrow represents the lamina propria. The GAGs are colored in blue, nuclei in red and cytoplasm in pink.

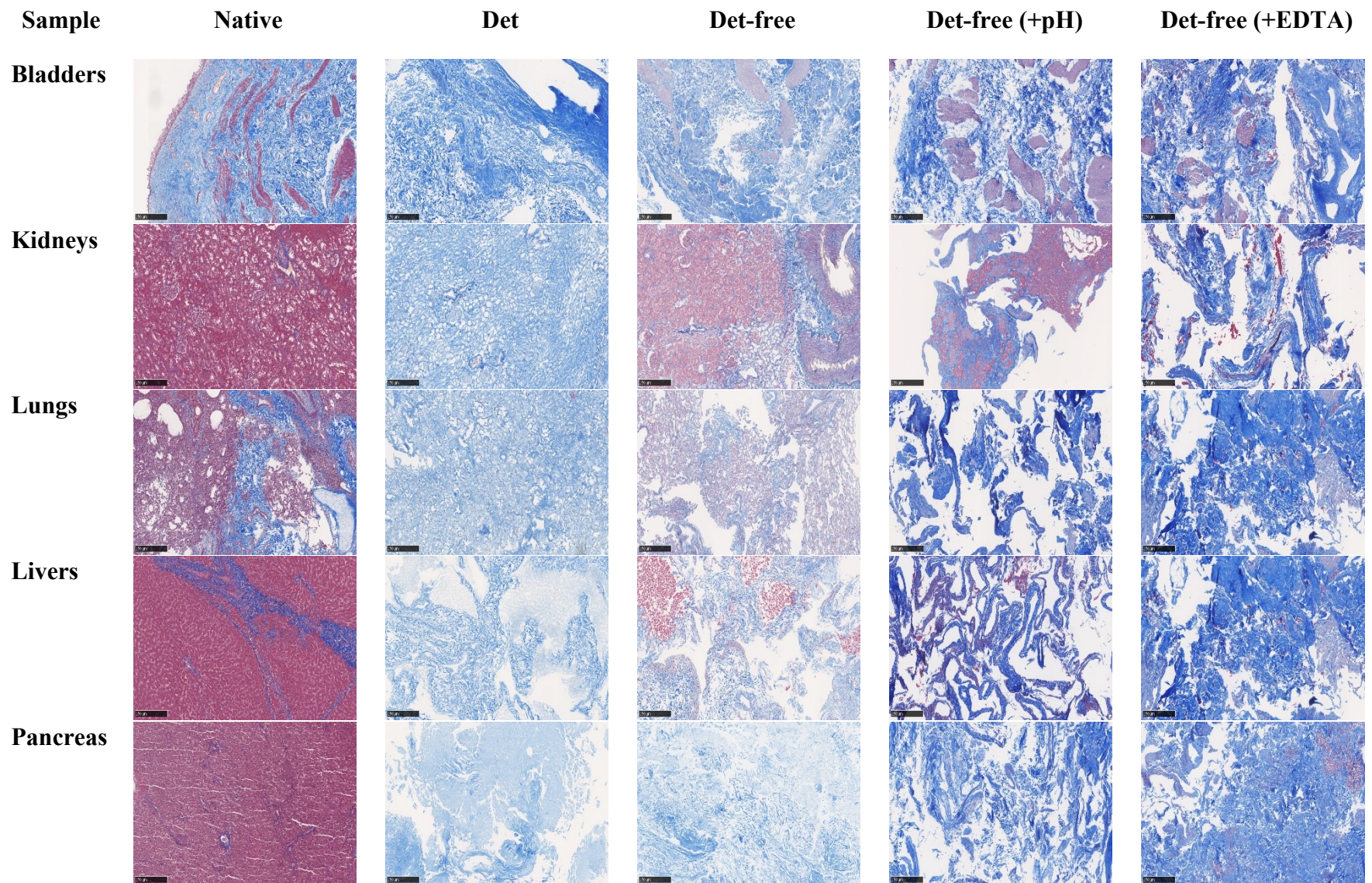


Figure 5.3 Trichrome-Masson staining of native and decellularized porcine organs. Collagen is coloured in blue, nuclei in black, and cytoplasm and muscle fibres in red. Scale bars represent 250 μm .

5.3.3 dsDNA and Protein Quantification

Estimation of dsDNA content in the native and decellularized organs allows assessing the efficiency of nuclear material removal. Figure 5.4a and 5.4b illustrate a decreased dsDNA concentration in decellularized organs, as compared to native ones. The concentrations of dsDNA in the wet decellularized organs were comparable to the dsDNA content in decellularized livers[363] and corneas[362] previously reported. The dsDNA content of native pancreas was considerably low as compared to other native organs and this could be a proof of auto-digestion of pancreas by the pancreatic digestive enzymes from the acinar cells[439]. The dsDNA content in the native porcine pancreas was less than the 150 ng/mg wet mass of ECM as reported in native rat pancreas elsewhere[443]. This observation is in agreement with the H&E observation of native pancreas from Figure 5.1 showing signs of auto-digestion.

Although a previous study reported a lower dsDNA concentration, i.e., <50 ng/mg dry weight, as a criterion for efficient decellularization[365], several commercial products contain considerably higher DNA content than this arbitrary stated value. Normalizing dsDNA extracted from wet organs to dry-weight increases the chances of errors[1]. In the present study, the dsDNA has been reported as ng/mg wet mass of the ECM sample. Although quantifying dsDNA has been used as a criterion for evaluating decellularization, the presence of single-stranded DNA and RNA could result in immunogenicity.

Quantification of protein content showed a slightly higher protein concentration in the detergent-free methods, as compared to the detergent (SDS)-based technique (Figure 5.4c). The BCA assay has been used to quantify protein content elsewhere following digestion with a mixture of acetic acid and pepsin. The protein content in decellularized ECM aggregates from differentiating embryoid bodies was significantly lower in comparison to native aggregates[444]. The concentration of proteins among the three detergent-free methods did not show a significant difference.

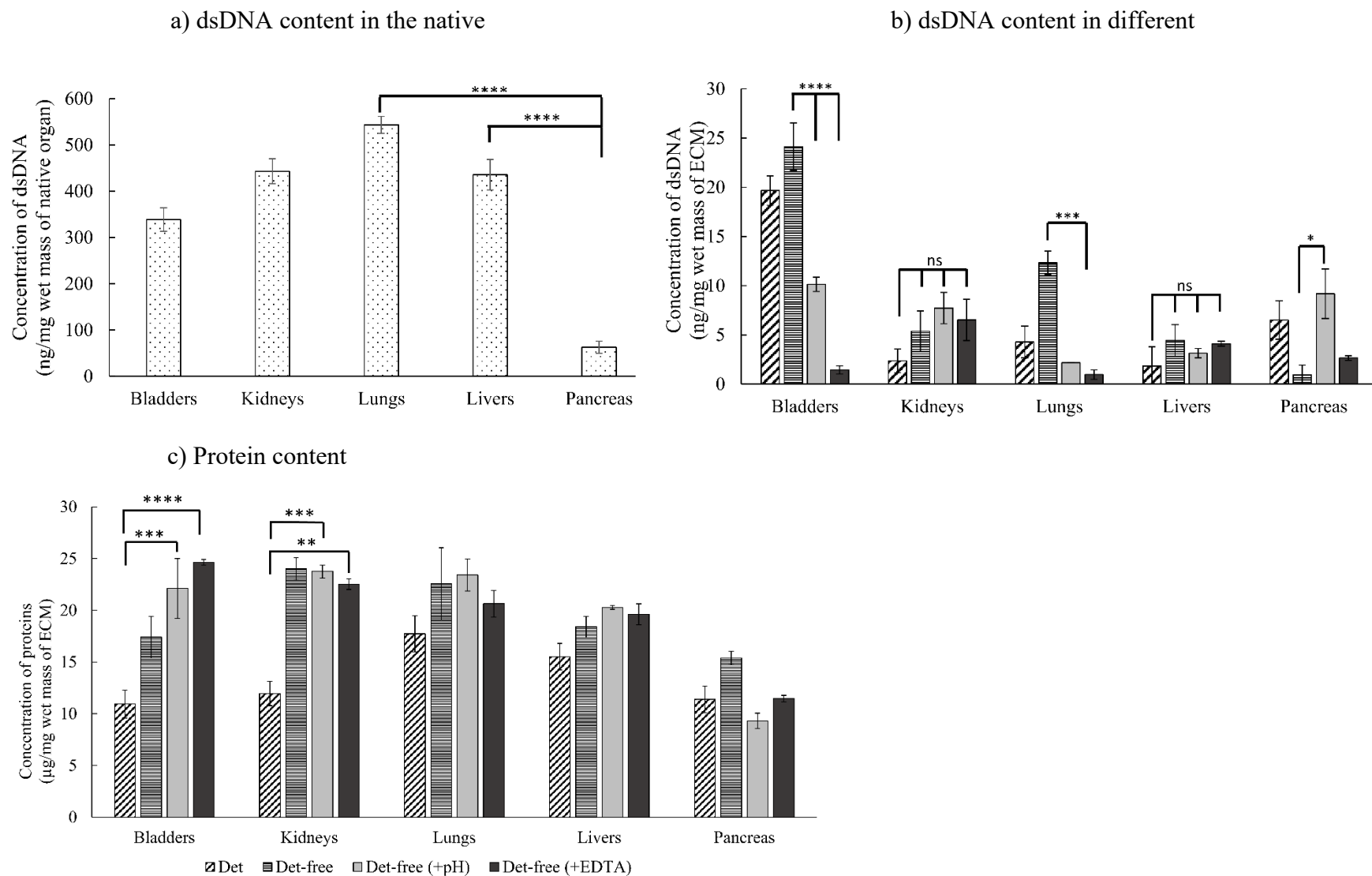


Figure 5.4 a-b) dsDNA quantification in native and decellularized organs. **c)** Protein content in the different ECMs. The protein content has been normalized per mass of wet ECM to compare the protein content of the ECM in its most native form as possible. The data for the dsDNA content in native, detergent-based and detergent-free alone decellularized bladder has been reported in an earlier study and has been used here to compare with other detergent-free decellularized bladders and other organs (Chapter 4)[1]. Also, the ambiguity surrounding the report of dsDNA content normalized to dry mass as reported elsewhere[1], has prompted the normalization per mass of wet ECM.

5.3.4 ECM Composition by Proteomics Analysis

Mass spectrometry of solubilized ECMs have revealed the presence of collagens, laminins, elastin, fibronectin and other ECM proteins[445,446]. The proteins of interest collagen IV, elastin, fibronectin, laminins, and others have been screened from mass spectrometric signal intensities and plotted in Figures 5.5-5.7. The list of other important proteins involved in the formation of the basement membrane, cell adhesion and signaling are shown in Appendix B (Supplemental Table 1)

Type IV collagen, laminin-1 and fibronectin are reported to be responsible for β -cell survival and insulin secretion[377–379]. Type IV collagens identified in the decellularized samples include COL4A2, COL4A4 and COL4A5 and their respective signal intensities are shown in Figure 5.5. The detergent-free methods were able to conserve type IV collagen in bladders, lungs and livers as compared to the detergent (SDS)-based method. Type IV collagen is the principle component of the basement membrane and is responsible for cell attachment, migration and proliferation[447].

Laminins were found to be more conserved in samples processed using detergent-free method, as compared to those treated using the detergent (SDS)-based technique (Figure 5.6). However, decellularized pancreas resulting from all the tested methods lacked laminins. The role of laminins in the basement membrane is to provide a point for cells to attach directly or by entrapping growth factors, as detailed elsewhere[448].

Other proteins such as fibronectin, elastin, and extracellular matrix protein 1 (ECM1) found in the decellularized organs are illustrated in Figure 5.7. The signal intensities of fibronectin and ECM1 in the detergent-free-processed samples indicated a conservation of the respective proteins, as opposed to those treated using the detergent (SDS)-based method. This could be due to the denaturation of the protein due to the SDS treatment[449]. Although, our results indicate less conserved composition using the detergent (SDS)-based method, another study comparing two detergent-based methods for decellularizing rat livers revealed the conservation of collagens, laminins, glycoproteins and other ECM proteins in both cases[363]. Sodium deoxycholate was used as detergent rather than SDS.

The total numbers of different proteins identified in the five organs decellularized by the four tested methods are shown in Figure 5.8. The figure shows the number of different proteins detected

in different conditions. Certain proteins were exclusive to the treatment, and some were found to overlap among different treatments. In all cases, the detergent-free methods were able to preserve a greater number of proteins, as compared to the detergent (SDS)-based method. Among the detergent-free methods, there was a big overlap of the different proteins preserved except for the pancreas, where the det-free (+pH) and det-free (+EDTA) were able to preserve more proteins compared to the det-free samples. Decellularization using anionic detergents such as CHAPS and 1% SDS has resulted in disruption of the native structure, denaturation of the ECM, and degradation of the basement membrane complex[450]. Decellularization using SDS was found to degrade GAGs, as compared to a freeze-thaw method[451] and to the use of the non-ionic detergent Triton X-100[452]. The degradation of proteins caused by detergents such as SDS may be the reason for the reduced number of proteins. Intracellular proteins such as the dyneins, tubulins, spectrins, filamin-A and plectins have been detected in the present study by mass spectrometry. Although multiple studies have used histological techniques confirming the removal of cytoplasm, very few uses sensitive techniques such as mass spectrometry to identify cytoplasmic proteins in the resulting matrices. Rat lungs have been decellularized using detergents such as SDS, sodium deoxycholate (SDC), and 3-([3-cholamidopropyl]dimethylammonio)-1-propanesulfonate hydrate (CHAPS) and all of them resulted in the retention of cytoplasmic proteins in the matrices[372].

The pH adjustment and EDTA treatment coupled to the detergent-free decellularization were able to retain certain laminins, and other important proteins such as tenascins, heparan sulfate proteoglycans, biglycans and fibrillin, as compared to the detergent-free decellularization used alone (Appendix B, Supplemental Table 1). Cysteine, threonine and aspartate proteinases are active at an acidic pH and are responsible for the degradation of the intracellular and extracellular proteins[453,454]. This could be the reason for the degradation of ECM proteins in the detergent-free method used alone as the pH of the solution was acidic compared to the pH-adjusted samples.

Application-oriented products derived from ECM should maintain the ultrastructure and composition of ECM as close to the native to increase the potential use of ECM. The ECM obtained by detergent-free decellularization would be better used for designing scaffolds for cell culture. However, for specific applications, multiple studies and analysis would be required to elucidate

the pathway linking the proteins conserved to the function i.e., for example, presence of basement membrane proteins such as type-IV collagen and increases insulin secretion in human islets[455].

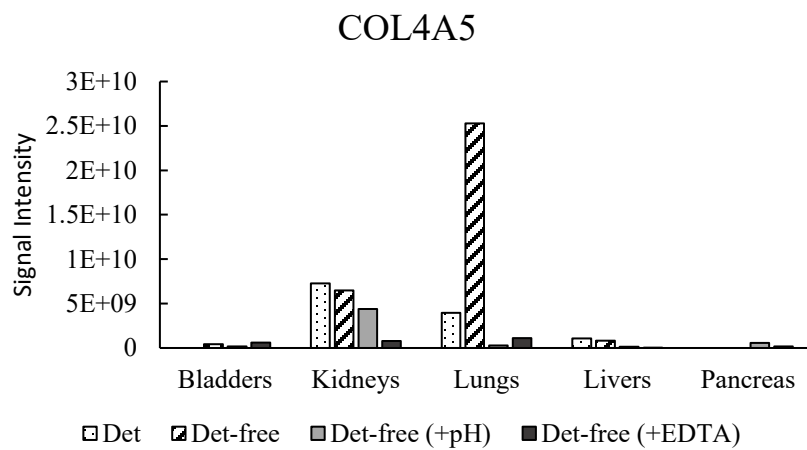
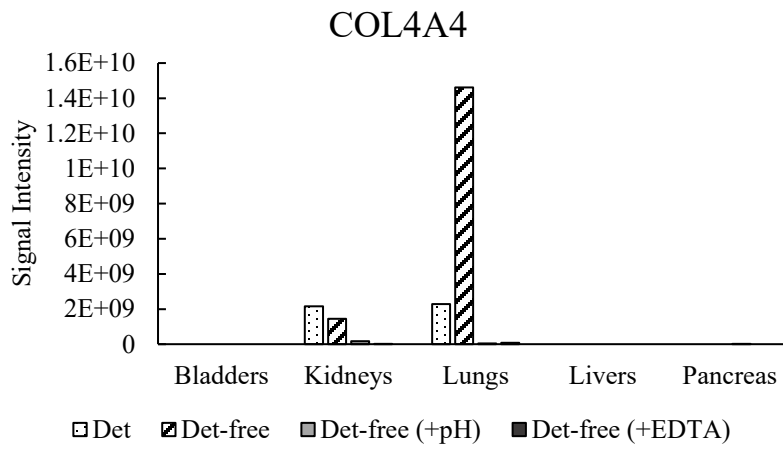
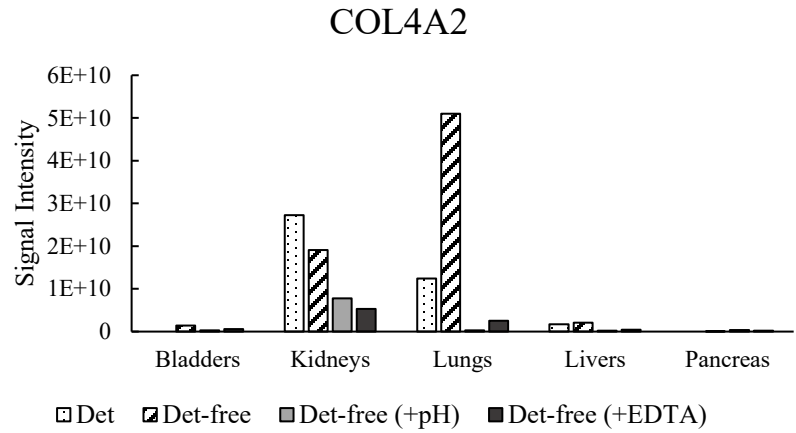
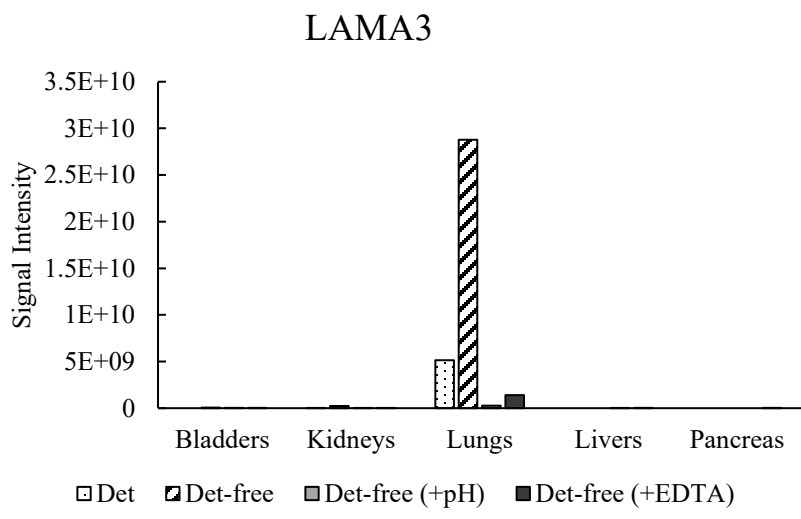
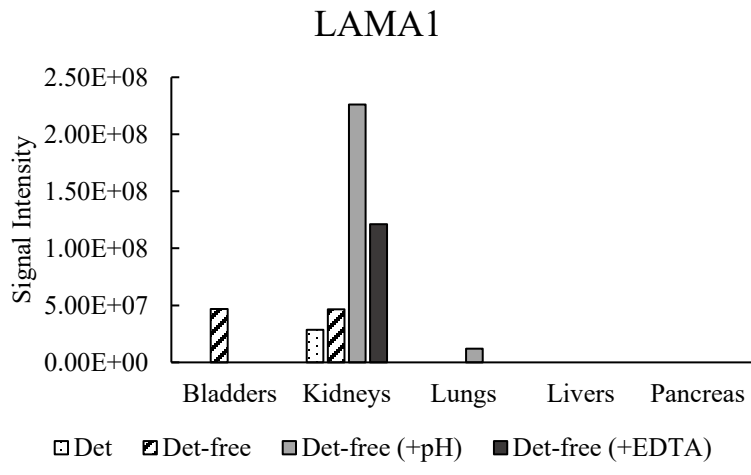
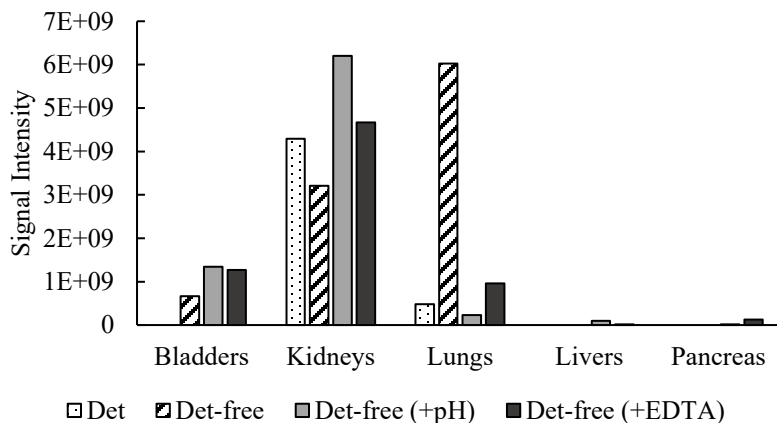


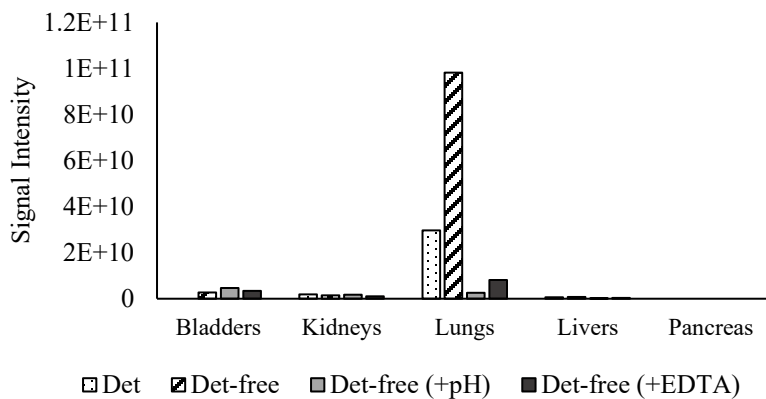
Figure 5.5 Type IV collagens detected in the decellularized organs: COL4A2, COL4A4, and COL4A5.



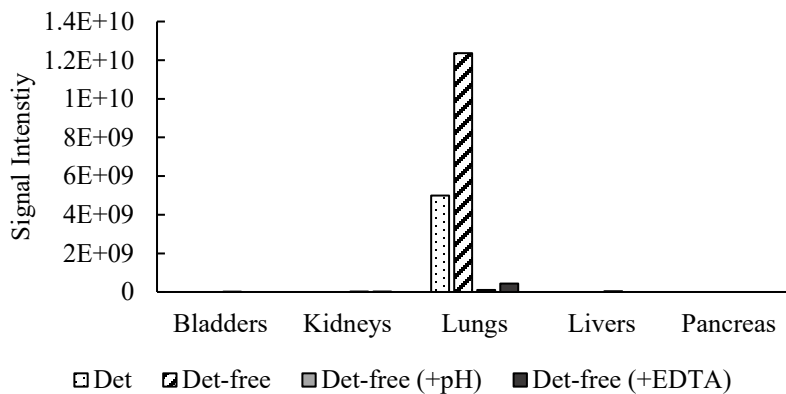
LAMB1



LAMB2



LAMB3



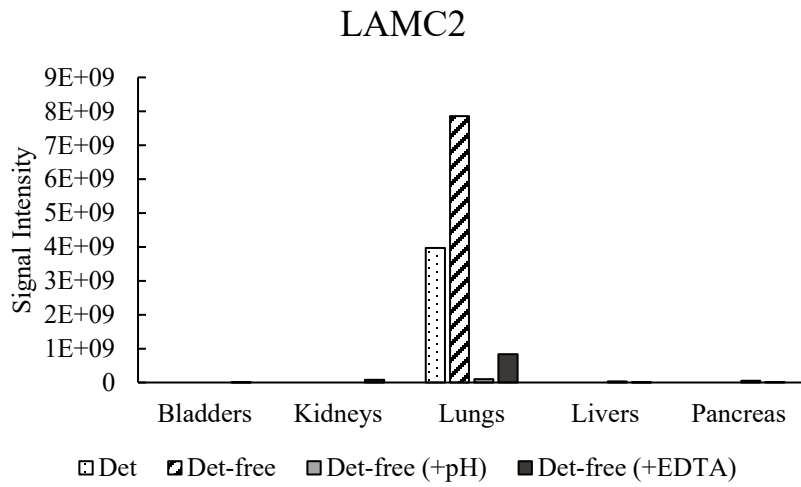
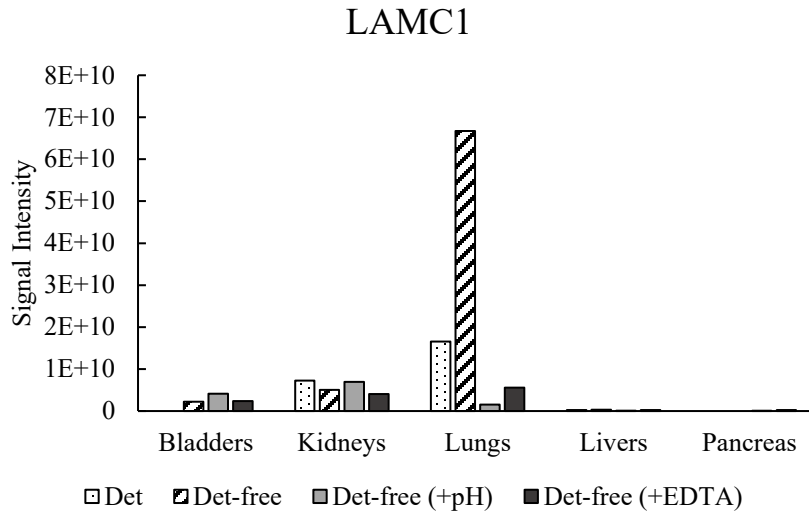


Figure 5.6 Laminins detected in the decellularized organs: LAM1, LAMA3, LAMB1, LAMB2, LAMB3, LAMC1, and LAMC2.

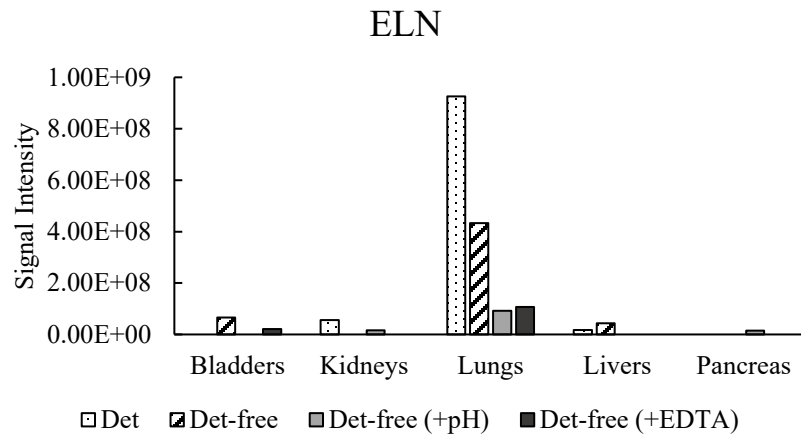
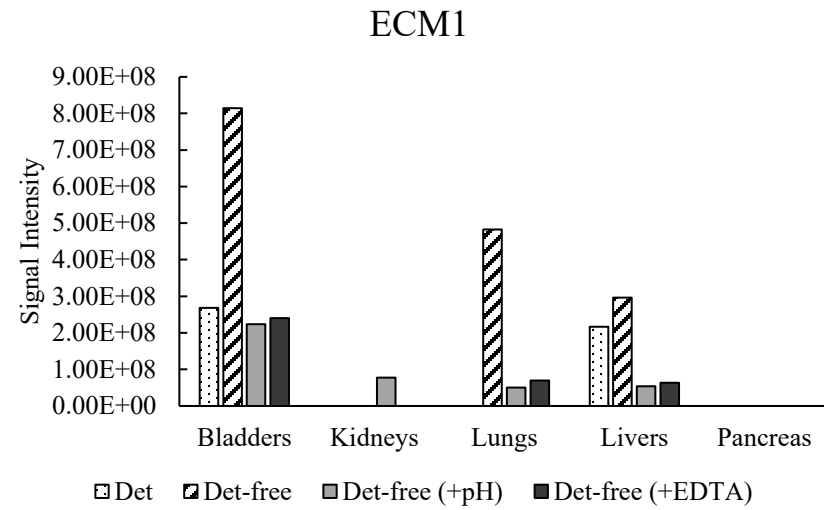
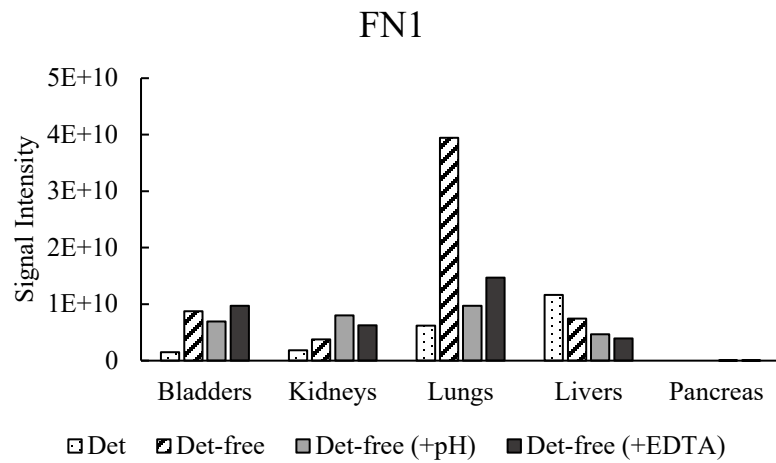


Figure 5.7 Other ECM proteins detected in the decellularized organs: Fibronectin 1 (FN1), ExtraCellular Matrix Protein 1 (ECM1), and Elastin (ELN).

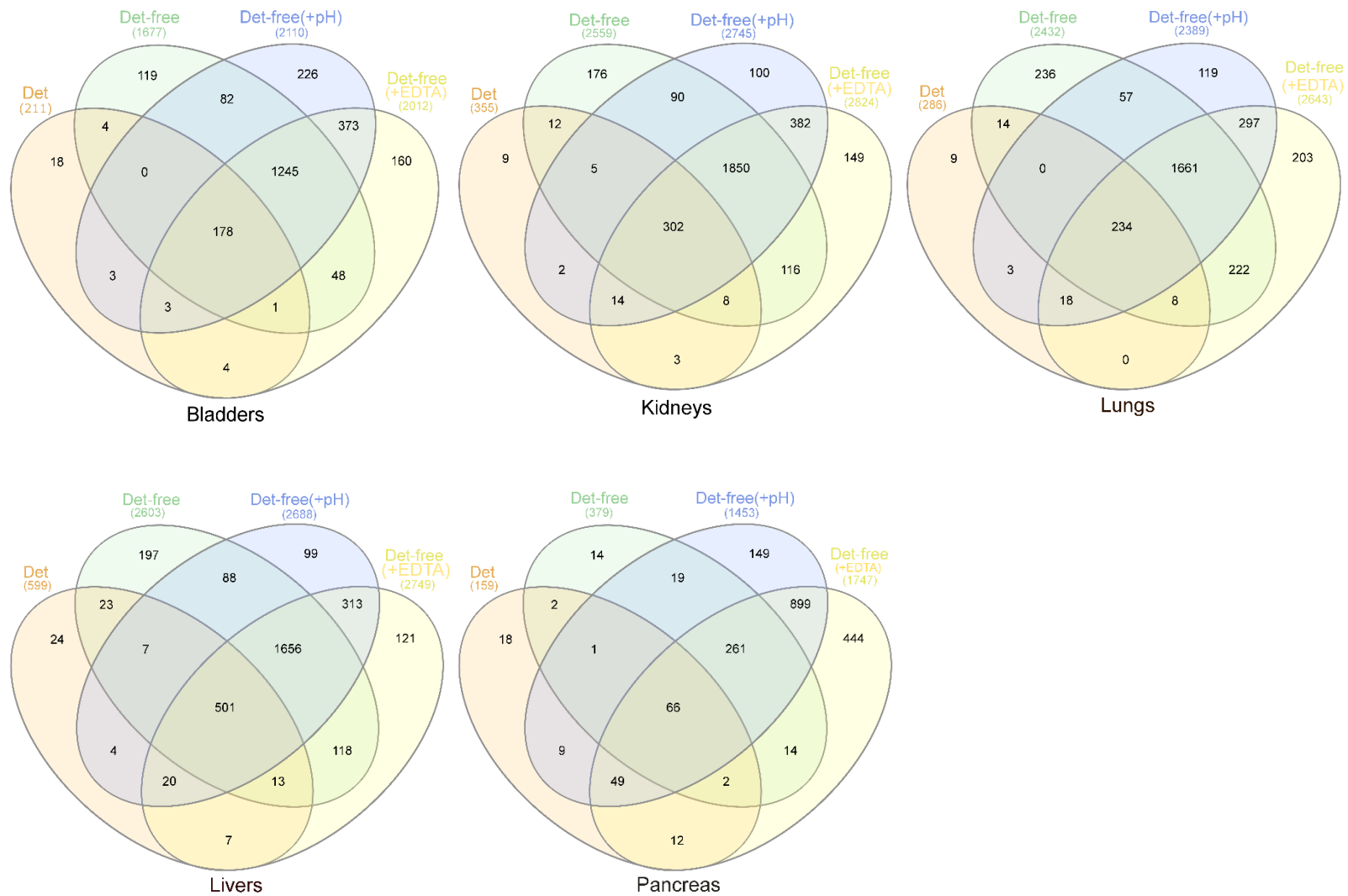


Figure 5.8 Venn diagrams of the total number of proteins detected in decellularized bladders, kidneys, lungs, livers, and pancreas.

Venn diagrams were prepared using InteractiVenn ©.

5.3.5 Collagen Fibers Orientation

Orientation of the collagen fibers was assessed using polarization microscopy of Picrosirius Red-stained samples. The colour of the birefringence under polarized light was able to distinguish between the different types of fibrillar collagen network. For example, yellow-red birefringence indicated type I collagen and green birefringence indicated type III collagen[456]. Introduction of polarized light reveals type I collagen and type III collagen in green.

The relative frequency percentages of collagen orientations is shown in Figure 5.9. For each condition, three independent samples were analysed, and in each section, the top, middle and bottom regions of the sections were imaged and analysed. Following the capture of the images, the images were converted to grayscale and were analysed pixel-by-pixel. Each pixel with a colour coding, corresponded to a particular orientation of collagen. OrientationJ plugin in ImageJ was used to identify the distribution of these colours, thereby calculating the number of pixels allowed for obtaining the orientation. An example of the image analysis is shown in Appendix B (Supplemental figure 6). The predominant collagen orientations found in decellularized bladders, livers and pancreas were $+45^\circ$ and -45° . However, the predominant orientation in decellularized lungs and kidneys was $+45^\circ$. Comparing the ECMs to native organs, the orientation was not altered based on the treatment for bladders, livers, and pancreas. But the orientation was altered for detergent-free decellularized kidneys and lungs, as the peak distribution was shifted by 45° compared to the native organs in both cases. Optimal orientation could not be deciphered from the literature as most studies have indicated the orientation in diseased models. Comparing the orientation of collagen fibers in decellularized samples to those found in native organs could indicate if the orientation of collagen has changed during the treatment.

The orientation of collagen fibers in an organ is an important property, as it aids in maintaining the organ structure[457]. An osteoarthritic mice model study revealed altered collagen orientation compared to controls[458]. Orientation of collagen in the bone provided greater insights into the biomechanical efficiency of the skeleton[459]. Another study indicated a change in the orientation of collagen fibers in cartilage upon compression[460]. The collagen fibers in tendons, small intestine sub-mucosa and porcine urinary bladder were found to be aligned longitudinally along the axis of the organ[461,462]. Thus, the orientation of collagen in an organ can be related to its

functionality. But it remains to be investigated whether collagen fibers orientation distribution affects cell responses.

Picrosirius Red-stained collagen of human dermis has been analysed using polarization microscopy[463]. Most of the studies with Picrosirius Red staining and polarization microscopy have been used to determine the density of collagen. Second harmonic generation (SHG) has been used to determine the orientation and alignment of collagen[464]. Although it proves to be a highly efficient technique, a limitation arises from the polarized beam's inability to penetrate and image in highly scattering tissues[465].

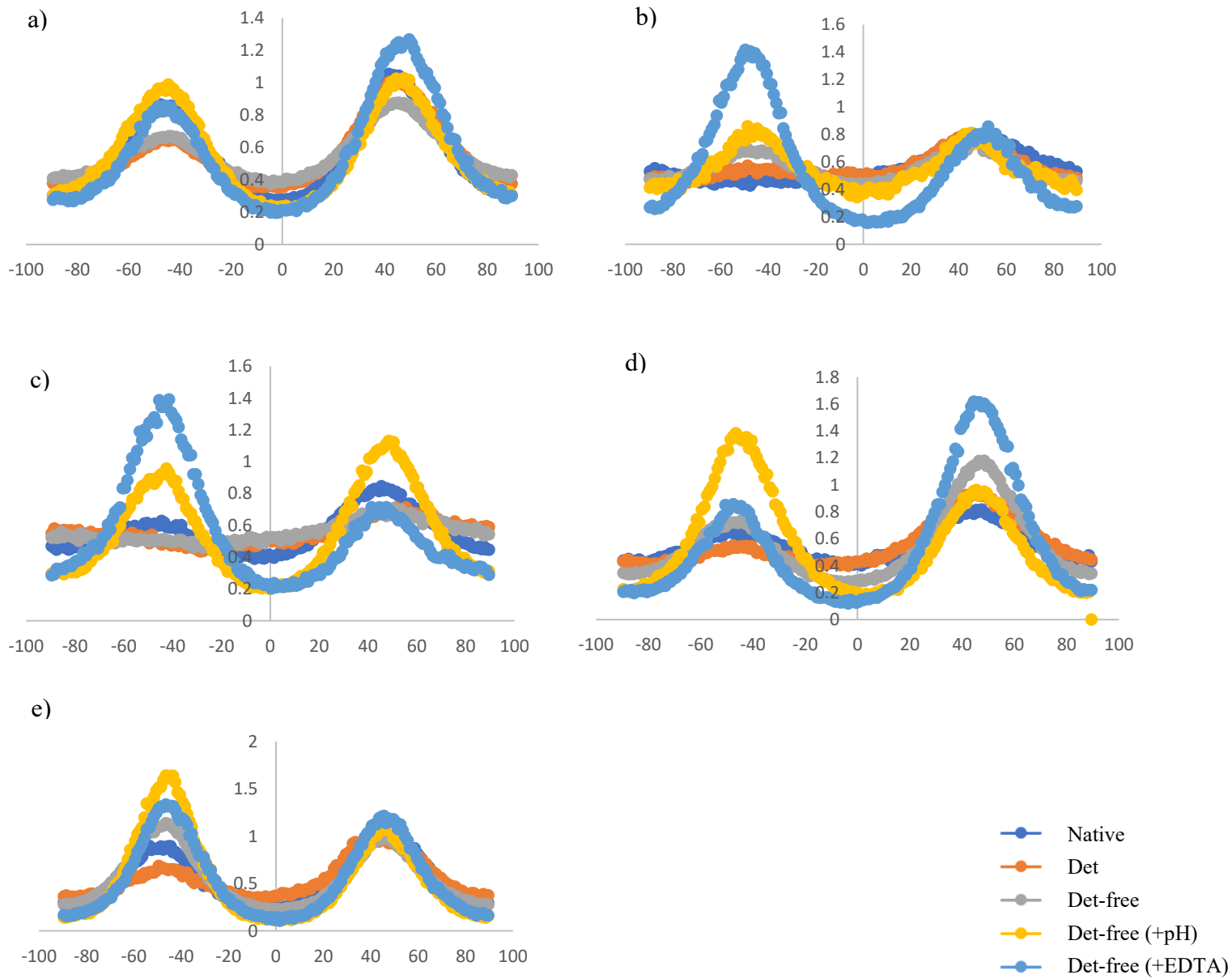


Figure 5.9 Percentage relative frequency of orientation of collagen fibers in **a)** bladders, **b)** kidneys, **c)** lungs, **d)** livers and **e)** pancreas.

5.4 Conclusions

Porcine bladders, kidneys, livers, lungs, and pancreas were decellularized. Detergent-free methods have resulted in better preserved ECM containing GAGs and collagens, while the detergent (SDS)-based method has induced more alterations into the ECM. Native pancreas showed necrosis due to auto-digestion by acinar cells during isolation and storage. This resulted in a reduced dsDNA content in the native pancreas and loss of collagen, laminins in the resulting ECM matrices. dsDNA quantification revealed a reduction of the nuclear material in the resulting ECM compared to native organs. Protein identification highlighted a greater prevalence of type IV collagen, laminins, and other ECM proteins with the detergent-free methods. Investigating the collagen fibers orientation showed that the process of decellularization did not alter much the fiber orientation.

This study describes a set of experimental protocols which helps understanding the organization and composition of ECM derived from the decellularization of organs. Although different decellularization techniques have been reported for porcine organs, there has been a smaller number of studies investigating protein composition. The significance of finding a balance between removal of DNA and of cellular materials and the conservation of ECM proteins in the extracted ECM, while maintaining the ultrastructure, has been enunciated. This study paves a new avenue to evaluate the efficiency of organ decellularization resulting from four methods by using a multi-technique characterization approach. It also points out that ECM composition and (ultra)structure depend upon the method used to perform the decellularization and on the organ itself.

Acknowledgements

We thank Tamara Challut for her technical help. We thank Marilène Paquette and the histology research core facility of the Faculté de Médecine et des Sciences de la Santé (Université de Sherbrooke) for the histology service, and Dominique Lévesque for mass spectrometry.

This research project was supported by NSERC through a Discovery Grant awarded to Patrick Vermette (Grant # 250296-2012). All authors have approved the final manuscript.

Conflict of interest

Patrick Vermette owns shares in SherMATRIX Inc., a company developing biomaterials for clinical uses.

Chapter 6

Extracellular matrix from decellularized porcine organs as scaffolds for insulin-secreting cells and pancreatic islets

Foreword

Authors and Affiliations:

Vignesh Dhandapani: Ph.D. candidate, Université de Sherbrooke, Département de génie chimique et de génie biotechnologique

Boabekoa Pakindame: Training student, Université de Sherbrooke, Département de génie chimique et de génie biotechnologique

Patrick Vermette: Professor, ingénieur, Université de Sherbrooke, Département de génie chimique et de génie biotechnologique

Date of Submission: June 20th, 2023

State of Acceptance: Under Review

Journal: Journal of Biomedical Materials Research Part B: Applied Biomaterials

Contribution:

The article compares the cell response of INS-1 cells cultured on different organs extracellular matrix (ECM) derived from different porcine organs decellularized by detergent-based and detergent-free techniques. Further, the article presents the culture of mouse primary islets seeded on the screened ECM. The article was submitted to the *Journal of Biomedical Materials Research Part B: Applied Biomaterials*. The experimental design was done mainly by Vignesh Dhandapani and Patrick Vermette. All the experimental work was performed by Vignesh Dhandapani, assisted by Boabekoa Pakindame. The results were interpreted and analyzed by Vignesh Dhandapani and Patrick Vermette. The article was mainly written by Vignesh Dhandapani and Patrick Vermette. It was reviewed by Patrick Vermette. All the work was done under the guidance and supervision of Patrick Vermette.

Titre en français :

Matrice Extracellulaire provenant d'organes porcins décellularisés comme échafaudages pour des cellules sécrétrices d'insuline et des îlots pancréatiques

Résumé :

La Matrice Extracellulaire (MEC) provenant de différents organes a été utilisée pour cultiver plusieurs types cellulaires. La MEC produite par décellularisation d'organes contient des collagènes, de la fibronectine, des glycosaminoglycanes (GAGs), des laminines et d'autres composants essentiels fournissant un soutien structural et des signaux biochimiques pour que les cellules s'attachent, fonctionnent et prolifèrent. Dans ce travail, nous avons fait l'hypothèse que l'organe à partir duquel la MEC est extraite et produite joue un rôle vital au niveau des réponses cellulaires lors de la recellularisation. Pour valider cette hypothèse, cinq organes porcins (vessies, reins, foies, poumons et pancréas) ont été décellularisés par une méthode à base de détergent ou par décellularisation sans détergent. Des cellules pancréatiques de type β de rat ayant la capacité de sécréter de l'insuline (INS-1) ont d'abord été utilisées pour évaluer, sur une période de 7 jours, l'effet des techniques de décellularisation testées, et ce, à partir des cinq organes sélectionnés, révélant que le traitement à base de SDS ne produisait pas des MECs supportant l'adhésion cellulaire, et ce, pour tous les organes testés. Les MECs dérivées des trois méthodes n'utilisant pas de détergent, en revanche, permettent l'attachement des cellules à l'exception de la MEC provenant du pancréas. La biocompatibilité des MECs produites à partir de méthodes sans détergent a ensuite été validée en utilisant des tests de prolifération et de métabolisme cellulaires, une immunocoloration pour investiguer l'expression de l'insuline et de l'actine, ainsi que la sécrétion d'insuline stimulée par le glucose (GSIS). Les cellules INS-1 ont proliféré sur certaines MECs dérivées des méthodes sans détergent et ont sécrété de l'insuline après 7 jours de culture. De plus, des îlots de souris pancréatiques primaires ont été isolés et cultivés pendant 48 heures sur des morceaux de vessie décellularisés avec les techniques sans détergent et l'analyse histologique a montré des îlots intacts intégrés à la MEC de la vessie. Le test GSIS a révélé des îlots fonctionnels après 48 heures de culture sur des morceaux de MEC de vessie produits par les méthodes sans détergent. Les îlots cultivés sur la MEC de vessie dérivée des méthodes sans détergent exprimaient

l'insuline et ont montré des cellules endothéliales (i.e., positives pour CD31) localisées à l'interface îlot-MEC.

Mots clés : Organes porcins décellularisés, Matrice Extracellulaire (MEC), Sécrétion d'insuline, Îlots pancréatiques de souris, Cellules endothéliales, Ingénierie tissulaire.

Abstract:

Extracellular Matrix (ECM) from different organs has been used to culture several cell types. ECM produced by organ decellularization contains collagens, fibronectin, glycosaminoglycans (GAGs), laminins and other components essential in providing structural support and biochemical cues for cells to attach, function, and proliferate. The organ from which ECM is extracted and produced is hypothesized to play a vital role in cell responses upon recellularization. To investigate this hypothesis, five porcine organs (bladders, kidneys, livers, lungs, and pancreas) were decellularized by a detergent-based method or by detergent-free decellularization. Insulin-secreting rat pancreatic β -like cells (INS-1) were first used to screen, over a 7-day culture, the effect of the ECM produced by the tested decellularization techniques from the five selected organs, revealing SDS treatment did not result in cell responsive ECMs for all the tested organs. Detergent-free-derived ECMs, on the other hand, allow cell attachment except for the pancreas ECM. The biocompatibility of the ECMs made from detergent-free methods was therefore subsequently validated using cell proliferation and cell metabolism assays, immunostaining for insulin and actin expression, and glucose-stimulated insulin secretion (GSIS). INS-1 cells proliferated on certain detergent-free ECMs and secreted insulin following 7 days of culture. Further, primary pancreatic mouse islets were isolated and grown 48 hours on detergent-free decellularized bladder pieces and histological analysis showed intact islets embedded within the bladder ECM. GSIS revealed functional islets following 48-hour culture on detergent-free-derived bladder ECM pieces. Islets grown on detergent-free-derived bladder ECM expressed insulin with endothelial cells (i.e., CD31-positive) localized at the islet-ECM interface.

Keywords: Decellularized porcine organs, ExtraCellular Matrix (ECM), Insulin secretion, Pancreatic mouse islets, Endothelial cells, Tissue engineering.

6.1 Introduction

Tissue engineering methods should apply the adequate combination of scaffolds, cells and biological materials to fabricate tissues or organs *in vitro* and/or *in vivo* to yield a product with a range of biological properties acceptable for the targeted application[466]. Scaffolds composed of or containing ExtraCellular Matrix (ECM) are of great interest owing to the ECM unique (ultra)structure and composition, making the ECM the gold standard for scaffolds. The ECM is a heterogenous fibrous network of glycoproteins structurally and functionally coordinated, providing mechanical stability, acting as a physical scaffold, as well as offering biochemical cues essential for tissue morphogenesis and homeostasis[467]. Decellularization of tissues and organs to produce ECMs has gained interest in the last decade, although soft tissues were decellularized as early as in the 1970s[468].

Briefly, organ decellularization refers to the process of removing cellular components from tissues or organs leaving a network of proteinaceous ECM[469]. Although different decellularization techniques i.e., physical, chemical and/or enzymatic, have been applied to decellularize tissues and organs with different efficiencies, often a combination of those techniques has proven to be efficient in removing cellular components and preserving the ECM (ultra)structure[334,350–352]. The impact of the applied decellularization method on the resulting matrix (ultra)structure is described elsewhere[346,470]. Basement membrane proteins (collagen IV and laminins), fibronectins and glycosaminoglycans have been evolutionarily conserved among allogenic and xenogenic scaffolds thereby eliciting similar cellular responses among xenogenic and allogenic scaffolds when implanted *in vivo* or seeded with cells *in vitro*[471–475]. On the other hand, the composition as well as structural and mechanical properties of the ECM vary among different organs because of the difference in the structural and functional molecules secreted by the organ resident cells[476–479].

A variety of products derived from ECMs are emerging. Tissue papers fabricated from different decellularized porcine and bovine organs aided in the proliferation of human mesenchymal stem cells[480]. Recently, 3D bioprinting with ECM embedded in scaffolds shows potential because of the ability to customize scaffolds architecture with the ECM[481]. Hydrogels derived from ECM were able to promote neurite outgrowth[478], bone and cartilage engineering[482], fibroblast

proliferation[343] and human corneal stromal cell attachment[346]. Several products have been derived from decellularized animal and human organs and are already commercialized. For example, Oasis® (porcine small intestine submucosa, Cook Biotech Inc. Indiana, USA), MatriStem® (urinary bladder mucosa, ACell, Columbia, USA), and Restore™ (porcine small intestine, DePuy Othopedics Inc., Indiana, USA)[6] are commercially available.

The bladder has been one of the most used tissue to extract and produce ECM to fabricate scaffolds and to culture cells, as exemplified by the bladder ECM used to support the proliferation of urothelial cells[353], human bone marrow stem cells, human muscle progenitor cells and fibroblasts[483]. Probably, one of the reasons is the good yield following decellularization. The utilization of decellularized urinary bladder-derived matrices to culture different cell types prompted us to carry out a study aiming to compare a single cell type or tissue response over ECM produced from different decellularized organs. This would allow investigating the potential, or limitations, to use other organs as ECM sources. Although few studies have reported comparison of cell responses on different decellularized organs, most of those studies have been conducted on modified ECMs such as ECM-derived or ECM-containing hydrogels, tissue papers and 3D printed scaffolds. In the present, it was decided to compare cell responses keeping the ECM as intact as possible to preserve as much as possible the ECM composition and (ultra)structure, making our study challenging experimentally, but unique.

An increase in the number of type 1 diabetes cases globally and the complications such as ischemia, loss of islet viability, hypoglycemia and harmful effects of long-term immunosuppression prompted the need for an alternative approach [323–327]. Tissue engineering approaches using decellularized organs to tackle the issue have been on the rise. An earlier study showed that the porcine bladder ECM obtained by detergent-free decellularization was able to aid in the attachment, proliferation and functionality of insulin-secreting pancreatic cells (INS-1)[1]. The objective of this study is an extension of the previous study to compare INS-1 cell responses on ECMs extracted and produced from five decellularized porcine organs including bladders, kidneys, lungs, livers, and pancreas. This first part of the study allowed us to screen and select the ECMs showing the most promising outcomes to study its effect on primary mouse islets. The organs were decellularized by four methods of which, three methods involved detergent-free decellularization and one the use of 0.5% sodium dodecyl sulfate (SDS) as the detergent. INS-1

cells were seeded on the ECM and grown for 7 days. Cell viability was visualized by a metabolism assay (MTT) and cell proliferation investigated using the CyQUANT test. Functionality was characterized by glucose-stimulated insulin secretion (GSIS) and immunostaining for insulin. Mouse primary pancreatic islets were isolated and seeded on the detergent-free decellularized bladder ECM and functionality characterized by glucose-stimulated insulin secretion (GSIS) and immunostaining for insulin and endothelial cells.

6.2 Materials and Methods

6.2.1 Organs decellularization

Porcine organs (bladders, kidneys, livers, lungs, and pancreas) from three different porcine donors (N=3) were freshly obtained from the slaughterhouse (Abattoir Régional de Coaticook, Coaticook, Québec) within 24 hours of animal sacrifice. The porcine bladders were procured from a licensed slaughterhouse and since the animal sacrifice was performed under strict regulated conditions, the tissues needed no approval from the ethics committee of the Université de Sherbrooke. They were placed on ice until further processing. Briefly, the bladder, being muscular, was delaminated and the resulting tissue was cut into pieces of approx. 5 mm x 5 mm. The other organs were diced into smaller pieces and fed into a meat grinder (Heavy-duty Electric Meat Grinder, Model #8 ¾ HP Motor, Weston). The slurry was collected and subject to detergent-based or detergent-free treatments[1,484].

Briefly, for the detergent-based method, 0.5% Sodium Dodecyl Sulfate (SDS) (161-032, Biorad) was used to decellularize the organs for 30 ± 1 hours at 200 rpm in a shaker (Innova® 44/44R, New Brunswick™). The decellularized samples were washed again in distilled water for 48 hours (4 changes of water) and the final water wash contained 1% penicillin/streptomycin (15140122, Life Technologies). The decellularized organs were filtered and stored at -20°C until further use.

The first applied detergent-free method involved two cycles of freeze-thaw and treatment with 2M sodium chloride. The second and third detergent-free methods were supplemented with either a 0.5% ethylene diamine tetra acetic acid (EDTA) treatment or a pH adjustment to reach a pH of 6.6. Finally, all the samples were washed and stored at -20°C until further use.

6.2.2 Culture setup and INS-1 cell culture

2% agarose (A0169, Sigma-Aldrich) solutions were prepared in either

- a) INS-1 cell culture medium composed of RPMI-1640 ((31800-022, Life Technologies) supplemented with 10 mM HEPES (BP310, Thermo Fisher Scientific), 10% foetal bovine serum (FBS) (12483020, Life Technologies), 1 mM sodium pyruvate (11360-070, Gibco), 50 μ M β - mercaptoethanol (M7522, Sigma-Aldrich), and a 1% penicillin/streptomycin mixture, or
- b) Islet culture medium made with 1:1 of DMEM (D5523, Sigma-Aldrich, low glucose): RPMI (R1383, Sigma-Aldrich) supplemented with 5% FBS, 15 mM HEPES, 10 mM nicotinamide and a 1% penicillin/streptomycin mixture.

First, layers of agarose resulting from 300 μ L of the agarose solution were made at the bottom of the wells of 24-well cell culture plates. Porcine organ ECM pieces were transferred to each well covering ca. 90% of the total surface area. A second layer of agarose was coated on the sides of the ECM (not covering the ECM pieces) to stick it to the first agarose layer as used in a previous study[1]. Wells with the ECM were soaked in 1X PBS for 90 minutes and simultaneously aseptitized under the laminar hood UV-light. The whole setup was soaked in sterile RPMI-1640 medium for 48 hours at 37°C and 5% CO₂.

Stock INS-1 cells (C0018007, AddexBio) were grown in INS-1 cell culture medium in T75 flasks at 37°C and 5% CO₂. Upon reaching confluence, cells were trypsinized (25200072, Life Technologies), counted and 25,000 cells per well were added. INS-1 cells passaged for 16-25 times were utilized for the experiments. Media were changed every 48 hours and cells were grown for 7 days.

6.2.3 Cell proliferation quantification

INS-1 cells grown on the ECMs for 4 hours (the time needed for INS-1 cells to attach to the ECM) and 7 days, as well as negative controls (i.e., wells with ECMs but with no cells), were quantified using the CyQUANT™ NF Cell Proliferation Assay Kit (C35006, Thermo Fisher Scientific). Briefly, the media from different wells were conserved in separate vials. Cells from each well were isolated by trypsinization (6-7 minutes) and vigorous repeated pipetting. They were transferred to vials containing media and centrifuged at 1200 rpm for 5 minutes. The supernatant media were discarded, the pellets rinsed in 1X Hanks Buffered Salt Solution (HBSS), centrifuged again and the supernatant discarded. Working concentration of CyQUANT™ NF reagent was prepared according to the protocol provided by the manufacturer, added to the cell pellet, and transferred to a 96-well microplate. The plate was incubated for 1 hour at 37°C and the fluorescence was read at 480 nm (Synergy HT Microplate Reader, Biotek).

6.2.4 Visual observation of viable cells on ECM pieces

A solution of 0.5 mg/mL thiazolyl blue tetrazolium bromide (M5655, Sigma-Aldrich) was prepared in 1X HBSS. The medium from each well was discarded and 1 mL of the prepared 3-(4,5-dimethylthiazol-2-yl)-2,5-diphenyltetrazolium bromide (MTT) solution was added in each well. The plate was incubated at 37°C for 1 hour under 5% CO₂ humidified conditions. Following incubation, the MTT solution was discarded and 1X PBS was added to the wells. A stereomicroscope (Leica MZFLIII, Germany) was used to visualize the cells and capture the images.

6.2.5 Islet isolation and culture

Adult mice (CD-1® IGS, Charles River, Boston, MA, USA) were euthanized under a CO₂ atmosphere according to the approved protocol (# 367-14) from the Université de Sherbrooke. The pancreas was injected with the dissociation solution consisting of 2.5 mg/mL collagenase (C9263, Sigma-Aldrich) through the pancreatic duct. The dissociation solution contained L-15 medium (L-4386, Sigma-Aldrich) supplemented with 10 mM nicotinamide, 15 mM HEPES, 2% FBS, 0.35 mg/mL sodium bicarbonate, 1 mg/mL glucose and a 1% penicillin/streptomycin mixture. The pancreas was excised off the mice and transferred on ice to the laboratory in a Falcon tube containing the dissociation solution. The tube was placed at 37°C for 18±2 minutes with manual shaking every 2-minutes. Ice-cold neutralization medium composed of HBSS (H1387, Sigma-Aldrich), supplemented with 5% FBS, 10 mM nicotinamide and 0.35 mg/mL sodium bicarbonate, was added to stop the collagenase digestion. The whole digest was poured into bacteriological Petri dishes and islets were handpicked under a stereomicroscope (Carl Zeiss, SteREO Lumar. V12, Germany) and transferred to vials containing the dissociation solution with no collagenase. The islets were centrifuged at 1200 rpm for 1 minute and resuspended in islet culture medium. Approximately 22 islets/well were seeded onto the soaked bladder ECM pieces or on TCPS (24-well plates). The islets were cultured for 48 hours considering the goal was to investigate the effect of seeding on insulin secretion. We have established that 48 hours was the minimal duration for islets to adapt to the condition (interact with the material) and secrete insulin[337]. The islets were isolated from the pancreas of three independent mice (N=3).

6.2.6 Insulin and actin expression by immunofluorescence

ECM pieces seeded with cells and islets were fixed in 4% PFA for 48 hours. Samples were processed, dehydrated, embedded in wax, and sections of 4- μ m thickness were cut. The dried sections were deparaffinized, hydrated and blocked with 2% bovine serum albumin. The primary antibodies to insulin (ab181547, Abcam) and β -actin (ab8226, Abcam) were added at the recommended dilution and left undisturbed overnight at 4°C to the samples with INS-1 cells. The secondary antibodies anti-rabbit Alexa 488 (Invitrogen) and anti-mouse Alexa 647 (Invitrogen) were added and left for 1 hour at room temperature and were counterstained with 4,6-diamidino-2-phenylindole, dichloride (DAPI, D1306, Invitrogen). For the islets, primary antibodies to insulin (ab181547, Abcam) were added and left undisturbed overnight at 4°C. Secondary antibodies anti-rabbit Alexa 488 (Invitrogen) were added at the recommended dilution and, incubated at room temperature for 1 hour. Endothelial cells visualization was performed by staining for CD31 using a polyclonal goat IgG primary antibody (R&D systems, AF3628) and horse anti-goat Dylight™ 488 (Vector laboratories, DI-3088-1.5) as the secondary antibody. Two fluorescence images from four different samples in each case were visualized using an Olympus IX83 inverted confocal microscope (Olympus life sciences, PA, USA) at 20x and the images were captured using the software Olympus FV-31S-SW.

6.2.7 Histological characterization

ECM pieces seeded with islets grown for 48 hours were fixed in 4% PFA for 48 hours. The samples were processed, dehydrated, embedded in wax, and sections of 4- μ m thickness were cut. The sections were dried, deparaffinized and hydrated. The sections were characterized using Hematoxylin and Eosin (H&E) staining to confirm the presence of islets embedded within the ECM. The images were acquired in visible mode at a 20x magnification using a NanoZoomer 2.0-RS slide scanner (Hamamatsu Photonics K.K, Bridgewater, NJ, USA) for digital pathology.

6.2.8 Functionality investigation by Glucose-Stimulated Insulin Secretion (GSIS)

The supernatant fluids from 7-day INS-1 cell cultures and 48-hour mouse pancreatic islet cultures were discarded after centrifuging the media. 1X PBS was used to wash the pellet, centrifuged, and the supernatant fluid was discarded. The cell pellet with the entire well content was washed twice (30 minutes and 1 hour of incubation) in a low-glucose (2.8 mM) solution containing Krebs-Ringer buffer (KRBH) supplemented with 115 mM NaCl, 5mM KCl, 25 mM HEPES, 24 mM NaHCO₃, 5mM CaCl₂, 1mM MgCl₂ and 0.1% bovine serum albumin to remove the residual insulin already present in the culture. Further, the whole well with the cells was incubated sequentially in low-glucose (2.8 mM, LG1), high glucose (28 mM, HG), high glucose ((28 mM) + 50 μ M 3-isobutyl-1-methylxanthine (IBMX, I5879, Sigma-Aldrich), HG+IBMX) and low-glucose (2.8 mM, LG2) for 1 hour at 37°C. KRBH buffer was used to prepare the glucose solutions. Post-incubation in each step, the buffer was collected, centrifuged and the supernatant fluid (containing the insulin) was stored at -20°C. Rinsing of the wells and cell pellets with 1X PBS following centrifugation was done in between each step with the rinsing solution discarded every time to remove residual insulin from the previous step. Insulin-containing solutions were stored at -20°C until running ELISA. Rat High Range Insulin ELISA (80-INSRTH-E01, Alpco Diagnostics) was used to estimate the insulin concentration from INS-1-seeded samples and Mouse High Range Insulin ELISA (80-INSMSH-E01) for islet-seeded samples. The secreted insulin was normalized to 100,000 cells and per islet, respectively, and the stimulation index was calculated for each condition by dividing the insulin concentration measured under high-glucose stimulation to that under low-glucose stimulation.

6.2.9 Statistical analysis

One or two-way analysis of variance (ANOVA) with Šidáks multiple comparisons tests was performed using GraphPad Prism. Microsoft Office 365 Excel was used to plot the graphs. A p value < 0.05 was considered statistically significant. The bars in the graph represent mean of three experiments \pm standard error.

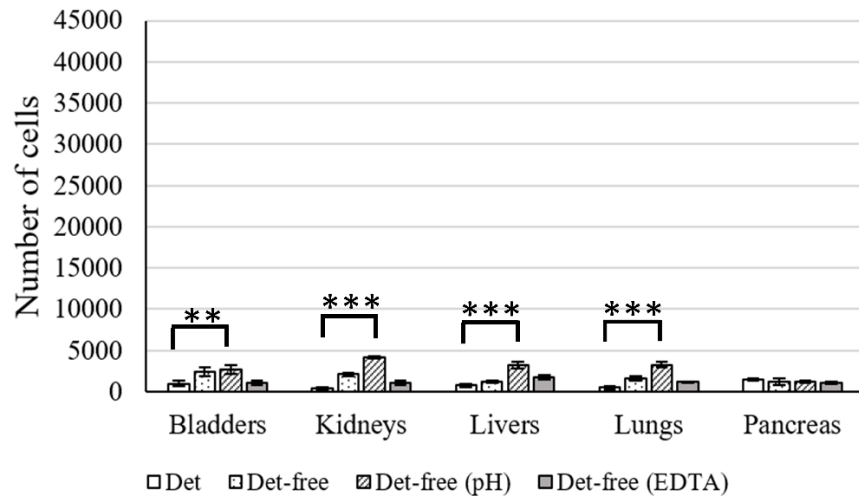
6.3 Results and Discussion

6.3.1 Proliferation of INS-1 cells on ECMs

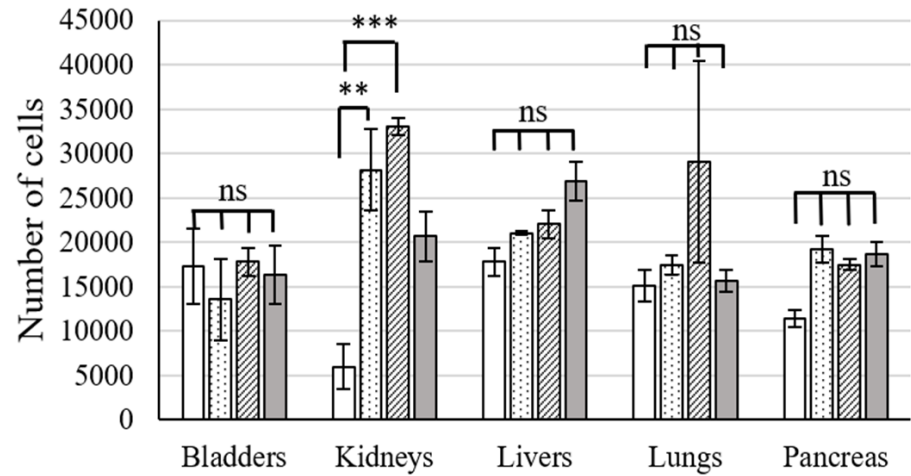
Characterization of ECMs derived from the different organs following detergent-free and detergent-based decellularization is described elsewhere[484]. ECMs were characterized for the removal of cellular components and dsDNA, and protein composition of the resulting ECMs analyzed.

Cell proliferation following 7 days of culture indicated that INS-1 cells proliferation was higher on bladders decellularized by the detergent-free method, as compared to cells on the other organs (Figure 6.1c). ECMs produced from bare detergent-free decellularization (i.e., with no additional treatment) did not result in cell proliferation in all cases, except for bladders. But INS-1 cells proliferated on detergent-free decellularized (alone, with pH and ethylene diamine tetraacetic acid (EDTA) treatments) bladders, kidneys (pH- and EDTA-treated ECM), livers (pH-treated), and lungs (EDTA-treated). Cell proliferation was not observed on decellularized pancreas, in all conditions. This could be due to the pancreas being necrotic on isolation due to the presence of exocrine enzymes, potentially digesting the pancreas upon isolation[484]. This points out to the absolute need to use freshly harvested pancreas (i.e., less than one hour) for decellularization. Even if the organs and the pancreas were obtained from the slaughterhouse less than 24 hours following animal sacrifice, this was not good enough for pancreas. Importance of pancreas preservation prior to its *in vivo* isolation and the need for qualified surgeons for transplants are reported elsewhere[485]. Cell proliferation on ECMs extracted using detergent-free processes (EDTA and/or pH treatments) for bladders, livers, lungs, and kidneys was significant as compared to detergent-based ECMs, where the cells did not proliferate. The negative controls without cells in Figure 6.1a indicated that the CyQUANT signals did not arise from the ECM itself. The number of cells after 4-hour seeding indicated viable cells on the different ECMs compared to the negative controls, as shown in Figure 6.1b. In summary, cell proliferation analysis indicates that INS-1 cells proliferated on at least one of the ECMs derived by detergent-free decellularization for all four organs (bladders, lungs, livers, and kidneys) but no for the pancreas ECM.

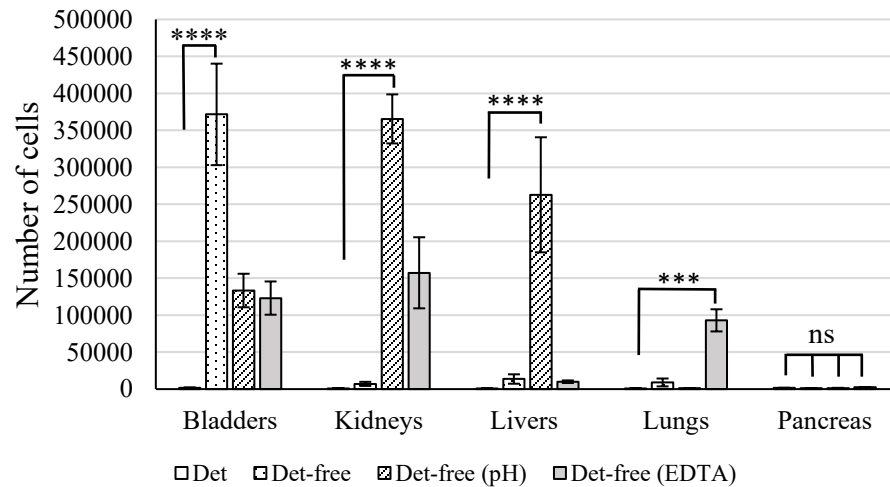
Basement membrane proteins such as collagens, laminins, heparan sulphate and fibronectin are essential for β -cell survival and proliferation[486]. Of all the collagens, collagen IV is key for INS-1 cells and MIN-6 cells proliferation[377,487]. Biomimetic materials incorporating decellularized urinary bladders have been used to culture fibroblasts[343], adipose-derived stem cells[369], skeletal muscle cells[368], and β -like rat cells[1]. Acellular kidneys were able to support the proliferation of embryonic stem cells[396,488], epithelial and endothelial cells[489] and primary renal cells[490]. Decellularized livers have been repopulated with primary hepatocytes[491], mesenchymal stem cells[492], and endothelial cells[493]. Decellularized lungs have been recellularized with lung fibroblasts, mesenchymal stem cells, and small airway epithelial cells[438]. Some studies describe the recellularization of pancreas with INS-1 cells, primary islets[337] and mesenchymal stem cells[494], but all of those studies indicated excision of fresh pancreas with decellularization initiated within 1 hour of excision. Again, our results validated the necessity of rapidly using the pancreas to perform decellularization. This was not the case for the other four tested organs (bladders, kidneys, livers, and lungs), as histological analysis revealed no obvious signs of damage, as it was observed for the pancreas[484].



a) Negative controls i.e., ECMs with no cells



b) 4 hours post-seeding of INS-1 cells on ECMs



c) 7 days post-seeding of INS-1 cells on ECMs

Figure 6.1 Number of INS-1 cells derived from the CyQUANT assay for **a)** ECMs with no cells as well as **b)** 4 hours, and **c)** 7 days post-seeding of INS-1 cells on ECMs. The statistical analysis was done comparing the detergent-based decellularization to the detergent-free ones. The data for the INS-1 cell number seeded on detergent-based and detergent-free alone decellularized bladder has been reported in an earlier study and has been used here to compare with other detergent-free decellularized bladders and other organs[1]. Tukey's two-way ANOVA was used to analyze significance. **** corresponds to $p < 0.0001$, *** represents $p < 0.001$, ** represents $p < 0.01$, * represents $p < 0.05$ and ns corresponds to non-significant. Bars represent average \pm standard error. Initial cell seeding density is 25,000 cells per well.

The metabolic activity of INS-1 cells, visualized by MTT staining following 7 days of culture, supported the CyQUANT cell proliferation results. Purple-colored crystals were visualized in all conditions where cells have proliferated, pinpointing metabolically active cells as shown in Figure 6.2. The ECMs where the cells did not proliferate and the negative controls were negative in terms of metabolic activity, as no purple-colored crystal was observed. MTT assay was successfully used to observe cell proliferation of human endometrial mesenchymal cells seeded on decellularized mouse liver[495]. The MTT assay was applied here to visually confirm cell viability and to supplement the CyQUANT proliferation analysis.

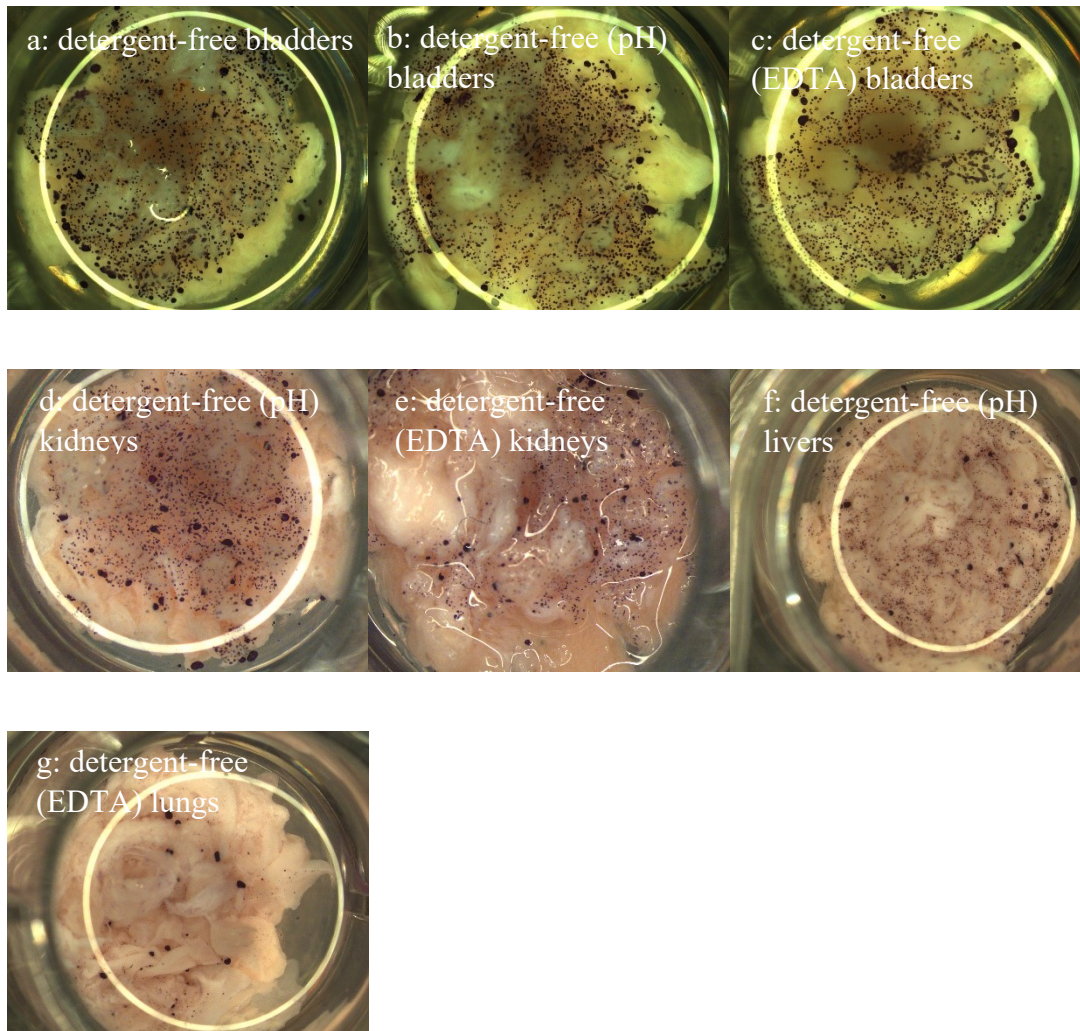


Figure 6.2 MTT staining allowing visualizing viable INS-1 cells on decellularized **a)** detergent-free bladders, **b)** detergent-free (pH) bladders, **c)** detergent-free (EDTA) bladders, **d)** detergent-free (pH) kidneys, **e)** detergent-free (EDTA) kidneys, **f)** detergent-free (pH) livers, and **g)** detergent-free (EDTA) lungs.

6.3.2 Functionality of INS-1 cells on ECMs

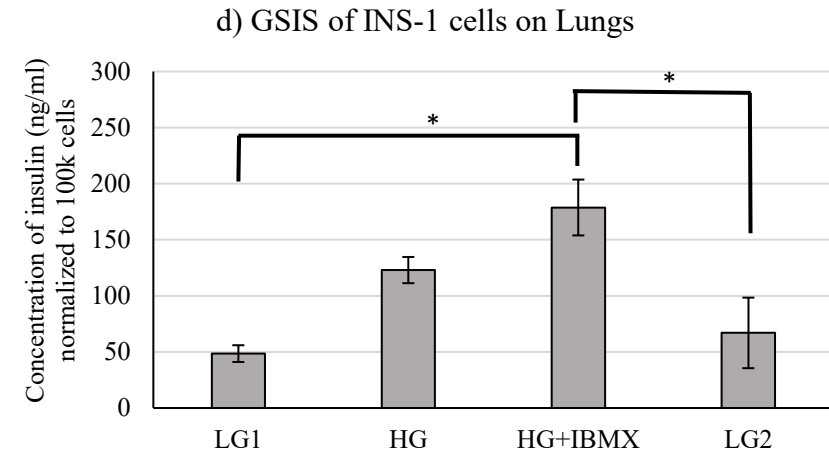
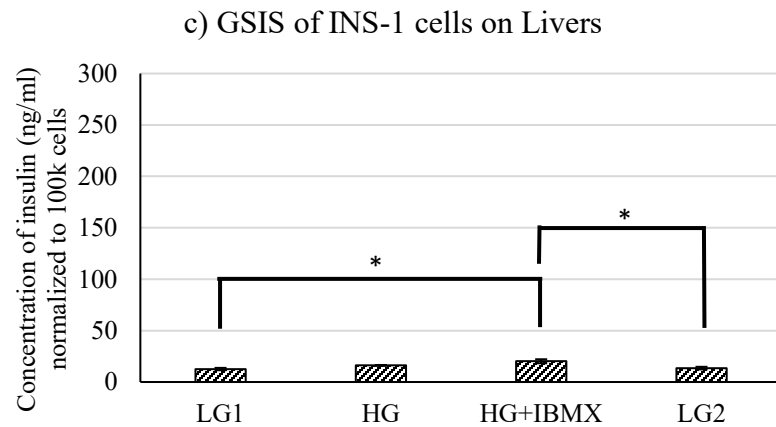
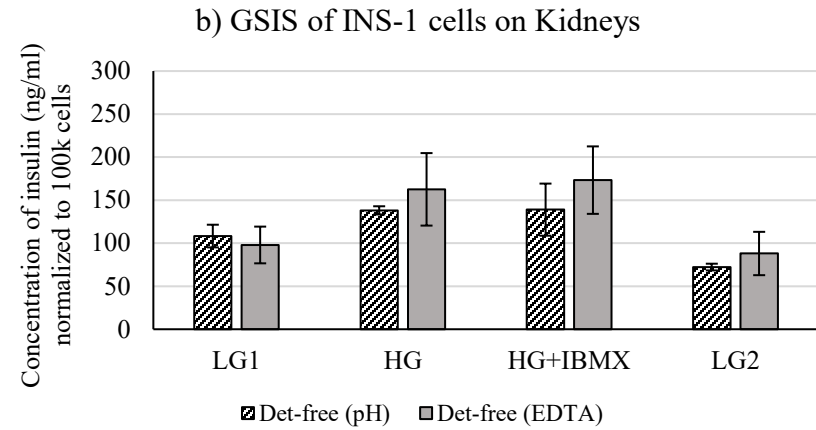
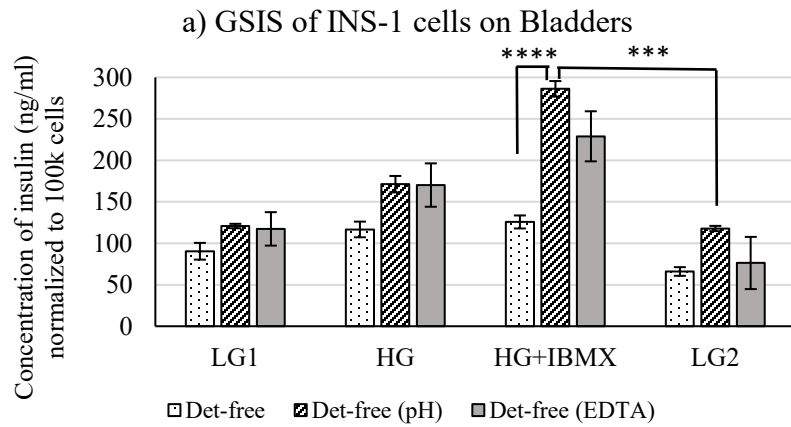
Functionality of INS-1 cells seeded on ECMs was evaluated using glucose-stimulated insulin secretion (GSIS). ECMs on which cells have proliferated also supported INS-1 cell functionality, as revealed by measuring insulin secretion after glucose stimulation (Figure 6.3).

Comparing insulin secretion of INS-1 cells on TCPS, insulin secretion was higher for INS-1 cells on ECMs in all conditions, except for the detergent-free (EDTA) livers (Figure 6.3a-e). Cells seeded on decellularized detergent-free bladders (bare, pH and EDTA), kidneys (pH and EDTA), livers (pH), and lungs (EDTA) were functional, as shown in Figure 6.3 (a-d). Since cells were metabolically inactive on the rest of the ECMs, confirmed by the MTT test, GSIS was not performed for the cells seeded on those ECMs. A previous study had described the conservation of collagen-4 and laminins in detergent-free decellularized bladders (bare, pH and EDTA)[484]. Basement membrane proteins such as type-4 collagen and laminins have been described to play a key role in insulin secretion from human islets[455]. This could explain the reason for insulin secretion by INS-1 cells seeded on detergent-free decellularized bladders, as observed in Figure 6.3 (a). Collagen-4 was not conserved in the detergent-free decellularized (bare, pH and EDTA) livers, whereas laminins were conserved in the detergent-free decellularized (pH) livers alone in an earlier study[484]. Reduced insulin secretion with decellularized liver in comparison to the other organs was observed in Figure 6.3 (c) corresponding to the proteomic results from the earlier study.

The stimulation index *i.e.*, the ratio of insulin concentration at high-glucose stimulation to that at low-glucose, was higher for cells on TCPS as shown in Figure 6.3e, compared to all conditions except for the detergent-free (EDTA)-treated lungs. The stimulation index of INS-1 cells seeded on decellularized lungs (EDTA) was significantly higher than the other conditions as shown in Figure 6.3f. The stimulation index of INS-1 cells on TCPS, as shown in Figure 6.3f, was comparable to that of a culture on fibronectin-coated plates[381]. The stimulation index of cells in all conditions, except that for the detergent-free (EDTA) lungs, was comparable to that of INS-1 cells grown in fibrin for 48 hours[376]. In a previous study, the stimulation index observed in 3D hydrogels was lower, as compared to that with 2D cultures[382]. However, it is risky to compare the two systems (TCPS and 3D cultures), as 3D culture systems can create a diffusional barrier

and/or can result in trapped insulin content[337,383]. The cell-matrix interactions influenced the survival and insulin secretion of β -cells by activation of NF- κ B signaling[374,384–386]. Collagen IV, laminins, fibronectins and other ECM proteins were conserved in detergent-free decellularized organs, as characterized by mass spectrometry[484]. Laminins in the basement membrane are key proteins responsible for insulin gene expression and β -cell proliferation[387]. Laminins were conserved in the detergent-free decellularized ECMs and could have supported insulin expression and thereby functionality[484].

Immunostaining for insulin in INS-1 cells has revealed green-coloured droplets of insulin, as shown in Figure 6.4. This supports that cells were functional on the screened ECMs. The staining for β -actin revealed the cytoskeleton of the cells, as shown in Figure 6.4. Focal cell adhesion points i.e., areas at which the cell interacts with the ECMs, were observed as extensions of actin filaments and shown in Figure 6.4. This is in accordance with another previous study reporting INS-1 cells on decellularized bladders[1]. Immunostaining indicated higher insulin fluorescence (green-droplets) on detergent-free decellularized bladder ECMs (bare, EDTA, pH) as compared to the insulin fluorescence on other organ ECMs (Figure 6.4). These results were coherent with the insulin secretion results, as shown in Figure 6.3 (a-d). Higher insulin secretion was observed for the INS-1 cells cultured on detergent-free decellularized bladders compared to other organ ECMs at low and high concentrations of glucose supplied. Since cells were metabolically inactive and did not proliferate on the rest of the ECMs, confirmed by the MTT test and CyQUANT assay, immunostaining was not performed for the cells seeded on those ECMs.



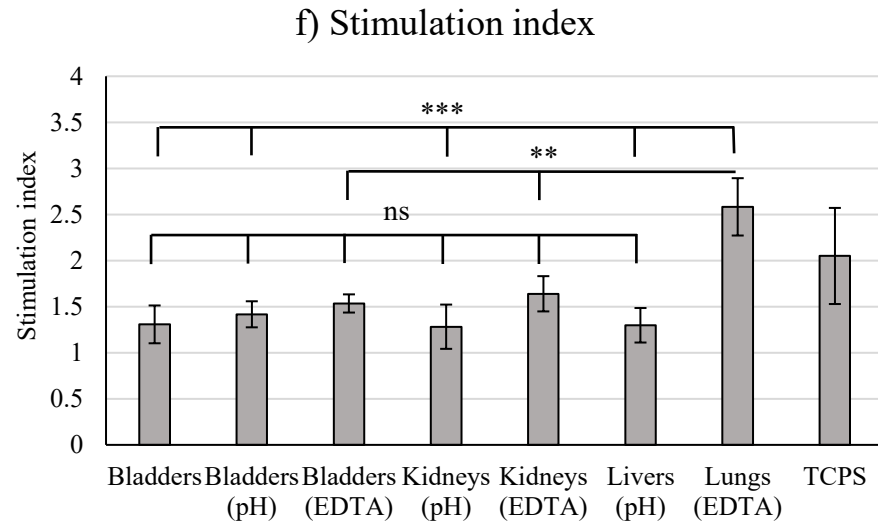
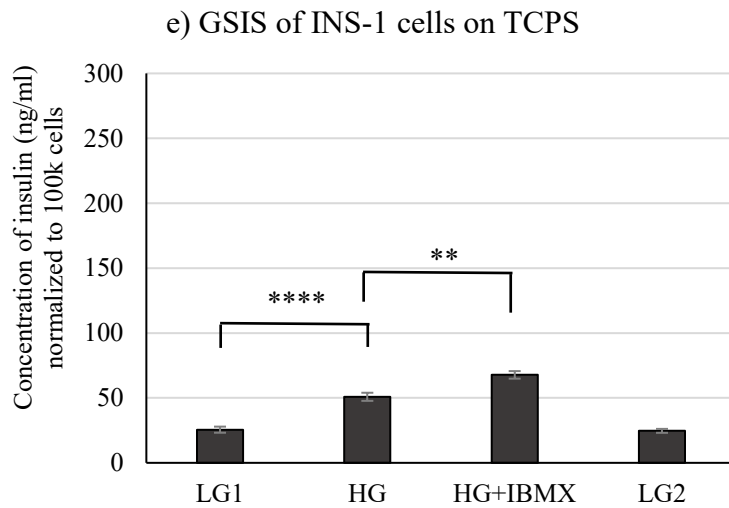


Figure 6.3 Functionality assessed by glucose-stimulated insulin secretion (GSIS) of INS-1 cells seeded on decellularized **a)** bladders, **b)** kidneys, **c)** livers, **d)** lungs, and **e)** TCPS. **f)** Stimulation index in each case (Stimulation index S.I. = concentration of insulin at HG/concentration of insulin at LG1). Glucose-stimulated insulin secretion data for INS-1 cells seeded on detergent-free alone decellularized bladder has been reported in an earlier study and has been used here to compare with other detergent-free decellularized bladders and other organs[1]. Ordinary one-way ANOVA with Šidáks multiple comparisons tests was used to determine significance. $p < 0.05$ was significant and indicated by *, $p < 0.01$ indicated by **, $p < 0.001$ indicated by *** and $p < 0.0001$ indicated by ****. TCPS means Tissue Culture Polystyrene.

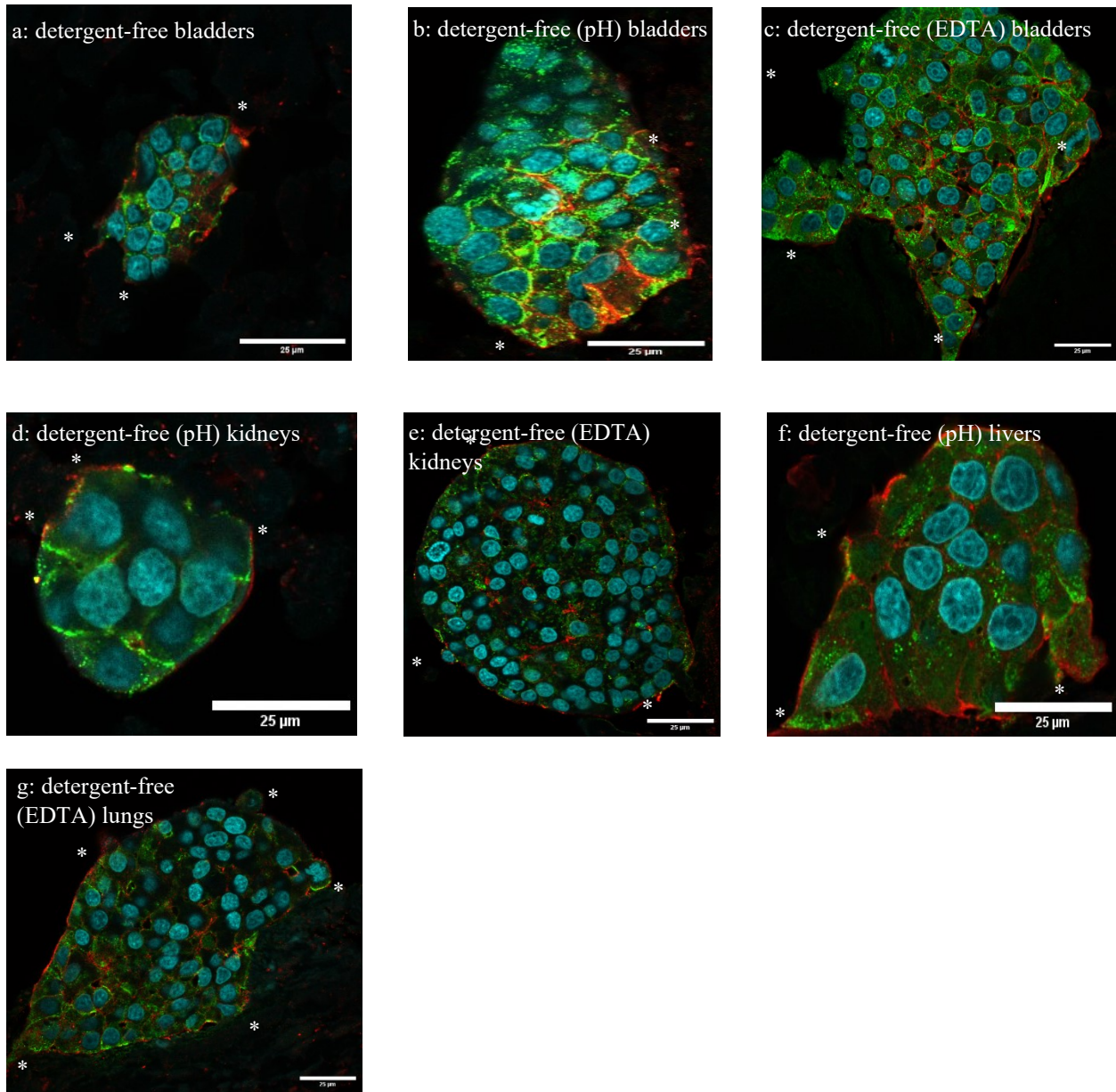


Figure 6.4 Immunostaining for insulin (green) and actin (red). INS-1 cells on bladder ECM obtained with the **a)** bare detergent-free method, **b)** detergent-free method with pH treatment, and **c)** detergent-free method with EDTA treatment. INS-1 cells on kidney ECM resulting from **d)** detergent-free (pH) and **e)** detergent-free (EDTA) treatments. INS-1 cells on liver ECM produced with the **f)** detergent-free (pH) method. INS-1 cells on lung ECM obtained from the **g)** detergent-free (EDTA) treatment. White * indicates focal adhesion points of cells to the ECM. Scale bars indicate 25 μm.

6.3.3 Functionality of pancreatic mouse islets seeded on detergent-free-produced bladder ECM

Considering the yield following decellularization and proliferation (Figure 6.1c), functionality of INS-1 cells on the different organ matrices, detergent-free decellularized bladder ECM was selected for further studies with mouse islets. Functionality of mouse islets measured by the GSIS assay is shown in Figure 6.5. As with INS-1 cells, islets were functional on the bladder ECM produced using the detergent-free method. The insulin secretion trend was as expected for the glucose concentrations used for stimulation. Previously, porcine[496] and rat [497] islets were used to recellularize decellularized pancreas. Although islets were seeded in the decellularized pancreas, the functionality was not reported. Later, a study reported a similar trend for islets seeded into decellularized mouse pancreas[337]. Islets seeded on ECM obtained from decellularized bladders secreted more insulin, as compared to those on TCPS. The stimulation index was slightly higher for the TCPS, as compared to that of cells on bladder ECM.

The pancreatic duct is closely associated with the islets in adult rats and the ductal ECM contains laminins, collagen IV and fibronectin, all responsible for β -cell survival[380,498,499]. Mass spectrometric analysis of the bladder ECM revealed the conservation of the necessary proteins and this could have supported islets functionality[484]. The presence of islets on the seeded ECM following 48 hours of culture was confirmed using H&E staining, as shown in Figure 6.6 (a-d). Histological characterization revealed intact islets with intact nuclei in the cells. Islets functionality was visualized by the expression of insulin within the islets, as shown in Figure 6.6 (e-g). In a previous study, mouse pancreatic islets grown 48 hours in decellularized mouse pancreas secreted insulin[337]. Staining for CD31 indicated the presence of endothelial cells, as pointed out in Figure 6.6 (h-j). Although not very prominent, endothelial cells were detected at the islet junction and near the ECM in Figure 6.6d and sparsely within the islets, shown by white arrows in Figures 6.6e and 6.6f. Islet capillaries consisting of endothelial cells are more extensive and crowded in rodents[500–502]. They are responsible for the secretion of certain growth factors and endothelin-1, which in turn increases insulin secretion in mouse islets by

triggering calcium influx into the β -cells[503,504]. Longer duration cultures would be essential to indicate angiogenesis onto the matrix.

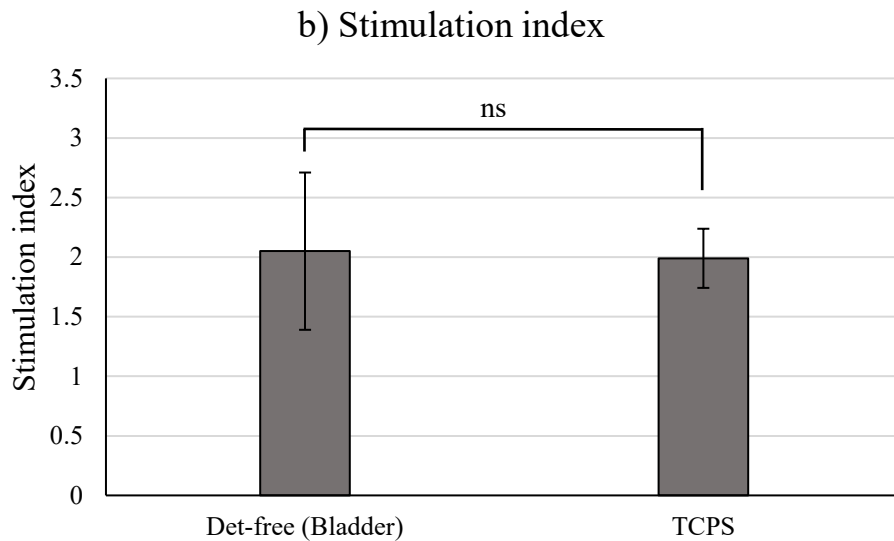
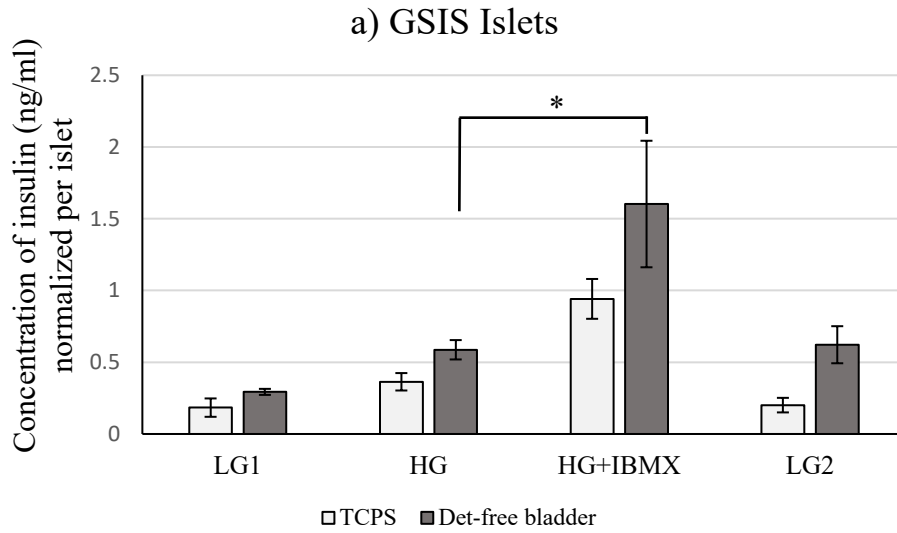


Figure 6.5 a) Glucose-stimulated insulin secretion (GSIS) from islets grown 48 hours on TCPS and bladder ECM obtained from the bare detergent-free decellularization method. **b)** Stimulation index of islets. Unpaired t-test was used to determine the significance. ns indicates no significance. Stimulation index = Concentration of secreted insulin at HG / Concentration of secreted insulin at LG1. TCPS refers to Tissue Culture Polystyrene. Bars in the graphs indicate a) Average \pm SE and b) Average \pm SD.

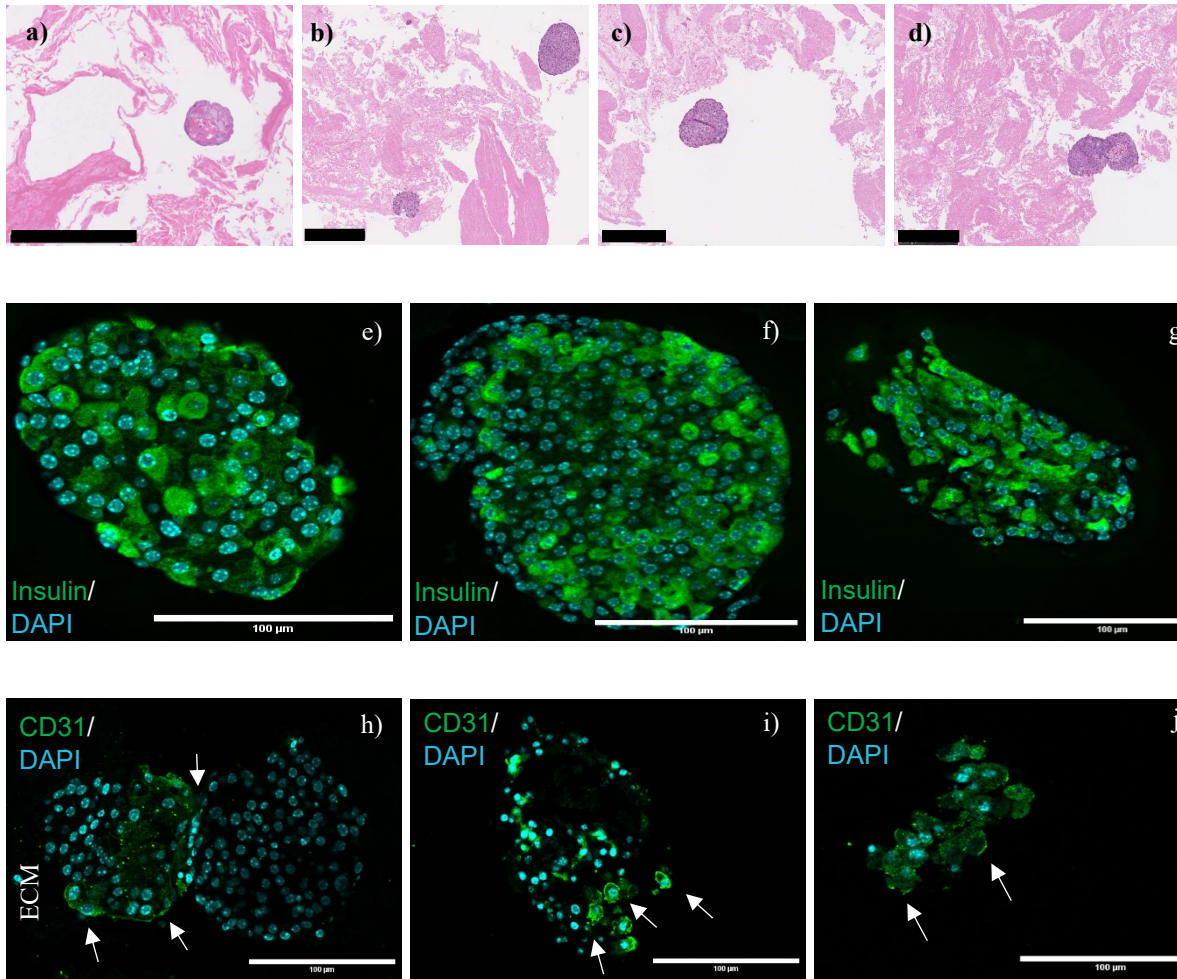


Figure 6.6 Islets grown 48 hours on detergent-free decellularized bladders stained by Haematoxylin and Eosin (H&E) (**a-d**), insulin expression (**e-g**) and endothelial cells (CD31-positive cells) (**h-j**). The white arrows indicate the endothelial cells. The islets in panel h correspond to the islets in panel d to highlight the presence and position of the ECM. Black scale bars correspond to 250 μm and white scale bars to 100 μm .

6.4 Conclusions

This study presents an overall comparison of the responses of a pancreatic β -like cell line (INS-1 cells) and mouse pancreatic islets towards ECMs obtained by decellularizing five porcine organs using three detergent-free methods and one detergent-based approach. The bare detergent-free method supported cell proliferation and functionality. The conservation of laminins, collagen-IV, and fibronectin in ECMs produced using detergent-free methods could be a significant factor. The additional use of EDTA-chelation and isoelectric treatment by pH adjustment coupled to the bare detergent-free technique yielded cell-compatible ECMs (for bladders, livers, lungs, and kidneys).

This study is one of the very few comparing the response of a single cell type (β -like cells) on different organ ECMs. Screening of different organ ECMs for tissue engineering could reveal better suited ECMs developed and tuned for the targeted application. The investigation with primary pancreatic mouse islets showed that the ECM resulting from the detergent-free-treated bladders is suitable to obtain ECM supporting islet survival and functionality.

The present study also opens the door for the development of different organ ECMs for a multitude of products depending on the need and on the anatomical site of application. Pluripotent stem cells could benefit from a combination of different ECMs stemming from different organs to support their expansion and sequential differentiation. This could allow making functional biologically active scaffolds. Application-oriented products such as scaffolds, sheets, meshes and bioadhesives could be derived from ECMs extracted and formulated from different organs.

Acknowledgements

The research project was supported by NSERC through a Discovery Grant awarded to Patrick Vermette (Grant # 250296-2012). We thank Marilène Paquette and the histology research core facility of the Faculté de Médecine et des Sciences de la Santé (Université de Sherbrooke) for the histology service. We thank Hadrien Le-Nghiem for technical help. All authors have approved the final manuscript.

Patrick Vermette owns shares in SherMATRIX Inc., a company developing biomaterials for clinical uses.

Chapter 7

Conclusions

Conclusions - Français

Le travail expérimental de cette thèse visait principalement à explorer les propriétés de la Matrice ExtraCellulaire (MEC) dérivée de différents organes porcins, afin de comprendre les différences entre elles et pour identifier leur utilisation potentielle pour la création de matériaux biomimétiques pour l'ingénierie tissulaire et la médecine.

Le travail expérimental présenté dans le chapitre 4, intitulé « Système de culture cellulaire pour étudier l'effet de la matrice extracellulaire sur des cellules pancréatiques sécrétrices d'insuline », visait à illustrer le potentiel de la MEC dérivée d'organes porcins décellularisés. Ici, un système de culture cellulaire a été conçu pour étudier les avantages potentiels de la MEC dérivée de vessies porcines décellularisées par deux techniques différentes (utilisant un détergent et sans détergent). Initialement, les MECs ont été validées pour l'élimination des composants cellulaires et la conservation de l'(ultra)structure de la MEC. Cette étude est l'une des très rares à exclure l'utilisation de détergent pour décellulariser des organes. Le broyage des vessies avant et pendant la décellularisation a permis de réduire la taille des particules de la MEC, augmentant ainsi la surface exposée et permettant une durée plus courte de décellularisation [356]. Plusieurs études ont modifié l'ultrastructure de la MEC pour former des papiers tissulaires et des gels solubilisés [480]. Des expériences de solubilisation et d'immobilisation avec la MEC ont montré la dégradation de l'ultrastructure et des protéines (comme indiqué dans l'Appendice D). L'importance de maintenir l'ultrastructure de la MEC pour permettre l'adhérence cellulaire a donc été mise au premier plan. Un système de culture cellulaire simple a été conçu pour faciliter l'interaction des cellules pancréatiques de rat sécrétant de l'insuline (INS-1) avec la MEC, dans lequel l'agarose a été utilisée comme moule pour maintenir la MEC au fond de la plaque. Les cellules INS-1 se sont agrégées lorsqu'elles ont étéensemencées sur l'agarose [505] et le ménisque du moule dans les puits a permis aux agrégats d'interagir avec la MEC. En outre, les MECs obtenues ont été validées pour leur cytotoxicité potentielle et leur fonctionnalité à l'aide de cellules INS-1. La MEC de vessie décellularisée sans détergent était non cytotoxique pour les cellules, supportant la prolifération et la fonctionnalité, confirmées par l'analyse de prolifération cellulaire CyQUANT NF et par la sécrétion d'insuline stimulée par le glucose (GSIS), respectivement, après 7 jours de culture *in vitro*. Précédemment, une étude a démontré que la matrice extracellulaire (ECM) dérivée de la lignée de cellules de carcinome de la vessie de rat 804G aidait à l'attachement et favorisait une

meilleure fonctionnalité des cellules β [380]. Le premier travail expérimental a permis de développer et de valider un système qui nous aiderait à cribler les MECs de différents organes porcins. Les limites de ce travail incluent le fait que les cellules INS-1 étant une lignée cellulaire immortalisée ne sont utiles que pour le criblage et l'élaboration de conclusions préliminaires. La réponse des cellules β natives dans les îlots pancréatiques primaires est différente de celle des lignées cellulaires [374,506]. Également, les résultats de culture en 3D ne pouvaient pas être comparés à ceux obtenus en culture 2D sur plaques de polystyrène de culture de tissus (TCPS) en raison de la barrière de diffusion dans le cas des cultures 3D pour extraire l'insuline des gels après 7 jours de culture [337,383].

Sur la base des résultats du premier travail expérimental présenté dans le chapitre 4, un deuxième travail expérimental (chapitre 5) a été réalisé et celui-ci est intitulé « Caractérisation de la matrice extracellulaire dérivée d'organes porcins décellularisés ». Ici, cinq organes porcins i.e., la vessie, les reins, les poumons, le foie et le pancréas, ont été décellularisés par quatre techniques de décellularisation, dont trois n'utilisaient pas de détergent (l'une impliquant l'ajustement du pH et l'autre l'ajout d'EDTA) et une était à base de détergent. L'étude visait à étudier l'effet de la méthode de décellularisation sur la composition en protéines et l'ultrastructure de la matrice extracellulaire. Les méthodes sans détergent ont permis de mieux conserver la matrice extracellulaire que la méthode à base de détergent. Une autodigestion du pancréas a été observée par analyse en histologie et a été confirmée par une diminution de l'ADN double brin ainsi qu'une perte de collagène et de laminines dans le pancréas natif. L'identification des protéines à l'aide de la spectrométrie de masse a indiqué la préservation de collagène IV, de laminines, de fibronectine et d'autres protéines de la matrice extracellulaire dans les MECs produites par méthodes sans détergent et a entraîné un plus grand nombre de protéines différentes dans la MEC. L'orientation du collagène n'a pas été modifiée après la décellularisation par rapport à l'état natif. Cette étude a révélé que la méthode de décellularisation exerce une grande influence sur l'ultrastructure et la composition de la matrice extracellulaire résultante et qu'une approche de caractérisation multifactorielle est nécessaire pour identifier l'équilibre entre l'élimination des composants cellulaires et le maintien de l'ultrastructure.

Le travail expérimental final de cette thèse, dans le chapitre 6 intitulé « Matrice Extracellulaire provenant d'organes porcins décellularisés comme échafaudages pour des cellules sécrétrices

d'insuline et des îlots pancréatiques », avait pour objectif de cribler les cinq matrices extracellulaires obtenues par des méthodes de décellularisation sans détergent et une utilisant un détergent d'abord avec des cellules INS-1, et ensuite, d'étudier l'effet de la matrice criblée sur des îlots pancréatiques primaires de souris. Les cellules ont proliféré plus rapidement sur les vessies produites à l'aide de méthodes sans détergent par rapport aux autres organes également décellularisés à l'aide de protocoles sans détergent. La prolifération cellulaire n'a pas été observée sur le pancréas décellularisé en raison de l'autodigestion du pancréas lors de son isolement par les enzymes de la partie exocrine, entraînant potentiellement la destruction du collagène IV, des laminines et de la fibronectine. Les profils GSIS des cellules INS-1 sur toutes les matrices extracellulaires sur lesquelles les cellules ont proliféré ont indiqué que celles-ci étaient fonctionnelles. Les indices de stimulation (le rapport de la concentration d'insuline sécrétée à haute concentration de glucose sur celle à faible concentration de glucose) étaient compris entre 1,25 et 2,25 pour les différentes matrices extracellulaires. Il est reconnu que les interactions cellules-matrice permettent d'améliorer la fonctionnalité des cellules β par l'activation de la signalisation NF- κ B [374,384–386]. En particulier, les laminines ont été identifiées comme jouant un rôle clé dans la survie et la fonctionnalité des cellules β , correspondant aux résultats de l'étude présente, car les laminines ont été conservées dans les échantillons sans détergent [387,484]. L'étude menée sur les îlots pancréatiques primaires de souris ensemencés sur des vessies décellularisées sans détergent après 48 heures de culture a révélé que ceux-ci étaient fonctionnels, car le profil de sécrétion d'insuline était en adéquation aux conditions de stimulation par le glucose. Les futurs travaux expérimentaux devraient inclure des tests sur les îlots sur différentes matrices extracellulaires d'organes afin d'identifier un candidat potentiel à tester *in vivo*.

Bien que les résultats de la thèse aient démontré la recellularisation de différentes matrices d'organes, il reste certains défis à explorer à l'avenir:

- L'évaluation de la quantité d'ADN double brin (dsDNA) a été utilisée comme l'un des critères pour évaluer l'efficacité de la décellularisation. Cependant, des restes d'ADN simple brin (ssDNA) et d'ARN pourraient être des sources potentielles rendant la matrice immunogène.
- La stérilisation de la matrice après la décellularisation est une préoccupation importante. Étant donné que les étapes de stérilisation altèrent la matrice extracellulaire (MEC), un examen attentif des différentes techniques disponibles doit être effectué. Les irradiations gamma sont

utilisées pour stériliser de nombreux dispositifs médicaux et entraînent la dégradation des protéines dans la matrice.

- Étant donné la source du tissu et les étapes de traitement (comme la filtration et la récupération du tissu), des variations entre les lots ont été observées. Une solution potentielle pourrait être l'optimisation de la source de tissu et la normalisation du traitement pour une mise à l'échelle optimale.

Un bio-adhésif incorporant la matrice extracellulaire de vessie décellularisée sans détergent a été également développé avec l'aide de Laurine Gallien. Celui-ci a été caractérisé *in vitro* pour sa cytotoxicité et, avec la participation de Dr Marco Sirois, *ex vivo* à l'aide d'un modèle de poumon porcin (comme indiqué dans l'Annexe C) et est actuellement testé *in vivo* dans un modèle de rat sous-cutané par Dr Sangamithirai Subramanian (stagiaire post-doctorante). Des expériences préliminaires ont été réalisées chez l'animal avec l'aide du Dr Marco Sirois. Une demande de brevet provisoire a été déposée auprès du United States Patent and Trademark Office (USPTO) pour ce produit. Des bio-adhésifs fabriqués à partir de matrices extracellulaires d'organes différents, en fonction de l'application, pourraient être explorés à l'avenir.

Initialement, au début du projet, des expériences ont été réalisées pour solubiliser et immobiliser les protéines de la matrice extracellulaire (MEC) sur les surfaces présentées dans l'Annexe D. Cependant, l'importance de conserver l'ultrastructure et la composition de la MEC a été réalisée et les expériences ont été orientées vers le développement de produits fabriqués à partir de MEC avec une ultrastructure suffisamment conservée.

En résumé, cette thèse présente un système de culture cellulaire pour étudier la réponse des cellules INS-1 et des îlots pancréatiques primaires en contact avec des morceaux de matrice extracellulaire (MEC) obtenus à partir de différents organes porcins décellularisés. Une caractérisation détaillée de la MEC pourrait conduire au criblage des MEC en fonction de l'application. Nous pourrions également conclure que la composition et l'organisation de la MEC sont totalement différentes entre les organes et diffèrent selon les méthodes utilisées pour effectuer la décellularisation. Un équilibre entre l'élimination du contenu cellulaire et le maintien de l'ultrastructure de la MEC pourrait être une façon d'extraire le potentiel maximal de cette MEC. Enfin, la MEC peut être utilisée pour formuler des matériaux biomimétiques fonctionnels tels que des bio-adhésifs, des échafaudages fabriqués par impression 3D, des pansements pour le traitement de plaies et des

patches régénératifs qui pourraient être utilisés pour résoudre certains des problèmes actuellement rencontrés en médecine.

Conclusions - English

The experimental work of this thesis primarily aimed to explore the properties of the ExtraCellular Matrix (ECM) derived from different porcine organs, to understand the differences among them and for their potential use in creating biomimetic materials for tissue engineering and medicine.

The experimental work presented in Chapter 4 entitled, “A cell culture system to investigate the effect of extracellular matrix on insulin-secreting pancreatic cells” attempted to highlight the potential of ECM derived from decellularized porcine organs. Here, a cell culture system was designed to investigate the potential benefit of ECM derived from porcine bladders decellularized by two different techniques (detergent-based and detergent-free). Initially, the ECMs were validated for the removal of cellular components and the conservation of the ECM (ultra)structure. This study is one of the very few excluding the use of detergent to decellularize organs. Dicing and grinding bladders prior and during decellularization reduce the particle size of the ECM, thereby, increasing the surface area of exposure and enabling a shorter duration for decellularization[356]. Several studies have modified the ultrastructure of the ECM to form tissue papers and solubilized gels[480]. The immobilization of solubilized ECM from decellularized organs (as shown in Appendix D) resulted in degradation of the proteins and, hence, led to the loss of ECM potential. The importance of maintaining the ultrastructure of the ECM to enable cell attachment was understood. A simple cell culture system was designed to facilitate the interaction of insulin-secreting rat pancreatic cells (INS-1) with the ECM wherein, agarose was used as a mold to hold the ECM at the bottom of the plate. INS-1 cells formed aggregates when seeded on agarose[505] and the meniscus of the mold in the wells aided the aggregates to interact with the ECM. Further, the ECMs obtained were validated for toxicity and functionality using INS-1 cells. The detergent-free decellularized bladder ECM was non-cytotoxic towards the cells, aided in proliferation and functionality as confirmed by the CyQUANT NF cell proliferation assay and glucose-stimulated insulin secretion (GSIS), respectively, following 7 days of culture *in vitro*. Previously, a study had demonstrated that ECM derived from rat bladder carcinoma cell line 804G aided in the attachment and enhanced functionality of β -cells[380]. The first experimental work allowed to develop and validate a system that would help us screen ECMs from different porcine organs. The limitations of the study include: INS-1 cells being an immortalized cell line, they can only be used to draw preliminary conclusions as the response of native β -cells in primary islets

vary as compared to cell lines[374,506]. 3D cell culture results could not be compared to those obtained with 2D cultures on tissue culture polystyrene (TCPS) due to the diffusional barrier in the case of 3D cultures. The storage of residual insulin in the 3D culture following longer periods of culture and difficulty associated with washing them completely from the setup makes it difficult to compare the 3D and 2D culture insulin secretion results [337,383].

Based on the results of the first experimental work described in Chapter 4, a second experimental work (Chapter 5) was designed and is entitled, “Characterization of ExtraCellular Matrix from decellularized porcine organs”. Here, five different porcine organs i.e., bladders, kidneys, lungs, livers, and pancreas were decellularized by four decellularization techniques, three of which were detergent-free (one involving the adjustment of pH and the other the addition of EDTA) and one was detergent-based. The study was designed to investigate the effect of the decellularization method on the protein composition and orientation in the ECM. The detergent-free methods conserved the ECM better as compared to the detergent-based method. Interestingly, self-digestion of pancreas was observed by staining and was supported by a reduced dsDNA content and loss of collagen and laminins. Protein identification using mass spectrometry indicated preservation of collagen IV, laminins, fibronectin, and other ECM proteins with the detergent-free methods and resulted in a higher number of different proteins in the ECM matrix. Collagen orientation was not altered following decellularization. This study revealed that the decellularization method has a great influence on the ultrastructure and composition of the resulting ECM and a multi-characterization approach is required to find the balance between the removal of cellular components and maintainance of the ultrastructure.

The final experimental work of this thesis (Chapter 6) is entitled, “Extracellular matrix from decellularized porcine organs as scaffolds for insulin-secreting cells and pancreatic islets”, aimed to screen the five different ECMs obtained by the detergent-free and detergent-based decellularization methods using INS-1 cells and further study the effect of the ECM on primary mouse islets. The cells proliferated more on the bladder ECM produced using detergent-free methods as compared to the other organ-derived ECMs. Cell proliferation was not observed on decellularized pancreas because of self-digestion of the pancreas on isolation by the enzymes from the exocrine part resulting in the destruction of collagen IV, laminins, and fibronectin. The GSIS profiles of INS-1 cells on all ECMs on which cells have proliferated indicated functionality. The

stimulation indices (the ratio of insulin secretion at high glucose concentration to that at low glucose concentration) were between 1.25 and 2.25 approx. for the different ECMs. Cells-matrix interactions enhanced the functionality of the β -cells by activation of the NF- κ B signaling[374,384–386]. Particularly, laminins were identified to play a key role in β -cells survival and functionality and this is in accordance with the results of the study, as laminins were conserved in the detergent-free samples[387,484]. The study with the primary islets from mouse seeded on detergent-free decellularized bladders following 48 hours of culture indicated functionality as the insulin secretion profile corresponded to the glucose-stimulation. Further experimental work should include testing the islets on the different organ ECMs and identifying a potential candidate to be tested *in vivo*.

Although results in the thesis demonstrated the recellularization of different organ matrices, there are certain challenges still to be explored in the future.

- Evaluation of dsDNA content was used as one of the criteria for evaluating the efficiency of decellularization. However, remnant ssDNA and RNA could be potential sources rendering an immunogenic matrix.
- Sterilization of the matrix following decellularization is an important concern. Since, sterilization steps alter the ECM, a careful screening of the different techniques available must be done. Gamma irradiation is used to sterilize multiple medical devices and is involved in the degradation of proteins in the matrix.
- Considering the source of the tissue and the processing (such as filtration and recuperation of tissue), batch variations were observed. Potential solution could be tissue source optimization and normalization of the processing for scale-up.

A bioadhesive incorporating the detergent-free decellularized bladder ECM has been developed with the help of Laurine Gallien. It has been characterized *in vitro* for cytotoxicity and, with the participation of Dr. Marco Sirois, *ex vivo* using a porcine lung model (as shown in Appendix C) and is currently being tested *in vivo* in a subcutaneous rat model by Dr. Sangamithirai Subramanian (post-doc). Preliminary animal experiments were performed with the help of Dr. Marco Sirois. A provisional patent application has been filed with the United States Patent Office (USPTO) for the same. Bioadhesives from different organ ECMs specific for application could be an avenue to be explored in the future. The bladder ECM (a component in the bioadhesive) has been characterized

and investigated in this thesis. Preliminary results drawn from the thesis would aid in progressing the research into bioadhesives. The future concerning this endeavor would require conducting multiple studies in animal models to confirm the safety of the bioadhesive developed and would be carried out by the research group in the future.

Initially, at the beginning of the project, experiments were performed to solubilize and immobilize the solubilized ECM on surfaces, as shown in Appendix D. However, the importance of conserving the ultrastructure and composition of ECM was realized and the experiments were thereafter directed towards developing application-oriented products using conserved ECM.

In summary, this thesis presents a cell culture system to study the culture of INS-1 cells and primary mouse islets in contact with ECM pieces obtained from different decellularized porcine organs. A detailed characterization of the ECM could lead to the screening of ECMs based on a given application. We could also conclude that the ECM composition and organization are different among organs and differ according to the method used to perform decellularization. A balance between cellular content removal and maintenance of the ECM ultrastructure could be a way to extract the maximal potential of the ECM. Finally, the ECM can be used to formulate functional biomimetic materials such as bioadhesives, 3D printed scaffolds, wound dressings and regenerative patches that could be used to resolve some of the issues currently faced in medicine. Future work is directed towards optimizing the scale up of ECM production and testing the application-oriented biomaterials *in vitro* and *in vivo*.

BIBLIOGRAPHY

1. Dhandapani V, Vermette P. Decellularized bladder as scaffold to support proliferation and functionality of insulin-secreting pancreatic cells. *Journal of Biomedical Materials Research Part B: Applied Biomaterials* [Internet]. [cited 2023 Jun 19]. Available from: <https://onlinelibrary.wiley.com/doi/abs/10.1002/jbm.b.35292>
2. Global Observatory on Donation and Transplantation (GODT). Transplant statistics [Internet]. [cited 2023 Feb 12]. Available from: <https://www.transplant-observatory.org/>
3. Human Resources and Service Administration. Organ Donation Statistics | organdonor.gov [Internet]. [cited 2023 Feb 12]. Available from: <https://www.organdonor.gov/learn/organ-donation-statistics>
4. Zhai Y, Petrowsky H, Hong JC, Busuttil RW, Kupiec-Weglinski JW. Ischaemia-reperfusion injury in liver transplantation--from bench to bedside. *Nat Rev Gastroenterol Hepatol*. 2013 Feb;10(2):79–89.
5. Kupiec-Weglinski JW. Grand Challenges in Organ Transplantation. *Frontiers in Transplantation* [Internet]. 2022 [cited 2023 Feb 12];1. Available from: <https://www.frontiersin.org/articles/10.3389/frtra.2022.897679>
6. Guruswamy Damodaran R, Vermette P. Tissue and organ decellularization in regenerative medicine. *Biotechnol Prog*. 2018 Nov;34(6):1494–505.
7. Liao J, Xu B, Zhang R, Fan Y, Xie H, Li X. Applications of decellularized materials in tissue engineering: advantages, drawbacks and current improvements, and future perspectives. *J Mater Chem B*. 2020 Nov 18;8(44):10023–49.
8. Duan W, Bian X, Bu Y. Applications of Bioadhesives: A Mini Review. *Frontiers in Bioengineering and Biotechnology* [Internet]. 2021 [cited 2023 Feb 12];9. Available from: <https://www.frontiersin.org/articles/10.3389/fbioe.2021.716035>
9. Coronado RE, Somaraki-Cormier M, Natesan S, Christy RJ, Ong JL, Halff GA. Decellularization and Solubilization of Porcine Liver for Use as a Substrate for Porcine Hepatocyte Culture. *Cell Transplant*. 2017 Dec;26(12):1840–54.
10. Shinde SU, Sangave PM, Chougule KB, Patil SV, Patil SS, Bhingardev D. Formulation and evaluation of bioadhesive pulsatile drug delivery system of an antilipidemic drug. *World Journal of Pharmacy and Pharmaceutical Sciences*. 2018 Jul 5;7(8):10.
11. Burks S, Spotnitz W. Safety and Usability of Hemostats, Sealants, and Adhesives. *AORN Journal*. 2014 Aug;100(2):160–76.
12. Zhu W, Chuah YJ, Wang DA. Bioadhesives for internal medical applications: A review. *Acta Biomaterialia*. 2018 Jul;74:1–16.

13. Spotnitz WD, Burks S. Hemostats, sealants, and adhesives III: a new update as well as cost and regulatory considerations for components of the surgical toolbox: hemostats, sealants and adhesives III. *Transfusion*. 2012 Oct;52(10):2243–55.
14. Bouten PJM, Zonjee M, Bender J, Yauw STK, van Goor H, van Hest JCM, Hoogenboom R. The chemistry of tissue adhesive materials. *Progress in Polymer Science*. 2014 Jul;39(7):1375–405.
15. US Food and Drug Administration. CFR - Code of Federal Regulations Title 21, Volume 8 [Internet]. [cited 2020 Aug 24]. Available from: <https://www.accessdata.fda.gov/scripts/cdrh/cfdocs/cfcfr/CFRSearch.cfm?fr=878.4010>
16. US Food and Drug administration. CFR - Code of Federal Regulations Title 21, Volume 8 [Internet]. [cited 2020 Aug 24]. Available from: <https://www.accessdata.fda.gov/scripts/cdrh/cfdocs/cfcfr/CFRSearch.cfm?fr=878.4490>
17. US Food and Drug Administration. Fibrin sealant (Human)- Clinical Review [Internet]. [cited 2020 Aug 24]. Available from: <https://www.fda.gov/media/109417/download>
18. Spotnitz WD, Burks S. Hemostats, sealants, and adhesives: components of the surgical toolbox. *Transfusion*. 2008 Jul;48(7):1502–16.
19. Guo M, Song W. The growing U.S. bioeconomy: Drivers, development and constraints. *New Biotechnology*. 2019 Mar;49:48–57.
20. Businesswire. \$1.4 Billion Bioadhesive Market: Global Industry Trends, Share, Size, Growth, Opportunity and Forecast 2017-2022 [Internet]. 2017 [cited 2020 Aug 24]. Available from: <https://www.businesswire.com/news/home/20171124005080/en/1.4-Billion-Bioadhesive-Market-Global-Industry-Trends>
21. Business Wire. Global Bioadhesive Market 2018 with Forecasts to 2023 - Henkel Corp, Dow Chemical Company, Ashland, Adhesives Research, and EcoSynthetix are Dominating [Internet]. [cited 2020 Aug 24]. Available from: <https://www.businesswire.com/news/home/20180412006056/en/Global-Bioadhesive-Market-2018-Forecasts-2023>
22. Viswanadh MK, Muthu MS. Targeted bioadhesive nanomedicine: an effective approach for synergistic drug delivery to cancers. *Nanomedicine*. 2018 Jun;13(12):1401–3.
23. Mehdizadeh M, Yang J. Design Strategies and Applications of Tissue Bioadhesives. *Macromolecular Bioscience*. 2013 Mar;13(3):271–88.
24. Athanasiadis T, Beule AG, Robinson BH, Robinson SR, Shi Z, Wormald PJ. Effects of a novel chitosan gel on mucosal wound healing following endoscopic sinus surgery in a sheep model of chronic rhinosinusitis. *Laryngoscope*. 2008 Jun;118(6):1088–94.
25. Ratner BD, editor. *Biomaterials science: an introduction to materials in medicine*. 3rd ed. Amsterdam ; Boston: Elsevier/Academic Press; 2013. 1519 p.

26. Zhao L, Li X, Zhao J, Ma S, Ma X, Fan D, Zhu C, Liu Y. A novel smart injectable hydrogel prepared by microbial transglutaminase and human-like collagen: Its characterization and biocompatibility. *Mater Sci Eng C Mater Biol Appl*. 2016 Nov 1;68:317–26.
27. Zheng Shu X, Liu Y, Palumbo FS, Luo Y, Prestwich GD. In situ crosslinkable hyaluronan hydrogels for tissue engineering. *Biomaterials*. 2004 Apr;25(7–8):1339–48.
28. Kuo CK, Ma PX. Maintaining dimensions and mechanical properties of ionically crosslinked alginate hydrogel scaffolds in vitro. *J Biomed Mater Res A*. 2008 Mar 15;84(4):899–907.
29. Ranson JM, Amin K, Schechter EMM, Kosutic D. Haemostatic property of cyanoacrylate in pedicled flaps. *British Journal of Oral and Maxillofacial Surgery*. 2016 Nov;54(9):1046–7.
30. Perera AN, Tavares MM. 2-Octyl Cyanoacrylate. In: StatPearls [Internet]. Treasure Island (FL): StatPearls Publishing; 2020 [cited 2020 Apr 6]. Available from: <http://www.ncbi.nlm.nih.gov/books/NBK532293/>
31. Leonardi M, Barbara C, Simonetti L, Giardino R, Aldini NN, Fini M, Martini L, Masetti L, Joechler M, Roncaroli F. Glubran 2: A New Acrylic Glue for Neuroradiological Endovascular Use. *Interventional Neuroradiology*. 2002;6.
32. Baxter. CoSeal, Baxter advanced surgery [Internet]. [cited 2020 Apr 6]. Available from: <https://advancedsurgery.baxter.com/products/coseal>
33. Integra. Integra®- DuraSeal® dural sealant system tender package insert [Internet]. [cited 2020 Aug 24]. Available from: http://www.neuromiss.gr/sites/default/files/DuraSeal_EN.pdf
34. BD. Progel™ pleural air leak sealant system- Brochure [Internet]. [cited 2020 Aug 24]. Available from: https://www.crbard.com/CRBard/media/ProductAssets/DavolInc/PF10139/en-US/PF10139_BD_Progel%20Brochure.pdf
35. Cohera Medical. TissuGlu-A new kind of glue [Internet]. Microverse Studios. [cited 2020 Aug 24]. Available from: <https://www.microversestudios.com/animations/cohera/>
36. Gilbert TW, Badylak SF, Gusenoff J, Beckman EJ, Clower DM, Daly P, Rubin JP. Lysine-Derived Urethane Surgical Adhesive Prevents Seroma Formation in a Canine Abdominoplasty Model: Plastic and Reconstructive Surgery. 2008 Jul;122(1):95–102.
37. Annabi N, Rana D, Shirzaei Sani E, Portillo-Lara R, Gifford JL, Fares MM, Mithieux SM, Weiss AS. Engineering a sprayable and elastic hydrogel adhesive with antimicrobial properties for wound healing. *Biomaterials*. 2017 Sep;139:229–43.

38. Pinkas O, Goder D, Noyvirt R, Peleg S, Kahlon M, Zilberman M. Structuring of composite hydrogel bioadhesives and its effect on properties and bonding mechanism. *Acta Biomater.* 2017 15;51:125–37.
39. Baxter. Tisseel- Baxter advanced surgery [Internet]. [cited 2020 Aug 24]. Available from: <https://advancedsurgery.baxter.com/products/tisseel>
40. Buchta C, Dettke M, Funovics PT, Hocker P, Knobl P, Macher M, Quehenberger P, Treitl C, Worel N. Fibrin sealant produced by the CryoSealR FS System: product chemistry, material properties and possible preparation in the autologous preoperative setting. *Vox Sanguinis.* 2004 May;86(4):257–62.
41. J&J Medical Devices. EVICEL® Fibrin Sealant (Human) [Internet]. [cited 2020 Aug 24]. Available from: <https://www.jnjmedicaldevices.com/en-US/product/evicel-fibrin-sealant-human>
42. Vyas KS, Saha SP. Comparison of hemostatic agents used in vascular surgery. *Expert Opinion on Biological Therapy.* 2013 Dec;13(12):1663–72.
43. Kullar P, Weerakkody R, Cathcart R, Yates P. Locally applied haemostatic agents in the management of acute epistaxis (nosebleeds). In: The Cochrane Collaboration, editor. *Cochrane Database of Systematic Reviews* [Internet]. Chichester, UK: John Wiley & Sons, Ltd; 2011 [cited 2020 Apr 6]. Available from: <http://doi.wiley.com/10.1002/14651858.CD009373>
44. Zhang YJ, Gao B, Liu XW. Topical and effective hemostatic medicines in the battlefield. *Int J Clin Exp Med.* 2015;8(1):10–9.
45. Fischer TH, Bode AP, Demcheva M, Vournakis JN. Hemostatic properties of glucosamine-based materials. *Journal of Biomedical Materials Research Part A.* 2007 Jan;80A(1):167–74.
46. Thatte HS, Zagarins S, Khuri SF, Fischer TH. Mechanisms of Poly-N-Acetyl Glucosamine Polymer-Mediated Hemostasis: Platelet Interactions: *The Journal of Trauma: Injury, Infection, and Critical Care.* 2004 Jul;57(Supplement):S13–21.
47. Clinique Chirurgicale de Laval. BST Cargel treatment [Internet]. [cited 2020 Aug 24]. Available from: <https://www.cliniquechirurgicaledeval.com/en/technology-cargel>
48. Bhamidipati CM, Coselli JS, LeMaire SA. BioGlue® in 2011: What Is Its Role in Cardiac Surgery? 2011;7.
49. Noshadi I, Hong S, Sullivan KE, Shirzaei Sani E, Portillo-Lara R, Tamayol A, Shin SR, Gao AE, Stoppel WL, Black III LD, Khademhosseini A, Annabi N. In vitro and in vivo analysis of visible light crosslinkable gelatin methacryloyl (GelMA) hydrogels. *Biomaterials Science.* 2017;5(10):2093–105.

50. Theodore P, Davis P. In vitro evaluation of physical characteristics for lung applications, as compared to other surgical sealants. :9.
51. Ge L, Chen S. Recent Advances in Tissue Adhesives for Clinical Medicine. *Polymers*. 2020 Apr 18;12(4):939.
52. Sierra DH, Eberhardt AW, Lemons JE. Failure characteristics of multiple-component fibrin-based adhesives. *J Biomed Mater Res*. 2002 Jan;59(1):1–11.
53. Strausberg R, Link R. Protein-based medical adhesives. *Trends in Biotechnology*. 1990;8:53–7.
54. Bitton R, Josef E, Shimshelashvili I, Shapira K, Seliktar D, Bianco-Peled H. Phloroglucinol-based biomimetic adhesives for medical applications. *Acta Biomaterialia*. 2009 Jun;5(5):1582–7.
55. Horowitz B, Busch M. Estimating the pathogen safety of manufactured human plasma products: application to fibrin sealants and to thrombin. *Transfusion*. 2008 Aug;48(8):1739–53.
56. US Food and Drug Administration. Pre-market approval, Summary of safety and effectiveness-BioGlue® Surgical Adhesive [Internet]. [cited 2020 Aug 24]. Available from: https://www.accessdata.fda.gov/cdrh_docs/pdf/P010003b.pdf
57. US Food and Drug Administration. Pre-market approval, Summary of safety and effectiveness- Omnex™ Ethicon™ Surgical sealant [Internet]. [cited 2020 Aug 24]. Available from: https://www.accessdata.fda.gov/cdrh_docs/pdf6/P060029B.pdf
58. Reece TB, Maxey TS, Kron IL. A prospectus on tissue adhesives. *The American Journal of Surgery*. 2001 Aug;182(2):S40–4.
59. Kd T, Cj B. • Engineered for appropriate strength and optimal duration, even in high-pressure areas. :2.
60. Kd T, Cj B. • DuraSeal® strengthens your repair and supports the body’s natural healing process. :2.
61. Lee SH, Park CW, Lee SG, Kim WK. Postoperative Cervical Cord Compression Induced by Hydrogel Dural Sealant (DuraSeal®). *Korean J Spine*. 2013;10(1):44.
62. Williams DF. On the mechanisms of biocompatibility. *Biomaterials*. 2008 Jul;29(20):2941–53.
63. Gray D, White R, Cooper P, Kingsley A. Applied wound management and using the wound healing continuum in practice. :8.
64. Bornstein P. Thrombospondins as matricellular modulators of cell function. *Journal of Clinical Investigation*. 2001 Apr 15;107(8):929–34.

65. Anderson J, Cramer S. Perspectives on the Inflammatory, Healing, and Foreign Body Responses to Biomaterials and Medical Devices. In: *Host Response to Biomaterials* [Internet]. Elsevier; 2015 [cited 2019 Jul 18]. p. 13–36. Available from: <https://linkinghub.elsevier.com/retrieve/pii/B9780128001967000025>
66. Nguyen LL, D’Amore PA. Cellular interactions in vascular growth and differentiation. *Int Rev Cytol.* 2001;204:1–48.
67. Hinz B, Mastrangelo D, Iselin CE, Chaponnier C, Gabbiani G. Mechanical Tension Controls Granulation Tissue Contractile Activity and Myofibroblast Differentiation. *The American Journal of Pathology.* 2001 Sep;159(3):1009–20.
68. Anderson JM. Biological Responses to Materials. *Annual Review of Materials Research.* 2001 Aug;31(1):81–110.
69. Bota PCS, Collie AMB, Puolakkainen P, Vernon RB, Sage EH, Ratner BD, Stayton PS. Biomaterial topography alters healing in vivo and monocyte/macrophage activation in vitro. *Journal of Biomedical Materials Research Part A.* 2010 Aug 19;95A(2):649–57.
70. Anderson JM, Rodriguez A, Chang DT. Foreign body reaction to biomaterials. *Seminars in Immunology.* 2008 Apr;20(2):86–100.
71. Revell P. Biological causes of prosthetic joint failure. In: *Joint Replacement Technology* [Internet]. Elsevier; 2008 [cited 2019 Jul 18]. p. 349–96. Available from: <https://linkinghub.elsevier.com/retrieve/pii/B9781845692452500159>
72. Bucala R. Review Series - Inflammation & Fibrosis * Fibrocytes and fibrosis. *QJM.* 2012 Jun 1;105(6):505–8.
73. Taboada GM, Yang K, Pereira MJN, Liu SS, Hu Y, Karp JM, Artzi N, Lee Y. Overcoming the translational barriers of tissue adhesives. *Nat Rev Mater.* 2020 Apr;5(4):310–29.
74. Mackensen A, Dräger R, Schlesier M, Mertelsmann R, Lindemann A. Presence of IgE antibodies to bovine serum albumin in a patient developing anaphylaxis after vaccination with human peptide-pulsed dendritic cells. *Cancer Immunology, Immunotherapy.* 2000 May 22;49(3):152–6.
75. Mogues T, Li J, Coburn J, Kuter DJ. IgG antibodies against bovine serum albumin in humans—their prevalence and response to exposure to bovine serum albumin. *Journal of Immunological Methods.* 2005 May;300(1–2):1–11.
76. Macy E, Bulpitt K, Champlin R, Saxon A. Anaphylaxis to infusion of autologous bone marrow: An apparent reaction to self, mediated by IgE antibody to bovine serum albumin. *Journal of Allergy and Clinical Immunology.* 1989 May;83(5):871–5.

77. Tanabe S, Kobayashi Y, Takahata Y, Morimatsu F, Shibata R, Nishimura T. Some human B and T cell epitopes of bovine serum albumin, the major beef allergen. *Biochemical and Biophysical Research Communications*. 2002;6.
78. Sung HW, Huang RN, Huang LLH, Tsai CC. In vitro evaluation of cytotoxicity of a naturally occurring cross-linking reagent for biological tissue fixation. *Journal of Biomaterials Science, Polymer Edition*. 1999 Jan;10(1):63–78.
79. Clair MBGSt, Bermudez E, Gross EA, Butterworth BE, Recio L, Carrano AV. Evaluation of the genotoxic potential of glutaraldehyde. *Environ Mol Mutagen*. 1991;18(2):113–9.
80. Christen V, Faltermann S, Brun NR, Kunz PY, Fent K. Cytotoxicity and molecular effects of biocidal disinfectants (quaternary ammonia, glutaraldehyde, poly(hexamethylene biguanide) hydrochloride PHMB) and their mixtures in vitro and in zebrafish eleuthero-embryos. *Science of The Total Environment*. 2017 May;586:1204–18.
81. Smith DR, Wang RS. Glutaraldehyde exposure and its occupational impact in the health care environment. :8.
82. Umashankar P, Kumari T, Mohanan P. Glutaraldehyde treatment elicits toxic response compared to decellularization in bovine pericardium. *Toxicology International*. 2012;19(1):51.
83. Ballantyne B, Myers RC. The acute toxicity and primary irritancy of glutaraldehyde solutions. *Vet Hum Toxicol*. 2001 Aug;43(4):193–202.
84. Beckman EJ, Buckley M, Agarwal S, Zhang J. Medical adhesive and methods of tissue adhesion [Internet]. US7264823B2, 2007 [cited 2021 Nov 4]. Available from: <https://patents.google.com/patent/US7264823B2/en>
85. Matsuda T, Nakajima N, Itoh T, Takakura T. Development of a compliant surgical adhesive derived from novel fluorinated hexamethylene diisocyanate. *ASAIO Trans*. 1989 Sep;35(3):381–3.
86. Singh I, Gupta NP, Hemal AK, Aron M, Seth A, Dogra PN. Severely encrusted polyurethane ureteral stents: management and analysis of potential risk factors. *Urology*. 2001 Oct;58(4):526–31.
87. Sen S, Pandey H, Jaiswal K, Gupta M, Basak P. A study on Invitro and Invivo immune response against polyurethane inserts. *Recent Advances in Applied Biosciences*. 2015;163–6.
88. Laschke MW, Strohe A, Scheuer C, Eglin D, Verrier S, Alini M, Pohlemann T, Menger MD. In vivo biocompatibility and vascularization of biodegradable porous polyurethane scaffolds for tissue engineering. *Acta Biomaterialia*. 2009 Jul;5(6):1991–2001.

89. Vermette P, editor. Biomedical applications of polyurethanes. Georgetown, Tex. : Austin, Tex: Landes Bioscience ; Eureka.com; 2001. 273 p. (Tissue engineering intelligence unit).
90. Sinclair TM, Kerrigan CL, Buntic R. Biodegradation of the polyurethane foam covering of breast implants. *Plast Reconstr Surg*. 1993 Nov;92(6):1003–13; discussion 1014.
91. García Cerdá D, Ballester AM, Aliena-Valero A, Carabén-Redaño A, Lloris JM. Use of cyanoacrylate adhesives in general surgery. *Surgery Today*. 2015 Aug;45(8):939–56.
92. Daane S. Alloplastic Implantation. In: *Plastic Surgery Secrets Plus* [Internet]. Elsevier; 2010 [cited 2020 Aug 24]. p. 28–32. Available from: <https://linkinghub.elsevier.com/retrieve/pii/B9780323034708000053>
93. Toriumi DM, Raslan WF, Friedman M, Tardy ME. Variable Histotoxicity of Histoacryl When Used in a Subcutaneous Site: An Experimental Study. *The Laryngoscope*. 1991 Apr;101(4):339–43.
94. Toriumi DM, Raslan WF, Friedman M, Tardy ME. Histotoxicity of Cyanoacrylate Tissue Adhesives: A Comparative Study. *Archives of Otolaryngology - Head and Neck Surgery*. 1990 May 1;116(5):546–50.
95. Aronson SB, McMaster PRB, Moore TE, Coon MA. Toxicity of the Cyanoacrylates. *Archives of Ophthalmology*. 1970 Sep 1;84(3):342–9.
96. Leonard F, Kulkarni RK, Brandes G, Nelson J, Cameron JJ. Synthesis and degradation of poly (alkyl α -cyanoacrylates). *J Appl Polym Sci*. 1966 Feb;10(2):259–72.
97. Mattamal GJ. US FDA perspective on the regulations of medical-grade polymers: cyanoacrylate polymer medical device tissue adhesives. *Expert Review of Medical Devices*. 2008 Jan;5(1):41–9.
98. Mizrahi B, Stefanescu CF, Yang C, Lawlor MW, Ko D, Langer R, Kohane DS. Elasticity and safety of alkoxyethyl cyanoacrylate tissue adhesives. *Acta Biomaterialia*. 2011 Aug;7(8):3150–7.
99. Wan X, Zhang J, Yu W, Shen L, Ji S, Hu T. Effect of protein immunogenicity and PEG size and branching on the anti-PEG immune response to PEGylated proteins. *Process Biochemistry*. 2017 Jan;52:183–91.
100. Webster R, Elliott V, Park BK, Walker D, Hankin M, Taupin P. PEG and PEG conjugates toxicity: towards an understanding of the toxicity of PEG and its relevance to PEGylated biologicals. In: Veronese FM, editor. *PEGylated Protein Drugs: Basic Science and Clinical Applications* [Internet]. Basel: Birkhäuser Basel; 2009 [cited 2020 Aug 25]. p. 127–46. Available from: http://link.springer.com/10.1007/978-3-7643-8679-5_8

101. Mima Y, Hashimoto Y, Shimizu T, Kiwada H, Ishida T. Anti-PEG IgM Is a Major Contributor to the Accelerated Blood Clearance of Polyethylene Glycol-Conjugated Protein. *Molecular Pharmaceutics*. 2015 Jul 6;12(7):2429–35.
102. Zhang H, Zhao T, Newland B, Duffy P, Annaidh AN, O’Cearbhaill ED, Wang W. On-demand and negative-thermo-swelling tissue adhesive based on highly branched ambivalent PEG–catechol copolymers. *J Mater Chem B*. 2015;3(31):6420–8.
103. Joo JY, Amin MdL, Rajangam T, An SSA. Fibrinogen as a promising material for various biomedical applications. *Mol Cell Toxicol*. 2015 Mar;11(1):1–9.
104. Pählman LI, Mörgelin M, Kasetty G, Olin AI, Schmidtchen A, Herwald H. Antimicrobial activity of fibrinogen and fibrinogen-derived peptides – a novel link between coagulation and innate immunity. *Thrombosis and Haemostasis*. 2013;109(05):930–9.
105. Santos SG, Lamghari M, Almeida CR, Oliveira MI, Neves N, Ribeiro AC, Barbosa JN, Barros R, Maciel J, Martins MCL, Gonçalves RM, Barbosa MA. Adsorbed fibrinogen leads to improved bone regeneration and correlates with differences in the systemic immune response. *Acta Biomaterialia*. 2013 Jul;9(7):7209–17.
106. Lovejoy AE, Reynolds TC, Visich JE, Butine MD, Young G, Belvedere MA, Blain RC, Pederson SM, Ishak LM, Nugent DJ. Safety and pharmacokinetics of recombinant factor XIII-A2 administration in patients with congenital factor XIII deficiency. *Blood*. 2006 Jul 1;108(1):57–62.
107. Dorion RP, Hamati HF, Landis B, Frey C, Heydt D, Carey D. Risk and clinical significance of developing antibodies induced by topical thrombin preparations. *Arch Pathol Lab Med*. 1998 Oct;122(10):887–94.
108. Ofosu FA, Crean S, Reynolds MW. A safety review of topical bovine thrombin-induced generation of antibodies to bovine proteins. *Clinical Therapeutics*. 2009 Apr;31(4):679–91.
109. Francesko A, Tzanov T. Chitin, Chitosan and Derivatives for Wound Healing and Tissue Engineering. In: Nyanhongo GS, Steiner W, Gübitz G, editors. *Biofunctionalization of Polymers and their Applications* [Internet]. Berlin, Heidelberg: Springer Berlin Heidelberg; 2010 [cited 2019 Jul 18]. p. 1–27. Available from: http://link.springer.com/10.1007/10_2010_93
110. Peluso G, Petillo O, Ranieri M, Santin M, Ambrosic L, Calabró D, Avallone B, Balsamo G. Chitosan-mediated stimulation of macrophage function. *Biomaterials*. 1994 Dec;15(15):1215–20.
111. Instituto de Engenharia Biomédica, Universidade do Porto, Rua do Campo Alegre 823, 4150-180-Porto, Portugal, Oliveira M, Santos S, Oliveira M, Torres A, Barbosa M. Chitosan drives anti-inflammatory macrophage polarisation and pro-inflammatory dendritic cell stimulation. *eCM*. 2012 Jul 24;24:136–53.

112. Fong D, Hoemann CD. Chitosan immunomodulatory properties: perspectives on the impact of structural properties and dosage. *Future Science OA*. 2018 Jan;4(1):FSO225.
113. Ohsaki M, Tsutsumi H, Kumagai T, Yamanaka T, Wataya Y, Furukawa H, Kojima H, Saito A, Yano S, Chiba S. The relevance of TH1 and TH2 cells in immediate and nonimmediate reactions to gelatin-containing vaccine. *Journal of Allergy and Clinical Immunology*. 1999 Feb;103(2):276–81.
114. Kumagai T, Yamanaka T, Wataya Y, Umetsu A, Kawamura N, Ikeda K, Furukawa H, Kimura K, Chiba S, Saito S. Gelatin-specific humoral and cellular immune responses in children with immediate- and nonimmediate-type reactions to live measles, mumps, rubella, and varicella vaccines. *Journal of Allergy and Clinical Immunology*. 1997 Jul;100(1):130–4.
115. Chen T, Janjua R, McDermott MK, Bernstein SL, Steidl SM, Payne GF. Gelatin-based biomimetic tissue adhesive. Potential for retinal reattachment. *Journal of Biomedical Materials Research Part B: Applied Biomaterials*. 2006 May;77B(2):416–22.
116. Raveendran R, Khan DA. Gelatin Anaphylaxis During Surgery: A Rare Cause of Perioperative Anaphylaxis. *The Journal of Allergy and Clinical Immunology: In Practice*. 2017 Sep;5(5):1466–7.
117. Kassam A, Nemoto E, Balzer J, Rao G, Welch WC, Kuwabara H, Boada F, Horowitz M. Effects of Tisseel Fibrin Glue on the Central Nervous System of Nonhuman Primates. *Ear, Nose & Throat Journal*. 2004 Apr;83(4):246–56.
118. Reuthebuch.O, Moehrlen.U, Kurrer.M.O,Stammberger.U, Lachat.M.L,Turina.M. Biocompatibility and Biodegradation of High Doses of FloSeal in Rats. *Journal of Applied Research in Clinical and Experimental therapeutics*. 2001;2(2)(XXI–XXII).
119. Gilbert TW, Badylak SF, Beckman EJ, Clower DM, Rubin JP. Prevention of seroma formation with TissuGlu® surgical adhesive in a canine abdominoplasty model: Long term clinical and histologic studies. *Journal of Plastic, Reconstructive & Aesthetic Surgery*. 2013 Mar;66(3):414–22.
120. Wallace DG, Cruise GM, Rhee WM, Schroeder JA, Prior JJ, Ju J, Maroney M, Duronio J, Ngo MH, Estridge T, Coker GC. A tissue sealant based on reactive multifunctional polyethylene glycol. *Journal of Biomedical Materials Research*. 2001;58(5):545–55.
121. Hill A, Estridge TD, Maroney M, Monnet E, Egbert B, Cruise G, Coker GT. Treatment of suture line bleeding with a novel synthetic surgical sealant in a canine iliac PTFE graft model. *J Biomed Mater Res*. 2001 May 1;58(3):308–12.
122. Slezak P, Klang A, Ferguson J, Monforte X, Schmidt P, Bauder B, Url A, Osuchowski M, Redl H, Spazierer D, Gulle H. Tissue reactions to polyethylene glycol and glutaraldehyde-based surgical sealants in a rabbit aorta model. *Journal of Biomaterials Applications*. 2020 Apr;34(9):1330–40.

123. Hewitt CW, Marra SW, Kann BR, Tran HS, Puc MM, Chrzanowski FA, Tran JLV, Lenz SD, Cilley JH, Simonetti VA, DelRossi AJ. BioGlue surgical adhesive for thoracic aortic repair during coagulopathy: efficacy and histopathology. *The Annals of Thoracic Surgery*. 2001 May;71(5):1609–12.
124. Kalsi P, Thom M, Choi D. Histological effects of fibrin glue and synthetic tissue glues on the spinal cord: are they safe to use? *British Journal of Neurosurgery*. 2017 Nov 2;31(6):695–700.
125. Stergios K, Frountzas M, Pergialiotis V, Korou LM, Kontzoglou K, Stefanidis K, Nikiteas N, Perrea DN, Vaos G. The Effect of TISSEEL® on Colorectal Anastomosis Healing Process in a Diabetic Animal Experimental Model. *In Vivo*. 2020;34(2):659–65.
126. Kobayashi H, Sekine T, Nakamura T, Shimizu Y. In vivo evaluation of a new sealant material on a rat lung air leak model. *Journal of Biomedical Materials Research*. 2001;58(6):658–65.
127. Fuller C. Reduction of intraoperative air leaks with Progel in pulmonary resection: a comprehensive review. *Journal of Cardiothoracic Surgery* [Internet]. 2013 Dec [cited 2021 Jan 20];8(1). Available from: <https://cardiothoracicsurgery.biomedcentral.com/articles/10.1186/1749-8090-8-90>
128. Thomas PJ, Tawfic SN. Eosinophil-rich inflammatory response to FloSeal hemostatic matrix presenting as postoperative pelvic pain. *American Journal of Obstetrics and Gynecology*. 2009 Apr;200(4):e10–1.
129. Gaffen A, Zheng H. BioGlue Surgical Adhesive: reported incidents of chronic inflammation and foreign-body reactions. *Can Adverse React Newsl* 16(4); 2006.
130. Fürst W, Banerjee A. Release of Glutaraldehyde From an Albumin-Glutaraldehyde Tissue Adhesive Causes Significant In Vitro and In Vivo Toxicity. *The Annals of Thoracic Surgery*. 2005 May;79(5):1522–8.
131. Gruber-Blum S, Petter-Puchner AH, Mika K, Brand J, Redl H, Öhlinger W, Benesch T, Fortelny RH. A comparison of a bovine albumin/glutaraldehyde glue versus fibrin sealant for hernia mesh fixation in experimental onlay and IPOM repair in rats. *Surgical Endoscopy*. 2010 Dec;24(12):3086–94.
132. Chen CT, Choi CL, Suen DT, Kwong A. A prospective randomised controlled trial of octylcyanoacrylate tissue adhesive and standard suture for wound closure following breast surgery. *Hong Kong Med J*. 2016 Jun;22(3):216–22.
133. Ferreira P, Gil MH, Alves P. An overview in surgical adhesives. :22.
134. Annabi N, Tamayol A, Shin SR, Ghaemmaghami AM, Peppas NA, Khademhosseini A. Surgical Materials: Current Challenges and Nano-enabled Solutions. *Nano Today*. 2014 Oct 1;9(5):574–89.

135. Simon HK, McLario DJ, Bruns TB, Zempsky WT, Wood RJ, Sullivan KM. Long-term appearance of lacerations repaired using a tissue adhesive. *Pediatrics*. 1997 Feb;99(2):193–5.
136. Soni A, Narula R, Kumar A, Parmar M, Sahore M, Chandel M. Comparing cyanoacrylate tissue adhesive and conventional subcuticular skin sutures for maxillofacial incisions--a prospective randomized trial considering closure time, wound morbidity, and cosmetic outcome. *J Oral Maxillofac Surg*. 2013 Dec;71(12):2152.e1-8.
137. Arunachalam P, King PA, Orford J. A prospective comparison of tissue glue versus sutures for circumcision. *Pediatr Surg Int*. 2003 Apr;19(1–2):18–9.
138. Ao A, Oa S. Wound Edge Complications and Cost Considerations in Closure of Herniotomy Wounds. *Annals of Pediatric Surgery*. 2009;5(2):94–7.
139. Oz MC, Rondinone JF, Shargill NS. FloSeal Matrix: new generation topical hemostatic sealant. *J Card Surg*. 2003 Dec;18(6):486–93.
140. Oz MC, Cosgrove DM, Badduke BR, Hill JD, Flannery MR, Palumbo R, Topic N. Controlled clinical trial of a novel hemostatic agent in cardiac surgery. *The Annals of Thoracic Surgery*. 2000 May 1;69(5):1376–82.
141. Nasso G, Piancone F, Bonifazi R, Romano V, Visicchio G, De Filippo CM, Impiombato B, Fiore F, Bartolomucci F, Alessandrini F, Speziale G. Prospective, Randomized Clinical Trial of the FloSeal Matrix Sealant in Cardiac Surgery. *The Annals of Thoracic Surgery*. 2009 Nov 1;88(5):1520–6.
142. Landi A, Gregori F, Marotta N, Delfini R. Efficacy, Security, and Manageability of Gelified Hemostatic Matrix in Bleeding Control during Thoracic and Lumbar Spine Surgery: FloSeal versus Surgiflo. *Journal of Neurological Surgery Part A: Central European Neurosurgery*. 2015 Sep 9;77(02):139–43.
143. Renkens KLJ, Payner TD, Leipzig TJ, Feuer H, Morone MA, Koers JM, Lawson KJ, Lentz R, Shuey HJ, Conaway GL, J. Andersson GB, An HS, Hickey M, Rondinone JF, Shargill NS. A Multicenter, Prospective, Randomized Trial Evaluating a New Hemostatic Agent for Spinal Surgery. *Spine*. 2001 Aug 1;26(15):1645–50.
144. Akar E, Haberal M, Dikis O. Efficacy of Surgical Tissue Glues and Supporters for Treatment of Prolonged Air Leaks in Bullous Emphysema. *Journal of the College of Physicians and Surgeons Pakistan*. 2020 Jan 1;30(01):57–61.
145. Esposito F, Cappabianca P, Angileri FF, Cavallo LM, Priola SM, Crimi S, Solari D, Germanò AF, Tomasello F. Gelatin-thrombin hemostatic matrix in neurosurgical procedures: hemostatic effectiveness and economic value of clinical and surgical procedure-related benefits. *J Neurosurg Sci [Internet]*. 2020 Mar [cited 2021 Feb 2];64(2). Available from: <https://www.minervamedica.it/index2.php?show=R38Y2020N02A0158>

146. Gall RM, Witterick IJ, Shargill NS, Hawke M. Control of bleeding in endoscopic sinus surgery: use of a novel gelatin-based hemostatic agent. *J Otolaryngol*. 2002 Oct;31(5):271–4.
147. Testini M, Marzaioli R, Lissidini G, Lippolis A, Logoluso F, Gurrado A, Lardo D, Poli E, Piccinni G. The effectiveness of FloSeal matrix hemostatic agent in thyroid surgery: a prospective, randomized, control study. *Langenbecks Arch Surg*. 2009 Sep;394(5):837–42.
148. Mozet C, Prettin C, Dietze M, Fickweiler U, Dietz A. Use of Floseal and effects on wound healing and pain in adults undergoing tonsillectomy: randomised comparison versus electrocautery. *European Archives of Oto-Rhino-Laryngology*. 2012 Oct;269(10):2247–54.
149. Sartelli M, Catena F, Biancafarina A, Tranà C, Piccardo A, Ceccarelli G, Tirone G, Agresta F, Di Giorgio A, Catani M, Tricarico F, Buonanno M, Piazza L. Use of Floseal Hemostatic Matrix for Control of Hemostasis During Laparoscopic Cholecystectomy for Acute Cholecystitis: A Multicenter Historical Control Group Comparison (The GLA Study Gelatin Matrix for Acute Cholecystitis). *Journal of Laparoendoscopic & Advanced Surgical Techniques*. 2014 Dec;24(12):837–41.
150. Martorana E, Ghaith A, Micali S, Pirola GM, De Carne C, Fidanza F, Bianchi G. A Retrospective Analysis of the Hemostatic Effect of FloSeal in Patients Undergoing Robot-Assisted Laparoscopic Radical Prostatectomy. *Urologia Internationalis*. 2016;96(3):274–9.
151. Glickman M, Gheissari A, Money S, Martin J, Ballard JL, CoSeal Multicenter Vascular Surgery Study Group. A polymeric sealant inhibits anastomotic suture hole bleeding more rapidly than gelfoam/thrombin: results of a randomized controlled trial. *Arch Surg*. 2002 Mar;137(3):326–31; discussion 332.
152. Natour E, Suedkamp M, Dapunt OE. Assessment of the effect on blood loss and transfusion requirements when adding a polyethylene glycol sealant to the anastomotic closure of aortic procedures: a case-control analysis of 102 patients undergoing Bentall procedures. *J Cardiothorac Surg*. 2012 Oct 8;7:105.
153. Konertz WF, Kostelka M, Mohr FW, Hetzer R, Hübner M, Ritter J, Liu J, Koch C, Block JE. Reducing the incidence and severity of pericardial adhesions with a sprayable polymeric matrix. *Ann Thorac Surg*. 2003 Oct;76(4):1270–4; discussion 1274.
154. Taflampas P, Sanidas E, Christodoulakis M, Askoxylakis J, Melissas J, Tsiftsis DD. Sealants after axillary lymph node dissection for breast cancer: good intentions but bad results. *The American Journal of Surgery*. 2009 Jul;198(1):55–8.
155. Lequaglie C, Giudice G, Marasco R, Morte AD, Gallo M. Use of a sealant to prevent prolonged air leaks after lung resection: a prospective randomized study. *Journal of Cardiothoracic Surgery* [Internet]. 2012 Dec [cited 2020 Apr 6];7(1). Available from: <https://cardiothoracicsurgery.biomedcentral.com/articles/10.1186/1749-8090-7-106>

156. Venuta F, Diso D, De Giacomo T, Anile M, Rendina EA, Coloni GF. Use of a polymeric sealant to reduce air leaks after lobectomy. *J Thorac Cardiovasc Surg.* 2006 Aug;132(2):422–3.
157. D'Andrilli A, Andreotti C, Ibrahim M, Ciccone AM, Venuta F, Mansmann U, Rendina EA. A prospective randomized study to assess the efficacy of a surgical sealant to treat air leaks in lung surgery. *Eur J Cardiothorac Surg.* 2009 May;35(5):817–20; discussion 820–821.
158. Tan C, Utley M, Paschalides C, Pilling J, Robb JD, Harrison-Phipps KM, Lang-Lazdunski L, Treasure T. A prospective randomized controlled study to assess the effectiveness of CoSeal® to seal air leaks in lung surgery. *Eur J Cardiothorac Surg.* 2011 Aug;40(2):304–8.
159. Feier H, Deutsch P, Gaspar M, Ursoniu S. The Influence of Albumin/glutaraldehyde Sealant in Early Results After Acute Type A Aortic Dissection. *Revista de Chimie.* 2019 Jul 15;70(6):2032–3035.
160. Chao HH, Torchiana DF. BioGlue: albumin/glutaraldehyde sealant in cardiac surgery. *J Card Surg.* 2003 Dec;18(6):500–3.
161. Coselli JS, Bavaria JE, Fehrenbacher J, Stowe CL, Macheers SK, Gundry SR. Prospective randomized study of a protein-based tissue adhesive used as a hemostatic and structural adjunct in cardiac and vascular anastomotic repair procedures. *Journal of the American College of Surgeons.* 2003 Aug;197(2):243–52.
162. Weiner J, Widman S, Golek Z, Tranquilli M, Elefteriades JA. Role of bovine serum albumin-glutaraldehyde glue in the formation of anastomatic pseudoaneurysms. *J Card Surg.* 2011 Jan;26(1):76–81.
163. Fink D, Klein JJ, Kang H, Ergin MA. Application of biological glue in repair of intracardiac structural defects. *The Annals of Thoracic Surgery.* 2004 Feb;77(2):506–11.
164. Bavaria JE, Brinster DR, Gorman RC, Woo YJ, Gleason T, Pochettino A. Advances in the treatment of acute type a dissection: an integrated approach. *The Annals of Thoracic Surgery.* 2002 Nov;74(5):S1848–52.
165. Tansley P, Al-Mulhim F, Lim E, Ladas G, Goldstraw P. A prospective, randomized, controlled trial of the effectiveness of BioGlue in treating alveolar air leaks. *The Journal of Thoracic and Cardiovascular Surgery.* 2006 Jul;132(1):105–12.
166. Rathinam S, Naidu BV, Nanjaiah P, Loubani M, Kalkat MS, Rajesh PB. BioGlue and Peri-strips in lung volume reduction surgery: pilot randomised controlled trial. *Journal of Cardiothoracic Surgery [Internet].* 2009 Dec [cited 2020 Apr 6];4(1). Available from: <http://cardiothoracicsurgery.biomedcentral.com/articles/10.1186/1749-8090-4-37>
167. Potaris K, Mihos P, Gakidis I. Preliminary results with the use of an albumin-glutaraldehyde tissue adhesive in lung surgery. *Med Sci Monit.* 2003 Jul;9(7):PI79-83.

168. Belcher E, Dusmet M, Jordan S, Ladas G, Lim E, Goldstraw P. A prospective, randomized trial comparing BioGlue and Vivostat for the control of alveolar air leak. *The Journal of Thoracic and Cardiovascular Surgery*. 2010 Jul;140(1):32–8.
169. Bahouth Z, Moskovitz B, Halachmi S, Nativ O. Bovine serum albumin-glutaraldehyde (BioGlue®) tissue adhesive versus standard renorrhaphy following renal mass enucleation: a retrospective comparison. *Ther Adv Urol*. 2017 Apr;9(3–4):67–72.
170. Kumar A, Maartens NF, Kaye AH. Evaluation of the use of BioGlue® in neurosurgical procedures. *Journal of Clinical Neuroscience*. 2003 Nov;10(6):661–4.
171. Anghelacopoulos SE, Tagarakis GI, Pilpilidis I, Kartsounis C, Chryssafis G. Albumin-glutaraldehyde bioadhesive (“Bioglue”) for prevention of postoperative complications after stapled hemorrhoidopexy: A randomized controlled trial. *Wien Klin Wochenschr*. 2006 Aug;118(15–16):469–72.
172. Chalmers RTA, Darling III RC, Wingard JT, Chetter I, Cutler B, Kern JA, Hart JC. Randomized clinical trial of tranexamic acid-free fibrin sealant during vascular surgical procedures. *Br J Surg*. 2010 Dec;97(12):1784–9.
173. Pryor SG, Sykes J, Tollefson TT. Efficacy of fibrin sealant (human) (Evicel) in rhinoplasty: a prospective, randomized, single-blind trial of the use of fibrin sealant in lateral osteotomy. *Arch Facial Plast Surg*. 2008 Oct;10(5):339–44.
174. Sroka G, Milevski D, Shteinberg D, Mady H, Matter I. Minimizing Hemorrhagic Complications in Laparoscopic Sleeve Gastrectomy—a Randomized Controlled Trial. *Obesity Surgery*. 2015 Sep;25(9):1577–83.
175. Randelli F, D’Anchise R, Ragone V, Serrao L, Cabitza P, Randelli P. Is the Newest Fibrin Sealant an Effective Strategy to Reduce Blood Loss After Total Knee Arthroplasty? A Randomized Controlled Study. *The Journal of Arthroplasty*. 2014 Aug;29(8):1516–20.
176. Tempesta BJ, Gharagozloo F, Margolis M, Schwartz A, Strother E. Aerostasis with human fibrin sealant (Evicel) in patients undergoing pulmonary resection. *Chest*. 2007 Oct;132(4):661C.
177. Zloto O, Greenbaum E, Fabian ID, Ben Simon GJ. Evicel versus Tisseel versus Sutures for Attaching Conjunctival Autograft in Pterygium Surgery. *Ophthalmology*. 2017 Jan;124(1):61–5.
178. D. Hornig J, Gillespie MB, J. Lentsch E, W. Fuller C, Condrey J, A. Nguyen S. Fibrin sealant use in thyroidectomy: A prospective, randomized, placebo-controlled double blind trial using EVICEL. *Otorhinolaryngology-Head and Neck Surgery*. 2016;1(1):21–4.
179. Rousou J, Levitsky S, Gonzalez-Lavin L, Cosgrove D, Magilligan D, Weldon C, Hiebert C, Hess P, Joyce L, Bergsland J. Randomized clinical trial of fibrin sealant in patients undergoing re-sternotomy or reoperation after cardiac operations. A multicenter study. *J Thorac Cardiovasc Surg*. 1989 Feb;97(2):194–203.

180. Spotnitz WD, Dalton MS, Baker JW, Nolan SP. Reduction of perioperative hemorrhage by anterior mediastinal spray application of fibrin glue during cardiac operations. *Ann Thorac Surg.* 1987 Nov;44(5):529–31.
181. Séguin JR, Frapier JM, Colson P, Chaptal PA. Fibrin sealant improves surgical results of type A acute aortic dissections. *Ann Thorac Surg.* 1991 Oct;52(4):745–8; discussion 748–749.
182. Saha SP, Muluk S, Schenk W, Dennis JW, Ploder B, Grigorian A, Presch I, Goppelt A. A prospective randomized study comparing fibrin sealant to manual compression for the treatment of anastomotic suture-hole bleeding in expanded polytetrafluoroethylene grafts. *J Vasc Surg.* 2012 Jul;56(1):134–41.
183. Ochsner MG, Maniscalco-Theberge ME, Champion HR. Fibrin glue as a hemostatic agent in hepatic and splenic trauma. *J Trauma.* 1990 Jul;30(7):884–7.
184. Allen MS, Wood DE, Hawkinson RW, Harpole DH, McKenna RJ, Walsh GL, Vallieres E, Miller DL, Nichols FC, Smythe WR, Davis RD. Prospective randomized study evaluating a biodegradable polymeric sealant for sealing intraoperative air leaks that occur during pulmonary resection. *The Annals of Thoracic Surgery.* 2004 May;77(5):1792–801.
185. Mortman KD, Corral M, Zhang X, Berhane I, Soleas IM, Ferko NC. Length of stay and hospitalization costs for patients undergoing lung surgery with Progel pleural air leak sealant. *J Med Econ.* 2018 Oct;21(10):1016–22.
186. Klijian A. A novel approach to control air leaks in complex lung surgery: a retrospective review. *J Cardiothorac Surg.* 2012 Jun 1;7:49.
187. Zaraca F, Vaccarili M, Zaccagna G, Maniscalco P, Dolci G, Feil B, Perkmann R, Bertolaccini L, Crisci R. Cost-effectiveness analysis of sealant impact in management of moderate intraoperative alveolar air leaks during video-assisted thoracoscopic surgery lobectomy: a multicentre randomised controlled trial. *J Thorac Dis.* 2017 Dec;9(12):5230–8.
188. Gologorsky RC, Alabaster AL, Ashiku SK, Patel AR, Velotta JB. Progel Use is Not Associated with Decreased Incidence of Postoperative Air Leak after Nonanatomic Lung Surgery. *Perm J.* 2019;23.
189. Walgenbach KJ, Bannasch H, Kalthoff S, Rubin JP. Randomized, prospective study of TissuGlu® surgical adhesive in the management of wound drainage following abdominoplasty. *Aesthetic Plast Surg.* 2012 Jun;36(3):491–6.
190. Hunstad JP, Michaels J, Burns AJ, Slezak S, Stevens WG, Clower DM, Rubin JP. A Prospective, Randomized, Multicenter Trial Assessing a Novel Lysine-Derived Urethane Adhesive in a Large Flap Surgical Procedure without Drains. *Aesthetic Plast Surg.* 2015 Aug;39(4):616–24.

191. Ohlinger R, Rutkowski R, Kohlmann T, Paepke S, Alwafai Z, Flieger C, Möller S, Lenz F, Zygmunt M, Unger J. Impact of the Lysine-urethane Adhesive TissuGlu® on Postoperative Complications and Interventions After Drain-free Mastectomy. *Anticancer Res.* 2020 May;40(5):2801–12.
192. Ohlinger R, Gieron L, Rutkowski R, Kohlmann T, Zygmunt M, Unger J. The Use of TissuGlu® Surgical Adhesive for Mastectomy With or Without Lymphonodectomy. In *Vivo.* 2018 Jun;32(3):625–31.
193. Boeer B, Schneider J, Schoenfisch B, Röhm C, Paepke S, Oberlechner E, Ohlinger R, Hartkopf A, Brucker SY, Hahn M, Marx M. Lysine-urethane-based tissue adhesion for mastectomy-an approach to reducing the seroma rate? *Arch Gynecol Obstet.* 2020 Nov 4;
194. Rocco PRM, Negri EM, Kurtz PM, Vasconcellos FP, Silva GH, Capelozzi VL, Romero PV, Zin WA. Lung Tissue Mechanics and Extracellular Matrix Remodeling in Acute Lung Injury. *Am J Respir Crit Care Med.* 2001 Sep 15;164(6):1067–71.
195. Carver W, Goldsmith EC. Regulation of Tissue Fibrosis by the Biomechanical Environment. *BioMed Research International.* 2013;2013:1–10.
196. Moser C, Opitz I, Zhai W, Rousson V, Russi EW, Weder W, Lardinois D. Autologous fibrin sealant reduces the incidence of prolonged air leak and duration of chest tube drainage after lung volume reduction surgery: A prospective randomized blinded study. *The Journal of Thoracic and Cardiovascular Surgery.* 2008 Oct;136(4):843–9.
197. Gonfiotti A, Santini PF, Jaus M, Janni A, Lococo A, De Massimi AR, D'Agostino A, Carleo F, Di Martino M, Larocca V, Cardillo G. Safety and effectiveness of a new fibrin pleural air leak sealant: a multicenter, controlled, prospective, parallel-group, randomized clinical trial. *Ann Thorac Surg.* 2011 Oct;92(4):1217–24; discussion 1224-1225.
198. Cardillo G, Carleo F, Carbone L, De Massimi AR, Lococo A, Santini PF, Janni A, Gonfiotti A. Adverse effects of fibrin sealants in thoracic surgery: the safety of a new fibrin sealant: multicentre, randomized, controlled, clinical trial. *European Journal of Cardio-Thoracic Surgery.* 2012 Mar 1;41(3):657–62.
199. Fabian T, Federico JA, Ponn RB. Fibrin glue in pulmonary resection: a prospective, randomized, blinded study. *The Annals of Thoracic Surgery.* 2003 May;75(5):1587–92.
200. Murdock MH, Chang JT, Luketich SK, Pedersen D, Hussey GS, D'Amore A, Badylak SF. Cytocompatibility and mechanical properties of surgical sealants for cardiovascular applications. *The Journal of Thoracic and Cardiovascular Surgery.* 2019 Jan;157(1):176–83.
201. Elefteriades JA. How I do it: utilization of high-pressure sealants in aortic reconstruction. *J Cardiothorac Surg.* 2009 Dec;4(1):27.

202. LeMaire SA, Carter SA, Won T, Wang X, Conklin LD, Coselli JS. The Threat of Adhesive Embolization: BioGlue Leaks Through Needle Holes in Aortic Tissue and Prosthetic Grafts. *The Annals of Thoracic Surgery*. 2005 Jul;80(1):106–11.
203. Mazuchowski EL, Thibault LE. Biomechanical properties of the human spinal cord and the pia matter. 2003;2.
204. Fiford RJ, Bilston LE. The mechanical properties of rat spinal cord in vitro. *Journal of Biomechanics*. 2005 Jul;38(7):1509–15.
205. Campbell P, Bennett S, Driscoll A, Sawhney A. Evaluation of Absorbable Surgical Sealants : In vitro Testing [Internet]. 2005 [cited 2021 Sep 16]. Available from: <https://www.semanticscholar.org/paper/Evaluation-of-Absorbable-Surgical-Sealants-%3A-In-Campbell-Bennett/0e72159a6027168d8ecb11dcd2375ad692c30ab3>
206. US Food and Drug Administration. Pre-market approval, Summary of safety and effectiveness- DuraSeal Xact Spine Sealant [Internet]. Available from: https://www.accessdata.fda.gov/cdrh_docs/pdf8/P080013b.pdf
207. DuraSeal® Xact Spinal Sealant System « Integra LifeSciences: Europe, Middle East and Africa [Internet]. [cited 2021 Sep 16]. Available from: <https://integralife.eu/products/neuro/duraplasty/duraseal-xact-sealant-system-adhesion-barrier-2/>
208. Klimo P, Khalil A, Slotkin JR, Smith ER, Scott RM, Goumnerova LC. Wound complications associated with the use of bovine serum albumin-glutaraldehyde surgical adhesive in pediatric patients. *Operative Neurosurgery*. 2007 Apr;60:305–9.
209. Duan W, Bian X, Bu Y. Applications of Bioadhesives: A Mini Review. *Frontiers in Bioengineering and Biotechnology*. 2021;9:702.
210. Gong C, Lu C, Li B, Shan M, Wu G. Injectable dopamine-modified poly(α,β -aspartic acid) nanocomposite hydrogel as bioadhesive drug delivery system. *J Biomed Mater Res A*. 2017 Apr;105(4):1000–8.
211. Han HK, Shin HJ, Ha DH. Improved oral bioavailability of alendronate via the mucoadhesive liposomal delivery system. *Eur J Pharm Sci*. 2012 Aug 15;46(5):500–7.
212. US Food and Drug Administration. Pre-market approval, Summary of safety and effectiveness- CoSeal Surgical sealant [Internet]. Available from: https://www.accessdata.fda.gov/cdrh_docs/pdf/P010022B.pdf
213. Vakalopoulos KA, Wu Z, Kroese L, Kleinrensink GJ, Jeekel J, Vendamme R, Dodou D, Lange JF. Mechanical Strength and Rheological Properties of Tissue Adhesives With Regard to Colorectal Anastomosis: An Ex Vivo Study. *Annals of Surgery*. 2015 Feb;261(2):323–31.

214. Baxter. Product Catalogue-CoSeal Surgical Sealant [Internet]. [cited 2021 Mar 15]. Available from:
<https://ecatalog.baxter.com/ecatalog/loadproduct.html?cid=10001&lid=10011&hid=10000&pid=288952>
215. Cryolife Inc.,. Bioglue, Instructions to use [Internet]. [cited 2021 Mar 15]. Available from:
https://www.cryolife.com/wp-content/uploads/stories/assets/docs/BG_Surgical_Adhesive_Syringe_IFU_dom.pdf
216. Herget GW, Kassa M, Riede UN, Lu Y, Brethner L, Hasse J. Experimental use of an albumin±glutaraldehyde tissue adhesive for sealing pulmonary parenchyma and bronchial anastomosesq. thoracic Surgery. 2001;6.
217. Baxter. Tisseel-Highlights of prescribing information https://baxterpi.com/pi-pdf/Tisseel_PI.pdf (accessed 24 Aug,2020) [Internet]. [cited 2020 Aug 24]. Available from: https://baxterpi.com/pi-pdf/Tisseel_PI.pdf
218. Shea L. Comparison of TissuePatchTM3 with other commonly used Surgical Sealants. 2009;2.
219. US Food and Drug Administration. Pre-market approval, Summary of safety and effectiveness- ProgelTM pleural air leak sealant system [Internet]. [cited 2020 Aug 24]. Available from: https://www.accessdata.fda.gov/cdrh_docs/pdf/P010047S036c.pdf
220. US Food and Drug Administration. Pre-market approval, Summary of safety and effectiveness- TissuGlu Surgical Adhesive [Internet]. Available from:
https://www.accessdata.fda.gov/cdrh_docs/pdf13/P130023B.pdf
221. Vakalopoulos KA, Wu Z, Kroese LF, Jeekel J, Kleinrensink G jan, Dodou D, Lam KH, Lange JF. Sutureless closure of colonic defects with tissue adhesives: an in vivo study in the rat. The American Journal of Surgery. 2017 Jan;213(1):151–8.
222. Kim KD, Wright NM. Polyethylene Glycol Hydrogel Spinal Sealant (DuraSeal Spinal Sealant) as an Adjunct to Sutured Dural Repair in the Spine: Results of a Prospective, Multicenter, Randomized Controlled Study. Spine. 2011 Nov;36(23):1906–12.
223. Kim KD, Ramanathan D, Highsmith J, Lavelle W, Gerszten P, Vale F, Wright N. DuraSeal Exact Is a Safe Adjunctive Treatment for Durotomy in Spine: Postapproval Study. Global Spine Journal. 2019 May;9(3):272–8.
224. Fransen P. Reduction of postoperative pain after lumbar microdiscectomy with DuraSeal Xact Adhesion Barrier and Sealant System. The Spine Journal. 2010 Sep;10(9):751–61.
225. Dhandapani V, Saseedharan P, Groleau D, Vermette P. Overview of approval procedures for bioadhesives in the United States of America and Canada. J Biomed Mater Res. 2021 Oct 22;jbm.b.34956.

226. Reimbursement: A Medical Device Company & Worst Nightmare? [Internet]. MasterControl. [cited 2021 Aug 31]. Available from: <https://www.mastercontrol.com/gxp-lifeline/reimbursement-a-medical-device-company-s-worst-nightmare->
227. Kuo TY, Manaker S. Reimbursement Strategies and CPT Codes for Device Development. In: Academic Entrepreneurship for Medical and Health Sciences [Internet]. 1st ed. PubPub; 2019 [cited 2021 Aug 31]. Available from: <https://academicentrepreneurship.pubpub.org/pub/1fani3y6>
228. Affairs O of R. Medical Device Overview, [Internet]. FDA; [cited 2021 Mar 15]. Available from: <https://www.fda.gov/industry/regulated-products/medical-device-overview>
229. How To Determine A Combination Product's Primary Mode of Action (PMOA) [Internet]. [cited 2021 Sep 1]. Available from: <https://www.meddeviceonline.com/doc/how-to-determine-a-combination-product-s-primary-mode-of-action-pmoa-0001>
230. Branch LS. Consolidated federal laws of canada, Medical Devices Regulations [Internet]. [cited 2021 Mar 15]. Available from: <https://laws-lois.justice.gc.ca/eng/regulations/sor-98-282/fulltext.html>
231. FITT H. Medical devices [Internet]. European Medicines Agency. 2018 [cited 2021 Sep 2]. Available from: <https://www.ema.europa.eu/en/human-regulatory/overview/medical-devices>
232. Commissioner O of the. What We Do [Internet]. FDA. FDA; 2021 [cited 2021 Sep 3]. Available from: <https://www.fda.gov/about-fda/what-we-do>
233. US Food and Drug Administration C for BE and R. Devices Regulated by the Center for Biologics Evaluation and Research. FDA [Internet]. 2019 Jan 7 [cited 2021 Sep 3]; Available from: <https://www.fda.gov/vaccines-blood-biologics/510k-process-cber/devices-regulated-center-biologics-evaluation-and-research>
234. US Food and Drug Administration O of the C. Intercenter Agreement Between the Center for Biologics Evaluation and Research and the Center for Devices and Radiological Health. FDA [Internet]. 2018 Mar 11 [cited 2021 Sep 3]; Available from: <https://www.fda.gov/combination-products/jurisdictional-information/intercenter-agreement-between-center-biologics-evaluation-and-research-and-center-devices-and>
235. Jin J. FDA Authorization of Medical Devices. JAMA. 2014 Jan 22;311(4):435–435.
236. US Food and Drug Administration C for D and R health. Classify Your Medical Device [Internet]. FDA. FDA; [cited 2021 Mar 15]. Available from: <https://www.fda.gov/medical-devices/overview-device-regulation/classify-your-medical-device>

237. US Food and Drug Administration. 510 (k) summary, ProDerma (K063202) [Internet]. [cited 2021 Mar 15]. Available from: https://www.accessdata.fda.gov/cdrh_docs/pdf6/K063202.pdf
238. US Food and Drug Administration. 510 (k) summary, Kerisure Advanced™ Liquid Bandage (K131384) [Internet]. [cited 2021 Mar 15]. Available from: https://www.accessdata.fda.gov/cdrh_docs/pdf13/K131384.pdf
239. US Food and Drug Administration. 510 (k) summary, Glustitch Twist Tissue Adhesive (K150032) [Internet]. [cited 2021 Mar 15]. Available from: https://www.accessdata.fda.gov/cdrh_docs/pdf15/K150032.pdf
240. US Food and Drug Administration. 510 (k) summary, LiquiBand Exceed (K151182) [Internet]. [cited 2021 Mar 15]. Available from: https://www.accessdata.fda.gov/cdrh_docs/pdf15/K151182.pdf
241. Factors to Consider When Making Benefit-Risk Determinations in Medical Device Premarket Approval and De Novo Classifications [Internet]. Available from: <https://www.fda.gov/media/99769/download>
242. US Food and Drug Administration C for D and R health. Factors to Consider Regarding Benefit-Risk in Medical Device Product Availability, Compliance, and Enforcement Decisions - Guidance for Industry and Food and Drug Administration Staff [Internet]. Available from: <https://www.fda.gov/media/98657/download>
243. US Food and Drug Administration C for D and R health. Premarket Notification 510(k) [Internet]. FDA. FDA; [cited 2021 Mar 15]. Available from: <https://www.fda.gov/medical-devices/premarket-submissions/premarket-notification-510k>
244. US Food and Drug Administration C for D and R. Premarket Approval (PMA) [Internet]. FDA. FDA; [cited 2021 Mar 15]. Available from: <https://www.fda.gov/medical-devices/premarket-submissions/premarket-approval-pma>
245. US Food and Drug Administration. Product Classification [Internet]. [cited 2021 Mar 15]. Available from: <https://www.accessdata.fda.gov/scripts/cdrh/cfdocs/cfpdc/classification.cfm>
246. Code of Federal Regulations. e-CFR: TITLE 21—Food and Drugs [Internet]. Electronic Code of Federal Regulations. Available from: https://www.ecfr.gov/cgi-bin/text-idx?SID=e26f14ae48980e817a8adb617334f9bb&mc=true&tpl=/ecfrbrowse/Title21/21CIs_ubchapH.tpl
247. Glustitch Inc. GluStitch® Twist [Internet]. GluStitch. [cited 2021 Mar 15]. Available from: <https://glustitch.com/products/glustitch-twist>
248. US Food and Drug Administration C for D and R health. General Controls for Medical Devices [Internet]. FDA; [cited 2021 Mar 13]. Available from:

- <https://www.fda.gov/medical-devices/regulatory-controls/general-controls-medical-devices>
249. US Food and Drug Administration C for D and R health. Regulatory Controls [Internet]. FDA. FDA; 2019 [cited 2021 Mar 15]. Available from: <https://www.fda.gov/medical-devices/overview-device-regulation/regulatory-controls>
 250. US Food and Drug Administration. Use of International Standard ISO 10993-1, “Biological evaluation of medical devices - Part 1: Evaluation and testing within a risk management process” - Guidance for Industry and Food and Drug Administration Staff [Internet]. Available from: <https://www.fda.gov/media/85865/download>
 251. US Food and Drug Administration C for D and R health. Biocompatibility Evaluation Endpoints by Device Category [Internet]. FDA; 2021 [cited 2021 Aug 31]. Available from: <https://www.fda.gov/medical-devices/biocompatibility-assessment-resource-center/biocompatibility-evaluation-endpoints-device-category>
 252. US Food and Drug Administration C for D and RH. Immunotoxicity Testing Guidance [Internet]. U.S. Food and Drug Administration. FDA; 2020 [cited 2021 Sep 3]. Available from: <https://www.fda.gov/regulatory-information/search-fda-guidance-documents/immunotoxicity-testing-guidance>
 253. Potter DR, Trivedi A, Lin M, Miyazawa BY, Vivona LR, McCully B, Nair A, Schreiber MA, Pati S. The effects of human prothrombin complex concentrate on hemorrhagic shock-induced lung injury in rats: Implications for testing human blood products in rodents. *Journal of Trauma and Acute Care Surgery*. 2020 Dec;89(6):1068–75.
 254. Van Norman GA. Limitations of Animal Studies for Predicting Toxicity in Clinical Trials. *JACC Basic Transl Sci*. 2020 Apr 27;5(4):387–97.
 255. Faisal S. DuraSeal Xact Adhesion Barrier and Sealant System: An Advanced Hydrogel Technology for Watertight Dural Repair in Spinal Cases. 2013;4.
 256. Fritz JM, Cleland J. Effectiveness Versus Efficacy: More Than a Debate Over Language. *J Orthop Sports Phys Ther*. 2003 Apr;33(4):163–5.
 257. US Food and Drug Administration C for D and R health. Recalls, Corrections and Removals (Devices) [Internet]. FDA. FDA; 2021 [cited 2021 Aug 31]. Available from: <https://www.fda.gov/medical-devices/postmarket-requirements-devices/recalls-corrections-and-removals-devices>
 258. US Food and Drug Administration. Class 2 Device Recall BioGlue Surgical Adhesive (BioGlue) [Internet]. [cited 2021 Mar 15]. Available from: <https://www.accessdata.fda.gov/scripts/cdrh/cfdocs/cfRES/res.cfm?id=127033>
 259. US Food and Drug Administration. Class 2 Device Recall BioGlue [Internet]. [cited 2021 Mar 15]. Available from: <https://www.accessdata.fda.gov/scripts/cdrh/cfdocs/cfRES/res.cfm?id=155852>

260. US Food and Drug Administration. Class 2 Device Recall BioGlue Surgical Adhesive [Internet]. [cited 2021 Mar 15]. Available from: <https://www.accessdata.fda.gov/scripts/cdrh/cfdocs/cfRES/res.cfm?id=165020>
261. US Food and Drug Administration. Class 2 Device Recall Progel Pleural Air Leak Sealant [Internet]. [cited 2021 Mar 15]. Available from: <https://www.accessdata.fda.gov/scripts/cdrh/cfdocs/cfRES/res.cfm?id=112705>
262. US Food and Drug Administration. Class 2 Device Recall Coseal Surgical Sealant (COH102 & COH 206) [Internet]. [cited 2021 Mar 15]. Available from: <https://www.accessdata.fda.gov/scripts/cdrh/cfdocs/cfRES/res.cfm?id=92113>
263. US Food and Drug Administration. Class 2 Device Recall Coseal Surgical Sealant. [Internet]. [cited 2021 Mar 15]. Available from: <https://www.accessdata.fda.gov/scripts/cdrh/cfdocs/cfRES/res.cfm?id=103883>
264. US Food and Drug Administration. Class 2 Device Recall COSEAL Surgical Sealant [Internet]. [cited 2021 Mar 15]. Available from: <https://www.accessdata.fda.gov/scripts/cdrh/cfdocs/cfRES/res.cfm?id=146449>
265. US Food and Drug Administration. Pre-market approval, Summary of safety and effectiveness-FloSeal™ Hemostatic Matrix sealant [Internet]. 2021. Available from: https://www.accessdata.fda.gov/cdrh_docs/pdf/P990009B.pdf
266. US Food and Drug Administration. Class 2 Device Recall FloSeal Endoscopic Applicator [Internet]. [cited 2021 Mar 15]. Available from: <https://www.accessdata.fda.gov/scripts/cdrh/cfdocs/cfRES/res.cfm?id=72773>
267. US Food and Drug Administration. Class 2 Device Recall FLOSEAL Special Applicator Tips [Internet]. [cited 2021 Mar 15]. Available from: <https://www.accessdata.fda.gov/scripts/cdrh/cfdocs/cfRES/res.cfm?id=166431>
268. US Food and Drug Administration C for D and R health. How to Determine if Your Product is a Medical Device [Internet]. FDA; [cited 2021 Mar 15]. Available from: <https://www.fda.gov/medical-devices/classify-your-medical-device/how-determine-if-your-product-medical-device>
269. US Food and Drug Administration. FDA and Industry Procedures for Section 513(g) Requests for Information under the Federal Food, Drug, and Cosmetic Act - Guidance for Industry and Food and Drug Administration Staff, Accessed 7 Jan 2021. <https://www.fda.gov/media/78456/download> . [Internet]. [cited 2021 Jan 7]. Available from: <https://www.fda.gov/media/78456/download>
270. US Food and Drug Administration C for D and R health. Requests for Feedback and Meetings for Medical Device Submissions: The Q-Submission Program [Internet]. U.S. Food and Drug Administration. FDA; [cited 2021 Mar 15]. Available from: <https://www.fda.gov/regulatory-information/search-fda-guidance-documents/requests-feedback-and-meetings-medical-device-submissions-q-submission-program>

271. US Food and Drug Administration. The Q-submission Program, Guidance for Industry and Food and Drug Administration Staff [Internet]. [cited 2021 Jan 7]. Available from: <https://www.fda.gov/media/114034/download>
272. US Food and Drug Administration. Device Classification under Section 513(f)(2)(de novo) [Internet]. [cited 2021 Mar 15]. Available from: <https://www.accessdata.fda.gov/scripts/cdrh/cfdocs/cfpmn/denovo.cfm?ID=DEN090005>
273. US Food and Drug Administration. Medical Device Exemptions 510(k) and GMP Requirements [Internet]. [cited 2021 Mar 15]. Available from: <https://www.accessdata.fda.gov/scripts/cdrh/cfdocs/cfpd/315.cfm>
274. US Food and Drug Administration C for D and R health. Medical Device User Fee Amendments (MDUFA) [Internet]. FDA. FDA; [cited 2021 Mar 5]. Available from: <https://www.fda.gov/industry/fda-user-fee-programs/medical-device-user-fee-amendments-mdufa>
275. US Food and Drug Administration C for D and R health. Quality System (QS) Regulation/Medical Device Good Manufacturing Practices [Internet]. FDA. FDA; 2021 [cited 2021 Sep 3]. Available from: <https://www.fda.gov/medical-devices/postmarket-requirements-devices/quality-system-qs-regulationmedical-device-good-manufacturing-practices>
276. US Food and Drug Administration. Overview of Quality System Regulations [Internet]. Available from: <https://www.fda.gov/files/drugs/published/Overview-of-Quality-System-Regulation.pdf>
277. US Food and Drug Administration. Quality system information for certain premarket application reviews, Guidance for industry and FDA staff [Internet]. Available from: <https://www.fda.gov/media/71083/download>
278. US Food and Drug Administration C for D and R health. PMA Review Process [Internet]. FDA; [cited 2021 Mar 13]. Available from: <https://www.fda.gov/medical-devices/premarket-approval-pma/pma-review-process>
279. US Food and Drug Administration. Recalls- Code of Federal Regulations [Internet]. [cited 2021 Apr 2]. Available from: <https://www.accessdata.fda.gov/scripts/cdrh/cfdocs/cfcfr/CFRSearch.cfm?CFRPart=7&showFR=1&subpartNode=21:1.0.1.1.6.3>
280. US Food and Drug Administration C for D and R health. PMA Supplements and Amendments [Internet]. FDA; [cited 2021 Mar 15]. Available from: <https://www.fda.gov/medical-devices/premarket-approval-pma/pma-supplements-and-amendments>
281. US Food and Drug Administration. Premarket Approval (PMA) CoSeal Surgical sealat [Internet]. [cited 2021 Mar 15]. Available from: <https://www.accessdata.fda.gov/scripts/cdrh/cfdocs/cfpma/pma.cfm?id=P030039>

282. US Food and Drug Administration. Premarket Approval (PMA) Focal Seal-L synthetic absorbable sealant [Internet]. [cited 2021 Mar 15]. Available from: <https://www.accessdata.fda.gov/scripts/cdrh/cfdocs/cfpma/pma.cfm?id=P990028>
283. US Food and Drug Administration C for D and R health. Postmarket Surveillance Under Section 522 of the Federal Food, Drug, and Cosmetic Act - Guidance for Industry and Food and Drug Administration Staff [Internet]. Available from: <https://www.fda.gov/media/81015/download>
284. Hurley C. Utilizing RWD and RWE: An Introduction to Core Concepts and Requirements. :7.
285. US Food and Drug Administration O of the C. Leveraging Real World Evidence in Regulatory Submissions of Medical Devices [Internet]. FDA; 2021 [cited 2021 Sep 2]. Available from: <https://www.fda.gov/news-events/fda-voices/leveraging-real-world-evidence-regulatory-submissions-medical-devices>
286. US Food and Drug Administration. Use of Real-World Evidence to Support Regulatory Decision-Making for Medical Devices - Guidance for Industry and Food and Drug Administration Staff [Internet]. Available from: <https://www.fda.gov/media/99447/download>
287. Canada H. Health Products and Food Branch [Internet]. 2002 [cited 2021 Sep 3]. Available from: <https://www.canada.ca/en/health-canada/corporate/about-health-canada/branches-agencies/health-products-food-branch.html>
288. Government of Canada HC. Medical Devices Active Licence Listing [Internet]. 2012 [cited 2021 Mar 15]. Available from: <https://health-products.canada.ca/mdall-limh/prepareSearch-preparerRecherche.do?type=active>
289. Canada H. Medical device application forms [Internet]. [cited 2021 Mar 15]. Available from: <https://www.canada.ca/en/health-canada/services/drugs-health-products/medical-devices/application-information/forms.html>
290. Canada H. Fees for the Examination of an Application for a Medical Device Licence [Internet]. [cited 2021 May 3]. Available from: <https://www.canada.ca/en/health-canada/services/drugs-health-products/funding-fees/fees-respect-human-drugs-medical-devices/medical-device-licence-application-review-funding-fees-drugs-health-products.html>
291. International Medical Device Regulators Forum. Non-In Vitro Diagnostic Device Market Authorization Table of Contents [Internet]. [cited 2021 Mar 15]. Available from: <http://www.imdrf.org/docs/imdrf/final/technical/imdrf-tech-190321-nivd-dma-toc-n9.pdf>
292. US Food and Drug Administration. Medical Device Single Audit Program [Internet]. [cited 2021 Mar 15]. Available from: <https://www.fda.gov/media/87544/download>

293. Canada H. Learning portal Health Canada- Pre-market regulations for medical devices [Internet]. [cited 2021 Mar 15]. Available from: <https://training-formation.phac-aspc.gc.ca/login/index.php>
294. Canada H. Guidance Document: Guidance for the Labelling of Medical Devices, not including in vitro diagnostic devices - Appendices for the Labelling of Soft, Decorative, Contact Lenses and Menstrual Tampons [Internet]. [cited 2021 Mar 15]. Available from: <https://www.canada.ca/en/health-canada/services/drugs-health-products/medical-devices/application-information/guidance-documents/guidance-labelling-medical-devices-including-vitro-diagnostic-devices-appendices.html>
295. International Medical Device Regulators Forum. IMDRF documents [Internet]. [cited 2021 Mar 15]. Available from: <http://www.imdrf.org/documents/documents.asp>
296. European Medicines Agency. What we do [Internet]. European Medicines Agency. 2018 [cited 2021 Sep 3]. Available from: <https://www.ema.europa.eu/en/about-us/what-we-do>
297. Classification Of Medical Devices And Their Routes To CE Marking [Internet]. Clever Compliance Support - Compliance system and CE marking information. [cited 2021 Sep 2]. Available from: <https://support.ce-check.eu/hc/en-us/articles/360008712879-Classification-Of-Medical-Devices-And-Their-Routes-To-CE-Marking>
298. Commission E. Guidance document for classification of medical devices in europe [Internet]. Available from: <https://ec.europa.eu/docsroom/documents/10337/attachments/1/translations/en/renditions/pdf>
299. Regulation (EU) 2020/561 of the European Parliament and of the Council of 23 April 2020 amending Regulation (EU) 2017/745 on medical devices, as regards the dates of application of certain of its provisions (Text with EEA relevance) [Internet]. OJ L, 32020R0561 Apr 24, 2020. Available from: <http://data.europa.eu/eli/reg/2020/561/oj/eng>
300. MDR vs. MDD: 13 Key Changes [Internet]. [cited 2021 Sep 3]. Available from: <https://www.thefdagroup.com/blog/mdr-vs-mdd-13-key-changes>
301. INGLING P. New regulations [Internet]. Internal Market, Industry, Entrepreneurship and SMEs - European Commission. [cited 2020 May 5]. Available from: https://ec.europa.eu/growth/sectors/medical-devices/new-regulations_en
302. Medical device regulations, classification & submissions [Internet]. MaRS Startup Toolkit. [cited 2021 Sep 3]. Available from: <https://learn.marsdd.com/article/medical-device-regulations-classification-and-submissions/>
303. 9 Ways Canadian Medical Device Regulations Differ From the US [Internet]. [cited 2021 Sep 3]. Available from: <https://www.qualio.com/blog/canadian-medical-device-regulations>

304. Kahanovitz L, Sluss PM, Russell SJ. Type 1 diabetes – A clinical perspective. *Point Care*. 2017 Mar;16(1):37–40.
305. American Diabetes Association. Diagnosis and classification of diabetes mellitus. *Diabetes Care*. 2013 Dec 16;37(Supplement_1):S81–90.
306. Pathak V, Pathak NM, O’Neill CL, Guduric-Fuchs J, Medina RJ. Therapies for type 1 diabetes: Current scenario and future perspectives. *Clin Med Insights Endocrinol Diabetes*. 2019 May 3;12:1179551419844521.
307. Yeh HC, Brown TT, Maruthur N, Ranasinghe P, Berger Z, Suh YD, Wilson LM, Haberl EB, Brick J, Bass EB, Golden SH. Comparative effectiveness and safety of methods of insulin delivery and glucose monitoring for diabetes mellitus: a systematic review and meta-analysis. *Ann Intern Med*. 2012 Sep 4;157(5):336–47.
308. Hypoglycemia in the diabetes control and complications trial. The diabetes control and complications trial research group. *Diabetes*. 1997 Feb;46(2):271–86.
309. Foster NC, Beck RW, Miller KM, Clements MA, Rickels MR, DiMeglio LA, Maahs DM, Tamborlane WV, Bergenstal R, Smith E, Olson BA, Garg SK. State of type 1 diabetes management and outcomes from the T1D exchange in 2016-2018. *Diabetes Technol Ther*. 2019 Feb;21(2):66–72.
310. American Diabetes Association. 6. Glycemic targets: Standards of medical care in diabetes—2020. *Diabetes Care*. 2019 Dec 16;43(Supplement_1):S66–76.
311. Priya G, Kalra S. A review of insulin resistance in type 1 diabetes: Is there a place for adjunctive metformin? *Diabetes Ther*. 2018 Feb;9(1):349–61.
312. Holt RIG, DeVries JH, Hess-Fischl A, Hirsch IB, Kirkman MS, Klupa T, Ludwig B, Nørgaard K, Pettus J, Renard E, Skyler JS, Snoek FJ, Weinstock RS, Peters AL. The management of type 1 diabetes in adults. A consensus report by the American Diabetes Association (ADA) and the European Association for the Study of Diabetes (EASD). *Diabetes Care*. 2021 Oct 18;44(11):2589–625.
313. Najarian JS, Sutherland DE, Matas AJ, Steffes MW, Simmons RL, Goetz FC. Human islet transplantation: a preliminary report. *Transplant Proc*. 1977 Mar;9(1):233–6.
314. Brendel MD, Hering BJ, Schultz AO, Bretzel RG. Intentional Islet transplant registry. 8(1). Available from: http://www.med.uni-giessen.de/itr/newsletter/no_9/news_9.pdf
315. Shapiro AM, Lakey JR, Ryan EA, Korbitt GS, Toth E, Warnock GL, Kneteman NM, Rajotte RV. Islet transplantation in seven patients with type 1 diabetes mellitus using a glucocorticoid-free immunosuppressive regimen. *N Engl J Med*. 2000 Jul 27;343(4):230–8.
316. Pancreas islet transplantation for patients with type 1 diabetes mellitus: A clinical evidence review. *Ont Health Technol Assess Ser*. 2015 Sep 1;15(16):1–84.

317. Shapiro AMJ, Ricordi C, Hering BJ, Auchincloss H, Lindblad R, Robertson RP, Secchi A, Brendel MD, Berney T, Brennan DC, Cagliero E, Alejandro R, Ryan EA, DiMercurio B, Morel P, Polonsky KS, Reems JA, Bretzel RG, Bertuzzi F, Froud T, Kandaswamy R, Sutherland DER, Eisenbarth G, Segal M, Preiksaitis J, Korbitt GS, Barton FB, Viviano L, Seyfert-Margolis V, Bluestone J, Lakey JRT. International trial of the Edmonton protocol for islet transplantation. *N Engl J Med*. 2006 Sep 28;355(13):1318–30.
318. Lablanche S, Vantyghem MC, Kessler L, Wojtusciszyn A, Borot S, Thivolet C, Girerd S, Bosco D, Bosson JL, Colin C, Tetaz R, Logerot S, Kerr-Conte J, Renard E, Penfornis A, Morelon E, Buron F, Skaare K, Grguric G, Camillo-Brault C, Egelhofer H, Benomar K, Badet L, Berney T, Pattou F, Benhamou PY, Malvezzi P, Tauveron I, Roche B, Noel C, Frimat L, Guerci B, Pernin N, Moisan A, Persoons V, Ezzouaoui R, Gmyr V, Thony F, Bricault Y, Rodière M, Sengel C, Greget M, Enescu I, Noel C, Hazzan M, Caiazzo R, Torres F, Mapihan KL, Raverdy V, Pierredon MA, Valette PJ, Muller A, Champagnac J, Chaillous L, Dantal J, Cattan P, Riveline JP, Moreau F, Baltzinger P, Bahoune T. Islet transplantation versus insulin therapy in patients with type 1 diabetes with severe hypoglycaemia or poorly controlled glycaemia after kidney transplantation (TRIMECO): a multicentre, randomised controlled trial. *The Lancet Diabetes & Endocrinology*. 2018 Jul 1;6(7):527–37.
319. Hering BJ, Clarke WR, Bridges ND, Eggerman TL, Alejandro R, Bellin MD, Chaloner K, Czarniecki CW, Goldstein JS, Hunsicker LG, Kaufman DB, Korsgren O, Larsen CP, Luo X, Markmann JF, Naji A, Oberholzer J, Posselt AM, Rickels MR, Ricordi C, Robien MA, Senior PA, Shapiro AMJ, Stock PG, Turgeon NA, Clinical Islet Transplantation Consortium. Phase 3 Trial of transplantation of human islets in type 1 diabetes complicated by severe hypoglycemia. *Diabetes Care*. 2016 Jul;39(7):1230–40.
320. Lablanche S, Borot S, Wojtusciszyn A, Bayle F, Tétaz R, Badet L, Thivolet C, Morelon E, Frimat L, Penfornis A, Kessler L, Brault C, Colin C, Tauveron I, Bosco D, Berney T, Benhamou PY, GRAGIL Network. Five-year metabolic, functional, and safety results of patients with type 1 diabetes transplanted with allogenic islets within the swiss-french GRAGIL network. *Diabetes Care*. 2015 Sep;38(9):1714–22.
321. Rickels MR, Peleckis AJ, Markmann E, Dalton-Bakes C, Kong SM, Teff KL, Naji A. Long-term improvement in glucose control and counterregulation by islet transplantation for type 1 diabetes. *The Journal of Clinical Endocrinology & Metabolism*. 2016 Nov 1;101(11):4421–30.
322. Paraskevas S, Maysinger D, Wang R, Duguid TP, Rosenberg L. Cell loss in isolated human islets occurs by apoptosis. *Pancreas*. 2000 Apr;20(3):270–6.
323. McCall M, James Shapiro AM. Update on islet transplantation. *Cold Spring Harb Perspect Med*. 2012 Jul;2(7):a007823.
324. Bottino R, Knoll MF, Knoll CA, Bertera S, Trucco MM. The future of islet transplantation is now. *Front Med (Lausanne)*. 2018;5:202.

325. Walker S, Appari M, Forbes S. Considerations and challenges of islet transplantation and future therapies on the horizon. *American Journal of Physiology-Endocrinology and Metabolism*. 2022 Feb;322(2):E109–17.
326. Vantyghem MC, Koning EJP de, Pattou F, Rickels MR. Advances in β -cell replacement therapy for the treatment of type 1 diabetes. *The Lancet*. 2019 Oct 5;394(10205):1274–85.
327. Ryan EA, Paty BW, Senior PA, Bigam D, Alfadhli E, Kneteman NM, Lakey JRT, Shapiro AMJ. Five-year follow-up after clinical islet transplantation. *Diabetes*. 2005 Jul;54(7):2060–9.
328. Badylak SF. Xenogeneic extracellular matrix as a scaffold for tissue reconstruction. *Transplant Immunology*. 2004 Apr;12(3–4):367–77.
329. Chen F, Yoo JJ, Atala A. Acellular collagen matrix as a possible “off the shelf” biomaterial for urethral repair. *Urology*. 1999 Sep;54(3):407–10.
330. Wainwright DJ. Use of an acellular allograft dermal matrix (AlloDerm) in the management of full-thickness burns. *Burns*. 1995 Jun;21(4):243–8.
331. Iozzo RV, Schaefer L. Proteoglycan form and function: A comprehensive nomenclature of proteoglycans. *Matrix Biol*. 2015 Mar;42:11–55.
332. Hillebrandt KH, Everwien H, Haep N, Keshi E, Pratschke J, Sauer IM. Strategies based on organ decellularization and recellularization. *Transplant International*. 2019;32(6):571–85.
333. Gilbert TW. Strategies for tissue and organ decellularization. *J Cell Biochem*. 2012 Jul;113(7):2217–22.
334. Gilpin A, Yang Y. Decellularization strategies for regenerative medicine: From processing techniques to applications. *BioMed Research International*. 2017;2017:1–13.
335. Zhang X, Chen X, Hong H, Hu R, Liu J, Liu C. Decellularized extracellular matrix scaffolds: Recent trends and emerging strategies in tissue engineering. *Bioactive Materials*. 2022 Apr 1;10:15–31.
336. Lichtenberg D, Ahyayauch H, Goñi FM. The mechanism of detergent solubilization of lipid bilayers. *Biophys J*. 2013 Jul 16;105(2):289–99.
337. Guruswamy Damodaran R, Vermette P. Decellularized pancreas as a native extracellular matrix scaffold for pancreatic islet seeding and culture. *J Tissue Eng Regen Med*. 2018 May;12(5):1230–7.
338. Schmitt A, Csiki R, Tron A, Saldamli B, Tübel J, Florian K, Siebenlist S, Balmayor E, Burgkart R. Optimized protocol for whole organ decellularization. *European Journal of Medical Research*. 2017 Sep 8;22(1):31.

339. Rashtbar M, Hadjati J, Ai J, Jahanzad I, Azami M, Shirian S, Ebrahimi-Barough S, Sadroddiny E. Characterization of decellularized ovine small intestine submucosal layer as extracellular matrix-based scaffold for tissue engineering. *J Biomed Mater Res B Appl Biomater*. 2018 Apr;106(3):933–44.
340. Kim H, Choi KH, Sung SC, Kim YS. Effect of ethanol washing on porcine pulmonary artery wall decellularization using sodium dodecyl sulfate. *Artificial Organs*. 2022;46(7):1281–93.
341. Bongolan T, Whiteley J, Castillo-Prado J, Fantin A, Larsen B, J. Wong C, Mazilescu L, Kawamura M, Urbanellis P, Jonebring A, Salter E, Collingridge G, Gladdy R, Hicks R, Gingras AC, Selzner M, M. Rogers I. Decellularization of porcine kidney with submicellar concentrations of SDS results in the retention of ECM proteins required for the adhesion and maintenance of human adult renal epithelial cells. *Biomaterials Science*. 2022;10(11):2972–90.
342. Balestrini JL, Gard AL, Liu A, Leiby KL, Schwan J, Kunkemoeller B, Calle EA, Sivarapatna A, Lin T, Dimitrievska S, Campbell SG, Niklason LE. Production of decellularized porcine lung scaffolds for use in tissue engineering. *Integrative Biology*. 2015 Dec 30;7(12):1598–610.
343. Kao CY, Nguyen HQD, Weng YC. Characterization of porcine urinary bladder matrix hydrogels from sodium dodecyl sulfate decellularization Method. *Polymers (Basel)*. 2020 Dec 16;12(12):3007.
344. Elder BD, Kim DH, Athanasiou KA. Developing an articular cartilage decellularization process toward facet joint cartilage replacement. *Neurosurgery*. 2010 Apr;66(4):722–7.
345. Bodnar E, Olsen EG, Florio R, Dobrin J. Damage of porcine aortic valve tissue caused by the surfactant sodiumdodecylsulphate. *Thorac Cardiovasc Surg*. 1986 Apr;34(2):82–5.
346. Fernández-Pérez J, Ahearne M. The impact of decellularization methods on extracellular matrix derived hydrogels. *Sci Rep*. 2019 Oct 17;9(1):14933.
347. White LJ, Taylor AJ, Faulk DM, Keane TJ, Saldin LT, Reing JE, Swinehart IT, Turner NJ, Ratner BD, Badylak SF. The impact of detergents on the tissue decellularization process: A ToF-SIMS study. *Acta Biomaterialia*. 2017 Mar;50:207–19.
348. Chen WCW, Wang Z, Missinato MA, Park DW, Long DW, Liu HJ, Zeng X, Yates NA, Kim K, Wang Y. Decellularized zebrafish cardiac extracellular matrix induces mammalian heart regeneration. *Sci Adv*. 2016 Nov 18;2(11):e1600844.
349. Xing Q, Yates K, Tahtinen M, Shearier E, Qian Z, Zhao F. Decellularization of fibroblast cell sheets for natural extracellular matrix scaffold preparation. *Tissue Engineering Part C: Methods* [Internet]. 2014 Jun 27 [cited 2022 Jun 25]; Available from: <https://www.liebertpub.com/doi/10.1089/ten.tec.2013.0666>

350. Burk J, Erbe I, Berner D, Kacza J, Kasper C, Pfeiffer B, Winter K, Brehm W. Freeze-thaw cycles enhance decellularization of large tendons. *Tissue Eng Part C Methods*. 2014 Apr;20(4):276–84.
351. Roth SP, Glauche SM, Plenge A, Erbe I, Heller S, Burk J. Automated freeze-thaw cycles for decellularization of tendon tissue - a pilot study. *BMC Biotechnology*. 2017 Feb 14;17(1):13.
352. Flynn LE. The use of decellularized adipose tissue to provide an inductive microenvironment for the adipogenic differentiation of human adipose-derived stem cells. *Biomaterials*. 2010 Jun;31(17):4715–24.
353. Rosario DJ, Reilly GC, Ali Salah E, Glover M, Bullock AJ, MacNeil S. Decellularization and sterilization of porcine urinary bladder matrix for tissue engineering in the lower urinary tract. *Regenerative Medicine*. 2008 Mar;3(2):145–56.
354. Gilbert TW, Freund J, Badylak SF. Quantification of DNA in biologic scaffold materials. *J Surg Res*. 2009 Mar;152(1):135–9.
355. Garriboli M, Deguchi K, Totonelli G, Georgiades F, Urbani L, Ghionzoli M, Burns AJ, Sebire NJ, Turmaine M, Eaton S, De Coppi P. Development of a porcine acellular bladder matrix for tissue-engineered bladder reconstruction. *Pediatr Surg Int*. 2022 May 1;38(5):665–77.
356. Choudhury D, Yee M, Sheng ZLJ, Amirul A, Naing MW. Decellularization systems and devices: State-of-the-art. *Acta Biomaterialia*. 2020 Oct;115:51–9.
357. Choi YJ, Kim TG, Jeong J, Yi HG, Park JW, Hwang W, Cho DW. 3D cell printing of functional skeletal muscle constructs using skeletal muscle-derived bioink. *Adv Healthcare Mater*. 2016 Oct;5(20):2636–45.
358. Ungerleider JL, Johnson TD, Rao N, Christman KL. Fabrication and characterization of injectable hydrogels derived from decellularized skeletal and cardiac muscle. *Methods*. 2015 Aug;84:53–9.
359. Goh SK, Bertera S, Olsen P, Candiello JE, Halfter W, Uechi G, Balasubramani M, Johnson SA, Sicari BM, Kollar E, Badylak SF, Banerjee I. Perfusion-decellularized pancreas as a natural 3D scaffold for pancreatic tissue and whole organ engineering. *Biomaterials*. 2013 Sep;34(28):6760–72.
360. Maloney SE, Broberg CA, Grayton QE, Picciotti SL, Hall HR, Wallet SM, Maile R, Schoenfisch MH. Role of Nitric Oxide-Releasing Glycosaminoglycans in Wound Healing. *ACS Biomater Sci Eng*. 2022 Jun 13;8(6):2537–52.
361. Casale J, Crane JS. Biochemistry, Glycosaminoglycans [Internet]. StatPearls [Internet]. StatPearls Publishing; 2022 [cited 2022 Aug 10]. Available from: <https://www.ncbi.nlm.nih.gov/books/NBK544295/>

362. Zhang Z, Niu G, Choi JS, Giegengack M, Atala A, Soker S. Bioengineered multilayered human corneas from discarded human corneal tissue. *Biomed Mater*. 2015 Jun 24;10(3):035012.
363. Maghsoudlou P, Georgiades F, Smith H, Milan A, Shangaris P, Urbani L, Loukogeorgakis SP, Lombardi B, Mazza G, Hagen C, Sebire NJ, Turmaine M, Eaton S, Olivo A, Godovac-Zimmermann J, Pinzani M, Gissen P, De Coppi P. Optimization of liver decellularization maintains extracellular matrix micro-architecture and composition predisposing to effective cell seeding. *PLoS One*. 2016 May 9;11(5):e0155324.
364. Bruyneel AAN, Carr CA. Ambiguity in the presentation of decellularized tissue composition: The need for standardized approaches. *Artif Organs*. 2017 Aug;41(8):778–84.
365. Crapo PM, Gilbert TW, Badylak SF. An overview of tissue and whole organ decellularization processes. *Biomaterials*. 2011 Apr;32(12):3233–43.
366. Pashos NC, Scarritt ME, Eagle ZR, Gimble JM, Chaffin AE, Bunnell BA. Characterization of an acellular scaffold for a tissue engineering approach to the nipple-areolar complex reconstruction. *Cells Tissues Organs*. 2017;203(3):183–93.
367. Derwin KA, Baker AR, Spragg RK, Leigh DR, Iannotti JP. Commercial extracellular matrix scaffolds for rotator cuff tendon repair. *The Journal of Bone & Joint Surgery*. 2006;88(12):2665–72.
368. Bolland F, Korossis S, Wilshaw SP, Ingham E, Fisher J, Kearney JN, Southgate J. Development and characterisation of a full-thickness acellular porcine bladder matrix for tissue engineering. *Biomaterials*. 2007 Feb;28(6):1061–70.
369. Moreno-Manzano V, Zaytseva-Zotova D, López-Mocholí E, Briz-Redón Á, Løkensgard Strand B, Serrano-Aroca Á. Injectable gel form of a decellularized bladder induces adipose-derived stem cell differentiation into smooth muscle cells in vitro. *Int J Mol Sci*. 2020 Nov 15;21(22):8608.
370. Brown BN, Buckenmeyer MJ, Prest TA. Preparation of decellularized biological scaffolds for 3D cell culture. In: Koledova Z, editor. *3D Cell Culture* [Internet]. New York, NY: Springer New York; 2017 [cited 2022 Jun 28]. p. 15–27. (Methods in Molecular Biology; vol. 1612). Available from: http://link.springer.com/10.1007/978-1-4939-7021-6_2
371. Kuehn C, Dubiel EA, Sabra G, Vermette P. Culturing INS-1 cells on CDPGYIGSR-, RGD- and fibronectin surfaces improves insulin secretion and cell proliferation. *Acta Biomaterialia*. 2012 Feb;8(2):619–26.
372. Gilpin SE, Guyette JP, Gonzalez G, Ren X, Asara JM, Mathisen DJ, Vacanti JP, Ott HC. Perfusion decellularization of human and porcine lungs: Bringing the matrix to clinical scale. *The Journal of Heart and Lung Transplantation*. 2014 Mar 1;33(3):298–308.

373. Syed O, Walters NJ, Day RM, Kim HW, Knowles JC. Evaluation of decellularization protocols for production of tubular small intestine submucosa scaffolds for use in oesophageal tissue engineering. *Acta Biomater.* 2014 Dec;10(12):5043–54.
374. Riopel M, Stuart W, Wang R. Fibrin improves beta (INS-1) cell function, proliferation and survival through integrin $\alpha v \beta 3$. *Acta Biomaterialia.* 2013 Sep 1;9(9):8140–8.
375. Riopel M, Li J, Trinder M, Fellows GF, Wang R. Fibrin supports human fetal islet-epithelial cell differentiation via p70s6k and promotes vascular formation during transplantation. *Lab Invest.* 2015 Aug;95(8):925–36.
376. Sharp J, Vermette P. An In-situ glucose-stimulated insulin secretion assay under perfusion bioreactor conditions. *Biotechnol Progress.* 2017 Mar;33(2):454–62.
377. Weber LM, Hayda KN, Anseth KS. Cell–matrix interactions improve β -cell survival and insulin secretion in three-dimensional culture. *Tissue Eng Part A.* 2008 Dec;14(12):1959–68.
378. Kragl M, Lammert E. Basement Membrane in Pancreatic Islet Function. In: Islam MdS, editor. *The Islets of Langerhans* [Internet]. Dordrecht: Springer Netherlands; 2010 [cited 2022 Jul 23]. p. 217–34. (Advances in Experimental Medicine and Biology; vol. 654). Available from: http://link.springer.com/10.1007/978-90-481-3271-3_10
379. Kaido T, Yebra M, Cirulli V, Montgomery AM. Regulation of human beta-cell adhesion, motility, and insulin secretion by collagen IV and its receptor $\alpha 1 \beta 1$. *J Biol Chem.* 2004 Dec 17;279(51):53762–9.
380. Bosco D, Meda P, Halban PA, Rouiller DG. Importance of cell-matrix interactions in rat islet beta-cell secretion in vitro: role of $\alpha 6 \beta 1$ integrin. *Diabetes.* 2000 Feb;49(2):233–43.
381. Dubiel EA, Vermette P. Solution composition impacts fibronectin immobilization on carboxymethyl-dextran surfaces and INS-1 insulin secretion. *Colloids and Surfaces B: Biointerfaces.* 2012 Jun;95:266–73.
382. Lan T, Guo J, Bai X, Huang Z, Wei Z, Du G, Yan G, Weng L, Yi X. RGD-modified injectable hydrogel maintains islet beta-cell survival and function. *Journal of Applied Biomaterials & Functional Materials.* 2020 Jan;18:228080002096347.
383. Dubiel EA, Lakey JRT, Lamb MW, Vermette P. Culturing free-floating and fibrin-embedded islets with endothelial cells: Effects on insulin secretion and apoptosis. *Cel Mol Bioeng.* 2014 Jun;7(2):243–53.
384. Kuehn C, Lakey JR, Lamb MW, Vermette P. Young porcine endocrine pancreatic islets cultured in fibrin show improved resistance toward hydrogen peroxide. *Islets.* 2013 Sep 1;5(5):207–15.

385. Nagata N, Gu Y, Hori H, Balamurugan AN, Touma M, Kawakami Y, Wang W, Baba TT, Satake A, Nozawa M, Tabata Y, Inoue K. Evaluation of insulin secretion of isolated rat islets cultured in extracellular matrix. *Cell Transplant*. 2001;10(4–5):447–51.
386. Hammar EB, Irminger JC, Rickenbach K, Ribaux P, Bosco D, Rouiller DG, Halban PA. Activation of NF- κ B by extracellular matrix is involved in spreading and glucose-stimulated insulin secretion of pancreatic beta cells. *Biological Chemistry*:2005, 280 (34): 30630-30637.
387. Nikolova G, Jabs N, Konstantinova I, Domogatskaya A, Tryggvason K, Sorokin L, Fässler R, Gu G, Gerber HP, Ferrara N, Melton DA, Lammert E. The vascular basement membrane: A niche for insulin gene expression and β cell proliferation. *Developmental Cell*. 2006 Mar 1;10(3):397–405.
388. Bachir AI, Horwitz AR, Nelson WJ, Bianchini JM. Actin-Based Adhesion Modules Mediate Cell Interactions with the Extracellular Matrix and Neighboring Cells. *Cold Spring Harb Perspect Biol*. 2017 Jul;9(7):a023234.
389. Frantz C, Stewart KM, Weaver VM. The extracellular matrix at a glance. *J Cell Sci*. 2010 Dec 15;123(Pt 24):4195–200.
390. Vorotnikova E, McIntosh D, Dewilde A, Zhang J, Reing JE, Zhang L, Cordero K, Bedelbaeva K, Gourevitch D, Heber-Katz E, Badylak SF, Braunhut SJ. Extracellular matrix-derived products modulate endothelial and progenitor cell migration and proliferation in vitro and stimulate regenerative healing in vivo. *Matrix Biol*. 2010 Oct;29(8):690–700.
391. Nagase H, Visse R, Murphy G. Structure and function of matrix metalloproteinases and TIMPs. *Cardiovasc Res*. 2006 Feb 15;69(3):562–73.
392. Vigier S, Fülöp T. Exploring the Extracellular Matrix to Create Biomaterials. In: Travascio F, editor. *Composition and Function of the Extracellular Matrix in the Human Body* [Internet]. InTech; 2016 [cited 2022 Aug 2]. Available from: <http://www.intechopen.com/books/composition-and-function-of-the-extracellular-matrix-in-the-human-body/exploring-the-extracellular-matrix-to-create-biomaterials>
393. Zhang R, Jiang J, Yu Y, Wang F, Gao N, Zhou Y, Wan X, Wang Z, Wei P, Mei J. Analysis of structural components of decellularized scaffolds in renal fibrosis. *Bioact Mater*. 2021 Jan 16;6(7):2187–97.
394. Agarwal T, Maiti TK, Ghosh SK. Decellularized caprine liver-derived biomimetic and pro-angiogenic scaffolds for liver tissue engineering. *Mater Sci Eng C Mater Biol Appl*. 2019 May;98:939–48.
395. Orlando G, Booth C, Wang Z, Totonelli G, Ross CL, Moran E, Salvatori M, Maghsoudlou P, Turmaine M, Delario G, Al-Shraideh Y, Farooq U, Farney AC, Rogers J, Iskandar SS, Burns A, Marini FC, De Coppi P, Stratta RJ, Soker S. Discarded human kidneys as a

- source of ECM scaffold for kidney regeneration technologies. *Biomaterials*. 2013 Aug;34(24):5915–25.
396. Bonandrini B, Figliuzzi M, Papadimou E, Morigi M, Perico N, Casiraghi F, Dipl C, Sangalli F, Conti S, Benigni A, Remuzzi A, Remuzzi G. Recellularization of well-preserved acellular kidney scaffold using embryonic stem cells. *Tissue Eng Part A*. 2014 May;20(9–10):1486–98.
 397. Sun JH, Li G, Wu TT, Lin ZJ, Zou JL, Huang LJ, Xu HY, Wang JH, Ma YH, Zeng YS. Decellularization optimizes the inhibitory microenvironment of the optic nerve to support neurite growth. *Biomaterials*. 2020 Nov;258:120289.
 398. Pérez ML, Castells-Sala C, López-Chicón P, Nieto-Nicolau N, Aiti A, Fariñas O, Casaroli-Marano RP, Porta O, Vilarrodona A. Fast protocol for the processing of split-thickness skin into decellularized human dermal matrix. *Tissue and Cell*. 2021 Oct 1;72:101572.
 399. Sant S, Wang D, Abidi M, Walker G, Ferrell N. Mechanical characterization of native and sugar-modified decellularized kidneys. *J Mech Behav Biomed Mater*. 2021 Feb;114:104220.
 400. Granato AEC, da Cruz EF, Rodrigues-Junior DM, Mosini AC, Ulrich H, Rodrigues BVM, Cheffer A, Porcionatto M. A novel decellularization method to produce brain scaffolds. *Tissue Cell*. 2020 Dec;67:101412.
 401. Sargazi Z, Zavareh S, Jafarabadi M, Salehnia M. An efficient protocol for decellularization of the human endometrial fragments for clinical usage. *Prog Biomater*. 2021 May 21;10:119–30.
 402. Kargar-Abarghouei E, Vojdani Z, Hassanpour A, Alaei S, Talaei-Khozani T. Characterization, recellularization, and transplantation of rat decellularized testis scaffold with bone marrow-derived mesenchymal stem cells. *Stem Cell Research & Therapy*. 2018 Nov 21;9(1):324.
 403. Prydz K. Determinants of Glycosaminoglycan (GAG) Structure. *Biomolecules*. 2015 Aug 21;5(3):2003–22.
 404. Sodhi H, Panitch A. Glycosaminoglycans in Tissue Engineering: A Review. *Biomolecules*. 2020 Dec 29;11(1):29.
 405. Collins MN, Birkinshaw C. Hyaluronic acid based scaffolds for tissue engineering--a review. *Carbohydr Polym*. 2013 Feb 15;92(2):1262–79.
 406. Hwang NS, Varghese S, Lee HJ, Theprungsirikul P, Canver A, Sharma B, Elisseeff J. Response of zonal chondrocytes to extracellular matrix-hydrogels. *FEBS Lett*. 2007 Sep 4;581(22):4172–8.

407. Liu Y, Cai S, Shu XZ, Shelby J, Prestwich GD. Release of basic fibroblast growth factor from a crosslinked glycosaminoglycan hydrogel promotes wound healing. *Wound Repair Regen.* 2007 Apr;15(2):245–51.
408. Kadler KE, Baldock C, Bella J, Boot-Handford RP. Collagens at a glance. *J Cell Sci.* 2007 Jun 15;120(Pt 12):1955–8.
409. Ricard-Blum S. The Collagen Family. *Cold Spring Harb Perspect Biol.* 2011 Jan;3(1):a004978.
410. Arseni L, Lombardi A, Orioli D. From Structure to Phenotype: Impact of Collagen Alterations on Human Health. *International Journal of Molecular Sciences.* 2018 May;19(5):1407.
411. Wang H. A Review of the Effects of Collagen Treatment in Clinical Studies. *Polymers.* 2021 Jan;13(22):3868.
412. Ottani V, Raspanti M, Ruggeri A. Collagen structure and functional implications. *Micron.* 2001 Apr;32(3):251–60.
413. Fang M, Goldstein EL, Turner AS, Les CM, Orr BG, Fisher GJ, Welch KB, Rothman ED, Banaszak Holl MM. Type I Collagen D-spacing in Fibril Bundles of Dermis, Tendon and Bone: Bridging Between Nano- and Micro-Level Tissue Hierarchy. *ACS Nano.* 2012 Nov 27;6(11):9503–14.
414. Eyre D. Articular cartilage and changes in Arthritis: Collagen of articular cartilage. *Arthritis Research & Therapy.* 2001 Oct 5;4(1):30.
415. LeBleu VS, Macdonald B, Kalluri R. Structure and function of basement membranes. *Exp Biol Med (Maywood).* 2007 Oct;232(9):1121–9.
416. Mak KM, Mei R. Basement Membrane Type IV Collagen and Laminin: An Overview of Their Biology and Value as Fibrosis Biomarkers of Liver Disease. *The Anatomical Record.* 2017;300(8):1371–90.
417. Aumailley M, Bruckner-Tuderman L, Carter WG, Deutzmann R, Edgar D, Ekblom P, Engel J, Engvall E, Hohenester E, Jones JCR, Kleinman HK, Marinkovich MP, Martin GR, Mayer U, Meneguzzi G, Miner JH, Miyazaki K, Patarroyo M, Paulsson M, Quaranta V, Sanes JR, Sasaki T, Sekiguchi K, Sorokin LM, Talts JF, Tryggvason K, Uitto J, Virtanen I, von der Mark K, Wewer UM, Yamada Y, Yurchenco PD. A simplified laminin nomenclature. *Matrix Biol.* 2005 Aug;24(5):326–32.
418. Tzu J, Marinkovich MP. Bridging structure with function: Structural, regulatory, and developmental role of laminins. *The International Journal of Biochemistry & Cell Biology.* 2008;40(2):199–214.
419. Barros D, Amaral IF, Pêgo AP. Laminin-Inspired Cell-Instructive Microenvironments for Neural Stem Cells. *Biomacromolecules.* 2020 Feb 10;21(2):276–93.

420. To WS, Midwood KS. Plasma and cellular fibronectin: distinct and independent functions during tissue repair. *Fibrogenesis Tissue Repair*. 2011 Sep 16;4:21.
421. Couchman JR, Austria MR, Woods A. Fibronectin-cell interactions. *J Invest Dermatol*. 1990 Jun;94(6 Suppl):7S-14S.
422. Ushiki T. Collagen fibers, reticular fibers and elastic fibers. A comprehensive understanding from a morphological viewpoint. *Arch Histol Cytol*. 2002 Jun;65(2):109–26.
423. Narciso M, Ulldemolins A, Júnior C, Otero J, Navajas D, Farré R, Gavara N, Almendros I. Novel Decellularization Method for Tissue Slices. *Frontiers in Bioengineering and Biotechnology* [Internet]. 2022 [cited 2023 Feb 18];10. Available from: <https://www.frontiersin.org/articles/10.3389/fbioe.2022.832178>
424. Oliveira AC, Garzón I, Ionescu AM, Carriel V, Cardona J de la C, González-Andrades M, Pérez M del M, Alaminos M, Campos A. Evaluation of Small Intestine Grafts Decellularization Methods for Corneal Tissue Engineering. *PLOS ONE*. 2013 Jun 14;8(6):e66538.
425. Banfi G, Salvagno GL, Lippi G. The role of ethylenediamine tetraacetic acid (EDTA) as in vitro anticoagulant for diagnostic purposes. *Clin Chem Lab Med*. 2007;45(5):565–76.
426. Wang NS. Enzyme purification by salt (ammonium sulfate) precipitation [Internet]. [cited 2022 Oct 1]. Available from: <https://user.eng.umd.edu/~nsw/ench485/lab6a.htm>
427. Raman R, Sasisekharan V, Sasisekharan R. Structural insights into biological roles of protein-glycosaminoglycan interactions. *Chem Biol*. 2005 Mar;12(3):267–77.
428. Babeu JP, Wilson SD, Lambert É, Lévesque D, Boisvert FM, Boudreau F. Quantitative Proteomics Identifies DNA Repair as a Novel Biological Function for Hepatocyte Nuclear Factor 4 α in Colorectal Cancer Cells. *Cancers*. 2019 May 5;11(5):626.
429. Chauvin A, Bergeron D, Vencic J, Lévesque D, Paquette B, Scott MS, Boisvert FM. Downregulation of KRAB zinc finger proteins in 5-fluorouracil resistant colorectal cancer cells. *BMC Cancer*. 2022 Apr 4;22(1):363.
430. Heberle H, Meirelles GV, da Silva FR, Telles GP, Minghim R. InteractiVenn: a web-based tool for the analysis of sets through Venn diagrams. *BMC Bioinformatics*. 2015 May 22;16(1):169.
431. Ahmed MH, Ghatge MS, Safo MK. Hemoglobin: Structure, Function and Allostery. *Subcell Biochem*. 2020;94:345–82.
432. Guerrero-Hue M, Rubio-Navarro A, Sevillano Á, Yuste C, Gutiérrez E, Palomino-Antolín A, Román E, Praga M, Egido J, Moreno JA. Adverse effects of the renal accumulation of haem proteins. Novel therapeutic approaches. *Nefrología (English Edition)*. 2018 Jan 1;38(1):13–26.

433. Devineau S, Inoue K ichi, Kusaka R, Urashima S hei, Nihonyanagi S, Baigl D, Tsuneshige A, Tahara T. Change of the isoelectric point of hemoglobin at the air/water interface probed by the orientational flip-flop of water molecules. *Phys Chem Chem Phys*. 2017 Apr 19;19(16):10292–300.
434. Yang B, Zhang Y, Zhou L, Sun Z, Zheng J, Chen Y, Dai Y. Development of a Porcine Bladder Acellular Matrix with Well-Preserved Extracellular Bioactive Factors for Tissue Engineering. *Tissue Engineering Part C: Methods*. 2010 Oct;16(5):1201–11.
435. Alaby Pinheiro Faccioli L, Suhett Dias G, Hoff V, Lemos Dias M, Ferreira Pimentel C, Hochman-Mendez C, Braz Parente D, Labrunie E, Souza Mourão PA, Rogério de Oliveira Salvalaggio P, Goldberg AC, Campos de Carvalho AC, dos Santos Goldenberg RC. Optimizing the Decellularized Porcine Liver Scaffold Protocol. *Cells Tissues Organs*. 2022;0–9.
436. Poornejad N, Buckmiller E, Schaumann L, Wang H, Wisco J, Roeder B, Reynolds P, Cook A. Re-epithelialization of whole porcine kidneys with renal epithelial cells. *J Tissue Eng*. 2017 Jul 3;8:2041731417718809.
437. Li Y, Wu Q, Li L, Chen F, Bao J, Li W. Decellularization of porcine whole lung to obtain a clinical-scale bioengineered scaffold. *Journal of Biomedical Materials Research Part A*. 2021;109(9):1623–32.
438. O'Neill JD, Anfang R, Anandappa A, Costa J, Javidfar J, Wobma HM, Singh G, Freytes DO, Bacchetta MD, Sonett JR, Vunjak-Novakovic G. Decellularization of human and porcine lung tissues for pulmonary tissue engineering. *Ann Thorac Surg*. 2013 Sep;96(3):1046–55; discussion 1055-1056.
439. Nagai H, Henrich H, Wünsch PH, Fischbach W, Mössner J. Role of pancreatic enzymes and their substrates in autodigestion of the pancreas. In vitro studies with isolated rat pancreatic acini. *Gastroenterology*. 1989 Mar;96(3):838–47.
440. Ito K, Matsuura K, Mihara Y, Sakamoto Y, Hasegawa K, Kokudo N, Shimizu T. Delivery of pancreatic digestive enzymes into the gastrointestinal tract by pancreatic exocrine tissue transplant. *Sci Rep*. 2019 Apr 11;9(1):5922.
441. White SA, Djaballah H, Hughes DP, Roberts DL, Contractor HH, Pathak S, London NJM. A Preliminary Study of the Activation of Endogenous Pancreatic Exocrine Enzymes during Automated Porcine Islet Isolation. *Cell Transplant*. 1999 May 1;8(3):265–76.
442. Uhl FE, Zhang F, Pouliot RA, Uriarte JJ, Rolandsson Enes S, Han X, Ouyang Y, Xia K, Westergren-Thorsson G, Malmström A, Hallgren O, Linhardt RJ, Weiss DJ. Functional role of glycosaminoglycans in decellularized lung extracellular matrix. *Acta Biomaterialia*. 2020 Jan 15;102:231–46.
443. Berkova Z, Zacharovova K, Patikova A, Leontovyc I, Hladikova Z, Cerveny D, Tihlarikova E, Nedela V, Girman P, Jirak D, Saudek F. Decellularized Pancreatic Tail as

- Matrix for Pancreatic Islet Transplantation into the Greater Omentum in Rats. *Journal of Functional Biomaterials*. 2022 Dec;13(4):171.
444. Goh SK, Olsen P, Banerjee I. Extracellular Matrix Aggregates from Differentiating Embryoid Bodies as a Scaffold to Support ESC Proliferation and Differentiation. Kerkis I, editor. *PLoS ONE*. 2013 Apr 18;8(4):e61856.
445. Johnson TD, Hill RC, Dzieciatkowska M, Nigam V, Behfar A, Christman KL, Hansen KC. Quantification of Decellularized Human Myocardial Matrix: A Comparison of Six Patients. *Proteomics Clin Appl*. 2016 Jan;10(1):75–83.
446. Vigier S, Gagnon H, Bourgade K, Klarskov K, Fülöp T, Vermette P. Composition and organization of the pancreatic extracellular matrix by combined methods of immunohistochemistry, proteomics and scanning electron microscopy. *Current Research in Translational Medicine*. 2017 Jan;65(1):31–9.
447. Kühn K. Basement membrane (type IV) collagen. *Matrix Biol*. 1995 Feb;14(6):439–45.
448. Aumailley M, Smyth N. The role of laminins in basement membrane function. *J Anat*. 1998 Jul;193(Pt 1):1–21.
449. Chen H, Mosher DF. Formation of sodium dodecyl sulfate-stable fibronectin multimers. Failure to detect products of thiol-disulfide exchange in cyanogen bromide or limited acid digests of stabilized matrix fibronectin. *J Biol Chem*. 1996 Apr 12;271(15):9084–9.
450. Faulk DM, Carruthers CA, Warner HJ, Kramer CR, Reing JE, Zhang L, D'Amore A, Badylak SF. The Effect of Detergents on the Basement Membrane Complex of a Biologic Scaffold Material. *Acta Biomater*. 2014 Jan;10(1):10.1016/j.actbio.2013.09.006.
451. Kim B, Ventura R, Lee BT. Functionalization of porous BCP scaffold by generating cell-derived extracellular matrix from rat bone marrow stem cells culture for bone tissue engineering. *J Tissue Eng Regen Med*. 2018 Feb;12(2):e1256–67.
452. Willemsse J, Versteegen MMA, Vermeulen A, Schurink IJ, Roest HP, van der Laan LJW, de Jonge J. Fast, robust and effective decellularization of whole human livers using mild detergents and pressure controlled perfusion. *Mater Sci Eng C Mater Biol Appl*. 2020 Mar;108:110200.
453. Green KA, Lund LR. ECM degrading proteases and tissue remodelling in the mammary gland. *Bioessays*. 2005 Sep;27(9):894–903.
454. Cawston TE, Young DA. Proteinases involved in matrix turnover during cartilage and bone breakdown. *Cell Tissue Res*. 2010 Jan;339(1):221–35.
455. Wieland FC, van Blitterswijk CA, van Apeldoorn A, LaPointe VLS. The functional importance of the cellular and extracellular composition of the islets of Langerhans. *Journal of Immunology and Regenerative Medicine*. 2021 Aug 1;13:100048.

456. Junqueira LC, Bignolas G, Brentani RR. Picrosirius staining plus polarization microscopy, a specific method for collagen detection in tissue sections. *Histochem J.* 1979 Jul;11(4):447–55.
457. Tomoda K, Kimura H, Osaki S. Distribution of Collagen Fiber Orientation in the Human Lung. *The Anatomical Record.* 2013;296(5):846–50.
458. Yoshioka NK, Young GM, Khajuria DK, Karuppagounder V, Pinamont WJ, Fanburg-Smith JC, Abraham T, Elbarbary RA, Kamal F. Structural changes in the collagen network of joint tissues in late stages of murine OA. *Sci Rep.* 2022 Jun 1;12(1):9159.
459. Bromage TG, Goldman HM, McFarlin SC, Warshaw J, Boyde A, Riggs CM. Circularly polarized light standards for investigations of collagen fiber orientation in bone. *The Anatomical Record Part B: The New Anatomist.* 2003;274B(1):157–68.
460. Schmid TM, Li J, Muehleman C, Wimmer M, Irving T. Cartilage compression changes collagen fiber orientation as measured by small angle x-ray diffraction. In 2004.
461. Gilbert TW, Wognum S, Joyce EM, Freytes DO, Sacks MS, Badylak SF. Collagen fiber alignment and biaxial mechanical behavior of porcine urinary bladder derived extracellular matrix. *Biomaterials.* 2008 Dec 1;29(36):4775–82.
462. Meyer M. Processing of collagen based biomaterials and the resulting materials properties. *BioMedical Engineering OnLine.* 2019 Mar 18;18(1):24.
463. Lattouf R, Younes R, Lutomski D, Naaman N, Godeau G, Senni K, Changotade S. Picrosirius Red Staining: A Useful Tool to Appraise Collagen Networks in Normal and Pathological Tissues. *J Histochem Cytochem.* 2014 Oct 1;62(10):751–8.
464. Narice BF, Green NH, MacNeil S, Anumba D. Second Harmonic Generation microscopy reveals collagen fibres are more organised in the cervix of postmenopausal women. *Reproductive Biology and Endocrinology.* 2016 Oct 21;14(1):70.
465. Chen X, Nadiarynkh O, Plotnikov S, Campagnola PJ. Second harmonic generation microscopy for quantitative analysis of collagen fibrillar structure. *Nat Protoc.* 2012 Mar 8;7(4):654–69.
466. McInnes AD, Moser MAJ, Chen X. Preparation and Use of Decellularized Extracellular Matrix for Tissue Engineering. *Journal of Functional Biomaterials.* 2022 Dec;13(4):240.
467. Kim Y, Ko H, Kwon IK, Shin K. Extracellular Matrix Revisited: Roles in Tissue Engineering. *Int Neurourol J.* 2016 May;20(Suppl 1):S23-29.
468. Gratzer PF. Decellularized Extracellular Matrix. In: Narayan R, editor. *Encyclopedia of Biomedical Engineering* [Internet]. Oxford: Elsevier; 2019 [cited 2023 Feb 6]. p. 86–96. Available from: <https://www.sciencedirect.com/science/article/pii/B9780128012383998702>

469. Chandra PK, Atala AA. Use of Matrix and Seeding With Cells for Vasculature of Organs. In: Reis RL, editor. *Encyclopedia of Tissue Engineering and Regenerative Medicine* [Internet]. Oxford: Academic Press; 2019 [cited 2023 Feb 6]. p. 425–46. Available from: <https://www.sciencedirect.com/science/article/pii/B9780128012383110785>
470. Keane TJ, Swinehart IT, Badylak SF. Methods of tissue decellularization used for preparation of biologic scaffolds and in vivo relevance. *Methods*. 2015 Aug;84:25–34.
471. Hutter H, Vogel BE, Plenefisch JD, Norris CR, Proenca RB, Spieth J, Guo C, Mastwal S, Zhu X, Scheel J, Hedgecock EM. Conservation and novelty in the evolution of cell adhesion and extracellular matrix genes. *Science*. 2000 Feb 11;287(5455):989–94.
472. Iozzo RV. Perlecan: a gem of a proteoglycan. *Matrix Biol*. 1994 Apr;14(3):203–8.
473. Keane TJ, Badylak SF. The host response to allogeneic and xenogeneic biological scaffold materials. *J Tissue Eng Regen Med*. 2015 May;9(5):504–11.
474. Omae H, Zhao C, Sun YL, An KN, Amadio PC. Multilayer tendon slices seeded with bone marrow stromal cells: a novel composite for tendon engineering. *J Orthop Res*. 2009 Jul;27(7):937–42.
475. Cramer M, Badylak S. Extracellular Matrix-Based Biomaterials and Their Influence Upon Cell Behavior. *Ann Biomed Eng*. 2020 Jul;48(7):2132–53.
476. Wolf MT, Daly KA, Reing JE, Badylak SF. Biologic scaffold composed of skeletal muscle extracellular matrix. *Biomaterials*. 2012 Apr;33(10):2916–25.
477. Kočí Z, Výborný K, Dubišová J, Vacková I, Jäger A, Lunov O, Jiráková K, Kubinová Š. Extracellular Matrix Hydrogel Derived from Human Umbilical Cord as a Scaffold for Neural Tissue Repair and Its Comparison with Extracellular Matrix from Porcine Tissues. *Tissue Eng Part C Methods*. 2017 Jun;23(6):333–45.
478. Medberry CJ, Crapo PM, Siu BF, Carruthers CA, Wolf MT, Nagarkar SP, Agrawal V, Jones KE, Kelly J, Johnson SA, Velankar SS, Watkins SC, MODO M, Badylak SF. Hydrogels derived from central nervous system extracellular matrix. *Biomaterials*. 2013 Jan;34(4):1033–40.
479. Keane TJ, DeWard A, Londono R, Saldin LT, Castleton AA, Carey L, Nieponice A, Lagasse E, Badylak SF. Tissue-Specific Effects of Esophageal Extracellular Matrix. *Tissue Eng Part A*. 2015 Sep;21(17–18):2293–300.
480. Jakus AE, Laronda MM, Rashedi AS, Robinson CM, Lee C, Jordan SW, Orwig KE, Woodruff TK, Shah RN. “Tissue Papers” from Organ-Specific Decellularized Extracellular Matrices. *Adv Funct Mater*. 2017 Sep 13;27(3):1700992.
481. Da Silva K, Kumar P, Choonara YE, du Toit LC, Pillay V. Three-dimensional printing of extracellular matrix (ECM)-mimicking scaffolds: A critical review of the current ECM materials. *J Biomed Mater Res A*. 2020 Dec;108(12):2324–50.

482. Kim YS, Majid M, Melchiorri AJ, Mikos AG. Applications of decellularized extracellular matrix in bone and cartilage tissue engineering. *Bioeng Transl Med*. 2018 Oct 26;4(1):83–95.
483. Simões IN, Vale P, Soker S, Atala A, Keller D, Noiva R, Carvalho S, Peleteiro C, Cabral JMS, Eberli D, da Silva CL, Baptista PM. Acellular Urethra Bioscaffold: Decellularization of Whole Urethras for Tissue Engineering Applications. *Sci Rep*. 2017 Feb 6;7(1):41934.
484. Dhandapani V, Boabekoa P, Vermette P. Characterization of ExtraCellular Matrix dervied from decellularized porcine organs.
485. Iwanaga Y, Sutherland DER, Harmon JV, Papas KK. Pancreas preservation for pancreas and islet transplantation. *Curr Opin Organ Transplant*. 2008 Aug;13(4):445–51.
486. Townsend SE, Gannon M. Extracellular Matrix–Associated Factors Play Critical Roles in Regulating Pancreatic β -Cell Proliferation and Survival. *Endocrinology*. 2019 Jul 4;160(8):1885–94.
487. Krishnamurthy M, Li J, Al-Masri M, Wang R. Expression and function of $\alpha\beta 1$ integrins in pancreatic beta (INS-1) cells. *J Cell Commun Signal*. 2008 Dec;2(3–4):67–79.
488. Ross EA, Williams MJ, Hamazaki T, Terada N, Clapp WL, Adin C, Ellison GW, Jorgensen M, Batich CD. Embryonic stem cells proliferate and differentiate when seeded into kidney scaffolds. *J Am Soc Nephrol*. 2009 Nov;20(11):2338–47.
489. Song JJ, Guyette JP, Gilpin SE, Gonzalez G, Vacanti JP, Ott HC. Regeneration and experimental orthotopic transplantation of a bioengineered kidney. *Nat Med*. 2013 May;19(5):646–51.
490. Abolbashari M, Agcaoili SM, Lee MK, Ko IK, Aboushwareb T, Jackson JD, Yoo JJ, Atala A. Repopulation of porcine kidney scaffold using porcine primary renal cells. *Acta Biomaterialia*. 2016 Jan 1;29:52–61.
491. Debnath T, Mallarpu CS, Chelluri LK. Development of Bioengineered Organ Using Biological Acellular Rat Liver Scaffold and Hepatocytes. *Organogenesis*. 2020 Apr 2;16(2):61–72.
492. Li Y, Wu Q, Wang Y, Li L, Chen F, Shi Y, Bao J, Bu H. Construction of bioengineered hepatic tissue derived from human umbilical cord mesenchymal stem cells via aggregation culture in porcine decellularized liver scaffolds. *Xenotransplantation*. 2017 Jan;24(1).
493. Kojima H, Yasuchika K, Fukumitsu K, Ishii T, Ogiso S, Miyauchi Y, Yamaoka R, Kawai T, Katayama H, Yoshitoshi-Uebayashi EY, Kita S, Yasuda K, Sasaki N, Komori J, Uemoto S. Establishment of practical recellularized liver graft for blood perfusion using primary rat hepatocytes and liver sinusoidal endothelial cells. *Am J Transplant*. 2018 Jun;18(6):1351–9.

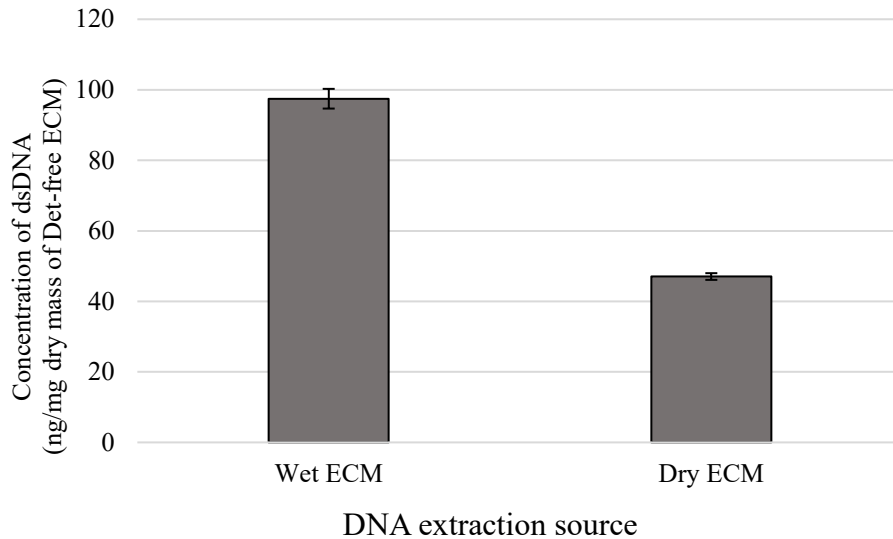
494. Uday Chandrika K, Tripathi R, Kameshwari Y, Rangaraj N, Mahesh Kumar J, Singh S. Refunctionalization of Decellularized Organ Scaffold of Pancreas by Recellularization: Whole Organ Regeneration into Functional Pancreas. *Tissue Eng Regen Med*. 2020 Oct 24;18(1):99–112.
495. Panahi F, Baheiraei N, Sistani MN, Salehnia M. Analysis of decellularized mouse liver fragment and its recellularization with human endometrial mesenchymal cells as a candidate for clinical usage. *Prog Biomater*. 2022 Sep 19;11:409–20.
496. Mirmalek-Sani SH, Orlando G, McQuilling J, Pareta R, Mack D, Salvatori M, Farney AC, Stratta RJ, Atala A, Opara EC, Soker S. Porcine pancreas extracellular matrix as a platform for endocrine pancreas bioengineering. *Biomaterials*. 2013 Jul;34(22):5488–95.
497. Napierala H, Hillebrandt KH, Haep N, Tang P, Tintemann M, Gassner J, Noesser M, Everwien H, Seiffert N, Kluge M, Teegen E, Polenz D, Lippert S, Geisel D, Reutzel Selke A, Raschzok N, Andreou A, Pratschke J, Sauer IM, Struecker B. Engineering an endocrine Neo-Pancreas by repopulation of a decellularized rat pancreas with islets of Langerhans. *Sci Rep*. 2017 Feb 2;7(1):41777.
498. Bertelli E, Regoli M, Orazioli D, Bendayan M. Association between islets of Langerhans and pancreatic ductal system in adult rat. Where endocrine and exocrine meet together? *Diabetologia*. 2001 May;44(5):575–84.
499. Bouwens L. Islet morphogenesis and stem cell markers. *Cell Biochem Biophys*. 2004;40(3 Suppl):81–8.
500. Brissova M, Shostak A, Fligner CL, Revetta FL, Washington MK, Powers AC, Hull RL. Human Islets Have Fewer Blood Vessels than Mouse Islets and the Density of Islet Vascular Structures Is Increased in Type 2 Diabetes. *J Histochem Cytochem*. 2015 Aug;63(8):637–45.
501. Cohrs CM, Chen C, Jahn SR, Stertmann J, Chmelova H, Weitz J, Bähr A, Klymiuk N, Steffen A, Ludwig B, Kamvissi V, Wolf E, Bornstein SR, Solimena M, Speier S. Vessel Network Architecture of Adult Human Islets Promotes Distinct Cell-Cell Interactions In Situ and Is Altered After Transplantation. *Endocrinology*. 2017 May 1;158(5):1373–85.
502. Narayanan S, Loganathan G, Dhanasekaran M, Tucker W, Patel A, Subhashree V, Mokshagundam S, Hughes MG, Williams SK, Balamurugan AN. Intra-islet endothelial cell and β -cell crosstalk: Implication for islet cell transplantation. *World J Transplant*. 2017 Apr 24;7(2):117–28.
503. Hogan MF, Hull RL. The islet endothelial cell: a novel contributor to beta cell secretory dysfunction in diabetes. *Diabetologia*. 2017 Jun;60(6):952–9.
504. Spelios MG, Afinowicz LA, Tipon RC, Akirav EM. Human EndoC- β H1 β -cells form pseudoislets with improved glucose sensitivity and enhanced GLP-1 signaling in the presence of islet-derived endothelial cells. *American Journal of Physiology-Endocrinology and Metabolism*. 2018 May;314(5):E512–21.

505. Hilderink J, Spijker S, Carlotti F, Lange L, Engelse M, van Blitterswijk C, de Koning E, Karperien M, van Apeldoorn A. Controlled aggregation of primary human pancreatic islet cells leads to glucose-responsive pseudoislets comparable to native islets. *Journal of Cellular and Molecular Medicine*. 2015;19(8):1836–46.
506. Asfari M, Janjic D, Meda P, Li G, Halban PA, Wollheim CB. Establishment of 2-mercaptoethanol-dependent differentiated insulin-secreting cell lines. *Endocrinology*. 1992 Jan;130(1):167–78.

APPENDIX A

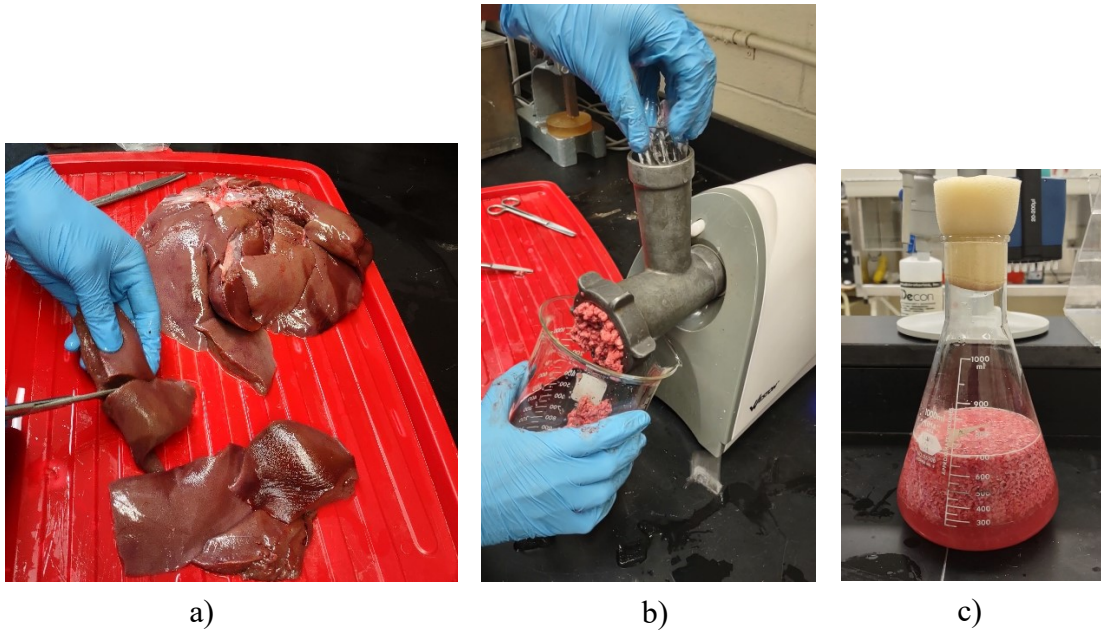


Supplemental Figure 1: **a)** Whole native bladder, **b)** Bladder with the fat and muscular layers excised, **c)** Diced bladder, **d)** Native bladder transferred to an Erlenmeyer flask, **e)** Detergent-based decellularization (15 hours after the process has been initiated), **f)** Detergent-free decellularized bladder ECM, **g)** Detergent-based decellularized bladder ECM.

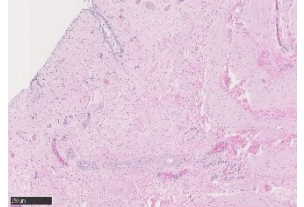
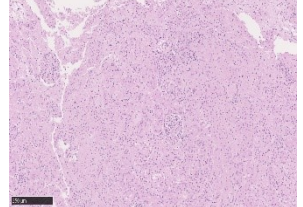
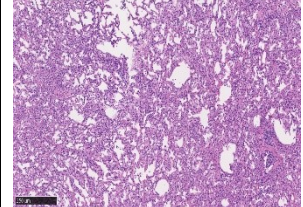
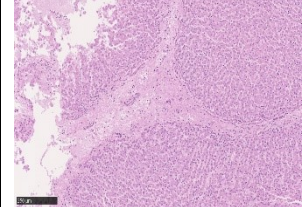
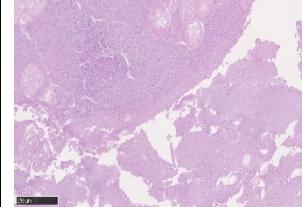


Supplemental Figure 2: The concentration of dsDNA extracted and quantified from Det-free ECM using two protocols: **1.** DNA extracted from wet ECM samples and dsDNA quantified and normalized per mg of dry ECM mass. The dry mass was estimated by weighing a lyophilized sample obtained from ECM having a wet mass equivalent to that used to extract the DNA. **2.** Lyophilized ECM was weighted, then DNA extracted from this same lyophilized ECM sample and dsDNA quantified and normalized per mg of dry mass of ECM. Hydrating the dry matrix completely to extract the dsDNA would be difficult in comparison with pre-wet ECMs and may have contributed to the difference observed.

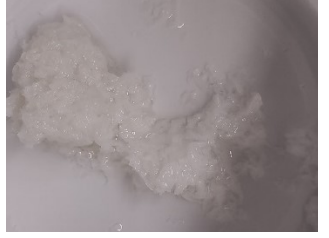











APPENDIX B



Supplemental Figure 3: Preparation for decellularization: **a)** Dicing porcine liver, **b)** weighed lung pieces processed in a meat grinder, and **c)** ground lung transferred to an Erlenmeyer flask in Milli-Q water.

Sample	Bladders	Kidneys	Lungs	Livers	Pancreas
H&E					

Supplemental Figure 4: H&E staining of ground organs, except bladders, as it could not be grinded. Bladders were diced. Necrosis of the native pancreas was also observed due to auto-digestion (similar to Figure 5.1).

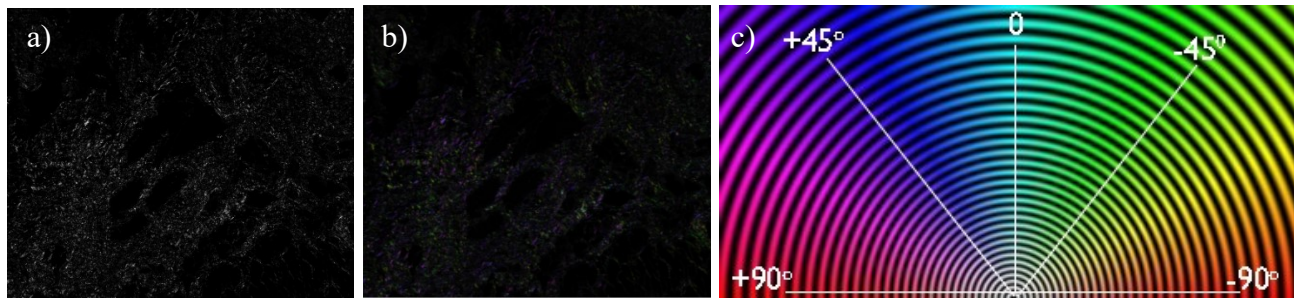
Organ/Method	Det	Det-free	Det-free (+pH)	Det-free (+EDTA)
Kidneys				
Lungs				
Livers				

Supplemental Figure 5: Visual organ coloration following decellularization.

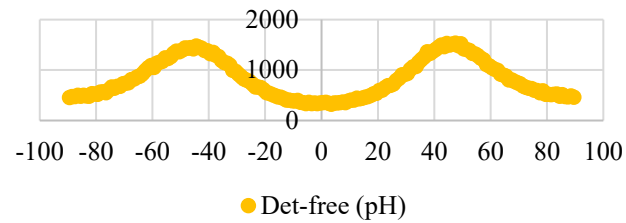
Gene names / Samples	Bladders				Kidneys				Lungs				Livers				Pancreas			
	D	DF	DFP	DFE	D	DF	DFP	DFE	D	DF	DFP	DFE	D	DF	DFP	DFE	D	DF	DFP	DFE
Collagens																				
COL4A3	-	-	-	+	+	+	+	+	+	+	+	+	-	-	-	-	-	-	-	-
COL4A6	-	+	+	+	+	+	+	+	+	+	+	+	-	-	-	+	-	-	+	+
COL1A1	+	+	+	+	+	+	+	+	+	+	+	+	+	+	+	+	+	+	+	+
COL1A2	+	+	+	+	+	+	+	+	+	+	+	+	+	+	+	+	+	+	+	+
COL6A3	+	+	+	+	+	+	+	+	+	+	+	+	+	+	+	+	+	+	+	+
COL6A1	+	+	+	+	+	+	+	+	+	+	+	+	+	+	+	+	-	+	+	+
COL6A2	+	+	+	+	+	+	+	+	+	+	+	+	+	+	+	+	+	+	+	+
COL6A5	+	+	+	+	+	+	+	+	+	+	+	+	+	+	+	+	+	-	+	+
COL6A6	+	-	+	+	+	+	+	+	+	+	+	+	+	+	+	+	+	-	+	+
Glycoproteins																				
FBN1	+	+	+	+	+	+	+	+	+	+	+	+	+	+	+	+	+	-	+	+
FBN2	-	-	-	-	-	-	-	-	+	-	+	+	+	-	-	-	-	-	+	+
BGN	+	+	+	+	+	+	+	+	+	+	+	+	+	+	+	+	-	-	+	-

HRG	+	+	+	+	-	+	+	+	+	+	+	+	+	+	+	+	-	-	+	+
TNC	-	+	+	+	-	+	+	+	+	+	+	+	+	+	+	+	-	-	+	+
HSPG2	+	+	+	+	+	+	+	+	+	+	+	+	+	+	+	+	+	+	+	+
Other ECM																				
Proteins																				
EFEMP1	+	+	+	+	+	+	+	+	+	+	+	+	+	+	-	+	-	-	-	-
EFEMP2	-	+	+	+	-	+	-	-	-	+	-	+	+	+	-	-	-	-	-	-
FRAS1	-	+	-	-	+	+	+	+	-	-	-	-	-	+	-	-	-	-	-	-
NID1	-	+	+	+	+	+	+	+	+	+	+	+	+	+	+	+	-	-	+	-
NID2	-	+	+	+	+	+	+	+	+	+	+	+	+	+	+	+	-	-	-	-

Supplemental Table 1: Proteins detected by mass spectrometry. D indicates detergent (SDS)-based, DF indicates detergent-free, DFP indicates detergent-free with pH adjustment and DFE indicates detergent-free coupled with EDTA-treatment decellularization. COL: collagen, FBN fibrillin, BGN: Biglycan, HRG: Histidine rich glycoprotein, TNC: Tenascin, HSPG2: Heparan sulfate proteoglycan 2, EFEMP: Epidermal growth factor containing fibulin like ECM protein, FRAS: Fraser ECM complex, NID: Nidogen.

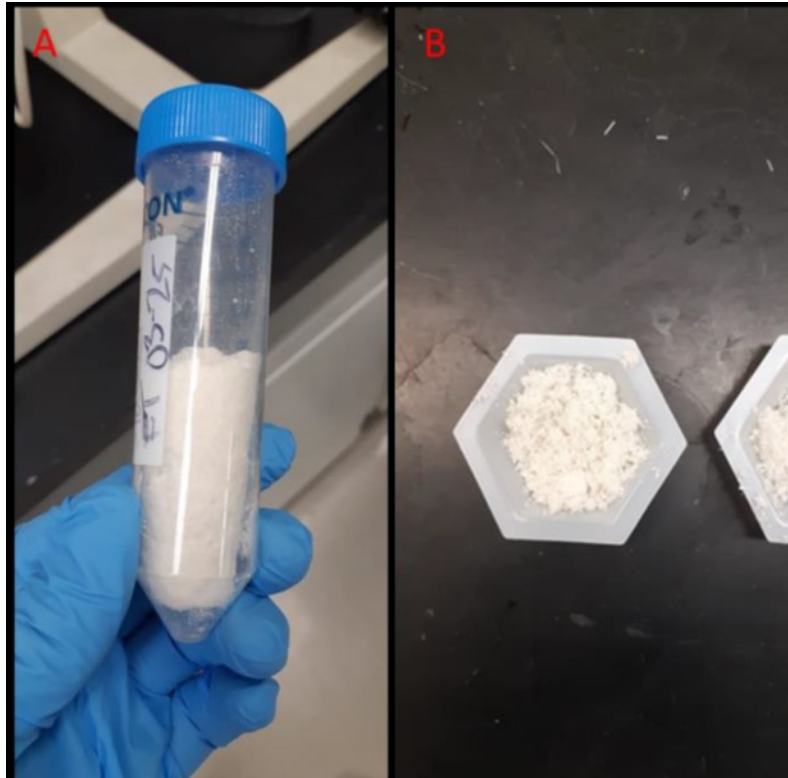


d) Orientation of collagen fibers
in bladders



Supplemental Figure 6: Collagen orientation in detergent-free with pH adjustment decellularized bladder. a) Polarization microscopy image. b) Image J Hue, saturation, and brightness colour coded map of the image. c) Angles corresponding to the color coding (<http://bigwww.epfl.ch/demo/orientation/>). d) Distribution obtained by the distribution function in ImageJ.

APPENDIX C

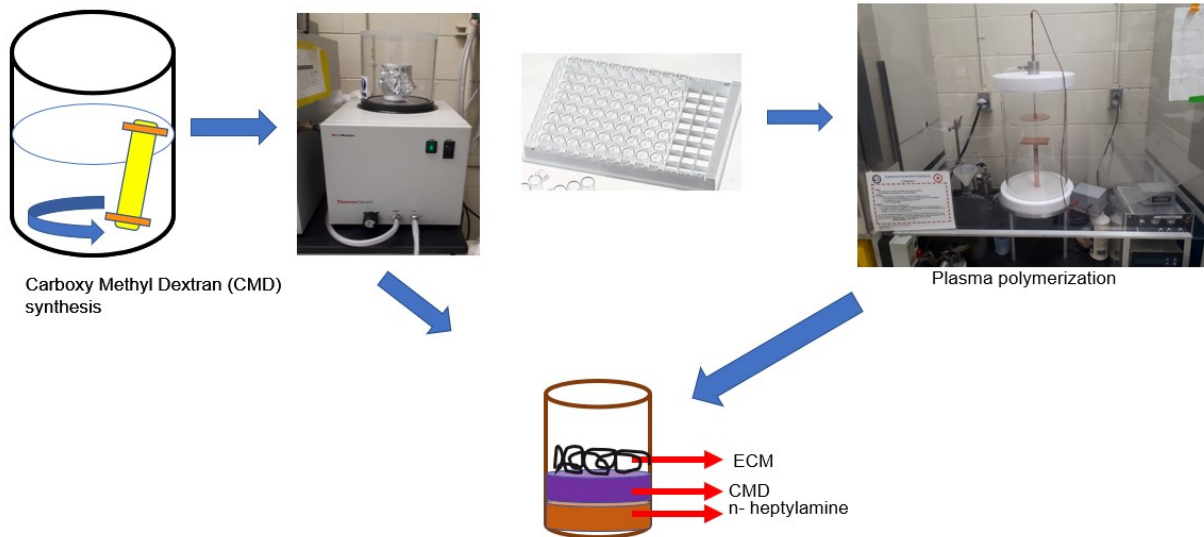


Supplemental Figure 7: Result of the process of decellularization of pig bladder in accordance with an embodiment showing in **(A)** extracellular matrix (ECM) stored following the protocol and in **(B)** ECM after grinding.

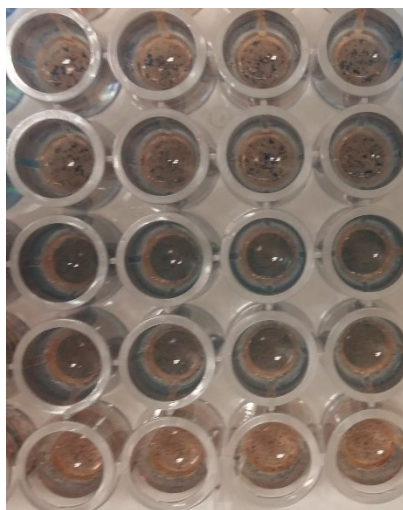


Supplemental Figure 8: Bioadhesives tested for airleak leak on an *ex vivo* porcine lung model.

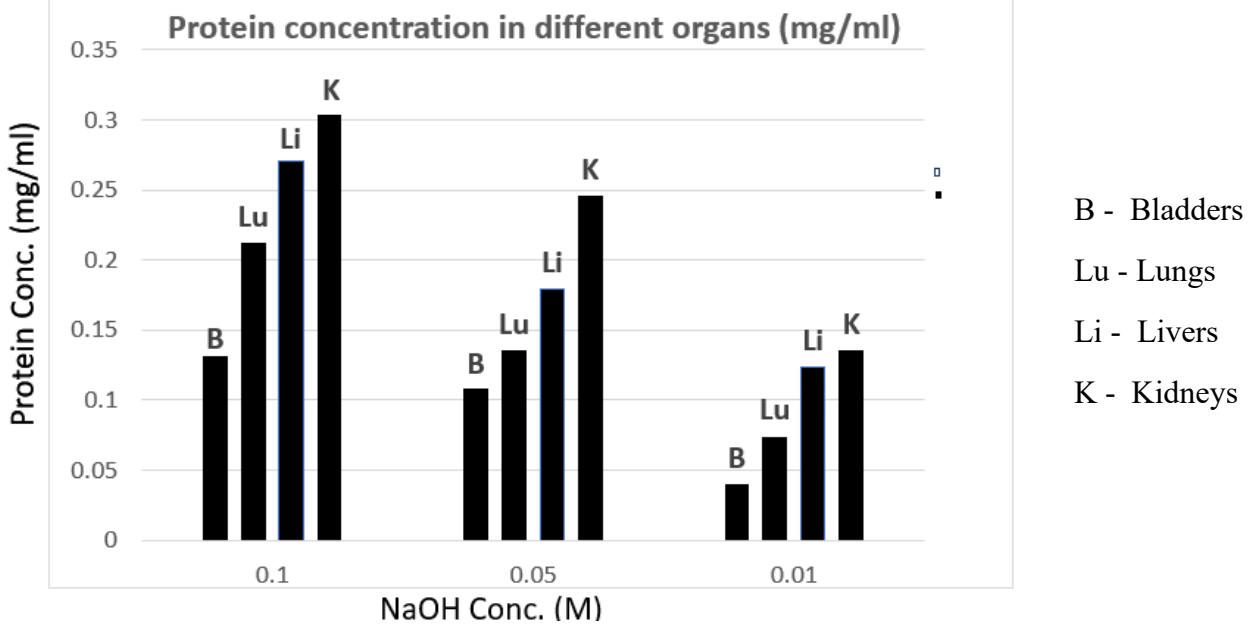
APPENDIX D



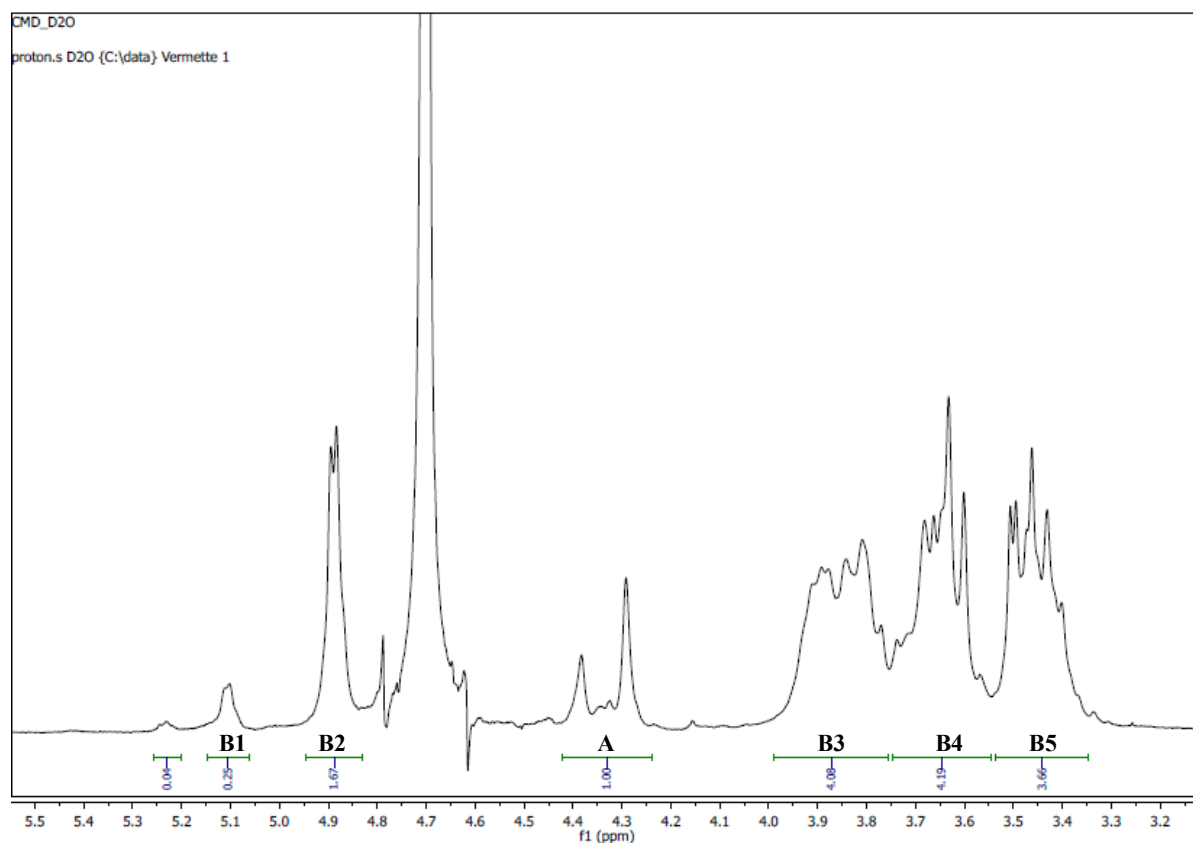
Supplemental Figure 9: Hypothesized process of immobilizing ECM proteins on cell culture plates. Briefly, carboxy methyl dextran was synthesized by dialysis, coupled to plasma coating of n-heptyl amine with further addition of solubilized ECM from decellularized organs.



Supplemental Figure 10: Bradford assay of 1 mg/mL of porcine lung dissolved in 1M, 0.5M, 0.1M, 0.05M, and 0.01M sodium hydroxide.



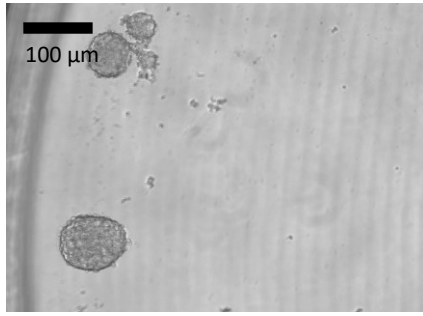
Supplemental Figure 11: BCA assay of 1 mg/ml of porcine organs dissolved in 0.1M, 0.05M, 0.01M sodium hydroxide.



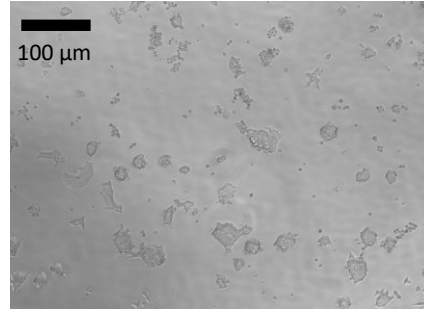
Supplemental Figure 12: Estimation of degree of carboxylation of carboxymethyl dextran using ¹H-NMR.

Ratios obtained, A= 1, B1= 0.25, B2= 1.67, B3= 4.08, B4= 4.19, B5= 3.66

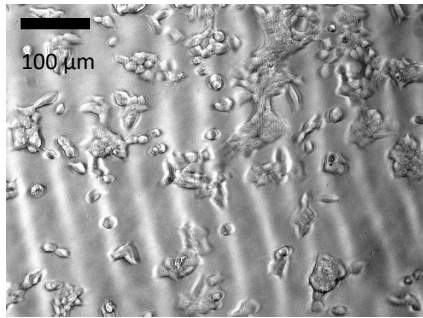
$$\begin{aligned} \text{\% degree of carboxylation} &= \left\{ \frac{A/2}{(B1+B2) + (B3+B4+B5)/6} \right\} \times 100 \\ &= \left\{ \frac{(1/2)}{(0.25+1.67) + (4.08+4.19+3.66)/6} \right\} \times 100 \\ &= 25.5\% \text{ (approx. 25\%)} \end{aligned}$$



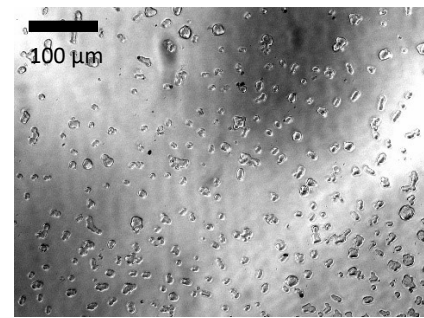
a) CMD surface



b) TCPS surface



c) GRGDS



d) GRGES

Supplemental Figure 13: INS-1 cells on **a)** CMD surface after 4 days of culture, **b)** Tissue Culture Polystyrene (TCPS) after 4 days of culture, **c)** GRGDS-coated CMD after 2 days of culture, **d)** GRGES-coated CMD after 2 days of culture.